Sponsored by the
European Association of Neurosurgical Societies

Advances and Technical Standards in Neurosurgery

Vol. 24

Edited by
F. Cohadon, Bordeaux (Editor-in-Chief),
V. V. Dolenc, Ljubljana, J. Lobo Antunes, Lisbon,
H. Nornes, Oslo, J. D. Pickard, Cambrigde,
H.-J. Reulen, Munich, A. J. Strong, London,
N. de Tribolet, Lausanne, C. A. F. Tulleken, Utrecht

Springer-Verlag Wien GmbH

With 57 partly coloured Figures

Originally published by Springer-Verlag Wien New York in 1998
Softcover reprint of the hardcover 1st edition 1998
Library of Congress Catalogue Card Number 74-10499

Graphic design: Ecke Bonk

Printed on acid-free and chlorine-free bleached paper

SPIN: 10635988

ISSN 0095-4829

ISBN 978-3-7091-7339-8 ISBN 978-3-7091-6504-1 (eBook)
DOI 10.1007/978-3-7091-6504-1

Preface

As an addition to the European postgraduate training system for young neurosurgeons we began to publish in 1974 this series of Advances and Technical Standards in Neurosurgery which was later sponsored by the European Association of Neurosurgical Societies.

This series was first discussed in 1972 at a combined meeting of the Italian and German Neurosurgical Societies in Taormina, the founding fathers of the series being Jean Brihaye, Bernard Pertuiset, Fritz Loew and Hugo Krayenbühl. Thus were established the principles of European cooperation which have been born from the European spirit, flourished in the European Association, and have throughout been associated with this series.

The fact that the English language is well on the way to becoming the international medium at European scientific conferences is a great asset in terms of mutual understanding. Therefore we have decided to publish all contributions in English, regardless of the native language of the authors.

All contributions are submitted to the entire editorial board before publication of any volume.

Our series is not intended to compete with the publications of original scientific papers in other neurosurgical journals. Our intention is, rather, to present fields of neurosurgery and related areas in which important recent advances have been made. The contributions are written by specialists in the given fields and constitute the first part of each volume.

In the second part of each volume, we publish detailed descriptions of standard operative procedures and in depth reviews of established knowledge in all aspects of neurosurgery, furnished by experienced clinicians. This part is intended primarily to assist young neurosurgeons in their postgraduate training. However, we are convinced that it will also be useful to experienced, fully trained neurosurgeons.

We hope therefore that surgeons not only in Europe, but throughout the world will profit by this series of Advances and Technical Standards in Neurosurgery.

The Editors

Contents

A. Advances

The Septal Region and Memory. D. Y. von Cramon and U. Müller, Max-Planck-Institute of Cognitive Neuroscience, Department of Neurology, Leipzig (Germany)

The in vivo Metabolic Investigation of Brain Gliomas with Positron Emission Tomography. J. M. DERLON, Service de Neurochirurgie, CHU, Caen (France)

Use of Surgical Wands in Neurosurgery. L. ZAMORANO, F. C. VINAS, Z. JIANG, and F. G. DIAZ, Department of Neurosurgery, Wayne State University, Detroit, MI (U.S.A.)

B. Technical Standards

Listed in Index Medicus

List of Contributors

Cramon, D. Y. von, Prof. Dr., Max-Planck-Institute of Cognitive Neuroscience, Department of Neurology, Inselstrasse 22–26, D-04103 Leipzig, Germany.

Derlon, J.-M., Prof., Service de Neurochirurgie, CHU, Av. de la Cote de Nacre, F-14033 Caen Cedex, France.

Diaz, F. G., Department of Neurosurgery, Wayne State University, 4160 John R. Suite 930, Detroit, MI 48201, U.S.A.

Guglielmi, G., Department of Neuroradiology, Los Angeles Medical School, University of California (UCLA), BL-428CHS Los Angeles, CA 90024-1721, U.S.A.

Jiang, Z., Department of Neurosurgery, Wayne State University, 4160 John R. Suite 930, Detroit, MI 48201, U.S.A.

Müller, U., Max-Planck-Institute of Cognitive Neuroscience, Department of Neurology, Inselstrasse 22–26, D-04103 Leipzig, Germany.

Pickard, J. D., Prof., Academic Neurosurgical Unit, Box 167, Level 4, A Block, Addenbrooke's Hospital, Hills Road, Cambridge CB2 2QQ, U.K.

Sarkies, N., Neuro-ophthalmology Department, University of Cambridge, Cambridge, U.K.

Sussman, J. D., Academic Neurology Department, University or Sheffield, U.K.

Valavanis, A., Prof. Dr., Institute of Neuroradiology, University of Zürich, Frauenklinikstrasse 10, CH-8091 Zürich, Switzerland.

Vinas, F. C., Department of Neurosurgery, Wayne State University, 4160 John R. Suite 930, Detroit, MI 48201, U.S.A.

Yasargil, M. G., Institute of Neuroradiology, University of Zürich, Frauenklinikstrasse 10, CH-8091 Zürich, Switzerland.

Zamorano, L., MD, PhD, Prof., Department of Neurosurgery, Wayne State University, 4160 John R. Suite 930, Detroit, MI 48201, U.S.A.

A. Advances

The Septal Region and Memory

D. Y. von Cramon and U. Müller

Max-Planck-Institute of Cognitive Neuroscience, Department of Neurology, Leipzig (Germany)

With 1 Figure

Contents

Introductory Remarks

There is a wealth of evidence indicating that the septal region, which can be considered synonymous with the anterior compartment of the basal forebrain, plays a role in cognitive processes. Impairments of memory and attention have been reported to follow damage involving the septum and adjacent cortical regions in animals and humans (Markowitsch, 1995).

In keeping with a two-system model separating the system that stores (cognitive) memories from another system involved in developing (noncognitive) habits, the basal forebrain seems an essential component of the former one. In the memory system (in contrast to the habit system) sensory input arriving in the higher-order sensory areas of the cerebral cortex triggers structures in the medial temporal lobe. The temporal-lobe structures activate structures in the medial thalamus. The medial thalamus, in turn, activates ventromedial areas in the orbital and prefrontal cortex. The medial temporal lobe and ventromedial cortex also extend projections to the basal forebrain which has connections that feed back to the medial thalamus as well as to medial-temporal and sensory cortical areas. This model, proposed by Petri and Mishkin (1994), presumes that storage of stimulus memories requires the activation of these loops and the feedback produced by structures in the basal forebrain onto higher-order sensory areas.

Neuropsychologists have proposed various terms to describe this split between the memories and the habit system. Some use the term *declarative* for memories and *nondeclarative* for habits as well as for other types of noncognitive learning (such as priming). Others have suggested the terms *explicit* and *implicit* memory for this major distinction between systems. In this chapter we will focus on the potential contribution of the septal region (as anterior portion of the basal forebrain) to declarative or, respectively, explicit memory.

Anatomy of the Septal Region

The term septal region (SR) denotes a topographical area that contains a rather heterogeneous collection of nuclear structures (e.g. the septal nuclei and the nucleus of the diagonal band) and major fiber tracts (e.g. fornix/FO, stria terminalis/ST, diagonal band of Broca/DB, medial forebrain bundle/MFB, anterior commissure/AC, thalamic peduncles) that could conceivably participate in cognitive and in particular in memory processes. Most likely, the SR is not an autonomous structure with solitary task, but one that plays an integrative role; a structure that is connected intimately with many other brain regions.

Focal vascular lesions of various etiology comprising the SR seem to be located within the supply area of perforating branches of the anterior

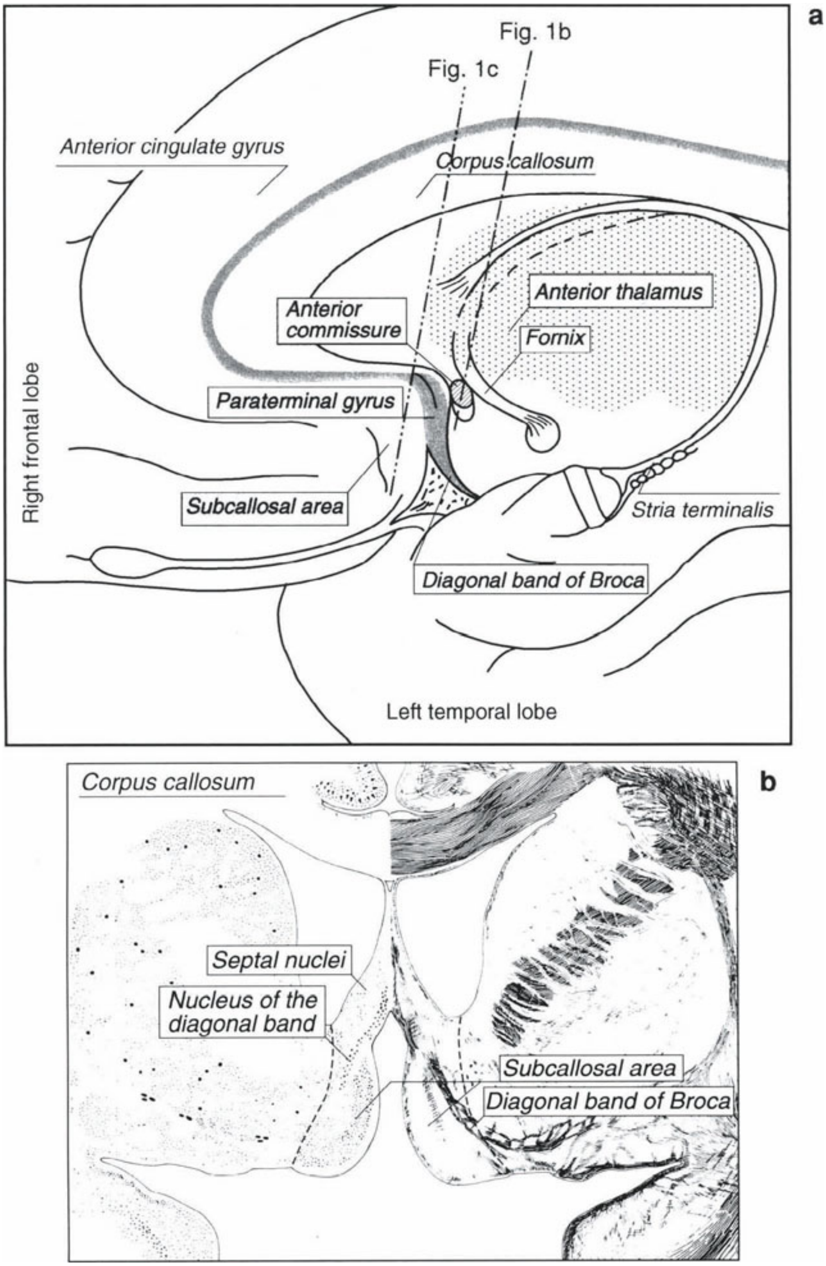

Fig. 1. Structures of the Septal Region (anterior commissure, anterior thalamus, diagonal band of Broca, fornix, paraterminal gyrus, septum, subcallosal area) in a schematic, slightly rotated sagittal section (Fig. 1a) and two coronal sections at the level of the septal nuclei (Fig. 1b) and of the anterior commissure (Fig. 1c) [modified from Nieuwenhuys et al. 1988, Mark et al. 1994, and Gade 1982]

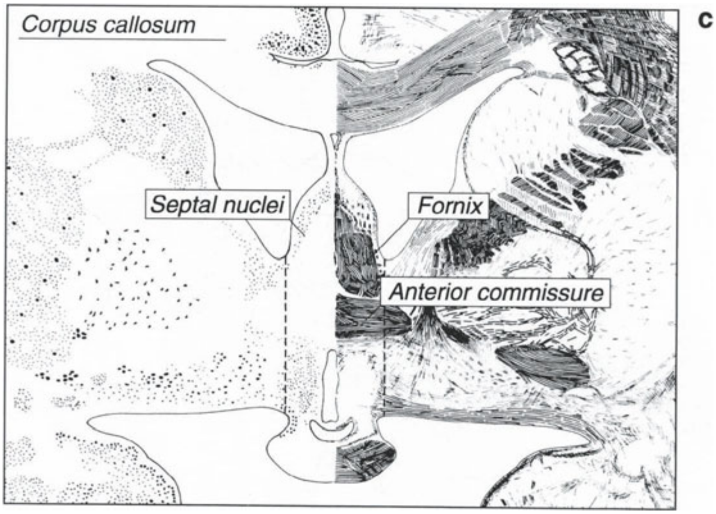

Fig. 1 (*continued*)

communicating artery (ACoA). Thus, since in human cases focal lesions will only in very rare cases be restricted to single brain structures like the medial septal nucleus (MS) or the DB, the best operationalization of the SR refers to those brain structures which in a high percentage of cases are perfused by branches of the ACoA.

This operational definition makes it necessary to include two gyri as part of the SR which are separated by two nearly vertically oriented sulci. The gyri are the subcallosal area and the smaller paraterminal gyrus which are referred to as part of the anterior cingulate cortex (ACC). The two sulci are the anterior and posterior parolfactory sulci. The anterior parolfactory sulcus forms the anterior border of the subcallosal area. The posterior parolfactory sulcus forms the anterior border of the paraterminal gyrus and separates the subcallosal area from the paraterminal gyrus.

Paraterminal gyrus, DB and indusium griseum form part of a continuous curve around the surface of the corpus callosum. This inner curve "is called the precommissural hippocampus or prehippocampal rudiment. As part of an outer curve" the subcallosal area merges superiorly with the ACC and continues to the inferior surface of the hemisphere in contact with the medial olfactory stria (Mark *et al.*, 1994).

Cortical Component: Brodmann Area 25

Brodmann area (BA) 25 largely coincides with the paraterminal gyrus, the subcallosal area and the rostrally adjacent portion of the ACC (Uylings

Table 1. *Brodmann Area* 25

Afferents from:
*entorhinal cortex
*hippocampal formation (including subiculum) via the precommissural fornix
*amygdaloid body (basolateral nucleus)
*thalamus (mediodorsal nucleus)
*nucleus basalis
Efferents to:
*entorhinal cortex
*hippocampal formation
*amygdaloid body (central nucleus)
*nucleus accumbens (shell)
*medial ventral striatum
*nucleus basalis
*thalamus (mediodorsal nucleus)
*hypothalamus
*various brain stem sites (including the dorsal raphe nucleus, the locus coeruleus, the nucleus of solitary tract, and the dorsal motor nucleus of vagus)
*the (sympathetic) thoracic intermediolateral cell column

and Van Eden, 1990). It lies ventral and caudal to BA 33 and has as the larger rest of the ACC a clearly defined layer V. It is one of the least differentiated areas in the agranular ACC with only external and internal pyramidal layers and a hint of large neurons in layer Va. The distinction between layers V and VI is not clear because layer Vb is poorly formed (Vogt *et al.*, 1995).

BA 25 has several projection sites (nucleus of the solitary tract, sympathetic thoracic intermediolateral cell columns) that may mediate visceromotor activity. It is considered as part of the affect division rather than of the cognitive division of ACC (Devinsky *et al.*, 1995). In the face of its connections to memory-related" structures (e.g. to entorhinal cortex, hippocampus, and mediodorsal thalamus) a role in possibly emotional or autonomic aspects of memory cannot be excluded. A survey of the main fiber projections of BA 25 is given in Table 1.

The Precommissural Septum

The precommissural septum or septum verum forms part of the medial wall of the hemisphere. It is situated directly rostral to the lamina terminalis in the depth of the paraterminal gyrus. It is bordered dorsally by the corpus callosum, rostrally by the precommissural hippocampus (BA 25) and caudally by the AC and the preoptic region. Ventrolaterally it borders on the nucleus accumbens septi (Nieuwenhuys *et al.*, 1988). Contrary to the prevailing opinion the septal nuclei are well developed in humans (Andy and Stephan, 1968).

They are composed of rather poorly individualized cell groups among which the lateral septal (LS) nucleus and the magnocellular MS complex may be mentioned. The latter comprises the MS nucleus and the medial or dorsal nucleus of the DB (MS/DB complex). An aggregation of rather large cells form the septal (vertical) limb of the nucleus of the DB. The ventral limb of the nucleus of the DB is the causal boundary of the olfactory tubercle (the latter being a striatal area rather than an olfactory one).

Fiber projections originating in the hippocampal formation and the amygdaloid body travel on their way to the septal nuclei first through the ventral amygdalofugal pathway and continue their course via the DB. In addition to the well-known "dorsal route" via ACC, stria terminalis, and longitudinal striae a major "ventral route" connecting temporomesial and septal structures is observed.

In Table 2 relevant afferent and efferent projections of the precommissural septum are listed. It appears that it forms part of a number of neuronal loops which include primarily the hippocampal formation but also the preoptic region, the hypothalamus and a number of monoaminergic sources in the brain stem as nodal points.

Septal fibers terminate predominantly in the fascia dentata, the CA3 segment of the cornu ammonis (CA), the subiculum, and the entorhinal cortex as well. It appears that CA1 does not receive septal inputs. All fields of the CA, the subiculum and the entorhinal cortex send projections back to the septum terminating in largely overlapping areas in the LS which in turn impinges upon septohippocampal afferents in the MS.

Cholinergic Cell Groups

According to the nomenclature proposed by Mesulam (1995, 1990) cholinergic cell groups centered around the general area of the MS/DB complex are designated Ch1 and Ch2 respectively. All neurons of the Ch1-Ch2 cell group contain acetylcholinesterase (AChE) and cholinacetyltransferase (ChAT) in the perikarya, dendrites and axons. In the rhesus monkey Ch1 consists of choline acetyltransferase (ChAT)-positive neurons within the traditional boundaries of the medial septal nucleus. Approximately 10 % of perikarya are cholinergic and belong to the Ch1 cell group. The boundary between the Ch1 and Ch2 groups is not sharp. Approximately 70 % of the cell bodies within the vertical nucleus of the DB are cholinergic and make up the Ch2 cell group. Ch1 and Ch2 cell groups collectively provide by way

Table 2

A: Lateral Septal Nucleus
Afferents from:
*hippocampal formation via the precommissural fornix
*preoptic region
*hypothalamus (including the anterior, periventricular, ventromedial nuclei, and the lateral hypothalamic area)
*(noradrenergic) locus coeruleus and A1/A2 areas
*(largely serotoninergic) raphe nuclei
*laterodorsal tegmental nucleus
*parabrachial nuclei
*Kölliker-Fuse nucleus
*dorsal vagal complex

Efferents to:
*MS/DB complex
*hypothalamic, supramammillary and ventral tegmental regions via the MFB
*thalamic nuclei via the stria medullaris

B: MS/DB Complex
Afferents from:
*lateral septal nucleus
*lateral preoptico-hypothalamic area
*medial mammillary nucleus
*dorsal tegmental nucleus

Efferents to:
*hippocampal formation (including the subicŭlum)
*entorhinal cortex
*preoptic region
*lateral hypothalamic area
*mammillary complex
*supramammillary region
*ventral tegmental area
*mesencephalic raphe nuclei

---

of the ACC, fimbria, and perhaps supracallosal fibers the major cholinergic innervation of the hippocampal formation (Dekker *et al.*, 1991; Butcher and Semba, 1989; Mesulam, 1988; Fibiger, 1982). Moreover, the cholinergic cell groups of the basal forebrain can be considered as a telencephalic extension of the brain-stem reticular formation and also as a direct extension of basomedial limbic cortex. This duality may account for their role in arousal and memory.

Non-cholinergic Neurotransmitters

Experiments based on retrogradely transported horseradish peroxidase and perikaryal cholinergic markers have shown that only about half of the projections from the SR to the hippocampal formation arise from cholinergic Ch1/Ch2 neurons. The septo-hippocampal pathway is therefore not uniformly cholinergic. Of special interest are GABAergic projection neurons (Amaral and Kurtz, 1985; Senut *et al.*, 1989). Anatomical, neurochemical and neurophysiological evidence indicates that many systems impinge indirectly on the septohippocampal projection via intraseptal GABAergic neurons. The latter exert potent and complex influences on intrinsic septal neurons and septohippocampal efferents (Jacab and Leranth, 1990).

Other neurotransmitter systems may also play a role in addition to or modulating the glutamergic, cholinergic, GABAergic, and β-noradrenergic synapses. Serotoninergic, dopaminergic, and various peptidergic fibers terminate upon the septum. Recently galanin has received much attention as a potential cotransmitter in cholinergic neurons of the basal forebrain in primates (Biesold *et al.*, 1989). A high concentration of galanin receptors in the septum and the co-localization of galanin with ACh in the MS suggests that galanin may act locally in the MS. The functional consequences of such galanin transmission in the SR are unknown even though galanin seems to inhibit MS neural activity (Givens *et al.*, 1992).

However, there are obviously considerable intraspecies differences. Ch1–Ch2 neurons of the monkey, for instance, express galanin whereas this does not occur in the human brain (Kordower and Mufson, 1990).

Cholinergic-Dopaminergic Interaction

A principal site for interaction of cholinergic and dopaminergic systems appears to be the SR where dopamine (DA) ligands have been found to affect the activity of hippocampal cholinergic projections arising from the MS/DB complex (Robinson *et al.*, 1979). DA projections from the ventral tegmental area (VTA) to the SR have been demonstrated in rodents and humans (Gasper *et al.*, 1985). DA fibers from the VTA project to the LS where they interact possibly via a GABA interneuron with cholinergic fibers which arise from the MS and project to the hippocampus (Levin *et al.* 1990).

DA input to the septum has an inhibitory control over the firing of septohippocampal cholinergic neurons (Costa *et al.*, 1983). DA may also have interactive effects with ACh via its actions directly in the hippocampus. Noteworthy, DA concentrations in the hippocampus are relatively low compared with those in the septum (approx. 1:60) and are much lower than those in the striatum (approx. 1:900).

Major Fiber Tracts Traversing the Septal Region

The *FO* is a compact fiber bundle connecting the hippocampal formation with the hypothalamus and various other basal forebrain structures. At the level of the anterior thalamus the fornical corpus separates into two columns which curve ventrally in front of the interventricular foramen and caudal to the AC to enter the hypothalamic region. Immediately behind the interventricular foramen a considerable amount of fibers leave the column to pass backwards to the anterior thalamic nucleus and the bed nucleus of the stria terminalis. Other fibers split off just above the AC to constitute the small precommissural portion of the FO. The fornical columns as well as the precommissural FO lie within the SR (see section "Introductory Remarks", p. 4). One should mention that the FO is a "neuromediator-rich" fiber bundle containing several classical neuromediators (e.g. acetylcholine/ACh, dopamine/DA, noradrenaline/NA, serotonin/5-HT, GABA, glutamate) and a variety of neuropeptides and hormones (e.g. Cholecystokinin and ACTH).

The *stria terminalis* (ST) emerges from the caudo-medial aspect of the amygdaloid body from where it runs along the medial border of the caudate nucleus to the AC. With respect to the SR, the precommissural fibers of the ST descending in front of the AC and its commissural component that enters the AC are of particular relevance.

The ST is accompanied in its whole subependymal course by neurons, (the bed nucleus) which can be seen as a small rim of gray matter on its medial aspect. At the point where the ST approaches the AC, the bed nucleus expands into a sizable nuclear mass surrounding the AC. The bed nucleus of the ST as well as portions of the nucleus accumbens septi with which it is in direct continuity are part of the so-called "extended amygdala" (Heimer and Alheid, 1991). The ST is composed of both amygdalofugal and amygdalopetal fibers. It contains a great many of neuromediators, in particular neuropeptides and hormones.

The *medial forebrain bundle* (MFB), composed of loosely arranged, mostly thin fibers, extends from the precommissural septum to the tegmental midbrain area. It is a major ascending and descending link between a variety of brain stem centers (among them noradrenergic, dopaminergic and serotoninergic cell groups as well as the ventrolateral reticular area and the dorsal vagal complex) and the (anterior component of the) basal forebrain. A majority of fibers from these various brain stem centers travel in the lateral hypothalamus and through the bottleneck in the SR to reach their respective cortical target areas. A major group of noradrenergic and serotonergic fibers, for instance, traverses the SR and encircles the corpus callosum to innervate the neocortex and the hippocampal formation.

The *AC*, which crosses the midline just posterior to the precommissural septum, is the commissure of the palaeocortex, the amygdaloid bodies, the olfactory bulbs ("decussatio olfactoria"), but it also contains fibers of neocortical origin. In monkeys, neocortical fibers originate from and terminate in relatively ample portions of the temporal and frontal lobes (Jouandet *et al.*, 1984; Jouandet and Gazzaniga, 1979), and their terminals are adjacent to, but probably do not overlap with those of callosal afferents to the same territories. The position of their cell bodies and the distribution of their terminals in the opposite cortex indicate that AC neurons as callosal neurons perform functions similar to those of associative neurons that make medium and long-range connections within each cortex.

The AC seems to be one of the most variable structures in the brain; it may have as much as three or four times as great a diameter in some people as in others (Demeter *et al.*, 1988). It seems to play a much greater role in interhemispheric transmission in monkeys than in cats (Hamilton, 1982). And one might expect it to be even more important (being larger) in humans. Overproduction and elimination of AC axons during postnatal development in primates might contribute to individual variations in AC size correlated with a wide range of physical and behavioral differences (LaMantia and Rakic, 1994).

Although the human AC is only 1/100 the size of the corpus callosum, we can appreciate how significant it might be when we consider the wealth of information conveyed over one optic nerve, the diameter of which is about the same as that of the AC (Bogen, 1993).

The *anterior thalamic peduncle* may contribute to the SR with a small number of fibers that form reciprocal connections between various thalamic nuclei (in particular the magnocellular and dorsal portion of the mediodorsal nuclei), BA 25 and the precommissural septum. The anterior thalamic peduncle breaks away from the anterior limb of the internal capsule.

Arterial Territories within the Septal Area

The anatomical details regarding the vascularization of the septal area are based on several sources: Lazorthes *et al.* (1976), Crowell and Morawetz (1977), Yasargil (1984), Ghika *et al.* (1990), and Vincentelli *et al.* (1991).

The Anterior Communicating Artery

The ACoA artery is a short artery which unites the two anterior cerebral arteries (ACA) in the lamina terminalis cistern to provide an important anastomotic channel for collateral circulation through the circle of Willis. It is commonly between 0.1 and 3 mm long. Its normal caliber is between 1.0 and 3.0 mm, but hypoplastic (0.1–1.0 mm) and hyperplastic (>3 mm) vessels are frequently seen. Aplasia of the ACoA was not observed either in the cadaver dissections or operative cases but extreme hypoplasia (<0.1 mm) was seen in rare cases. In one cadaver brain the two anterior cerebral arteries were fused in the prechiasmatic region.

This artery as well as the adjoining A1 and A2-segments of the ACA are common sites of anomalies of the arterial circle. The ACoA often retains its embryonic multichannel vascular form including fenestrations, duplications, triplications, reticular patterns, loops and bridges.

The fetal type shows the ACoA equivalent in caliber to the A1 segment and a large median callosal artery is present. In the transitional type ACoA is smaller than the A1 segment and the median callosal artery is also small. The adult type is characterized by an ACoA caliber which is less than one third of that of the A1 segment. (De Vrièse, 1904/1905).

Branches of the ACoA

Crowell and Morawetz (1977) first reported the constant presence of perforators arising from the ACoA ranging from 3 to 13 ($N = 10$). Vincentelli *et al.* (1991) confirmed the assertion ($N = 60$). Earlier studies had reported branches in only less than 50 % of cases. Some had denied their very existence, others (e.g. Lazorthes *et al.*, 1976) found a median callosal artery as the only branch arising from the ACoA.

The average number of the perforating branches of the ACoA is 4.1+/– 1.8 (range 1–11). The diameter of 40 % of the branches ranges from 250 to 500 μm, for 60 % the diameter is less than 250 μm. Frequently a larger trunk of about 1 mm diameter, the median callosal artery, is accompanied by several microbranches or the main trunk itself divides into many small branches. Microradiograms confirm a postero-superior direction of the ACoA branches. Apparently, there are no laterally directed branches, similar to the recurrent artery of Heubner. The angle between the A2 segment of the ACA and the ACoA branches have an average value of 96° (range 90 to 120° in 70 % of cases) allowing in most cases a clip application for ACoA aneurysms perpendicular to the A2 segment (Vincentelli *et al.*, 1991).

Supply Area of the ACoA Branches

Based on various material it seems reasonable to assume that the middle portion of the AC, the fornical columns and the septal nuclei including the MS/DB complex are supplied by ACoA perforators in the vast majority of cases. In more than 40 % of cases in the study of Vincentelli *et al.* (1991) ACoA branches additionally vascularized the cortical region of BA 25. In a few cases (13 %) the vascular territory extended beyond the genu of the corpus callosum. Likewise, an exclusive supply of the lamina terminalis and the hypothalamus seemed a rather infrequent case (12 %).

Thus, ACoA perforators are best qualified as "septo-commissural" arteries rather than hypothalamic. In addition, one should emphasize that the substantia innomminata including the major portion of the basal nucleus of Meynert is not perfused by ACoA branches.

The Septal Region in Animal Research

Considerable evidence has been accumulated from animal studies (in particular from rodents) indicating that the septum verum as well as its septohippocampal and septoentorhinal projection (Mizumori *et al.*, 1992) seems a critical substrate of (working/episodic) memory. Originating in the MS, this projection is the dorsomedial-most extension of the magnocellular basal nucleus (of Meynert). Particular attention has been paid to septo-hippocampal interactions because of the reciprocal interconnections between the septum and the hippocampus and the similarity in behavioral deficits associated with their manipulation (Gray, 1987). Electrical or pharmacological modulation of septal activity alters neurophysiological parameters in the hippocampus and disrupts the performance of behavioural tasks dependent on hippocampal integrity. The importance of such modulation may depend upon the demands made on the system, i.e. its value increasing with greater processing demands. Future research will need to evaluate the relationship between increasing task demands and septohippocampal neuronal activity (Chrobak and Napier, 1992).

Septal Lesions and Hippocampal Theta Activity

Lesions of the MS but not of the LS deplete most of the hippocampal cholinergic activity (Wieraszko and Oderfeld-Nowak, 1977). As can be seen from electroencephalographic recordings MS lesions abolished cholinergic theta activity in both the hippocampal CA1 pyramidal cell field and the dentate gyrus. In most MS rats the damage extended ventrally to include the vertical limb of the DB. Unlike MS lesions LS lesions have little effect on hippocampal theta activity (M'Harzi and Jarrard, 1992). In several LS animals the ventral corpus callosum and/or septofimbrial nuclei were slightly damaged, but hippocampal theta was normal in all subjects of this group.

Superimposing an artificial stimulating ("theta-like") rhythm to the hippocampus of rats with prior lesion of the SR, during testing in the Morris water maze improves performance in a test of working memory. This lends support to the view that intrinsic rhythmic activity may play an important role in normal physiology, and in certain disease states (Turnbull *et al.*, 1994).

Electrical Stimulation of the Medial Septum

Post-training MS electrical stimulation facilitates subsequent retention of various memory tasks. It has been suggested that activation of this part of the septohippocampal system may facilitate retroactive interference processes involved in working memory, leading thereby to better memorisation of this changing situation (Galey and Jaffard, 1992).

The effects of focal electrical stimulation of the MS on regional cerebral blood flow (rCBF) were examined in rats using the ^{14}C-Iodoantipyrine method (Adachi *et al.*, 1990; Cao *et al.*, 1989). The electrical stimulation produced significant increases in bilateral hippocampal rCBFs together with an increased release of ACh whereas rCBFs in other brain regions were not influenced. The finding of bilateral responses following unilateral stimulation seems to be due to the spread of currents from the MS controlateral to the stimulated nucleus. What is more, the rCBF responses were restricted to regions that receive cholinergic projections from the MS. Conversely, the stimulation of the unilateral basal nucleus did not influence the hippocampus but produced significant increases in frontal, parietal, and occipital cortical blood flows in the hemisphere ipsilateral to the stimulated basal nucleus (Adachi *et al.*, 1990).

The Medial Septum in Aged Animals

The study of Stroessner-Johnson *et al.* (1992) found a 19 % decrease in the number of ChAT-positive cells in aged monkeys across all rostrocaudal levels of the MS. This loss was regionally selective and ranged from a low of 6 % rostrally to 41 % caudally. Interestingly, changes in the ChAT-positive cells failed to distinguish between memory impaired and unimpaired aged subjects. Thus, it would appear that a decrease in cell number alone is not sufficient to produce significant (recognition) memory impairment in monkeys.

These results do not fit in with studies in aged rodents likewise demonstrating a substantial loss of cholinergic cells in the MS. In these cases, changes were most pronounced among subjects that exhibited robust deficits on learning and memory tasks that are dependent on the functional integrity of the hippocampal formation. In the Morris water maze, for example, age-related memory and learning deficits were correlated with both the number and size of cholinergic cells in the MS (Fischer *et al.*, 1989).

Although relatively few investigations have specifically analyzed the MS in the aging human brain, there is some evidence (de Lacalle *et al.*,

1991) that loss of cholinergic cells is most pronounced not in the MS but rather at caudal levels of the basal nucleus.

Septal Lesions and Cognition

A great variety of studies support the hypothesis that the MS is necessary for the maintenance of spatial memories in rodents. Damage to MS neurons or their hippocampal projections produce severe and permanent spatial memory deficits in rats that cannot be restored through training (Janis *et al.*, 1994). Damage to the MS, for instance, has been shown to disrupt spatial mapping in the Morris water tank (Kelsey and Landry, 1988), acquisition of the radial arm maze task (Hepler *et al.*, 1985; Fukuda *et al.*, 1993), spatial delayed-nonmatch-to-sample (DNMTS) in a T-maze (Hepler *et al.*, 1985), and spatial delayed alternation in a two-lever operant chamber (Numan and Quaranta, 1990). The study of Kelsey and Vargas (1993) underlines that damage to the septohippocampal system disrupts spatial more than it disrupts nonspatial memory processes.

Impairments in memory have been quite subtle following similar lesions in monkeys. Ibotenic acid injections in the MS/DB complex, and nucleus basalis of Meynert in cynomolgus monkeys, using a large series of cognitive tasks that examined different mnemonic and attentional abilities suggest that the primate basal forebrain may be more involved in attentional than mnemonic processes. For instance, these lesions did not impair accuracy in DNMTS, delayed response, visual or spatial discriminations (Voytko *et al.*, 1994). In sum, the more selective the (nuclear) basal forebrain lesion the more subtle is obviously the memory impairment.

Intraseptal Drug Manipulation

The MS in particular seems sensitive to the effect of various drugs on memory processes (Izquierdo *et al.*, 1992). Alterations in the acquisition or performance of behavioral tasks dependent on hippocampal integrity have been reported following pharmacological manipulations within the septum suggesting that these effects may be mediated by an alteration of septohippocampal afferents. Intraseptal manipulations will obviously disrupt both septohippocampal cholinergic and GABAergic projections. Disruption of either, based upon their connectivity to hippocampal circuitry would appear sufficient to disrupt physiological processes with the hippocampal and entorhinal cortices that seem to serve as neural substrates for (working and episodic) memory.

Intraseptal infusion of various agents can influence memory storage, maintenance or retrieval processes, among them β-endorphin, naloxone (Bostock *et al.*, 1989), muscimol, scopolamine, oxotremorine (Pang *et al.*, 1993), neuropeptide Y (Flood *et al.*, 1989), substance P (Staubli and

Huston, 1980), the M_1 antagonist pirenzepine (Messer Jr. *et al.*, 1990), NMDA (Murtha and Pappas, 1994), tetracaine (Givens and Olton, 1994), colchicine (Barone *et al.*, 1991), and anti-nerve growth factor antibody (Nitta *et al.*, 1993).

Intraseptal infusion of the GABAergic agonist muscimol produces alterations of cholinergic indices and theta activity within the hippocampus and disrupts performance of mnemonic tasks. Interestingly, intraseptal administration of the GABAergic antagonist bicuculline can induce a similar effect as muscimol. These findings suggest that either activation or blockade of intraseptal GABA receptors is sufficient to disrupt (working/episodic) memory processes. The impairment associated with both agonist and antagonist presumably reflects a disruption of intraseptal GABAergic communication and potentially the ability of septal afferents to regulate the activity of the septohippocampal projection.

Direct infusions of tetracaine and scopolamine into the septum reduce the power of hippocampal theta and impair choice accuracy in a working memory (i.e. continuous conditional discrimination) task. The magnitude of both effects was greater for larger doses and steadily decreased over time after the infusion (Givens and Olton, 1994).

Intraseptal infusion of the muscarinic agonist oxotremorine, which excites MS neurons, improves memory in aged rats. There is some evidence that oxotremorine enhances memory in aged rats through mechanisms other than enhancement of long-term potentiation in the dentate gyrus of the hippocampal formation (Pang *et al.*, 1993).

Local infusions of the DA antagonist haloperidol into the septum increases the ACh turnover in the hippocampus but do not affect ACh turnover in the cortex (Robinson *et al.*, 1979). In mice haloperidol causes an immediate and long-lasting increase in high-affinity choline uptake in the hippocampus which is accompanied by increased hippocampal CA1 pyramidal cell excitability (Durkin *et al.*, 1986). The finding that intraseptal application of haloperidol causes enhanced ACh release (and facilitates extinction of a conditioned response) is evidence in favor of the SR as a critical site for DA-ACh interactions (important at least for radial-arm maze performance).

Finally, the direct infusion into the rat's septum of an anti-nerve growth factor monoclonal antibody causes very severe damage to the hippocampal cholinergic system. It produces a dysfunction of memory and decereases ChAT activity and AChE staining in the hippocampus (Nitta *et al.*, 1993).

Lesions of Fiber Tracts Traversing the Septal Region

The animal literature on the *fornices* leaves one with the impression that the FO may be a relatively less important conduit of hippocampal afferent and efferent projections in primates than, for instance, in rodents. This might in part be due to the fact that in rodents 90 % of the cholinergic innervation of the hippocampal formation arrives via the FO and transection of this fiber bundle produces a nearly complete cholinergic deafferentation of the hippocampus whereas in primates the FO carries much less of the cholinergic input, and a more significant ventral cholinergic pathway through the amygdaloid body and the external capsule is observed.

One promising approach to understanding the anatomy of amnesia is afforded by the recent development of an animal model of human amnesia in the monkey (Mishkin, 1982). The model has relied especially on the DNMTS task, an object-recognition memory task that is sensitive to human amnesia (Squire *et al.*, 1988) Monkeys with bilateral lesions of the hippocampal formation are impaired on this object-recognition task (Zola-Morgan and Squire, 1986). Another study of the San Diego group (Zola-Morgan *et al.*, 1989) revealed that bilateral FO transection as well as mammillary lesions in monkeys produced only transient memory impairment. The aninmals were impaired only on the first DNMTS task administered after surgery. However, they performed all the other tasks normally and were unimpaired when the DNMTS task was readministerd 18 months after surgery. On the basis of these findings it seems unlikely that similar damage in humans can cause a severe or permanent amnesia.

Although performance on DNMTS and kindred tasks are intact following FO transection monkeys are impaired, for instance, in remembering the spatial arrangements of objects in artificially constructed as well as in complex naturalistic scenes (Gaffan and Harrison, 1989; Gaffan, 1994). The apparent contradiction between earlier findings of unimpaired object discrimination learning could be resolved by taking into account that the monkeys had already acquired many and varied long-term visual memories before they performed the object discrimination learning task. In this respect they offered a better analogue to the conditions of human memory than is offered by experimentally naive monkeys.

With respect to the *AC* severe memory deficit in monkey can be produced by section of the AC (with corpus callosum left largely intact) if this has been preceded by two other ablations: inferior temporal cortex on one side and amygdala-hippocampus on the other (Mishkin and Phillips, 1990).

Section of the ST, the main afferent-efferent pathway of the amygdaloid body attenuates the effect of β-endorphin, naloxone, and epinephrine on memory. Similar lesions attenuate the effect of systematic oxotremorine and atropine, suggesting that the amygdaloid body is also involved in the memory-modulating effects of drugs active upon cholinergic muscarinic receptors (Izquierdo *et al.*, 1992).

The Septal Region in Human Research

There are only a few pathological conditions producing focal brain lesions restricted to the SR region. Among them ruptured aneurysms of the anterior communicating artery (ACoA) are most frequent, followed at a considerable distance by brain tumours, traumatic lesions, and other vascular accidents to ACoA branches mostly of unknown origin. Our comprehensive review of hitherto published cases with SR lesions focuses on memory dysfunctions and the functional neuroanatomy of SR amnesia.

Aneurysms of the Anterior Communicating Artery

The ACoA is a typical site of cerebral aneurysms that may rupture and produce subarachnoid hemorrhage. Since advances in microsurgical techniques and intensive medical care have considerably increased the chances of acute phase survival (Yasargil, 1984; Appuzzo, 1993) these patients are frequently seen in neurorehabilitation units. Brain damage in ACoA aneurysm patients may be due to (1) extra-/intracerebral hemorrhages, (2) ischemic lesions, and (3) CSF blockade (McCormick, 1984). It may also be due to side-effects of neurosurgical intervention. The most relevant pathophysiological mechanism seems to be cerebral *vasospasm* caused by vasoconstricting effects of oxyhemoglobin and other blood components (Findlay *et al.*, 1991). This feared complication of subarachnoid hemorrhage may occur up to 3 weeks after aneurysm rupture (Ohno *et al.*, 1991) and is primarily responsible for ischemic lesions especially in the supply area of the anterior cerebral arteries including the branches supplying the SR (see section “Arterial Territories”, p. 12). In addition, lesions of basal forebrain structures may cause functional deactivation of interacting cortical structures. According to the orientation of subcortico-cortical projections such effects can also be expected to affect memory-relevant frontal and temporal lobe structures (Volpe *et al.*, 1984; Rousseaux *et al.*, 1994).

Ruptur and repair of ACoA aneurysms may result in a variety of behavioral and cognitive disturbances that are not necessarily manifested in all patients (DeLuca, 1993; DeLuca and Diamond, 1995). The classical *ACoA syndrome* with amnesia, confabulation, and personality changes is a characteristic, but not representative symptom constellation. The latter, in particular, are only poorly defined and may often be reduced to other cognitive or affective disorders such as apathy or unawareness of deficits. It remains true, however, that memory deficits is a core problem in patients with ACoA aneurysm. In order to specify them in more detail we at first review the relevant neurosurgical outcome studies and then proceed to the discussion of single case studies or series of patients with amnesia due to ACoA aneurysms.

Neurosurgical Outcome Studies

Outcome studies, initiated by neurosurgeons, have the basic aim to evaluate and optimize treatment protocols. The main results of 17 studies including 504 patients with ruptured and repaired aneurysms of the ACoA are summarized in Table 3. The first studies were retrospective and used rather crude outcome criteria. More recent studies included control groups and applied standardized batteries of neuropsychological tests at fixed days for follow-up measurement.

The rate of persistent memory deficits after ACoA aneurysm varied widely between 3 and 83 % of all patients. Some studies presenting an all too optimistic view of the problem are of limited value because follow-up intervals were too short and memory functions tested inadequately. On the other hand, poor cognitive outcome in ACoA aneurysm patients was reported from a relatively small group of preselected subjects concentrating in rehabilitation units. In this context, it should be emphasized that a good neurological outcome indicated, for instance, by the Glasgow Outcome Scale, does not exclude persisting neuropsychological deficits (Hütter and Gilsbach, 1993).

It is safe to say that more than one third of all patients surviving rupture and repair of ACoA aneurysms do so without chronic memory problems. *Risk factors* for amnesia seem to be (1) late surgery (Laiacona *et al.*, 1989), (2) old age (Säveland *et al.*, 1986), (3) neuroradiologically documented vasospasm of ACoA and neighbouring arteries (Larsson *et al.*, 1989; Richardson, 1991), (4) combined lesions with striatal involvement (Irle *et al.*, 1992), and (5) "trapping" the ACoA aneurysm (Gade, 1982).

Noteworthy, most studies mentioned above could not find a close association of aneurysm location (as regards the anterior circle of Willis) and cognitive outcome measures, whereas cognitive deficits seemed closely related to focal/global vasospasm, or respectively global/diffuse tissue damage after subarachnoid hemorrhage (Ogden *et al.*, 1990; 1993; Tidswell *et al.*, 1995).

The time interval between subarachnoid hemorrhage and memory assessment ranged from one week to several years both between and within studies. Hence, the time course of the ACoA syndrome can only roughly be estimated. In the acute phase (week 1 to 6) after surgery neuropsychological memory assessment is hardly valid due to both medical constraints and globally reduced cognitive powers. The initial period may be dominated by a confusional state including disorientation (Lipowski, 1990) and (productive) confabulations (DeLuca, 1993; Fischer *et al.*, 1995). On the other hand, cognitive assessment in the postacute stage (month 2 to 6) tends to be unreliable because the patients' handicaps in everyday life are not yet fully recognizable.

Table 3. *Aneurysms of the Anterior Communicating Artery—Neurosurgical Outcome Studies*

Study	*n*	Etiology	TSL [months]	Persistent memory and/or cognitive deficits	Comment(s)
Lindqvist/Norlén, 1966	**33**	**ACoA aneurysm/SAH**	<6	15 %	short follow-up
Logue *et al.*, 1968	**79**	**ACoA aneurysm/SAH**	40 (7–101)	9–56 %	good functional outcome (56% back to work)
Gade, 1982	**48**	**ACoA aneurysm/SAH**	3 + 24	31 %	more memory deficits after damage to perforating ACoA branches, no improvement in follow-up
Teissier du Cros/Lhermitte, 1984	**32**	**ACoA aneurysm/SAH**	(12–50)	3–38 %	more memory deficits after gyrus rectus resection
Ljunggren *et al.*, 1985 Säveland *et al.*, 1986	**15** 25	**ACoA aneurysm/SAH** other SAH	19 (14–84)	46–83 %	more cognitive deficits in old age patients
Bornstein *et al.*, 1987	**17** 29	**ACoA aneurysm/SAH** other SAH	27 (1–66)	24–59 %	more cognitive deficits after ACoA aneurysms
Fasanaro *et al.*, 1987	**10**	**ACoA aneurysm/SAH**	12 (10–14)	60 %	
Desantis *et al.*, 1989; Laiacona *et al.*, 1989	**43** 71	**ACoA aneurysm/SAH** other aneurysms	46 (7–115)	23–58 %	more cognitive deficits after late surgery, no influences of aneurysm location
Larsson *et al.*, 1989	**50** 169	**ACoA aneurysm/SAH** other SAH	84 (24–168)	23–52 %	more memory deficits after vasospasm and left ACoA aneurysms, no influences of lesion size
Maurice-Williams *et al.*, 1991	**14** 13	**ACoA aneurysm/SAH** other SAH	(12–16)	?	no memory deficits

Table 3 (*continued*)

Study	*n*	Etiology	TSL [months]	Persistent memory and/or cognitive deficits	Comment(s)
Richardson, 1989; 1991	**24**	**ACoA aneurysm/SAH**	2.0 + 5.7	?	more memory deficits after vasospasm, no influences of aneurysm location
	52	other SAH			
Tarel *et al.*, 1990	**22**	**ACoA aneurysm/SAH**	5 (3–10)	23–68 %	
DeLuca/Cicerone, 1991	**14**	**ACoA aneurysm/SAH**	3.3	79 %	confabulations more frequent in ACoA patients
DeLuca 1992, 1993	13	other ICH	(1–4)		
Stenhouse *et al.*, 1991	**27**	**ACoA aneurysm/SAH**	54 (12–84)	26–59 %	
Hütter/Gilsbach, 1992	**18**	**ACoA aneurysm/SAH**	34	30–60 %	more memory deficits in aneurysmal SAH
Hütter *et al.*, 1994	30	SAH			
Irle *et al.*, 1992	**30**	**ACoA aneurysm/SAH**	29	15–60 %	more memory deficits after combined lesions with striatal involvement
	27	aneurysms without SAH			
Ogden *et al.*, 1993	**22**	**ACoA aneurysm/SAH**	2.5 + 12	35 %	no influences of aneurysm location on memory functions
	58	other aneurysms			
Tidswell *et al.*, 1995	**20**	**ACoA aneurysm/SAH**	27	46 %	no influences of aneurysm location on memory functions
	17	other SAH	(6–45)		

ACoA anterior communicating artery; *ICH* intracranial hemmorrhages; *SAH* subarachnoid haemorrhage; *TSL* time since lesion (SAH to memory assessment)

Neuropsychological Case Studies

A second group of studies deal with detailed neuropsychological findings in single patients or series of cases with memory deficits after ACoA aneurysm as the main inclusion criteria. Besides ACoA cases, there are a few cases where the SR was more or less exclusively damaged in the course of arterio-venous malformations or other cerebrovascular accidents to ACoA branches (Damasio *et al.*, 1985; von Cramon *et al.*, 1993; Tranel *et al.*, 1994). Table 4 summarizes the main results of 18 studies with 93 patients (in the case series age and memory quotients of the Wechsler Memory Scale are given as mean values). Table 5 gives short definitions of memory aspects mentioned in those studies (Bauer *et al.*, 1993; Eysenck *et al.*, 1990).

The most consistent neuropsychological finding is a mild to moderate *anterograde amnesia* whereas retrograde amnesia is mainly seen in acute patients and tends to remit during the course of recovery. However, some patients remain severely amnestic in both temporal domains. Active (free) recall seems more impaired than recognition of newly learned material and delayed recall to be more affected than the immediate reproduction of learned items. In contrast to obvious explicit memory dysfunctions, implicit memory, measured as the ability to learn complex motor (Bondi *et al.*, 1993; Tranel *et al.*, 1994) or arithmetic skills (Milberg *et al.*, 1988) remains largely spared. The memory deficits also contrast with largely preserved intellectual and attentional powers.

The patient of Delbecq-Derouesné *et al.* (1990) does not follow this rule. He presented with a reverse pattern of poor recognition and preserved recall. This might be due to additional bifrontal lesions which may also account for the occurrence of spontaneous confabulations (Kapur and Coughlan, 1980; Fischer *et al.*, 1995). Frontal lobe damage or lesions of the caudate nucleus with frontal lobe deactivation are frequent findings in patients with ACoA aneurysm and may be responsible for a wide range of behavioral disturbances, namely executive dysfunctions, apathy, increased distractibility, or unawareness of deficits (Van der Linden *et al.*, 1993; von Cramon *et al.*, 1993; Phillips *et al.*, 1987; Alexander and Freedman, 1984). At least some of these symptoms may also be attributed to the interruption of ascending monoaminergic and in particular dopaminergic projections traversing the SR (Müller and von Cramon, 1994).

Basal Forebrain Tumors

In a small number of amnestic patients following neurosurgical removal of small brain tumors in the SR memory functions have been thoroughly documented (Table 6). Not surprisingly, we find a test profile largely comparable with the amnestic ACoA group. A somewhat unexpected finding,

Table 4. *Memory Deficits After Basal Forebrain Vascular Lesions—Neuropsychological Studies*

Study	*n* [age]	etiology	TSL [months]	Memory deficits	WMS(-R) MQ	other observations
Talland *et al.*, 1967	2 [29.5]	ACoA aneurysm/SAH	29	chronic amnesia (antero- > retrograde)	89.0	lack of concern and spontaneity
Volpe/Hirst, 1983	2 [43.0]	ACoA aneurysm/SAH	18	free recall severely impaired, sensitivity to interference	85.0	disorientation and confusion only in the early stage
Alexander/Freedman, 1984	11 [45.0]	ACoA aneurysm/SAH, ACA infarctions	28 (2–132)	anterograde amnesia	82.5	flat affect and apathy frequent, poor word list generation
Eslinger/Damasio, 1984 Damasio *et al.*, 1985	4 1 [46.2]	ACoA aneurysm/SAH basal forebrain AVM	? (1–4)	global (antero-/retrograde) amnesia, impaired retrieval, poor temporal ordering of memory content, confabulations	86.6	"frontal" behavior disturbances
Vilkki, 1985	5 [38.0]	ACoA aneurysm/SAH	3 + 11 (1–18)	heterogeneous amnestic syndromes	–	restlessness and disorientation in the acute stage
Steinman/Bigler, 1986	7 [44.1]	ACoA aneurysm/SAH, ACA infarctions	38 (11–108)	deficits in short-term memory with comparatively intact remote memory	83.0	additional frontal lesions; marked personality changes

Phillips *et al.*, 1987	1 [37]	ACoA aneurysm/SAH	6 + 34	anterograde amnesia	84	apathy, altered arousal
Milberg *et al.*, 1988	2 [41.5]	ACoA aneurysm/SAH	2 + 9	severe (global) amnesia, arithmetic skill learning intact	75.5 + 86.0	
Parkin *et al.*, 1988	1 [42]	ACoA aneurysm/SAH	25–27	sensitivity to inteference, pour source retrieval	89	left frontal white matter lesion
Delbecq-Derouesné *et al.*, 1990	1 [54]	ACoA aneurysm/SAH	96–120	poor recognition, recall preserved, confabulations	94	additional bifrontal lesions; unawareness for memory deficits
Gade/Mortensen, 1990	20 [50.0]	ACoA aneurysm/SAH	24 (1–73)	retrograde amnesia (not different from dementia or other amnesias)	–	
Parkin/Barry, 1991	1 [46]	ACoA aneurysm/SAH, ACA infarction left	1 (?)	delayed recall impaired	93	executive dysfunctions, alien hand sign
Van der Linden *et al.*, 1992; 1993	8 [50.3]	ACoA aneurysm/SAH	16 (4–48)	anterograde amnesia, intrusive errors (proactive interfer-ence)	?	executive dysfunctions, frontal lobe damage in 6 patients
Bondi *et al.*, 1993	3 [46.3]	ACoA aneurysm/SAH	35 (6–90)	explicit memory impaired, implicit memory (skill learning and lexical priming) intact	59.0	all patients with additional cortical/ subcortical lesions

Table 4 (*continued*)

Study	*n* [age]	etiology	TSL [months]	Memory deficits	WMS(-R) MQ	other observations
von Cramon *et al.*, 1993	1 [61]	APA + RAH infarction	4–7	impaired free recall (long-term), good recognition memory, poor usage of learning strategies	89	left head of caudate nucleus damaged; increased distractibility
Hanley *et al.*, 1994	1 [42]	ACoA aneurysm	6–14	impaired recall of verbal material, excellent recognition memory	69	left caudate nucleus damaged
Tranel *et al.*, 1994	10 3 [52.0]	ACoA aneurysm/SAH other cerebrovascular diseases	55.5 (12–144)	explicit memory impaired, implicit memory (sensori-motor skill learning) normal	84	
Fischer *et al.*, 1995	9 [48.2]	ACoA aneurysm/SAH	<4	anterograde amnesia	–	spontaneous confabulations after frontal lobe damage

ACA anterior cerebral artery; *ACoA* anterior communicating artery; *APA* anterior perforating arteries; *AVM* arterio-venous malformation; *ICV* internal cerebral vein; *BFB* basal forebrain; *RAH* Recurrent artery of Heubner; *SAH* subarachnoid hemorrhage; *TSL* time since lesion (SAH to memory assessment); *WMS(-R)* Wechsler Memory Scale (Revised), *MQ* Memory Quotient

Table 5. *Short Definitions of Neuropsychological Memory Terms*

Memory term	Short definition
amnesia	profound defect in learning of new material (*anterograde amnesia*) and in recall of material that was learned before the damaging event (*retrograde amnesia*)
anomia	failure to name objects or persons that have been recognized
confabulation	report of fallacious memories, not due to error or lying and usually in connection with amnesia
episodic memory	memory for concrete personal episodes or events dated in the subjective past
explicit (declarative) memory	knowledge to which an individual has conscious access and which can therefore be stated directly
implicit memory	knowledge which derives from previous experiences, but with enhancement occuring in the absence of conscious recollection
interference	tendency for prior learning to interfere with subsequent learning (*proactive interference*) and vice versa (*retroactive interference*) with typical intrusive errors (*intrusions*)
primary/secondary memory	short-term information that forms part of the psychological present (*primary memory*), whereas information in long-term (*secondary*) memory forms part of the psychological past
priming	improvement of recall or recognition when part of the learned information or details of the context of a learning situation are given as cues
procedural (skill) learning	learning of motor, perceptual, and cognitive skills such as how to handle a device or performing a calculation usually by repetition and automatisation
recall	process of active reproduction of learned material
recognition	discrimination of learned (old) items from (new) distractors
retrieval	remembering of material that has been encoded in a special context
working memory	active cognitive process involved in the transient storage and manipulation of short-term information

Table 6. *Memory Deficits After Basal Forebrain Tumors—Neuropsychological Studies*

Study	*n* [age]	Etiology / damaged structures	TSL [months]	Memory deficits	WMS(-R) MQ	Other observations
Berti *et al.*, 1990	1 [43]	subependynoma, postsurgical/septal region (lower part), anterior cingulate	<1	global (antero-/retrograde) amnesia	–	mild confabulations, little concern about memory impairment
Gaffan *et al.*, 1991; Hodges/Carpenter, 1991	2 [39.0]	colloid cyst, transcallosal removal/fornical columns bilateral	1–24	severe anterograde amnesia, recognition superior to recall	–	
Morris *et al.*, 1992; Chatterjee *et al.*, 1993	1 [31]	astrocytoma, postsurgical/diagonal band of Broca (and adjacent structures)	1 + 18	global (antero-/retrograde) amnesia	74 + 96	no memory improvement during physostigmine treatment
Laatsch *et al.*, 1994	1 [32]	oligodendroglioma	2	anterograde amnesia	–	alcohol abuse
Calabrese *et al.*, 1995	1 [14]	astrocytoma, postsurgical/fornical columns bilateral	?	anterograde amnesia, episodic memory impaired	56	
Jacobs *et al.*, 1995	1 [67]	brain tumor, postsurgical/inferior septal region, diagonal band of Broca, orbitofrontal cortex left, gyrus rectus	1(?) + 12	anterograde amnesia, anomia (famous faces)	66 + 84	

McMackin *et al.*, 1995	2 [43]	colloid cyst, transfrontal removal/fornical columns bilateral;	44	(anterograde) amnesia;	–
	2 [32]	colloid cyst, transcallosal removal/fornical column right	69	visuo-spatial memory impairment	–

TSL time since lesion (surgery to memory assessment); *WMS(-R)* Wechsler Memory Scale (Revised), *MQ* Memory Quotient however, is anomia for famous faces as reported by Jacobs *et al.* (1995). Of particular interest is the case of an amnestic patient suffering from a basal forebrain low-grade glioma that after its removal was said to have damaged the (cholinergic) right DB (see section "Precommissural Septum", p. 7) including the adjacent preoptic area, anterior hypothalamus, lamina terminalis and the paraterminal gyrus; the septal nuclei and the nucleus basalis of Meynert appeared to have been spared. Postsurgical memory deficit did not respond favourably to physostigmine, an acetylcholine enhancing substance, which might be explained by the non-cholinergic lesions and neurotransmitter deficits (Morris *et al.*, 1992; Chatterjee *et al.*, 1993).

Anterior Fornical Lesions

In earlier human cases, impaired as well as intact memory function has been reported following bilateral FO damage. In a series of 193 patients of whom 180 underwent anterior fornicotomy for the treatment of epilepsy, and 13 underwent removal of third ventricle colloid cysts, only 4 were reported to have persistent memory loss postoperatively and they were in the colloid cyst group (García-Bengochea and Friedman, 1987). However, the assessment of memory function in these historical cases was based on anecdotal reports or clinical observations and in no case a comprehensive neuropsychological assessment had been performed.

Gaffan's group (Gaffan and Gaffan, 1991) stressed the point that there are patients with severe and persistent amnesia resulting from selective damage to the FO following surgical removal of colloid cysts from the third ventricle. They observed impairments in object discrimination learning comparable to what they had found many times in monkeys (Gaffan *et al.*, 1991). The four cases reported by Hodges and Carpenter (1991) and McMackin *et al.* (1995) underline this assumption. All patients suffered from persistent anterograde amnesia following the transcallosal removal of third ventricle colloid cysts and bilateral interruptions of the fornical columns. According to well-known principles of lateralization the two patients of McMackin *et al.* (1995) with unilateral lesions of the right fornical column show only visuo-spatial memory impairments.

There are also a few reports on patients with penetrating head injuries damaging the SR. In a series of 15 veterans of the Vietnam Head Injury Study reported by Salazar *et al.* (1986) the main neuropsychological findings were deficits of episodic memory, reasoning and calculation despite of preserved intelligence, attentional and language functions. Another patient with amnesia after a gunshot injury to the basal forebrain was recently reported by D'Esposito *et al.* (1995). The authors claimed a bilateral fornix transection to be responsible for the memory deficits. However, these results contrast with the findings of Gale *et al.* (1993) indicating that fornix

Table 7. *Neuropsychology of Septal Region Amnesia*

Memory function/dysfunction	
primary/working memory	generally preserved
recognition	preserved
retrieval/recall	impaired, but less severe than in Korsakoff's and medial temporal lobe amnesia
retention	preserved
fast forgetting	needs further investigation
priming/procedural (skill) learning	preserved
remote memory	impaired in the acute stage, tends to remit during recovery with a temporal gradient
confabulations	frequent in acute phase (delirium), chronically only in patients with additional frontal lobe lesion

atrophy following traumatic brain injury does not relate systematically to neuropsychological outcome. Given the limitations inherent to *in vivo* "neuropathological analysis" by neuroimaging procedures the hitherto published material lacks convincing evidence that fornical lesions were truly exclusive. Conversely, it appears evident that with anterior (pre- and postcommissural) fornicotomy we are interfering with a relevant though perhaps minor part of the structural systems subserving memory functions.

Conclusions

Historically, the SR is the latest region in the human brain that has been identified to produce amnesia after focal brain damage. Compared to patients with Kosakoff's disease, diencephalic or mesial temporal lesions memory deficits due to SR lesions are generally less severe and obviously do not affect implicit (non-declarative) memory functions (Table 7). It remains to be evaluated whether damage to the nucleus accumbens, a complex nuclear structure bordering on the SR and located within the supply area of Heubner's artery, is required to additionally impede the (non-declarative) "habit" system as proposed by Petri and Mishkin (1994).

It is safe to say that amnesia due to SR lesions occurs independent of tissue damage to temporomesial and diencephalic structures. However, amnesia in these cases seems to result primarily from indirect effects the SR exerts on temporomesial and diencephalic memory-related structures as well as on neocortical areas.

The interruption of the "dorsal route" of the septo-hippocampal/entorhinal system (i.e. fibers travelling via the cingulate bundle, the longitudinal striae, and the FO) may have a major role herein. There is some evidence that circumscribed lesions of the septohippocampal system sparing the SR itself, nevertheless, produce a largely comparable memory deficit (Valenstein *et al.*, 1987; von Cramon and Schuri, 1992). Although the FO is the center-piece of the septo-hippocampal system (exclusive) fornical damage seems to produce a narrower deficit than is characteristic of amnesia due to hippocampal, diencephalic, and presumably even SR injury. Whether the interruption of the "ventral route" (i.e. fibers travelling from the SR through the amygdaloid complex to the anterior hippocampal formation) makes any difference in respect to the pattern and severity of explicit memory dysfunction is another point at issue.

Besides the septo-hippocampal system, various ascending mainly monoaminergic fiber pathways both innervating and traversing the SR may be relevant to the maintenance of explicit memory functions. DA input to the septum, for instance, seems to have an inhibitory control over the firing of septohippocampal cholinergic neurons.

In sum, it seems plausible that evident memory dysfunctions depend on a combination of nuclear and fiber lesions in the SR rather than on damage to a single structure.

References

Adachi T, Biesold D, Inanami O, Sato A (1990) Stimulation of the nucleus basalis of Meynert and substantia innominata produces widespread increases in cerebral blood flow in the frontal, parietal and occipital cortices. Brain Res 514: 163–166

Adachi T, Inanami O, Ohno K, Sato A (1990) Responses of regional cerebral blood flow following focal electrical stimulation of the nucleus basalis of Meynert and the medial septum using the (^{14}C) iodoantipyrine method in rats. Neurosci Lett 112: 263–268

Alexander MP, Freedman M (1984) Amnesia after anterior communicating artery aneurysm rupture. Neurology 34: 752–757

Amaral DG, Kurz J (1985) An analysis of the origins of the cholinergic and non-cholinergic septal projections to the hippocampal formation of the rat. J Comp Neurol 240: 37–59

Andy OJ, Stephan H (1968) The septum in the human brain. J Comp Neurol 133: 383–410

Appuzzo MLJ (ed) (1993) Brain surgery: complication avoidance and management. Churchill Livingstone, New York

Barone S Jr, Nanry KP, Mundy WR, McGinty JF, Tilson HA (1991) Spatial learning deficits are not solely due to cholinergic deficits following medial septal lesions with colchicine. Psychobiology 19: 41–50

Bauer RM, Tobias B, Valenstein E (1993) Amnesic disorders. In: Heilman KM, Valenstein E (eds) Clinical neuropsychology, 3rd edn. Oxford University, New York

Berti A, Arienta C, Papagno C (1990) A case of amnesia after excision of the septum pellucidum. J Neurol Neurosurg Psychiatry 53: 922–924
Biesold D, Bigl V, Arendt T (1989) In: Kewitz, Thomsen, Bickel (eds) Pharmacological intervention on central cholinergic mechanisms in senile dementia (Alzheimer's disease). Zuckschwerdt, München, pp 121–128
Bogen JE (1993) The callosal syndromes. In: Heilman KM, Valenstein E (eds) Clinical Neuropsychology, 3rd edn. Oxford University, New York, pp 337–407
Bondi MW, Kaszniak AW, Rapcsak SZ, Butters MA (1993) Implicit and explicit memory following anterior communicating artery aneurysm rupture. Brain Cogn 22: 213–229
Bornstein RA, Weir BKA, Petruk KC, Disney LB (1987) Neuropsychological function in patients after subarachnoid hemorrhage. Neurosurgery 21: 651–654
Bostock E, Gallagher M, King RA (1989) Effects of opioid microinjections into the medial septal area on spatial memory in rats. Behav Neurosci 103: 643–652
Butcher LL, Semba K (1989) Reassessing the cholinergic basal forebrain: nomenclature schemata and concepts. Trends Neurosci 12: 483–485
Calabrese P, Markowitsch HJ, Harders AG, Scholz M, Gehlen W (1995) Fornix damage and memory: a case report. Cortex 31: 555–564
Cao WH, Inaunami O, Sato A, Sato Y (1989) Stimulation of the septal complex increases local cerebral blood flow in the hippocampus in anaesthetized rats. Neurosci Lett 98: 39–44
Chatterjee A, Morris MK, Bowers D, Williamson DJ, Doty L, Heilman KM (1993) Cholinergic treatment of an amnestic man with a basal forebrain lesion: theoretical implications. J Neurol Neurosurg Psychiatry 56: 1282–1289
Chrobak JJ, Napier TC (1992) Antagonism of GABAergic transmission within the septum disrupts working/episodic memory in the rat. Neuroscience 47: 833–841
Costa E, Panula P, Thompson HK, Cheney DL (1983) The transsynaptic regulation of the septo-hippocampal cholinergic neurons. Life Sci 32: 165–179
von Cramon DY, Markowitsch HJ, Schuri U (1993) The possible contribution of the septal region to memory. Neuropsychologia 11: 1159–1180
von Cramon DY, Schuri U (1992) The septo-hippocampal pathways and their relevance to human memory: a case report. Cortex 28: 411–422
Crowell RM, Morawetz RB (1977) The anterior communicating artery has significant branches. Stroke 8: 272–273
Damasio AR, Graff-Radford NR, Eslinger PJ, Damasio H, Kassell N (1985) Amnesia following basal forebrain lesions. Arch Neurol 42: 263–271
Dekker JAM, Connor DJ, Thal LJ (1991) The role of cholinergic projections from the nucleus basalis in memory. Neurosci Behav Rev 15: 299–317
De Lacalle S, Iraizoz I, Gonzalo LM (1991) Differential changes in cell size and number in topographic subdivisions of human basal nucleus in normal aging. Neuroscience 43: 445–456
Delbecq-Derouesné J, Beauvois MF, Shallice T (1990) Preserved recall versus impaired recognition: a case study. Brain 113: 1045–1074
DeLuca J, Diamond BJ (1995) Aneurysms of the anterior communicating artery: a review of neuroanatomical and neuropsychological sequelae. J Clin Exp Neuropsychol 17: 100–121

DeLuca J (1993) Predicting neurobehavioral patterns following anterior communicating artery aneurysm. Cortex 29: 639–647

DeLuca J (1992) Cognitive dysfunction after aneurysms of the anterior communicating artery. J Clin Exp Neuropsychol 14: 924–934

DeLuca J, Cicerone KD (1991) Confabulation following aneurysm of the anterior communicating artery. Cortex 27: 17–423

Demeter S, Ringo JL, Doty RW (1988) Morphometric analysis of the human corpus callosum and anterior commissure. Hum Neurobiol 6: 219–226

D'Esposito M, Verfaellie M, Alexander MP, Katz DI (1995) Amnesia following traumatic bilateral fornix transection. Neurology 45: 1546–1550

Desantis A, Laiacona M, Barbarotto R, Basso A, Villani R, Spagnoli D, Capitani E (1989) Neuropsychological outcome of patients operated upon for an intracranial aneurysm: analysis of general prognostic factors and of the effects of the location of the aneurysm. J Neurol Neurosurg Psychiatry 52: 1135–1140

Devinsky O, Morrell MJ, Vogt BA (1995) Contributions of anterior cingulate cortex to behavior. Brain 118: 279–306

De Vrièse B (1904/1905) Sur la signification morphologique des artères cérébrales. Arch Biol 21: 357–457

Durkin T, Galey D, Micheau J, Beslon J, Jaffard R (1986) The effects of intraseptal injections of haloperidol in vivo on hippocampal cholinergic function in the mouse. Brain Res 376: 420–424

Eslinger P, Damasio AR (1984) Behavioral disturbances associated with rupture of anterior communicating artery aneurysm. Semin Neurol 4: 385–389

Eysenck MW, Ellis A, Hunt E, Johnson-Laird P (eds) (1990) The Blackwell dictionary of cognitive psychology. Blackwell, Oxford

Fasanaro AM, Valiani R, Russo G, Scarano E, De Falco R, Profeta G (1987) Memory performances after anterior communicating artery aneurysm surgery. Acta Neurol (Napoli) 11: 272–278

Fibiger HC (1982) The organization and some projections of cholinergic neurons of the mammalian forebrain. Brain Res Rev 4: 327–388

Findlay JM, Macdonald RL, Weir BKA (1991) Current concepts of pathophysiology and management of cerebral vasospasm following aneurysmal subarachnoid hemorrhage. Cerbrovasc Brain Metab Rev 3: 336–361

Fischer RS, Alexander MP, D'Esposito M, Otto R (1995) Neuropsychological and neuroanatomical correlates of confabulation. J Clin Exp Neuropsychol 17: 20–28

Fischer W, Gage FH, Björklund A (1989) Degenerative changes in forebrain cholinergic nuclei correlate with cognitive impairments in aged rats. Eur J Neurosci 1: 34–45

Flood JF, Baker ML, Hernandez EN, Morley JE (1989) Modulation of memory processing by neuropeptide Y varies with brain injection site. Brain Res 503: 73–82

Fukuda M, Masuda R, Ono T (1993) Contribution of monkey basal forebrain to learning and memory. In: Ono T (ed) Brain mechanisms of perception and memory: from neuron to Behavior. Oxford University, New York

Gade A, Mortensen EL (1990) Temporal gradient in the remote memory impairment of amnesic patients with lesions in the basal forebrain. Neuropsychologia 9: 985–1001

Gade A (1982) Amnesia after operations of the anterior communicating artery. Surg Neurol 18: 46–49

Gaffan D (1994) Scene-specific memory for objects: a model of episodic memory impairment in monkeys with fornix transection. J Cogn Neurosci 6: 305–320

Gaffan D, Gaffan EA (1991) Amnesia in man following transsection of the fornix: a review. Brain 114: 2611–2618

Gaffan D, Harrison S (1989) Place memory and scene memory: effects of fornix transection in the monkey. Exp Brain Res 74: 202–212

Gaffan EA, Gaffan D, Hodges JR (1991) Amnesia following damage to the left fornix and to other sites: a comparative study. Brain 114: 1297–1313

Gale SD, Burr RB, Bigler ED, Blatter D (1993) Fornix degeneration and memory in traumatic brain injury. Brain Res Bull 32: 345–349

Galey D, Jaffard R (1992). Post-training medial septal stimulation improves spatial information processing in BALB/c mice. Neurosci Lett 143: 87–90

García-Bengochea F, Friedman WA (1987) Persistent memory loss following section of the anterior fornix in humans: a historical review. Surg Neurol 27: 361–364

Gasper P, Berger B, Alvarez C, Vigny A, Henry JP (1985) Catecholaminergic innervation of the septal area in man: Immunocytochemical study using TH and DBH antibodies. J Comp Neurol 241: 12–33

Ghika JA, Bogousslavsky J, Regli F (1990) Deep perforators from the carotid system. Arch Neurol 47: 1097–1100

Givens B, Olton DS (1994) Local modulation of basal forebrain: effects on working and reference memory. J Neurosci 14: 3578–3587

Givens BS, Olton DS, Crawley JN (1992) Galanin in the medial septal area impairs working memory. Brain Res 582: 71–77

Gray JA (1987) The Neuropsychology of Anxiety: An enquiry into the functions of the septo-hippocampal system. Oxford University, New York

Hamilton CR (1982). Mechanisms of interocular equivalence. In: Ingle D, Goodale M, Mansfield R (eds) Advances in the analysis of visual behavior. MIT Press, Cambridge, pp 693–717

Hanley JR, Davies ADM, Downes JJ, Mayes AR (1994) Impaired recall of verbal material following rupture and repair of an anterior communicating artery aneurysm. Cogn Neuropsychol 11: 543–578

Heimer L, Alheid GF (1991). Piecing together the puzzle of basal forebrain anatomy. In: Napier TC, Kalivas PW, Hanin I (eds) The basal forebrain. Plenum, New York, pp 1–42

Hepler DJ, Olton DS, Wenk GL, Coyle JT (1985) Lesions in nucleus basalis magnocellularis and medial septal area of rats produce qualitatively similar memory imapirments. J Neurosci 5: 866–873

Hodges JR, Carpenter K (1991) Anterograde amnesia with fornix damage following removal of IIIrd ventricle colloid cyst. J Neurol Neurosurg Psychiatry 54: 633–638

Hütter BO, Gilsbach JM, Kretschmann I (1994) Is there a difference in cognitive deficits after aneurysmal subarachnoid haemorrhage and subarachnoid haemorrhage of unknown origin? Acta Neurochir (Wien) 127: 129–135

Hütter BO, Gilsbach JM (1993) Which neuropsychological deficits are hidden behind a good outcome (Glasgow = I) after aneurysmal subarachnoid hemorrhage? Neurosurgery 33: 999–1006

Hütter BO, Gilsbach JM (1992) Cognitive deficits after rupture and early repair of anterior communicating artery aneurysms. Acta Neurochir (Wien) 116: 6–13

Irle E, Wowra B, Kunert HJ, Hampl J, Kunze S (1992) Memory disturbances following anterior communicating artery rupture. Ann Neurol 31: 473–480

Izquierdo I, Da Cunha C, Rosat R, Jerusalinsky D, Ferreira MBC, Medina JH (1992) Neurotransmitter receptors involved in post-training memory processing by the amygdala, medial septum, and hippocampus of the rat. Behav Neural Biol 58: 16–26

Jacobs DH, Shuren J, Bowers D, Heilman KM (1995) Anomia in a patient with a basal forebrain lesion. Neuropsychiatry Neuropsychol Behav Neurol 8: 200–207

Jakab RL, Leranth C (1990) Catecholaminergic, GABAergic, and hippocamposeptal innervation of GABAergic somatospiny neurons in the rat lateral septal area. J Comp Neurol 302: 305–321

Janis LS, Bishop TW, Dunbar GL (1994) Medial septal lesions in rats produce permanent deficits for strategy selection in a spatial memory task. Behav Neurosci 108: 892–898

Jouandet ML, Garey LJ, Lipp HP (1984) Distribution of the cells of origin of the corpus callosum and anterior commissure in the marmoset monkey. Anat Embryol 169: 45–59

Jouandet ML, Gazzaniga MS (1979) Cortical field of origin of the anterior commissure of the rhesus monkey. Exp Neurol 66: 381–397

Kapur N, Coughlan AC (1980) Confabulation and frontal lobe dysfunction. J Neurol Neurosurg Psychiatry 43: 461–463

Kelsey JE, Vargas H (1993) Medial septal lesions disrupt spatial, but not nonspatial, working memory in rats. J Neurosci 10: 565–574

Kelsey JE, Landry BA (1988) Medial septal lesions disrupt spatial mapping ability in rats. Behav Neurosci 107: 565–574

Kordower JH, Mufson J (1990) Galanin-like immunoreactivity within the primate basal forebrain: differential staining patterns between humans and monkeys. J Compa Neurol 294: 281–292

Laatsch L, Hartman D, Stone J (1994) Transcallosal intraventricular tumour excision, alcohol abuse, and amnestic syndrome: a case study. J Neurol Neurosurg Psychiatry 57: 766–767

Laiacona M, De Santis A, Barbarotto R, Basso A, Spagnoli D, Capitani E (1989) Neuropsychological follow-up of patients operated for aneurysms of anterior communicating artery. Cortex 25: 261–273

LaMantia AS, Rakic P (1994) Axon overproduction and elimination in the anterior commissure of the developing rhesus monkey. J Comp Neurol 340: 328–336

Larsson G, Rönnberg J, Forssell Å, Nilsson LG, Lindberg M, Ängquist KA (1989) Verbal memory funcitons after subarachnoid haemorrhage determined by the localisation of the ruptured aneurysm. Br J Neurosurg 3: 549–560

Lazorthes G, Gouaze A, Salamon G (1976) Les artères centrales du cerveau. In: Vascularisation et circulation de l'encéphale. Masson, Paris, pp 154–182

Levin ED, McGurk SR, Rose JE, Butcher LL (1990) Cholinergic-dopaminergic interactions in cognitive performance. Behav Neural Biol 54: 271–299

Lindqvist G, Norlén G (1966) Korsakoff's syndrome after operation on ruptured aneurysm of the anterior communicating artery. Acta Psychiatr Scand 42: 24–34

Lipowski ZJ (1990) Delirium: acute confusional states. Oxford University, New York

Ljunggren B, Sonesson B, Säveland H, Brandt L (1985) Cognitive impairment and adjustment in patients without neurological deficits after aneurysmal SAH and early operation. J Neurosurg 62: 673–679

Logue V, Durward M, Pratt RTC, Piercy M, Nixon WLB (1968) The quality of survival after rupture and repair of an anterior cerebral aneurysm. Br J Psychiatry 114: 137–160

Mark LP, Daniels DL, Naidich TP, Hendrix LE, Maas E (1994) The septal area. American Journal of Neuroradiology 15: 273–276

Markowitsch HJ (1995) Anatomical basis of memory disorders. In: Gazzaniga MS (ed) The cognitive neurosciences. Bradford/MIT, Cambridge

Maurice-Williams RS, Willison JR, Hatfield R (1991) The cognitive and psychological sequelae of uncomplicated aneurysm surgery. J Neurol Neurosurg Psychiatry 54: 335–340

McCormick WF (1984) Pathology and pathogenesis of intracranial saccular aneurysms. Semin Neurol 4: 291–303

McMackin D, Cockburn J, Anslow P, Gaffan D (1995) Correlation of fornix damage with memory impairment in six cases of colloid cyst removal. Acta Neurochir (Wien) 135: 12–18

Messer WS Jr, Bohnett M, Stibbe J (1990) Evidence for a preferential involvement of M_1 muscarinic receptors in representational memory. Neurosci Lett 116: 184–189

Mesulam MM (1995) Cholinergic pathways and the ascending reticular activating system of the human brain. Ann NY Acad Sci 757: 169–179

Mesulam MM (1990) Human brain cholinergic pathways. In: Aquilonius SM, Gillberg PG (eds) Progress in brain research, vol 84. Elsevier, Amsterdam, pp 231–241

Mesulam MM (1988) Central cholinergic pathways. In: Avoli M, Reader TA, Dykes RW, Gloor P (eds) Neurotransmitters and cortical function, vol 15. Plenum, New York, pp 237–260

M'Harzi M, Jarrard LE (1992) Effects of medial and lateral septal lesions on acquisition of a place and cue radial maze task. Behav Brain Res 49: 159–165

Milberg W, Alexander MP, Charness N, McGlinchey-Berroth R, Barrett A (1988) Learning of a comple arithmetic skill in amnesia: evidence for a dissociation between compilation and production. Brain Cogn 8: 91–104

Mishkin M, Phillips RR (1990) A corticolimbic memory path revealed through its disconnection. In: Trevarthen C (ed) Brain circuits and functions of the mind: essays in honour of R.W. Sperry. Cambridge University, Cambridge

Mishkin M (1982) A memory system in the monkey. Phil Transact Roy Soc Lond B298: 85–95

Mizumori SJY, Ward KE, Lavoie AM (1992) Medial septal modulation of entorhinal single unit activity in anesthesized and freely moving rats. Brain Res 570: 188–197

Morris MK, Bowers D, Chatterjee A, Heilman KM (1992) Amnesia following a discrete basal forebrain lesion. Brain 115: 1827–1847

Müller U, von Cramon DY (1994) The therapeutic potential of bromocriptine in neuropsychological rehabilitation of patients with acquired brain damage. Prog Neuro-Psychopharmacol Biol Psychiatry 18: 1103–1120

Murtha SJE, Pappas BA (1994) Neurochemical, histopathological and mnemonic effects of combined lesions of the medial septal and serotonin afferents to the hippocampus. Brain Res 651: 16–26

Nieuwenhuys R, Voogd J, van Huijzen C (1988) The human nervous system: a synopsis and atlas, 3rd edn. Springer, Berlin Heidelberg New York Tokyo

Nitta A, Murase K, Furukawa Y, Hayashi K, Hasegawa T, Nabeshima T (1993) Memory impairment and neural dysfunction after continuous infusion of anti-nerve growth factor antibody into the septum in adult rats. Neuroscience 57: 495–499

Numan R, Quaranta JR (1990) Effects of medial septal lesions on operant delayed alternation in rats. Brain Res 531: 232–241

Ogden JA, Mee EW, Henning M (1993) A prospective stud of impairment of cognition and memory after subarachnoid hemorrhage. Neurosurgery 33: 572–587

Ogden JA, Levin PL, Mee EW (1990) Long-term neuropsychological and psychosocial effects of subarachnoid hemorrhage. Neuropsychiatry Neuropsychol Behav Neurol 3: 260–274

Ohno K, Masaoka H, Suzuki R, Monma S, Matsushima Y (1991) Symptomatic cerebral vasospasm of unusually late onset after aneurysm rupture. Acta Neurochir (Wien) 108: 163–166

Pang K, Wiliams MJ, Egeth H, Olton DS (1993) Nucleus basalis magnocellularis and attention: effects of muscimol infusion. Behav Neurosci 107: 1031–1038

Parkin AJ, Leng NRC (1993) Neuropsychology of the amnesic syndrome. Lawrence Erlbaum, Hove

Parkin AJ, Barry C (1991) Alien hand sign and other cognitive deficits following ruptured aneurysm of the anterior communicating artery. Behav Neurol 4: 167–179

Parkin AJ, Leng NRC, Stanhope N (1988) Memory impariment following ruptured aneurysm of the anterior communicating artery. Brain Cogn 7: 231–243

Petri HL, Mishkin M (1994) Behaviorism, cognitivism and the neuropsychology of memory. American Scientist 82: 30–37

Phillips S, Sangalang V, Sterns G (1987) Basal forebrain infarction: a clinicopathologic correlation. Arch Neurol 44: 1134–1138

Richardson JTE (1991) Cognitive performance following rupture and repair of intracranial aneurysm. Acta Neurol Scand 83: 110–122

Richardson JTE (1989) Performance in free recall following rupture and repair of intracranial aneurysm. Brain Cogn 9: 210–226

Robinson SE, Malthe-Soerenssen D, Wood PL, Commisiong J (1979) Dopaminergic control of the septo-hippocampal cholinergic pathway. J Pharmacol Exp Therap 208: 476–479

Rousseaux M, Huglo D, Steinling M (1994) Cerebral blood flow in frontal lesions of aneuryms of the anterior communicating artery. Stroke 25: 135–140

Salazar AM, Grafman J, Schlesselman S, Vance SC, Mohr JP, Carpenter M, Pevsner P, Ludlow C, Weingartner H (1986) Penetrating war injuries of the basal forebrain: neurology and cognition. Neurology 36: 459–465

Säveland H, Sonesson B, Ljunggren B, Brandt L, Uski T, Zygmunt S, Hindfelt B (1986) Outcome evaluation following subarachnoid hemorrhage. J Neurosurg 64: 191–196

Senut MC, Menetrey D, Lamour Y (1989) Cholinergic and peptidergic projections from the medial septum and the nucleus of the diagonal band of Broca to dorsal hippocampus, cingulate cortex, and olfactory bulb: a combined wheatgerm agglutinin-apohorseradish peroxidase-gold immunohistochemical study. Neuroscience 30: 385–403

Squire LR, Zola-Morgan S, Chen K (1988) Human amnesia and animal models of amnesia: performance of amnesic patients on tests designed for the monkey. Behav Neurosci 102: 210–221

Staubli U, Huston JP (1980) Facilitation of learning by post-trial injection of substance P into the medial septal nucleus. Behav Brain Res 1: 245–255

Steinman DR, Bigler ED (1986) Neuropsychological sequelae of ruptured anterior communicating artery aneurysm. Int J Clin Neuropsychol 8: 135–140

Stenhouse LM, Knight RG, Longmore BE, Bishara SN (1991) Long-term cognitive deficits in patients after surgery on aneurysms of the anterior communicating artery. J Neurol Neurosurg Psychiatry 54: 909–914

Stroessner-Johnson HM, Rapp PR, Amaral DG (1992) Cholinergic cell loss and hypertrophy in the medial septal nucleus of the behaviorally characterized aged rhesus monkey. J Neurosci 12: 1936–1944

Talland GA, Sweet WH, Ballantine HT (1967) Amnesic syndrome with anterior communicating artery aneurysm. J Nerv Mental Dis 145: 179–192

Tarel V, Pellat J, Naegele B, Carbonnel S, Chirossel JP, de Rougemont J (1990) Troubles mnésiques après rupture d'anévrysme de l'artère communicante antérieure: 22 cas. Rev Neurol 146: 746–751

Teissier du Cros J, Lhermitte F (1984) Neuropsychological analysis of ruptured saccular aneurysms of the anterior communicating artery after radical therapy (32 cases). Surg Neurol 22: 353–359

Tidswell P, Dias PS, Sagar HJ, Mayes AR, Battersby RDE (1995) Cognitive outcome after aneurysm rupture: relationship to aneuryms site and perioperative complications. Neurology 45: 875–882

Tranel D, Damasio AR, Damasio H, Brandt JP (1994) Sensorimotor skill learning in amnesia: additional evidence for the neural basis of nondeclarative memory. Learn Mem 1: 165–179

Turnbull J, Jiang F, Racine R (1994) Hippocampal stimulation of fornical-lesioned rats. Can J Neurol Sci 21: 100–103

Uylings HBM, Van Eden CG (1990) Qualitative and quantitative comparison of the prefrontal cortex in rat and in primates, including humans. In: Uylings HBM, Van Eden CG, de Bruin JPC, Corner MA, Feenstra MGP (eds) The prefrontal cortex: its structure, function and pathology (Progress in brain research, vol 85). Elsevier, Amsterdam, pp 31–62

Valenstein E, Bowers D, Verfaellie M, Heilman KM, Day A, Watson RT (1987) Retrosplenial amnesia. Brain 110: 1631–1646

Van der Linden M, Bruyer R, Roland J, Schils JP (1993) Proactive interference in patients with amnesia resulting from anterior communicating artery aneurysm. J Clin Exp Neuropsychology 15: 525–536

Van der Linden M, Roland J, Schils JP, Bruyer R (1992) Approche neuropsychologique du syndrome amnésique consécutif à une rupture d'anévrysme de l'artère communicante antérieure. Rev Neuropsychol 2: 169–192

Vicentelli F, Lehman G, Caruso G, Grisoli F, Rabehanta P, Gouaze A (1991) Extracerebral course of the perforating branches of the anterior communicating artery: microsurgical anatomical study. Surg Neurol 35: 98–104

Vilkki J (1985) Amnesic syndromes after surgery of anterior communicating artery aneurysms. Cortex 21: 431–444

Vogt BA, Nimchinsky EA, Vogt LJ, Hof PR (1995) Human cingulate cortex: Surface features, flat maps, and cytoarchitecture. J Comp Neurol 359: 490–506

Volpe BT, Herscovitch P, Raichle ME (1984) Positron emission tomography defines metabolic abnormality in mesial temporal lobe of two patients with amnesia after rupture and repair of anterior communicating artery aneurysm [abstract]. Neurology 34 [Suppl] 1: 188

Volpe BT, Hirst W (1983) Amnesia following the rupture and repair of an anterior communicating artery aneurysm. J Neurol Neurosurg Psychiatry 46: 704–709

Voytko ML, Olton DS, Richardson RT, Gorman LK, Tobin JR, Price DL (1994) Basal forebrain lesions in monkeys disrupt attention but not learning and memory. J Neurosci 14: 167–186

Wieraszko A, Oderfeld-Nowak B (1977) Ipsi- and contralateral changes in acetylcholinesterase and choline acetyltransferase activities in the hippocampus following unilateral septal lesions in the rats. Neuroscience 2: 649–654

Yasargil MG (1984) Anterior cerebral and anterior communicating artery aneurysms. In: Yasargil MG, Smith RG, Young PH, Teddy PJ (eds) Microneurosurgery 2: clinical considerations, surgery of the intracranial aneurysms and results. Thieme, Stuttgart, pp 165–223

Zola-Morgan S, Squire LR, Amaral DG (1989) Lesions of the hippocampal formation but not lesions of the fornix or the mammillary nuclei produce long-lasting memory imapirment in monkeys. J Neurosci 9: 898–913

Zola-Morgan S, Squire LR (1986) Memory impairment in monkeys following lesions limited to the hippocampus. Behav Neurosci 100: 155–160

The in vivo Metabolic Investigation of Brain Gliomas with Positron Emission Tomography

J. M. DERLON

Service de Neurochirurgie, CHU, Caen (France)

With 5 Figures

Contents

I. Introduction

Despite the major contribution it provides to practical neurooncolgy, morphological imaging by CT-scanner or magnetic resonance imaging techniques (MRI) is not always able to give definite answers about the histology of the tumor, its prognosis, or to predict early the response to therapy. Stereotactic biopsy usually provides a histopathological diagnosis and sometimes allows a grading of anaplasia; but most often this information is relevant only for a limited area within the tumor. In addition, biopsies cannot be performed repeatedly during the clinical follow-up of the patient and they do not always afford an individual assessment of the evolution of the tumor nor of the presumed sensitivity to any eventual therapeutic intervention. On the other hand, it is obvious that parameters which are closely related to tumor growth are not readily identified by radiological or histological investigations since most are biochemical, pharmacological or genetic in nature. Positron emission tomography (PET) affords a simultaneous *in vivo* measurement of some of these parameters, both within the tumor and in the surrounding, presumably healthy, brain.

The method (Ell *et al.* 1982, Magistretti 1983, Phelps *et al.* 1986, Reivich *et al.* 1985, Sokoloff *et al.* 1985, books for reference) employs the injection (usually intravenously) of a molecule which is integrated into a physiological process, a metabolic route or a pharmacological binding, after which it therefore becomes a ≪tracer≫. During the synthesis of the molecule, a positron emitting isotope is substituted to one of its constitutive atoms. It is thus possible to measure the tissue concentration of this now radioactive molecule by external detectors. Such a molecule is termed a ≪radiopharmaceutic≫; the denomination is currently used even in the case where the molecule itself is devoid of any pharmacological effects. Detection of the tracer is possible by performing a positron tomograph made up of a set of detectors of annular design or movement, disposed around the patient's head, and which measures the concentration of the radiopharmaceutic throughout the entire brain. The number of slices (more than 30 in the latest generation of PET cameras), their orientation, their thickness and the spatial resolution of the measurements (usually around 5 mm), depends upon the device used. The number of acquisitions (*i.e.* the number of different measurements performed from the time of the tracer injection up to the time where the radioactive decay would make the measurements inaccurate) depends upon the investigation protocol.

Two types of quantitative functional images can be produced. In either case, one obtains the tissue tracer concentration, expressed in nanocuries per ml of tissue (1 nanocurie $= 10^{-10}$ curie), or in nanomoles per ml (calculated from the specific radioactivity of the tracer). In some cases, it is possible to determine in an animal model the mathematical relationship which exists between the uptake and use of the tracer in the tissue on the one hand, and that of the endogenous molecule with which it interacts, on the other hand. It is then possible, through a calculation taking into account not only the tissue tracer concentration (measured by the PET camera) but also the plasma concentration of both the radioactive tracer and the endogenous molecule as well as the mathematical relationships previously determined, to build ≪modelized images≫. These modelized images are the transcription (along a grey scale or a colour scale) of the real physiological parameter (for instance the tissue glucose consumption) and for this reason they are also called ≪parametric images≫.

The main objectives aimed at by research and diagnosis protocols in neurooncology can be summarized as follows (Beaney 1984, Blasberg 1994, Coleman *et al.* 1991, Di Chiro 1994, Roelcke 1994): (i) – to define the relationships between functional parameters and the histopathology of tumor groups; (ii) – to characterize the correlations between functional parameters and the evolution of the tumor (functional grading), allowing one to identify different prognostic forms within the same histological group); (iii) – to assess early biological modifications induced by the treatment and to correlate them with the late clinical and radiological response; (iv) – to clarify the mechanisms underlying tumor growth and identify the factors which are likely to inhibit this process.

We shall see to what extent previous studies have addressed these issues and fulfilled at least partly these objectives. We will also discuss the role of PET in ≪daily≫ practical neurooncology.

II. Perfusion and Oxygen Metabolism

Some *in vitro* works have shown that glioma growth is associated with endothelial and capillary proliferation, which is itself stimulated by the production of vascular growth factors by the tumor cells (Plate *et al.* 1992, Shweiki *et al.* 1992). Moreover, the frequent necrosis exhibited by anaplastic gliomas in their central part when they are of sufficient size has often be attributed to a tissue ischemia which developes despite the hyperplasia of the feeding vessels of the tumor. The previous arguments led to a hypothesis of the existence of some correlation between the perfusion of a glioma and its growth. As such, its prognosis could be assessed. On the other hand, the conditions of supply and use of oxygen by the tumor are supposed to modify its growth, and to interfere with the occurrence of its necrosis, spontaneously as well as induced by radiotherapy.

Positron emission tomography is a relevant method to address the previous issues (Frackowiak *et al.* 1982, Gwan Go *et al.* 1981, Lammertsma *et al.* 1981, Pantano *et al.* 1985). Thus, tissue perfusion can be investigated by the measurement of both cerebral and tumor blood flow (CBF and TumBF, expressed in ml/100 g of tissue per minute), by using plasma water as a diffusible tracer ($H_2{}^{15}O$ is usually produced by a continuous inhalation of $C^{15}O_2$ which, at the level of the capillaries in the lungs, transfers its labelled oxygen according to the the reaction $C^{15}O_2 + H_2O > H_2{}^{15}O + CO_2$). The intra-tissular vascular volume (cerebral blood volume or CBV) can be obtained following the continuous inhalation of tracer doses of $C^{15}O$ which binds itself to erythrocytes. Lastly, the continuous inhalation of tracer doses of $^{15}O_2$ allows the measurement of the fraction of blood oxygen extracted by the tissue (oxygen extraction fraction, OEF) and the calculation of the oxygen consumption of the tissue (in the case of brain tissue, it is referred to as the cerebral metabolic rate of oxygen, $CMRO_2$).

From the various investigations performed to assess tissue characteristics of tumors (Beaney *et al.* 1985, Brooks *et al.* 1986b, Ito *et al.* 1982, Lammertsma *et al.* 1985, Leenders *et al.* 1985, McKenzie *et al.* 1978, Mineura *et al.* 1986, Tyler *et al.* 1987) the following general conclusions can be made: (i) – The blood flow is much lower in the tumor than in the healthy brain tissue, but with a great variability from one case to the other and with no correlation between perfusion rate and histological grade. (ii) – The blood volume is also variable; usually smaller in the tumor than in the healthy brain tissue, but shows some correlation with the histological grade: it is higher in anaplastic gliomas than in a benign lesion. (iii) – The oxygen extraction fraction is significantly lower in the tumor tissue than in the healthy brain tissue (as it this case for the $CMRO_2$) and has no correlation with the histological grade of the tumor. This latter observation is especially important. Actually, an impairment of tissue oxygen consumption can result from three different mechanisms: an ischemia—a situation during which perfusion is insufficient for the metabolic requirements, (*e.g.* there is a decrease of both the blood flow and the $CMRO_2$), but the OEF is higher than normal (the normal value for the OEF in brain is close to 40 percent); a primary decrease of the metabolic demand with a coupled reduction of both blood flow and $CMRO_2$, and an OEF close to the normal range; lastly, a luxury perfusion,—a situation in which the blood flow, even if rather low, is superior to the metabolic needs, which in turn results in a decreased OEF (frequently around 20 percent in gliomas). Clearly this latter mechanism is involved in gliomas, whatever their degree of anaplasia. It is therefore possible to conclude that tumor tissue is not in a situation of ischemia, but that it spontaneously exhibits a weak oxygen metabolism in contrast to that of normal brain tissue.

III. Glucose Metabolism

The findings from the early studies on cell cultures suggested that malignant tumors exhibited an enhancement of glycolysis which in turn led to a hyperproduction of lactate and not to the Krebs' Cycle, because of the low rate of oxygen use by these lesions (Bustamante *et al.* 1978, Graham *et al.* 1985, Warburg *et al.* 1956). With PET, the measurement of the glucose consumption (in the brain CMRGlu, or in the tumor TumMRGlu) has been implemented from the method which was initially designed by Sokoloff for the *ex vivo* autoradiographic measurement of this parameter in experimental animals (Sokoloff *et al.* 1977). Most often, the tracer used is not glucose itself, but the deoxyglucose form, which is labelled usually by ^{18}F (^{18}F-fluorodeoxyglucose, or ^{18}F-FDG) and less frequently by ^{11}C. The deoxyglucose is a glucose analog which is actively transported from plasma to brain tissue by the same system, and in a competitive way with the endogenous glucose. It is then phosphorylated in the brain under the action of hexokinase and is blocked at this metabolic stage (Horton *et al.* 1973).

If one knows the brain concentration of the tracer (as measured by the positron camera), the plasma concentration curve of the tracer and the endogenous glucose (glycemia) during the time of the measurement (usually at one hour), then the CMRGlu can be calculated from these data by introducing their values in the equation giving the kinetics constants of the two molecules in a three-compartment model (Brooks 1982, Brooks *et al.* 1987, Huang *et al.* 1980, Mineura *et al.* 1986, Patronas *et al.* 1983, Phelps *et al.* 1979, Reivich *et al.* 1985, Tyler *et al.* 1988). This measurement can be performed in the tumor areas and in different areas of the surrounding and presumably normal brain tissue.

Previous studies have shown that there is a correlation between tumor CMRGlu and histological grading (Di Chiro *et al.* 1982, Di Chiro 1986, Yamaguchi *et al.* 1986): low grade astrocytomas actually have a mean CMRGlu which is much lower than that of white matter, anaplastic astrocytomas and glioblastomas have on the other hand a CMRGlu which may reach, or even exceed, that of healthy gray matter (normal gray matter CMRGlu is itself approximately three times higher than normal white matter CMRGlu). However, some contradictory results have been reported by other groups and it appears that there was a large overlap between the individual higher values in the former group and lower values in the latter group (Kim *et al.* 1991, Tyler *et al.* 1987). On the other hand, CMRGlu values in the healthy brain (and especially in cortical areas) are highly variable from one patient to another, probably because of the variable repercussion of the tumor on the activation and metabolism of the distant cortex (De La Paz *et al.* 1983, Fishbein *et al.* 1987, Newmark *et al.* 1983, Hossmann *et al.* 1982). Rather than documenting only the absolute values of CMRGlu in the tumor, most studies published after 1982 have sought to consider the ratio of the CMRGlu which exists between tumor and healthy brain tissue [T/H]. This ratio can be roughly approached by a purely qualitative visual analysis—the identification of a ≪hot spot≫ within the tumor volume being indicative of a hypermetabolic area (Fig. 1). Visual analysis, however, can be misleading as regards parametric PET images and as such, determination of the absolute values must be measured in these regions. The choice of a suitable reference region of healthy tissue

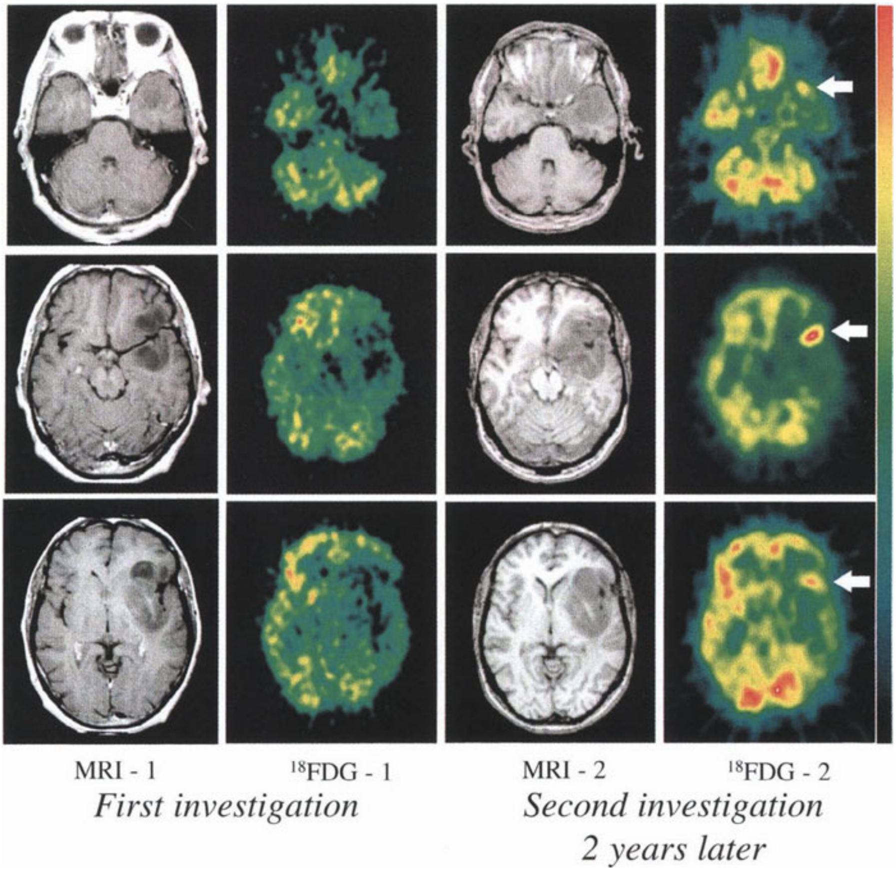

Fig. 1. Progression of an astrocytoma. The first investigation of this 50 year old patient who was referred for partial seizures showed a T1 hypointense left fronto-temporo-operculo-insular tumor, without Gadolinium enhancement, and with a low glucose metabolism. The stereotactic biopsy concluded to a low-grade astrocytoma. Two years later, the patient was still well controlled, clinically, by antiepileptic drugs without other treatment. The new MRI study showed only a very mild enlargement of the tumor, but a definite focus of abnormally high glucose metabolism in the opercular part of the tumor area (arrows). This metabolic modification was indicative of progression of the lesion toward an an plastic stage, requiring active surgical then radiation therapy

is also variable from one publication to another, but normally a white matter area located at distance from the tumor or in the contralateral hemisphere is selected. With such an approach, a correlation has been shown between the [T/H] ratio and each of the four grades of the Kernohan classification for astrocytomas with only a moderate overlap between individual values of the different groups (Di Chiro *et al.* 1984, Di Chiro 1986, Kim 1991).

Moreover, several studies have shown that, within a same histology grading, the prognosis was different when the [T/H] ratio was high or low (Di Chiro 1986, Patronas *et al.* 1985). The threshold between slowly growing astrocytomas and those with an aggressive evolution (Delbeke *et al.* 1995) has been established at around 1.4 (with a reference healthy tissue chosen in a white matter area); the median survival being almost four times longer in patients whose ratio is below this threshold than in those with a ratio above it. Does this latter observation allow us to say that this ≪metabolic grading≫ is more reliable than the ≪histopathology grading≫? This may not be the case. Indeed, in works here referenced, the histological diagnosis was often established on a small tissue sample and the sampling site had been determined on data which did not always have a link with a presumability of anaplasia. This is the case, in particular, for stereotactic biopsies of expanding lesions without contrast uptake and located in highly eloquent areas. Recent studies have shown that, when the target of the stereotacitc sampling was defined from the fiducial coordinates of the metabolically most active areas, there was a good correlation between functional and histological data, for instance cell density or criteria of anaplasia (Hanson *et al.* 1991, Herholz *et al.* 1993, Levivier *et al.* 1992). However, a long clinical follow-up of these patients, and a larger series, will have to be studied before firm conclusions can be reached.

Lastly, among low grade gliomas, everybody knows that it is difficult, if not impossible, to differentiate with confidence astrocytomas from oligodendrogliomas on the basis of clinical symptomatology or neuroradiological data. The assessment of glucose metabolism with PET is no more helpful for this purpose, despite the fact that the mean [T/H] ratio is slightly lower in the former than in the latter group (Derlon *et al.* 1994, Derlon *et al.* 1997).

IV. Amino Acids Uptake

In vitro observations suggest that there is a relationship between tumor growth on one hand, and amino acids (AA) use and protein synthesis on the other hand. This is especially true for neutral amino acids, which are not produced endogenously and must be supplied by energy supplying processes (Berlinguet *et al.* 1962, Busch *et al.* 1959, Ishiwata *et al.* 1988b and c, Kirikae *et al.* 1989, Kubota *et al.* 1984, Rogers and Robertson 1981). Thus, it was shown that glial tumor cells in culture stop growing if methionine is removed from the culture medium (Hoffman *et al.* 1976, Wison *et al.* 1978). The choice of the labelled AA is determined by two requirements which are not necessarily compatible with each other (Hubner *et al.* 1982, Kubota *et al.* 1984, Phelps *et al.* 1985): simplicity and reproducibility of the radiochemistry synthesis, providing a tracer easily available for daily clinical activity, on one hand; tracer tissue metabolism following a route which can be mathematically analyzed with a three-compartment model allowing the measurement of protein synthesis, on the other hand. It seems that the second requirement is best achieved with the use ^{11}C-L-leucine (Phelps *et al.* 1986) and ^{18}F-fluoro-tyrosine (Coenen *et al.* 1989, Ishiwata *et al.* 1988c, Murakami *et al.* 1988), at least as far as healthy brain tissue is concerned. Until now, the first requirement has been best satisfied by ^{11}C-L-methyl-methionine (^{11}C-MET), whose automatized synthesis was described some time ago (Bolster *et al.* 1986, Comar *et al.* 1976, Ishiwata *et al.* 1988a, Ishiwata *et al.* 1989, Meyer *et al.* 1985) is perfectly reproducible with a good radiochemical yield, and which is by far the most extensively and universally labelled AA used in neurooncology (Bergstrom *et al.* 1983, Bergstrom *et al.* 1987a and b, Bustany *et al.* 1986, Ericson *et al.* 1985, Ericson *et al.* 1987, Hatazawa *et al.* 1989, Lilja *et al.* 1985, Meyer *et al.* 1985, Mineura *et al.* 1991, Mosskin *et al.* 1987) as well as in the field of pituitary adenomas investigations (Bergström *et al.* 1987c, d and e). Despite early prospects, the intermediate metabolism of this tracer is far too complex to be analyzed following a three-compartment model and to provide protein synthesis values from appropriate algorithms. Measurements therefore must relate to tissue concentrations of ^{11}C-L-methyl-methionine (^{11}C-MET), either absolute or relative (as a percentage of injected dose, and/or as the ratio of concentration between tumor and healthy tissue [T/H] in the same subject), for reasons similar to those discussed for ^{18}F-FDG investigations.

A number of studies have shown that most of glial tumors exhibit a higher AA uptake than that of the healthy tissue. Studies dedicated to astrocytomas suggest that there is a relationship between the [T/H] ratio of AA uptake, and the histopathological grade (Bustany *et al.* 1986, Derlon *et al.* 1989, Ericson *et al.* 1985, Kaschten *et al.* 1994, Lilja *et al.* 1985, Meyer *et al.* 1985).

In the case of low grade gliomas, there is still some disagreement between different investigators. However, a recent work has shown that there is a highly significant difference between benign astrocytomas, in which the mean ^{11}C-MET uptake is identical or slightly superior to that of the normal tissue, on one hand; and oligodendrogliomas whose mean ratio is around 1.4, with a significant proportion of the tumor volume harbouring ratios of 2 or more (Derlon *et al.* 1994). We shall see later the practical consequences of this observation (Derlon *et al.* 1997).

V. Nucleic Acids Metabolism

There is no doubt about the importance of investigating the incorporation of the nucleic acids to DNA in tumor cells. Such an *in vivo* measurement would provide the knowledge of a parameter directly linked with the tumor growth, non-invasively and repeatedly at different stages of the treatment, which is not the case with tissue sampling for molecular biology analysis (flow cytometry, Ki67, BUdR, *etc.*). Two tracers especially have been proposed for such PET investigations: ^{18}F-fluorodeoxyruidine is taken up in most glial tumors, seems to be a good marker of DNA synthesis on experimental models (Tsurumi *et al.* 1990) and has a grade related uptake in human gliomas (Kameyama *et al.* 1987). ^{11}C-thymidine has been more extensively used in experimental models (Christman *et al.* 1972, Kubota *et al.* 1991, Shields *et al.* 1986, Shields *et al.* 1990) and for the investigation of non-brain tumors (Martiat *et al.* 1988), although its preliminary use in human brain gliomas did not display any correlation between the tracer uptake and histological grade. A better accumulation in recurrent tumors than that obtained with ^{18}F-FDG was observed (Vander Borght *et al.* 1994).

VI. Miscellaneous Parameters

1. *Blood-Tissue Permeability*

Several tracers can enter the brain or tumor tissue only if the blood-tissue barrier (BTB, a more general concept than blood-brain barrier or BBB) is permeable (Groothuis and Vick 1982). Gallium 68 (^{68}Ga), when injected intravenously (Hoop *et al.* 1976), is linked to the plasma transferrin and is then trapped in tissues with a BTB permeable to high molecular weight proteins. This also is the case for ^{68}Ga-EDTA (Bergstrom *et al.* 1983, Hawkins *et al.* 1984, Iannotti *et al.* 1987, Kessler *et al.* 1984). Rubidium 82 (^{82}Rb) has the same behavioural profile as potassium or Thallium 201 (^{201}Th): it does not penetrate into the extra-cellular space except when the capillary membranes are permeable to small molecules and when underlying cells are structurally and functionally intact (Brooks *et al.* 1984, Chi-Kwan and Badinger 1981, Chi-Kwan *et al.* 1982). Theoretically, investigating the uptake of both tracers (^{68}Ga and ^{82}Rb) allows one to differentiate between necrotic tissue and viable tumor tissue with an open BTB. Actually, the investigation of plasma-tissue permeability with PET does not seem to provide information which is different from that which can be obtained with a CT-scanner and contrast, MRI and Gadolinium, or SPECT (with ^{99m}Tc-EDTA or ^{201}Th). For this reason, therefore, it is seldom used in current practice.

2. *Acid-Base Equilibrium*

Measuring tumor pH is relevant with several experimental data: human glioma cells in culture appear to be less sensitive to radiotherapy at lower pH values (Röttinger and Mendouca 1980); local pH can modify the efficacy of certain cytotoxic agents (Born and Eichotte-Wirth 1981); more generally, pH influences cancer cells growth and contact inhibition (Ceccarini *et al.* 1971). The fact that most anaplastic tumors exhibit an enhanced glycolysis resulting in a high rate of lactate production would predict that their pH would be more acidic than that of normal tissue. Such was the conclusion of some *in vivo* measurements performed using microelectrodes (Wike-Hooley *et al.* 1985.) But such studies measure the interstitial pH of tissue, which cannot always reflect the intracellular pH which is actually investigated with PET methods. Tissue pH measurement with PET uses a weak acid, which is either $^{11}CO_2$ (Brooks *et al.* 1986c) or ^{11}C-DMO (Rottenberg *et al.* 1984, Rottenberg *et al.* 1985, Tyler *et al.* 1987). Both acids pass through the BTB, but accumulate in the tissue only when they are dissociated, which is the case when tissue pH is higher than plasma pH. A few studies have shown that the glioma pH was, actually, alkaline when compared with that of the healthy tissue. A similar result has been found also with *in vitro* NMR spectroscopy. The luxury perfusion of these tumors, with an uncoupling between perfusion and oxidative metabolism, would determine an increased leakage of the $[H^+]$ ions which could explain this phenomenon.

3. *Receptor Studies*

There is yet little knowledge about the relationship between expression of specific receptors by gliomas and their prognosis or their response to a given treatment. This is one explanation for the paucity of labelled ligands available for PET in this indication and of the reduced number of clinical investigations performed with such molecules. However, peripheral benzodiazepine receptors (PBZDr) have already been employed in some basic (Ferrarese *et al.* 1989, Ikezaki *et al.* 1990a and b, Olson *et al.* 1992, Richfield *et al.* 1988) and clinical (Black *et al.* 1989, Ferrarese *et al.* 1994, Junck *et al.* 1989, Pappata *et al.* 1991) research. These receptors are not present in normal brain tissue, but are expressed—sometimes at high concentrations—in reactive glia in or around an inflammatory or ischemic lesion and in glial tumor cells. A specific ligand of PBZDr, the PK 11186, labelled with carbon 11, thus binds to astrocytomas, whereas it does not exhibit any detectable accumulation in healthy brain. However, this ligand has not been extensively used because the measurement of its specific binding to PBZDr requires the simultaneous injection of a non-tracer amount of cold PK (non-radioactive)—a procedure which could carry some risk of toxicity. Other projects are currently under implementation, addressing ligands to interferon, enzymes, angiogenesis factors, EGF or retinoids.

4. *Polyamine Metabolism*

Polyamines (putrescine, spermine, spermidine) are derived from ornithine. Their metabolism is strongly involved in regeneration and normal or abnormal cell growth processes (Moulinoux *et al.* 1984, Pegg *et al.* 1982a, Pegg 1988b, Quemener *et al.* 1986) as well as in a number of pathological situations. As a relationship has been shown betwenn the frequency of glioblastoma recurrence and the increase of plasma polyamine levels, it was reasonable to attempt to also measure their tissue metabolism *in vivo*. A study performed with ^{14}C-putrescine on an experimental model of glioma was encouraging (Volkow *et al.* 1983), since the tracer accumulated selectively in the tumor tissue, and at only negligeable amounts in healthy brain tissue. Studies in humans with ^{11}C-putrescine (Hiesiger *et al.* 1987), however, provided results of limited interest, partly because this molecule does not cross the normal blood-brain barrier. Even when the barrier is permeable, the tracer accumulates in a non-specific way in all tissues and lesions alike, whether they are tumorous or not. Moreover, in tumor tissue, it seems that only a very small part of the labelled putrescine is actually incorporated to the polyamine metabolism most likely because it is in competition with a high disponibility of endogenous polyamines (Warnick *et al.* 1989). For these different reasons, the use of this tracer has not been pursued further subsequent to these preliminary studies.

5. *Tissue Pharmacokinetics of Antimitotic Drugs*

Among the different parameters likely to modify the chemosensitivity of a glioma, the biodisponibility of the antimitotic drug has been considered, since it can be limited because of permeability factors at the plasma-tissue level (Groothuis *et al.* 1982). Several currently used drugs have been labelled for use in PET investigations: BCNU, labelled with nitrogen 13 or carbon 11 (Diksic *et al.* 1982a and b); Sar-CNU (Conway *et al.* 1988); CCNU (Diksic *et al.* 1984, Diksic *et al.* 1985); Cis-platine (Ginos *et al.* 1987) or Fotemustine (Lasne *et al.* 1986) for example. A correlation has been demonstrated between tumor concentration of the drug on one hand and the BTB and way of drug administration (intravenous or intra-arterial routes) on the other hand (Diksic *et al.* 1982b, Diksic *et al.* 1984, Ginos *et al.* 1987, Tyler *et al.* 1986). However, no study has established any correlation between tumor concentration of the drug and the clinico-radiological response to treatment, because only a few patients were investigated with each molecule. Moreover, some agents such as nitrosoureas are chemically unstable and split into secondary molecules (among which some keep antimitotic properties) shortly after their tissue diffusion. One is therefore unable to know which of these secondary molecules is bound to the radioelement and, as such, one cannot reliably interpret the results of these measurements.

VII. The Contribution of PET to Clinical Neurooncology

Positron emission tomography can be, in some clinical situations, a useful tool complementary of neuroradiological and histological methods with the prospect to accurately establish the nature and the prognosis (grading) of the lesion, to predict then assess its response to therapy and to prove recurrency (as a differential diagnosis from scar, radionecrosis, or any inflammatory or ischemic process).

1. To Establish the Diagnosis

The variations of a given metabolic parameter have no absolute specificity relevant to a given tumor cell type. For instance, a high amino acid uptake can be observed in a meningioma, a schwannoma, a benign oligodendroglioma and sometimes a benign astrocytoma, but also in an anaplastic astrocytoma, a glioblastoma, a metastasis, and also an abscess (Ishii *et al.* 1993, Sasaki *et al.* 1990) or the periphery of a spontaneous subacute hematoma (Dethy *et al.* 1994). Similarly, high deoxyglucose activity has been encountered in different types of primary and secondary malignant tumors but also in abscesses (Sasaki *et al.* 1990) or subacute non-tumor hematomas (Dethy *et al.* 1994). It is only by the comparison of metabolic parameters on one hand, clinical, radiological (Weisberg 1980, Dean *et al.* 1990) and histological (Daumas-Duport 1992, Fulling and Garcia 1985, Rutten *et al.* 1982) data on the other hand, that a highly reliable diagnosis can be established. Each of these parameters, when considered independently, can be misleading both with diagnosis and prognosis setup. It has been shown that stereotactic biopsy itself sometimes fails to provide the correct diagnosis, and specially the appropriate grading of the tumor (Chandrasoma *et al.* 1989, Feiden *et al.* 1991), which is explainable by the heterogeneity of such lesions: there are not always neuroradiological abnormalities which could orientate the targeting toward its most specific part, which could therefore be ignored by the tissue sampling procedure. PET, on the other hand, has been shown in some cases to delineate the tumor margins more accurately than CT-scanner (Bergstrom *et al.* 1983, Mosskin *et al.* 1987). Moreover the use of PET for defining the target of stereotactic biopsy seems to improve the ≪yield≫ of the histology sampling in comparison with the results obtained with purely neuroradiological methods (Hanson *et al.* 1991, Levivier *et al.* 1992, Levivier *et al.* 1995, Pirotte *et al.* 1994): the most anaplastic part of the tumor corresponds in all reported cases to the area of higher metabolism, even if there is no contrast or Gadolinium uptake at the same location, whereas in some cases an area of contrast uptake can be observed in a non-tumor part of the brain. The use of a multiparameter investigation can improve the effectiveness of PET for the diagnosis and the metabolic characterization of human gliomas (Erickson *et al.* 1985, Kameyama *et al.* 1987, Meyer *et al.* 1989, Mineura *et al.* 1986, Rhodes *et al.* 1983, Tyler *et al.* 1987, Vander Borght *et al.* 1994) as well as of experimental tumor models (Hossmann *et al.* 1982, Kirikae *et al.* 1989, Sato *et al.* 1992). Thus, a recent study (Derlon *et al.* 1994, Derlon *et al.* 1997) has shown that it was possible to differentiate with PET two kinds of low grade gliomas, astrocytomas and oligodendrogliomas, which are almost indistinguishable one from the other when one considers only their clinical or neuroradiological features. Actually, both tumors have a low glucose metabolism but astrocytomas have a methionine uptake close, or slightly superior, to that of the healthy brain tissue (Fig. 2), whereas oligodendrogliomas always display a high accumulation of this tracer (Fig. 3). Moreover, if there is a high ^{18}F-FDG uptake in a tumor which has the radiological features of a benign astrocytoma, this diagnosis should seriously been reconsidered, even if it was based on biopsy histological procedures: repeating the biopsy after targeting the PET hypermetabolic area will usually conclude at an anaplastic focus in a heterogeneous tumor. Similarly, a high methionine uptake in a tumor whose biopsy reported a low grade astrocytoma should raise doubts about the diagnosis and lead to a re-oriented tissue sampling: it is likely to be an oligoastrocytoma or a heterogeneous anaplastic astrocytoma.

2. *To Define the Prognosis*

The prognosis of a glioma is currently defined on two morphological criteria: one is radiological, with the pejorative significance of the occurrence of contrast or Gadolinium uptake (Weisberg 1980, Dean *et al.* 1990); the other one is the histological grading (Daumas-Duport 1992, Fulling *et al.* 1985, 1992, Rutten *et al.* 1982). Unfortunately, the neuroradiological criterion is not entirely specific: a malignant glioma can keep a closed BTB for some time and some low grade gliomas have a slight enhancement after contrast injection. But there can be also, as we have seen previously, a failure of prognosis based on biopsy (Chandrasoma *et al.* 1989, Feiden *et al.* 1991), if a benign looking tissue has been sampled at some distance of an ignored anaplastic foci. Moreover, biopsy cannot be easily repeated since it is an invasive procedure, whereas PET can repeatedly sample the full tumor volume. In several studies, a correlation has been shown to exist between ^{18}F-FDG uptake on one hand, and prognosis on the other hand,

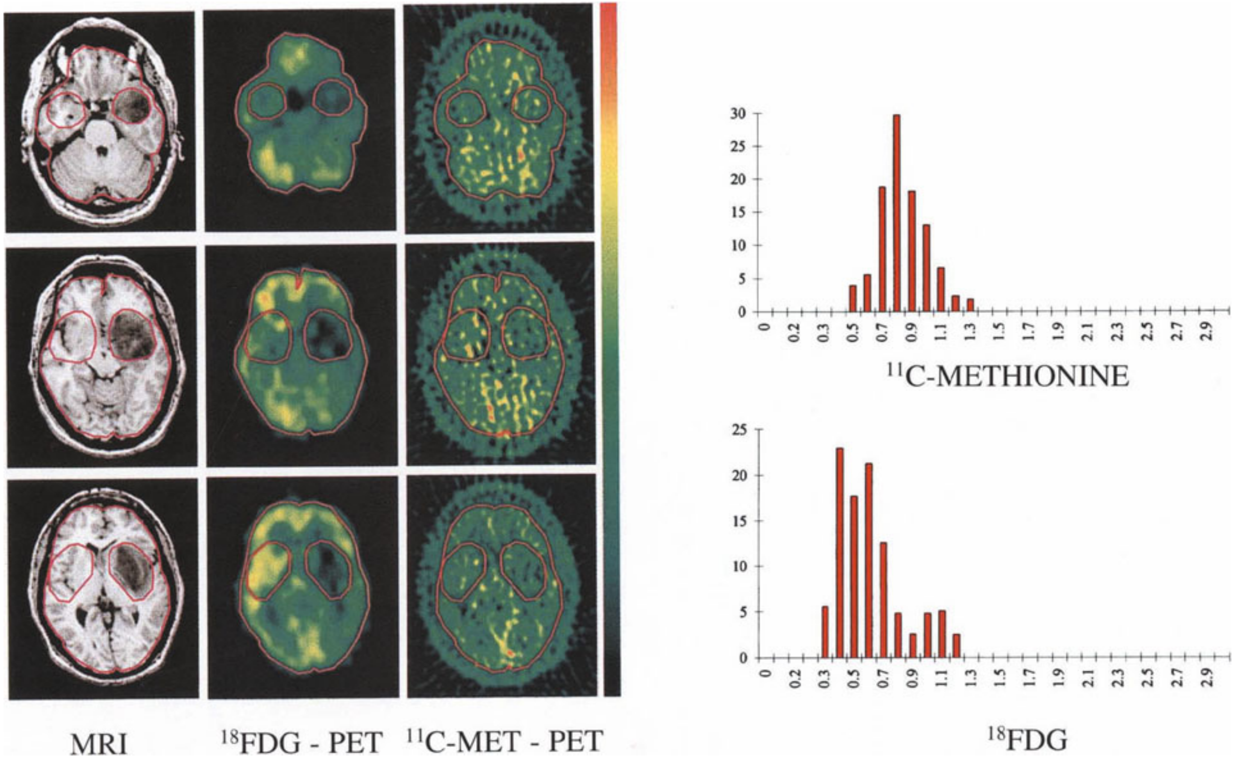

Fig. 2. Left temporo-insular low-grade astrocytoma (diagnosis obtained on large tissue sampling during surgery) in a 34 year old man presenting with generalized seizures. The MRI showed, on T1, a hypointense lesion without Gadolinium uptake (not shown). The tumor region of interest (ROI) has been delineated on the MRI images segmented at the appropriate slice levels, then copied onto the two PET scanners (^{18}F-DG and ^{11}C-MET). The healthy tissue ROI was the symmetric area of the tumor ROI, on the normal hemisphere. The tumor ROI has been itself divided into voxels of 8 x 8 x 9 mm^3, and the ratio between the tracer concentration in each voxel and the average concentration in the healthy ROI was calculated. Visual analysis shows clearly a glycolytic hypometabolism in the tumor area, with a methionine uptake close to normal values. Distribution analysis of the relative tracer concentration in the tumor voxels is displayed histograms, with the volume percentage of the tumor area exhibiting a definite range of uptake along the y-axis, and the tracer concentration ratio (between discrete tumor voxels and mean healthy tissue values) along the x-axis. This analysis confirms the pronounced glycolytic hypometabolism of the tumor (almost all values of glucose consumption are far below the normal uptake, corresponding to a ratio value of 1); shows the mild decrease of methionine uptake (the mean uptake is around 0.8, or 80 percent of the uptake in the healthy brain tissue); but, moreover, shows the extreme heterogeneity of the tumor metabolism between different areas, which was not as clear on pure visual observation

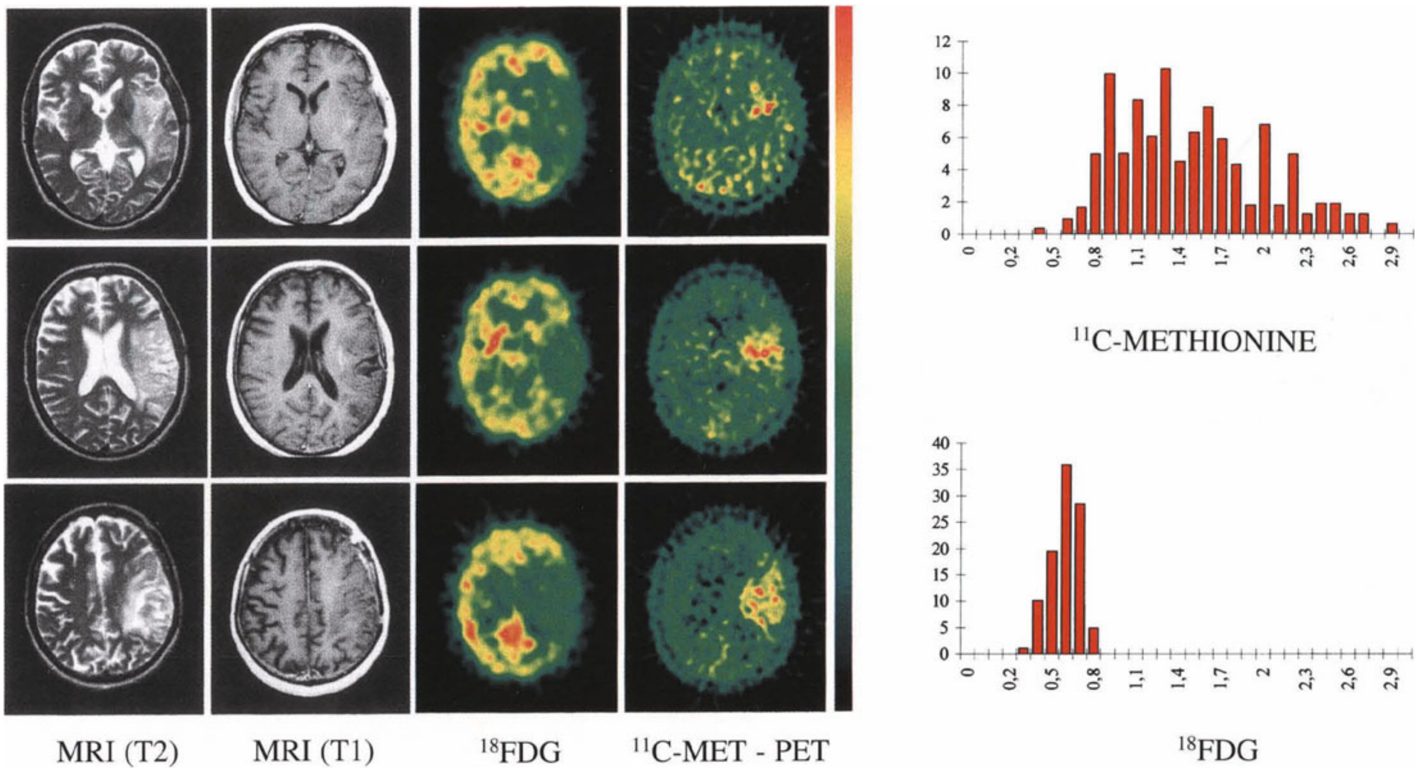

Fig. 3. Left fronto-parietal low-grade oligodendroglioma in a 50 year old woman with seizures and mild dysphasia. There is no Gadolinium uptake (not shown). In the tumor ROI, there is a hypometabolic glucose consumption and an abnormally high but heterogeneous uptake of methionine, as shown both by visual analysis and histograms of the relative tracer concentration in the different tumor areas (same analysis method than for case illustrated in Fig. 4)

in some way independently from the histological grade (Alavi *et al.* 1987, Alavi *et al.* 1988, Delbeke *et al.* 1995, Di Chiro *et al.* 1986, Holzer *et al.* 1993, Ishikawa *et al.* 1993, Kim *et al.* 1991, Patronas *et al.* 1985, Schifter *et al.* 1993): when the [T/R] tissue ratio of this tracer was above 1.4, the median survival of the patients was approximately three times shorter than when the ratio was below this threshold. Such a correlation has not yet been shown with AAs uptake, but studies to address this issue are currently underway. In some studies, already referenced in a previous section, a partial correlation has been shown between the histological grade of an astrocytoma and its methionine uptake (Derlon *et al.* 1989, Ericson *et al.* 1985, Kaschten *et al.* 1994, Lilja *et al.* 1985, Meyer *et al.* 1985).

3. To Predict and Assess the Response to Therapy

Anatomical imaging sometimes fails to provide unequivocal and early information about the effectiveness of a given therapy. A more accurate assessment of the residual tumor volume and of the early biological response to radiotherapy or chemotherapy, would likely be more helpful for a better therapeutic timing than is currently the case.

Surgery: It has been shown that, after lobectomy for non-tumour epilepsy, there is sometimes observed a contrast enhancement of the limits of resection (Laohaprasit *et al.* 1990): this feature is therefore poorly specific in cases of tumour resection even if the postoperative CT-scanner or MRI are performed within the first 48 hours (Albert *et al.* 1994, Frosting *et al.* 1993). On the other hand, in case of removal of a non-tumour epileptic focus, it has been shown that there was no high uptake of ^{18}F-FDG along the margins of the resection (Hanson *et al.* 1990), which suggests that this parameter would be also more relevant for the post-operative assessment of a tumour resection area (Fig. 4). The case report of a small recurrent oligodendroglioma in which MRI was unconclusive but which exhibited a definitely abnormal area of high ^{11}C-MET uptake (Viader *et al.* 1993) also suggested that a high uptake of ^{11}C-MET on the site of a previously resected tumour is indicative of residual or recurrent tumour tissue rather than of gliosis or an inflammatory process (Fig. 5). However, it is not certain that such assumption would be correct at all times after surgery, since we know that high deoxyglucose or methionine uptakes can be observed in non-tumour subacute hematomas (Dethy *et al.* 1994).

Radiotherapy and chemotherapy: In several experimental models, it was shown that the modifications of the tumor volume after radiotherapy, chemotherapy, or an association of both procedures, were preceded by early metabolic modifications. These modifications include perfusion, glucose metabolism, amino acid uptake and DNA synthesis, but they do not occur simultaneously or within the same range, depending on the protocol used (Abe *et al.* 1986, Kubota *et al.* 1991, Sato *et al.* 1992). Several clinical studies tried to demonstrate a correlation between immediate modifications of ^{18}F-FDG tumour uptake after chemotherapy, on one hand, and the radioclinical efficacy of the treatment on the other hand. The results are still difficult to interpret, since in some series an immediate decrease of the deoxyglucose uptake predicted a good delayed response (Rozental 1989, Rozental 1993), but in some others it was the reverse (De Witte *et al.* 1994a and b). In a prospective series of primary oligodendrogliomas, the ^{11}C-MET uptake was repeatedly measured before, then at different times after completion of radiotherapy for incompletely resected tumours (Derlon, unpublished data). It has been observed that the degree of reduction of this uptake, measured two months after the end of radiotherapy, was predictive of the late clinical and radiological response: in five patients in whom this uptake was significantly reduced, no seizure or permanent neurological deficit was recorded during the five years of follow-up; the two patients with no reduction of the methionine uptake worsened, and one of them died rapidly despite a PCV chemotherapy. Some studies have addressed the prediction of response to combined radiochemotherapy protocols. One group showed that tumour $CMRO_2$ and perfusion were not significantly modified by the treatment whereas a modification of the [T/H] ratio with ^{18}F-FDG resulted in a good prediction about the duration and quality of remission (Ogawa *et al.* 1988b). Another study (Holzer *et al.* 1993) showed that, in patients with glioblastoma treated with surgery, chemotherapy and radiotherapy, there was a good correlation between prognosis (time to recurrence and length of survival) on one hand, and ratio of ^{18}F-FDG between tumor tissue and contralateral normal brain on the other hand. The absolute values of tumor glucose consumption were of no prognostic significance, but the values of normal brain CMRGlu were linked to prognosis.

4. *To Differentiate Between Tumor Recurrency and Other Late Processes*

A frequent issue is the situation where clinical worsening (for instance with an increasing rate of seizures) or radiological modifications suggest a recurrency or a radiation necrosis. Conventional neuroradiology investigations can be confusing when one tries to establish the correct differential diagnosis between both pathophysiological hypotheses (Ashdown *et al.* 1993, Dooms *et al.* 1986, Forsting *et al.* 1993, Martins *et al.* 1977). In glioblastomas and anaplastic astrocytomas, glucose consumption is a reliable parameter for addressing this issue (Di Chiro *et al.* 1987, Doyle *et al.* 1987, Glantz *et al.* 1991, Ishikawa *et al.* 1993, Patronas *et al.* 1982): finding a hypermetabolic focus in the lesion area is indicative of recurrency, whereas a hypometabolism is likely to be due predominantly or exclusively

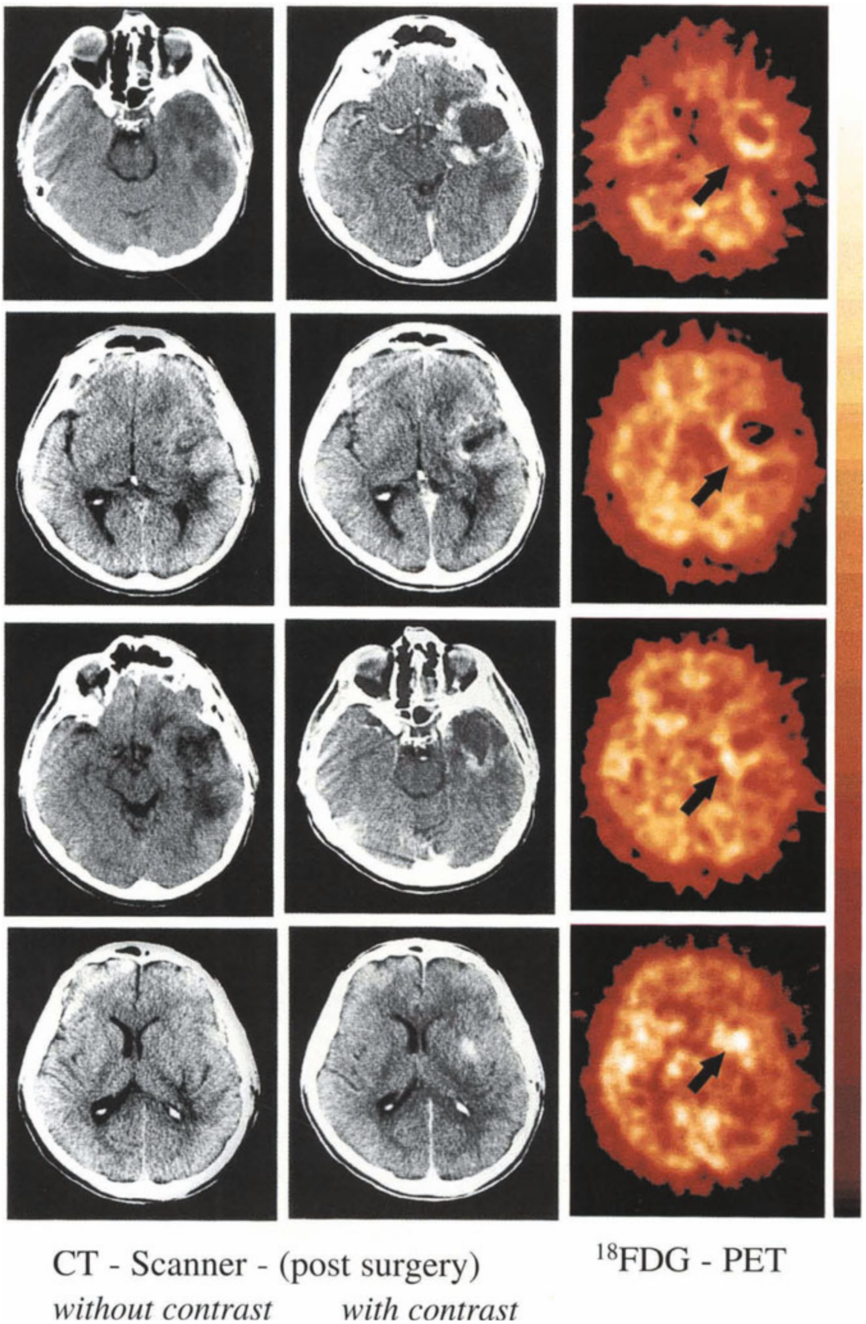

Fig. 4. A postoperative investigation was performed two weeks after surgical removal of a left temporal glioblastoma. The CT-scan shows contrast uptake at the periphery of the tumor resection area, which might be due either to non-specific disruption of the blood-tissue barrier or to residual tumor. The ^{18}F-DG-PET study shows a clear hypermetabolism in the same areas (arrows): glucose consumption is at the same level or even higher at the periphery of the tumor than in the contralateral normal cortex, which is highly in favour of the second diagnosis

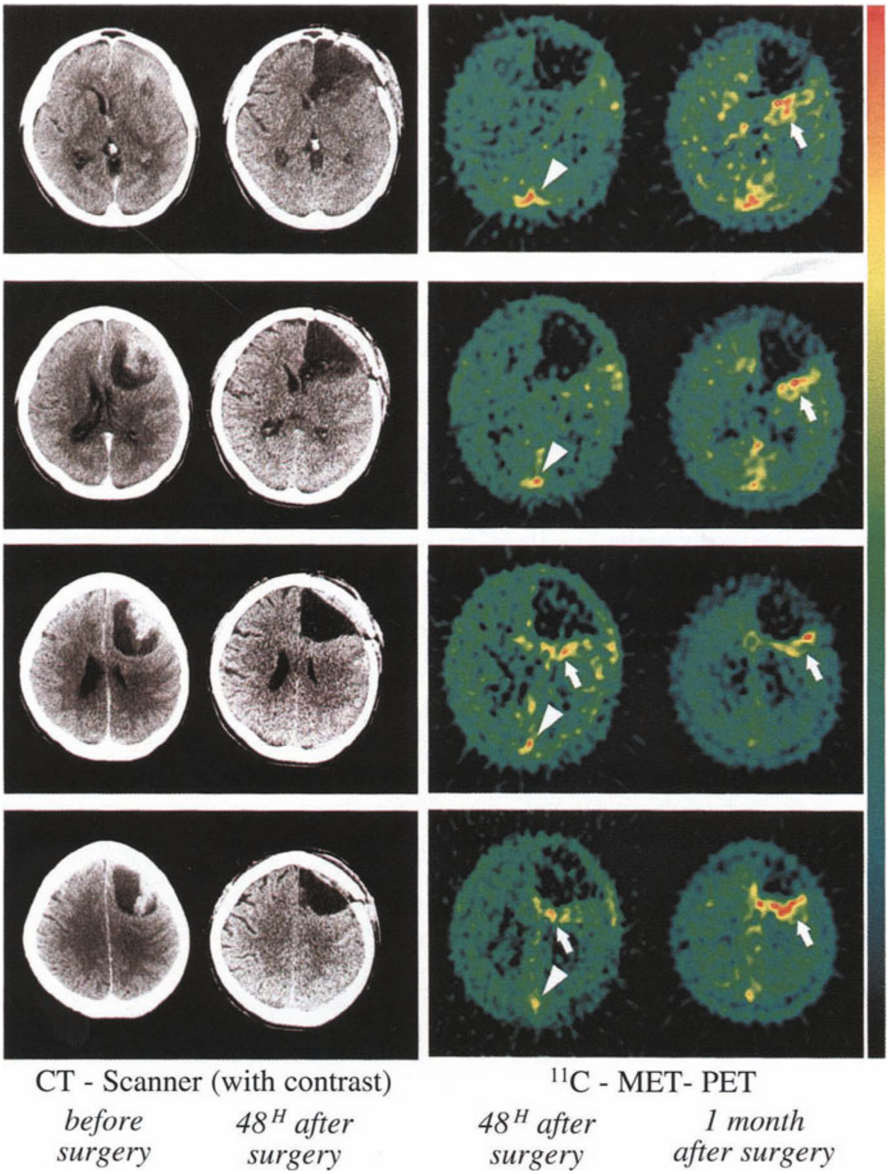

Fig. 5. The early CT-scan in this case of left frontal glioblastoma after lobectomy has not shown contrast uptake at the periphery of the resection area, which is indicative of a total tumor removal. However, the early PET investigation shows a definite though limited abnormally high methionine uptake in part of the resection margins (arrows). The clinical follow-up of the patient showed progressive disease with a rapidly worsening of the mild preoperative right-sided hemiparesis. One month after surgery, a new investigation demonstrated enlargement of the abnormal methonine uptake area (arrows), confirming that there was active residual tumor even during the early postoperative period. Notice that the area of higher methionine uptake in the medial occipital cortex (arrowheads) is a physiological phenomenon, due to the high cell density of this area

to radionecrosis. For the follow-up of benign oligodendrogliomas, the most reliable parameter is the measurement of methionine (or likely any other amino acid) uptake: a focus of abnormally high ^{11}C-MET in the tumor area is practically always associated with recurrency, whereas a decreased or normal uptake excludes this hypothesis (Viader *et al.* 1993).

VIII. Conclusions: Specificity of PET and Alternative Methods

Positron emission tomography provides, in clinical neurooncology, data which are complementary to those obtained by morphological neuroradiological investigations, such as CT-scan and MRI. This contribution is either diagnostic—particularly by the combined use of a glucose analog and of an amino acid; prognostic—and for this purpose ^{18}F-FDG has proved its relevance; and therapeutic, through an identification of those parameters with early modifications correlated with the delayed clinical response. However, the interpretation of PET investigations is not unequivocal. It is only after a number of investigations performed in a large series of patients with different pathologies that we will be able to define metabolic patterns relevant to tumor cell type, grade, prognosis, and lastly to measure the efficacity of response to therapy. We are still far from such an extensive reliability and accuracy of the method. Moreover, PET is a relatively expensive method and is not readily available in daily practice to a large number of neurooncologists. Two alternative approaches to measure tumor metabolism *in vivo* which are likely to be more widely used than PET in the near future and will provide complementary information are single photon emission computerized tomography (SPECT) and nuclear magnetic resonance spectroscopy (NMRS).

1. SPECT

There are several differences between PET and «conventional» tomoscintigraphy, usually referred to as SPECT (Single Photon Emission Computerized Tomography).

Physical differences: the gamma photons produced by the positron emission have an energy (511 KeV) which is much higher than that of the photons resulting from the disintegration of the gamma emitting isotopes and are, therefore, less absorbed (or more correctly, less «attenuated») by the tissue between the area where they are produced in the organ and the detector. The attenuation is measured in each individual subject and taken into account for the eventual calculation of the radiotracer tissue concentration. Therefore, the measurement of the tracer concentration is as accurate in the center as it is at the periphery of the organ under investigation. Moreover, the emission of two photons from each disintegration (instead of one with the single photon emitting isotopes) further increases the sensitivity of the detection. It results from these considerations that SPECT is less sensitive and less suitable for providing quantitative data than PET.

Physico-chemical differences: the positron emitting isotopes have a short half-life (*e.g.* two min for ^{15}O; 10 min for ^{13}N; 20 min for ^{11}C and 120 min for ^{18}F, which can be compared, for instance, with the six hours for ^{99m}Technetium—one of the most currently used gamma emitters). This short half-life considerably decreases the dosimetry of each investigation and allows sequential investigations to be performed in the same subject. On the other hand, this property needs the extemporaneous production of the isotope (by a cyclotron) and of the labelled molecule (by a fast radiochemistry synthesis) and allows only a relatively short period of observation and measurement of the biological process under investigation.

Radiobiological differences: the positron emitters (^{15}O, ^{11}C, ^{13}N, ^{18}F) which are isotopes of atoms constituting biological molecules, do not disturb their biochemical or pharmacological characteristics and are therefore suitable for a true study of functional parameters, which is seldom the case with gamma emitters.

In opposition to what is encountered in radiochemistry for PET, it is difficult to label a biological molecule with a gamma emitting (single photon) isotope without a strong modification of its metabolic and pharmacological properties because such isotopes have steric configurations which are greatly different from those of the stable isotopes. Some labelled molecules seem however to be useful in the assessment of different functional patterns of brain tumors. Thallium 201 (^{201}Th) behaves like Rubidium 82 and potassium: it crosses the plasma-tissue barrier only if it is permeable but accumulates in cells (by a ionic pump process) only when they are living and biologically active (Kim *et al.* 1990). The uptake of ^{201}Th in a lesion therefore allows one to differentiate between necrosis on the one hand, and recurrency or residual tumor on the other hand. The MIBI (2-methoxy isobutyl isonitrile) and its derivate molecules are easily labeled with Technetium 99m (^{99m}Tc) and have been used as well as ^{201}Th as a tracer of myocardial perfusion and viability (Bisi *et al.* 1995, Maublant *et al.* 1988, Wackers *et al.* 1989). It can image primary or recurrent non-necrotic tumors with permeable blood-tissue barrier (O'Tuama *et al.* 1993). EDTA labelled with ^{99m}Tc accumulates in tumor areas with both permeable capillary barrier and predominantly necrotic cells. The major drawback of the previous molecules is that they do not penetrate in tumor tissue with an intact barrier, which is the case for most if not all benign gliomas, but also to some extent of some anaplastic ones. Such is not the case with the iodo-methyl-tyrosine labelled with iodine 123 (^{123}I), which is transported between plasma and cells by the same system (facilitated transport) as that used by branched aminoacids and in a competitive way (Kawai *et al.* 1991, Langen *et al.* 1990, Langen *et al.* 1991). Therefore, this molecule is useful for assessing the amino acids uptake in brain tumors, even with an intact plasma-tissue barrier. The main problem is that this compound is not available from the pharmaceutical industries as is the case with other single photon emitting radiotracers. In return, no glucose analog has been labelled up to now which could be successful for measuring glucose metabolism with SPECT. Finally, it has been proposed to measure the DNA synthesis through the incorporation of iododeoxyuridine (IUdR) labelled with ^{123}I, but studies are only at a preliminary stage (Tsuvajev *et al.* 1993a, Tsuvajev *et al.* 1993b). The last remark is that SPECT data are essentially semi-quantitative, and a full absolute quantification is very difficult to achieve with most radiopharmaceuticals and this technique.

2. *NMRS*

The *in vivo* spectral analysis of some elements (proton, phosphorus, or carbon) gives access to an indirect assessment of their environmental biochemical structure and therefore of the metabolism of the tissue volume under assessment. Until recently, this technique could be applied in only rather large tissue volumes, with a poor spatial resolution, which is a serious limitation for the assessment of lesions which are presumably heterogenous. Recent developments of spectroscopic imaging are likely to improve considerably the possibilities of this method in neurooncology and some preliminary results indicate that it should be able to differentiate not only between different cell lines but also between different grades (Preul *et al.* 1996).

IX. Conclusions

Positron emission tomography is a unique method for the assessment of some functional parameters of brain gliomas which are relevant with their histological structure, prognosis and sensitivity to different therapies. However, its specificity for these different aspects are not unequivocally established because of the few number of patients included in some studies, especially with some radiopharmaceuticals. As in general oncology and in cardiology, PET should be in the near future not only a clinical research method, but also a more largely accessible diagnostic tool for daily neurooncology practice. It will then be possible to better establish its true potential. Other methods of *in vivo* metabolic assessment must also be considered, as alternative and less expensive methods than PET, or as a way to obtain data complementary to those provided by the former method. In any case, the metabolic information obtained must be correlated with accurate clinical, neuroradiological and histopathological data in order to achieve a complete and effective assessment of patients at the different stages of their disease and thus to improve their treatment.

Acknowledgements

We are grateful to Brigitte David, who provided care to the edition of this text; to Allan Young who made all corrections in order to get it in correct English language; and to Dominique Luet who managed inconography selection and printing.

References

1. Abe Y, Matsuzawa T, Fujiwara T, Fukuda H, Itoh M, Yamada K, Yamaguchi K, Sata T, Ito T (1986) Assessment of radiotherapeutic effects on experimental tumors using ^{18}F-fluoro-2-deoxy-D-glucose. Eur J Nucl Med 12: 325–328
2. Alavi JB, Alavi A, Goldberg HI, Dann R, Hickey W, Reivich M (1987) Sequential computerized tomography and positron emission tomography studies in a patient with malignant glioma. Nucl Med Commun 8: 457–468
3. Alavi JB, Alvi A, Chawluc J, Kushner M, Powe J, Hickey W, Reivich M (1988) Positron emission tomography in patients with glioma. A predictor of prognosis. Cancer 62: 1074–1078
4. Albert KF, Forsting M, Sartor K, Adams HP, Wilson CB, Kunze S, Salcman M (1994) Early post-operative magnetic resonance imaging after resection of malignant glioma—objective evaluation of residual tumor and its influence on regrowth and prognosis. Neurosurgery 34: 45–91
5. Ashdown BC, Boyko OB, Uglietta JP, Friedman HS, Hockenberger B, Oakes WJ, Fuller GN (1993) Postradiation cerebellar necrosis mimicking tumor: MR appearance. J Comput Assist Tomogr 17: 124–126
6. Beaney RP (1984) Positron emission tomography in the study of human tumors. Semin Nucl Med 14(4): 324–341
7. Beaney RP, Brooks DJ, Leenders KL, Thomas DGT, Jones T, Holnan KE (1985) Blood flow and oxygen utilisation in the contralateral cortex of patients with untreated intracranial tumour as studied by positron emission tomography, with observation on the effect of decompressive surgery. J Neurol Neurosurg Psychiatry 48: 310–319
8. Bergstrom M, Collins VP, Ehrin E, Ericson K, Ericson L, Greitz T, Halldin C, Von Holst H, Langstrom B, Lija A, Lundovist H, Nagren K (1983) Discreapancies in brain tumor extent as shown by computed tomography and positron emission tomography using (^{68}GA) EDTA, (^{11}C) glucose, and (^{11}C) methionine, J Comp Assist Tomogr 7: 1062–1066
9. Bergstrom M, Ericson K, Hagenfeld L, Mosskin M, Von Holst H, Noren G, Eriksson L, Ehrin E, Johnstrom P (1987a) PET study of methionine accumu-

lation in glioma and normal brain tissue: competition with branched chain amino acids. J Comput Assist Tomogr 11: 208–213
10. Bergstrom M, Lundqvist H, Ericson K, Lilja A, Johnstrom P, Langstrom B, Von-Host H, Eriksson L, Blomqvist G (1987b) Comparison of the accumulation kinetics of L-(methyl-11C)-methionine and D-(methyl-11C)-methionine in brain tumors studied with positron emission tomography. Acta Radiol 28: 225–229
11. Bergstrom M, Muhr C, Ericson K, Lundqvist H, Lilja A, Eriksson L, Blomqvist G, Langstrom B, Johnstrom P (1987c) The normal pituitary examined with PET and methyl-11C-L-methionine and methyl-11C-D-methionine. Neuroradiology 29: 221–225
12. Bergstrom M, Muhr C, Lundberg PO, Gee AD, Fasth KJ, Langstrom B (1987d) Rapid decrease in amino acid metabolism in prolactin-secreting pituitary adenomas after bromocriptine treatment: A PET study. J Comput Assist Tomogr 11: 815–819
13. Bergstrom M, Muhr C, Lundberg PO, Bergstrom K, Lungsvist H, Antoni G, Fasth KJ, Langstrom B (1987e) Amino acid distribution and metabolism in pituitary adenomas using positron emission tomography with D-^{11}C-methionine and L-^{11}C-methionine. J Comput Assist Tomogr 11: 384–389
14. Berlinguet L, Begin N, Babineau LM (1962) Autoradiographic studies of the distribution of 1-aminocyclopentane-carboxylic acid in normal and cancerous mice. Can J Biochem Physiol 40: 1111–1114
15. Bisi G, Sciagra R, Santoro GM, Rossi V, Fazzini PF (1995) Technicium-99m-sestamibi imaging with nitrate infusion to detect vialbe hibernating myocardium and predict postrevascularization recovery. J Nucl Med 36: 1994–2000
16. Black KL, Ikezaki K, Toga AW (1989) Imaging of brain tumors using peripheral benzodiazepine receptor ligands. J Neurosurg 71: 113–118
17. Blasberg RG (1994) Prediction of brain tumor therapy response by PET. J Neurooncol 22: 281–286
18. Bolster JM Vaarlburg W, Elsinga PH, Ishiwata K, Vissering H, Voldring MG (1986) The preparation of 11C-carboxylic labelled L-methionine for measuring protein synthesis rates. J Label Comput Radiopharmaceut 23: 1081–1082
19. Born R, Eicholtz-Wirth H (1981) Effect of different physiological conditions on the action of Adriamycin on Chinese hamster cells in vitro. Brit J Cancer 44: 241–246
20. Brooks RA (1982) Alternative formula for glucose utilization using labeled deoxyglucose. J Nucl Med 23: 538–530
21. Brooks DJ, Beaney RP, Lammertsma AA, Leenders KL, Horlock PL, Kensett MJ, Marshall J, Thomas DG, Jones T (1984) Quantitative measurement of blood-brain barrier permeability using Rubidium-82 and positron emission tomography. J Cerb Blood Flow Metab 4: 535–545
22. Brooks DJ, Beaney RP, Lammerstma AA, Herold S, Turton DR, Luthra SK, Frackowiak RSJ, Thomas DG, Marshall J, Jones T (1986a) Glucose

transport across the blood-brain barrier in normal human subjects and patients with cerebral tumors studied using (^{11}C)3-0-methyl-D-glucose and positron emission tomography. J Cereb Blood Flow Metab 6: 230–239

23. Brooks DJ, Beaney RP, Lammertsma AA, Turton DR, Marshall J, Thomas DG, Jones T (1986b) Studies on regional cerebral haematocrit and blood flow in patients with cerebral tumours using positron emission tomography. Microvasc Res 31: 267–276
24. Brooks DJ, Beaney RP, Thomas DGT, Marshall J, Jones T (1986c) Studies on regional cerebral pH in patients with cerebral tumours using continuous inhalation of $^{11}CO_2$ and positron emission tomography. J Cereb Blood Flow Metab 6: 529–535
25. Brooks RA, Hatazawa J, Di Chiro G, Larson SM, Fishbein DS (1987) Human cerebral glucose metabolism determined by positron emission tomography: a revisit. J Cereb Blood Flow Metab 7: 427–432
26. Busch H, Davis JR, Honig GR, Anderson DC, Nair PV, Nyhan WL (1959) The uptake of a variety of amino acids into nuclear proteins of tumors and other tissues. Cancer Res 19: 1030–1039
27. Bustamante E, Morris HP, Pedersen PL (1978) Hexokinase: the direct link between mitochondrial and glycolytic reactions in rapidly growing cancer cells. Adv Exp Med Bill 92: 363–380
28. Bustany P, Chatel M, Derlon JM, Darcel F, Sgouropoulos P, Soussaline F, Syrota A (1986) Brain tumor protein synthesis and histological grades: A study by positron emission tomography (PET) with C11-L-methionine. J Neurooncol 3: 397–404
29. Ceccarini C, Eagle H (1971) pH as a determinant of cellular growth and contact inhibition. Proc Natl Acad Sci USA 68: 229–233
30. Chandrasoma P, Smith M, Apusso M (1989) Stereotactic biopsy in the diagnosis of brain masses: comparison of results of biopsy and resected surgical specimen. Neurosurgery 24: 160–165
31. Chi-Kwan Y, Budinger TF (1981) Evaluation of blood brain barrier permeability changes in rhesus monkeys and man using Rb-82 and positron emission tomography. J Comput Assist Tomogr 5: 792–799
32. Chi-Kwan Y, Yano Y, Budinger TF, Friedland RP, Derenzo SE, Huesman RH, O'Brien HA (1982) Brain tumor evaluation using Rb-82 and positron emission tomography. J Nucl Med 23: 532–537
33. Christman D, Crawford EJ, Friedkin M, Wolf APP (1972) Detection of DNA synthesis in intact organisms with positron-emitting methyl-(11C) thymidine. Proc Natl Acad Sci USA 69: 988–992
34. Coenen HH, Kling P, Stocklin G (1989) Cerebral metabolism of L-(2-^{18}F) Fluorotyrosine, a new PET tracer of protein synthesis. J Nucl Med 30: 1367–1372
35. Coleman RE, Hoffman JM, Hanson MW, Sostman HD, Clifford-Schold S (1991) Clinical application of PET for the evaluation of brain tumors. J Nucl Med 32: 616–622
36. Comar D, Cartron JC, Mazière M, Marazano (1976) Labelling and metabolism of methionine-methyl-C11. Eur J Nucl Med 1: 11–14

37. Conway T, Diksic M (1988) Synthesis of "no-carrier-added" carbon-11 SarCNU: The sarcosinamide analog of the chemotherapeutic agent BCNU. J Nucl Med 29: 1957–1960
38. Daumas-Duport C (1992) Histological grading of gliomas. Curr Opin Neurol Neurosurg 5: 924–931
39. De La Paz RL, Patronas NJ, Brooks RA, Smith BH, Kornblith PL, Milam H, Di Chriro G (1983) Positron emission tomography study of suppression of gray matter glucose utilisation by brain tumors. AJNR 4: 826–829
40. De Witte O, Hildebrand J, Luxen A, Goldman S (1994a) Acute effect of BCNU on glucose metabolism in brain and glioblastoma. J Neurooncol 21: 4
41. De Witte O, Hildebrand J, Luxen A, Goldman S (1994b) Acute effect of carmustine on glucose metabolism in brain and glioblastoma. Cancer 74: 2836–2842
42. Dean BI, Drayer BP, Bird CR, Flom RA, Hodak JA, Coons SW, Carey RE (1990) Gliomas: classification with MR imaging. Radiology 174: 411–415
43. Delbeke D, Meyerowitz C, Lapidus RL, Maciunas RJ, Jenning MT, Moots PL, Kessler RM (1995) Optimal cutoff levels of F-18 fluorodeoxyglucose uptake in the differentiation of low-grade from high-grade brain tumors with PET. Radiology 195: 47–52
44. Derlon JM, Bourdet C, Bustany P, Chatel M, Theron J, Darcel F, Syrota A (1989) (^{11}C)L-methionine uptake in gliomas. Neurosurgery 25: 720–728
45. Derlon JM, Petit-Taboué MC, Dauphin F, Courtheoux P, Chapon F, Creissard P, Darcel F, Houtteville JP (1994) The in vivo metabolic assessment of benign brain gliomas with PET: different patterns and their implications. J Neurooncol 21: 1
46. Derlon JM, Petit-Taboué MC, Chapon F, Beaudouin V, Noël MH, Creveuil C, Courtheoux P, Houtteville JP (1997) The in vivo metabolic pattern of low grade brain gliomas; a PET study with ^{18}F-fluorodeoxyglucose and ^{11}C-L-methyl methionine. Neurosurgery 40: 276–288
47. Dethy S, Goldman S, Blecic S, Luxen A, Levivier M, Hildebrand J (1994) Carbon-11-methionine and fluorine-18-FDG PET study in brain hematoma. J Nucl Med 35: 1162–1166
48. Di Chiro G, De La Paz RL, Sokoloff L, Kornblith PL, Smith BH, Patronas NJ, Kufta CV, Kessler RM, Johnston GS, Manning RG, Wolf AP (1982) Glucose utilisation of cerebral gliomas measured by (18F) fluorodeoxyglucose and positron emission tomography. Neurology 32: 1323–1329
49. Di Chiro G, Books RA, Patronas NJ, Bairamian D, Kornblith PL, Smith BH, Mansi L, Barker J (1984) Issues in the in vivo measurement of glucose metabolism of human central nervous system tumors. Ann Neurol 15 [Suppl] S1: 38–S146
50. Di Chiro G (1986) Positron emission tomography using (18F) fluorodeoxyglucose in brain tumors: A powerful diagnostic and prognostic tool. Invest Radiol 22: 360–371

51. Di Chiro G, Oldfield E, Wright DC, De Michele D, Patz DA, Patronas NJ, Doppman JL, Larson SM, Ito M, Kufta CV (1987) Cerebral necrosis after radiotherapy and/or intraarterial chemotherapy for brain tumors. AJNR 8: 1083–1091
52. Di Chiro G (1994) Which PET radiopharmaceuticals for brain tumors? J Nucl Med 32: 1346–1347
53. Diksic M, Farrokhzad S, Yamamoto L, Feindel W (1982a) Synthesis of ≪no carrier added≫ 11C-labeled BCNU. J Nucl Med 23: 895–898
54. Diksic M, Farrokhzad S, Yamamoto YL, Feinderl W (1982b) 11C and 13N-labelled BCNU and its in vivo pharmacokinetic study with PET. J Labelled Comput Radiopharm 19: 1394
55. Diksic M, Sako K, Feindel W, Kato A, Yamamoto YL, Farrohzad S, Thompson C (1984) Pharmacokinetics of positron-labeled 1,3-bis(2-chloroethyl) nitrosourea in human brain tumors using positron emission tomography. Cancer Res 44: 3120–3124
56. Diksic M, Farrakhzad S, Yamamoto YL, Feindel W (1985) Synthesis of ≪no carrier-added≫ 11C-labeled nitrosoureas. J Radioanal Nucl Chem 89: 45–54
57. Dooms GC, Hecht S, Brant-Zawadski M, Berthiaume Y, Norman D, Newton TH (1986) Brain radiation lesions: MR imaging. Radiology 158: 149–155
58. Doyle WK, Budinger TR, Valk PE, Levin VA, Gutin Ph (1987) Differentiation of cerebral radiation necrosis from tumor recurrence by (18F) FDG and 82Rb positron emission tomography. J Comput Assist Tomogr 11: 563–570
59. Ell PJ, Holman BL (1982) Computed emission tomography. Oxford University Press, Oxford
60. Ericson K, Lilja A, Bergstrom M, Collins VP, Eriksson L, Ehrin E, Von-Holst H, Lundqvist H, Langstrom BB, Mosskin M (1985) Positron emission tomography with (^{11}C) methyl)-L-methionine, (^{11}C)D-glucose and (^{68}Ga) EDTA in supratentorial tumors. J Comput Assist Tomogr 9: 683–689
61. Ericson K, Blomqvist G, Bergstrom M, Eriksson L, Stone-Elander S (1987) Application of a kinetic model on the methionine accumulation in intracranial tumors studied with positron emission tomography. Acta Radiol 28: 505–509
62. Feiden W, Steude U, Bise K, Gündisch O (1991) Accuracy of stereotactic brain tumor biopsy: comparison of the histologic findings in biopsy cylinders and resected tumor tissue. Neurosurg Rev 14: 51–56
63. Ferrarese C, Appollonio I, Frigo M, Gaini SM, Piotri R, Frattola L (1989) Benzodiazepine receptors and diazepam-binding inhibitor in human cerebral tumors. Ann Neurol 26: 564–568
64. Ferrarese C, Pierapoli C, Linfante I, Bobo RH, Guthrie B, Kufta C, Duhaney MO, Melisi J, Fulham MJ (1994) Peripheral benzodiazepine receptors and glucose metabolism in human gliomas. J Neurooncol 22: 15–22
65. Fishbein DS, Chrousos GA, Di Chiro G, Wayner RE, Patronas NJ, Larson SM (1987) Glucose utilization of visual cortex following extra-occipital

interruptions of the visual pathways by tumor. A positron emission tomography study. J Clin Neuro Ophtalmol 7: 63–68
66. Forsting M, Albert FK, Kunze S, Adams HP, Zenner D, Sartor K (1993) Extirpation of glioblastomas: MR and CT follow-up of residual tumor and regrowth patterns. AJNR 14: 776–787
67. Frackowiak RSJ, Lenzi GL, Jones T, Heather JD (1982) Quantitative measurement of regional cerebral blood flow and oxygen metabolism in man using ^{15}O and positron emission tomography: theory, procedure and normal values. J Comput Assist Tomogr 4: 727–736
68. Fulling KH, Garcia DM (1985) Anaplastic astrocytoma of the adult cerebrum. Prognostic value of histologic featrues. Cancer 55: 928–931
69. Ginos JZ, Cooper AJL, Dhawan V (1987) [13N] Cisplatin PET to assess pharmacokinetics of intra-arterial versus intravenous chemotherapy for malignant brain tumors. J Nucl Med 28: 1844–1852
70. Glantz MJ, Hoffman JM, Coleman RE, Firedman AH, Hanson MW, Burger PC, Herndon J, Meisler WJ, Schold S Jr (1991) Identification of early recurrence of primary central nervous system tumors by 18F-fluorodeoxyglucose positron emission tomography. Ann Neurol 29: 347–355
71. Graham JF, Cummins CJ, Smith BH, Kornblith PL (1985) Regulation of hexokinase in cultured gliomas. Neurosurgery 17: 537–542
72. Groothuis DR, Vick NA (1982) Brain tumors and the blood-brain barrier. Elsevier, Amsterdam, pp 232–235
73. Gwan Go K, Lammmertsma A, Paans AMJ, Vaalburg W, Woldring MG (1981) Extraction of water labeled with oxygen 15 during single-capillary transit. Influence of blood pressure, osmolarity, and blood-brain damage. Arch Neurol 38: 581–584
74. Hanson MW, Hoffman JM, Glantz MJ, Schold SC, Radtke RA, Friedman AH, Coleman RE (1990) FDG-PET in the early postoperative evaluation of patients with brain tumors. J Nucl Med (Abstract) 31: 799
75. Hanson MW, Glantz MJ, Hoffman JM (1991) FDG-PET in the selection of brain lesions for biopsy. J Comput Assist Tomogr 15: 796–801
76. Hatazawa J, Ishiwata K, Itoh M, Kameyama M, Kubota K, Ido T, Matsuzawa T, Yoshimoto T, Watanuki S, Seo S (1989) Quantitative evaluation of L-(methyl-C-11) methionine uptake in tumor using positron emission tomography. J Nucl Med 30: 1809–1813
77. Hawkins RA, Phelps ME, Huang SC, Wapenski JA, Grimm PD, Parker RG, Juillard G, Greenberg P (1984) A kinetic evaluation of blood-brain barrier permeability in human brain tumors with (68-Ga) edta and positron computed tomography. J Cereb Blood Flow Metab 4: 507–515
78. Herholz K, Pietrzyk U, Voges J, Schröeder R, Halber M, Treuer H, Sturm V, Heiss WD (1993) Correlation of glucose consumption and tumor cell density in astrocytomas. A sterotactic PET study. J Neurosurg 79: 853–858
79. Hiesiger E, Fowler JS, Wolf AP, Logan J, Brodie JD, McPherson D, McGregor RR, Christman DR, Wolkow ND, Flamm E (1987) Serial PET studies of human cerebral malignancy with (1-^{11}C) putrescine and (1-^{11}C)2-deoxy-D-glucose. J Nucl Med 28: 1251–1261

80. Hoffman RF, Werbe R (1976) High in vivo rates of methionine biosynthesis in transformed human and malignant rat cells auxotrophic for methionine. Proc Natl Acad Sci 73: 1523–1527
81. Holzer T, Herholz K, Jeske J, Heiss WD (1993) FDG-PET as a prognostic indicator in radiochemotherapy of glioblastoma. J Comput Assist Tomogr 17: 681–687
82. Hoop B, Hnatowich DJ, Brownell GL, Jones T, McKusick KA, Ojemann RG, Parker JA, Subramanyam R, Taveras JM (1976) Techniques for positron scintigraphy of the brain. J Nucl Med 17: 473–479
83. Horton RW, Meldrum BS, Bachelard HS (1973) Enzymic and cerebral metabolic effects of 2-deoxy-D-glucose. J Neurochem 21: 507–520
84. Hossmann KA, Niebuhr I, Tamura M (1982) Local cerebral blood flow and glucose consumption of rats with experimental gliomas. J Cereb Blood Flow Metab 2: 25–32
85. Huang SC, Phelps ME, Hoffman EJ, Sideris K, Selin CJ, Kuhl DE (1980) Non-invasive determination of local cerebral metabolic rate of glucose in man. Am J Physiol 238: E69–E82
86. Hubner KF, Purvis JT, Mahaley SM, Robertson Fr JT, Rogers S, Gibbs WD, King P, Partain CL (1982) Brain tumor imaging by positron emission computed tomography using ^{11}C-labeled amino acids. J Comput Assist Tomogr 6: 544–550
87. Iannotti F, Fieschi C, Alfano B, Picozzi P, Mansi L, Pozzilli C, Punzo A, Del Vecchio L, Lenzi GL, Salvatore M, Conforti P (1987) Simplified, non-invasive PET measurement of blood-brain-barrier permeability. J Comput Assist Tomogr 11: 390–397
88. Ikezaki K, Black KL, Toga AW, Santori EM, Becker DP, Smith ML (1990a) Imaging peripheral benzodiazepine receptors in brain tumors in rats: in vitro binding characteristics. J Blood Flow Metabol 10: 580–587
89. Ikezaki K, Black KL, Santori EM, Becker DP, Payne BA, Toga AW (1990b) Three-dimensional comparison of peripheral benzodiazepine binding with histological findings in rat brain tumor. Neurosurgery 27: 78–82
90. Ishii K, Ogawa T, Hatazawa J, Kanno I, Inugami A, Fujita H, Shimosegawa E, Murakami M, Okudera T, Uemura K (1993) High L-methyl-C11 methionine uptake in brain abcess: a PET study. J Comput Assist Tomogr 17: 660–666
91. Ishiwata K, Ido T, Vaalburg W (1988a) Increased amounts of D-enantiomer dependent on alkaline concentration in the synthesis of L-methyl-11C-methionine. Appl Radiat Isot 39: 311–314
92. Ishiwata K, Vaalburg W, Elsinga PH, Paans AMJ, Woldring MG (1988b) Comparison of L-[1-11C]methionine and L-methyl-[11C]methionine for measuring in vivo protein syntheis with PET. J Nucl Med 29: 1419–1427
93. Ishiwata K, Vaalburg W, Elsinga PH, Paans AMJ, Woldring MG (1988c) Metabolic studies with L-1-14C Tyrosine for the investigation of a kinetic model to measure protein synthesis rates with PET. J Nucl Med 29: 524–529

94. Ishiwata K, Hatazawa J, Kubota K, Kameyama M, Itoh M, Matzuzawa T, Takahashi T, Iwata R, Ido T (1989) Metabolic fate of L-(methyl-11C)-methionine in human plasma. Eur J Nucl Med 15: 665–669
95. Ishikawa M, Kikuchi H, Miyatake S, Oda Y, Yonekura Y, Nishizawa S (1993) Glucose consumption in recurrent gliomas. Neurosurgery 33: 28–33
96. Ito M, Lammentsma AA, Wise RJJ, Bernadi S, Frackowiak RJJ, Heather JD, McKenzie LG, Thomas DGT, Jones T (1982) Measurement of regional cerebral blood flow and oxygen utilisation in patients with cerebral tumor using ^{15}O and positron emission tomography: analytical technics and preliminary results. Neuroradiology 23: 63–74
97. Junck L, Olson JMM, Ciliax BJ, Koeppe RA, Watkins GL, Jewett DM, Mackeever PE, Wieland DM, Kilbourn JM, Starosta-Rubinstein S, Mancini WR, Kuhl DE, Greenberg HS, Young AB (1989) PET imaging of human gliomas with ligands for the peripheral benzodiazepine binding site. Ann Neurol 26: 752–758
98. Kameyama M, Tsurumi Y, Shirane R, Katakura R, Suzuki J, Itoh M, Fukuda H, Matzuzawa T, Watanuki S, Ido T (1987) Multi-parametric analysis of brain tumor with PET. J Cereb Blood Flow Metabol 7 [Suppl 1]: S466
99. Kaschten B, Sadzot B, Stevenaert A (1994) Evaluation of brain tumor metabolism by PET J. Neurooncology 21: 1
100. Kawai K, Fujibayashi Y, Saji H (1991) A strategy for the study of cerebral amino acid transport using iodine 123 labeled amino acid radiopharmaceutical: 3-idio-alpha-methyl-L-tyrosine. J Nucl Med 32: 819–824
101. Kessler RM, Goble JC, Bird JH, Girton ME, Doppman JL, Rapoport SI, Barranger JA (1984) Measurement of blood-brain barrier permeability with positron emission tomography and 68Ga EDTA. J Cereb Blood Flow Metab 4: 324–328
102. Kim KT, Black KL, Marciano D, Mazziotta JC, Guze BH, Grafton S, Hawkins RA, Becker DP (1990) Thallium-201 SPECT imaging of brain tumors: methods and results. J Nucl Med 31: 965–969
103. Kim CK, Alavi JB, Alavi A, Reivich M (1991) New grading system of cerebral gliomas using positron emission tomography with F-18 fluorodeoxyglucose. J Neurooncol 10: 85–91
104. Kirikae M, Diksic M, Yamamoto YL (1989) Quantitative measurements of regional glucose utilization and rate of valine incorporation into proteins by double-tracer autoradiography in the rat brain tumor model. J Cereb Blood Flow Metab 9: 87–95
105. Kubota K, Yamada K, Fukada H, Endo S, Ito M, Abe Y, Yamaguchi T, Fujimara T, Saro T, Ito K, Yoshioka S, Hatazawa J, Marsuzawa T, Iwata R, Ido T (1984) Tumor detection with carbon 11 labelled amino acids. Eur J Nucl Med 9: 136–140
106. Kubota K, Ishiwata K, Kubota R, Yamada S, Tada M, Sato T, Ido T (1991) Tracer feasibility for monitoring tumor radiotherapy: A quadruple tracer study with fluorine-18 fluorodeoxyglucose or fluorine-18 fluorodeoxyuridine, L-(methyl-14C) methionine, (6-3H) thymidine and gallium-67. J Nucl Med 32: 2118–2123

107. Lammertsma AA, Jones T, Frackowiak RSJ, Lenzi GL (1981) A theoretical study of the steady-state model for measuring cerebral blood flow and oxygen utilization using oxygen-15. J Comput Assist Tomogr 5: 544–550
108. Lammertsma AA, Wise RJ, Cox TC, Thomas DG, Jones T (1985) Measurement of blood flow, oxygen utilisation, oxygen extraction ratio, and fractional blood volume in human brain tumors and surrouding oedematous tissue. Br J Radiol 58: 725–734
109. Langen KJ, Coenen HH, Roosen N, Kling P, Muzik O, Herzog H, Kuwert T, Stöcklin G, Feinendegen LE (1990) SPECT studies of brain tumors with L-3-1231-iodo-alpha-methyl tyrosine: comparison with PET, 124 IMT and first clinical results. J Nucl Med 31: 281–286
110. Langen KJ, Roosen N, Coenen H, Kuikka JT, Kuwert T, Herzog H, Stoöcklin G, Feinendegen LE (1991) Brain and brain tumor uptake of L-3-1231-iodo-alpha-methyl tyrosine: competition with natural L-amino acids. J Nucl Med 32: 1225–1228
111. Laohaprasit V, Silbergeld DL, Ojemann GA, Eskridge JM, Winn HR (1990) Postoperative CT contrast enhancement following lobectomy for epilepsy. J Neurosurg 73: 392–395
112. Lasne MC, Barré L, Piarraud A, Lalaoui K, Giroux B, Derlon JM (1991) Synthesis of "no-carrier added" carbon-11 fotemustine. J labelled Comp radiopharma 30: 440–445
113. Leenders KL, Beaney RP, Brooks DJ, Lammertsma AA, Heather JD, McKenzie CG (1985) Dexamethasone treatment of brain tumor patients: Effects on regional blood flow, blood volume, and oxygen utilization. Neurology 35: 1610–1616
114. Levivier M, Goldman S, Bidaut L, Luxen A, Stanus E, Przedborski S, Balériaux D, Hildebrand J, Brotchi J (1992) Positron tomography guided stereotactic brain biopsy. Neurosurgery 31: 792–797
115. Levivier M, Goldman S, Pirotte B, Brucher J, Balériaux D, Luxen A, Hildebrand J, Brotchi J (1995) Diagnostic yield of stereotactic brain biopsy guided by positron emission tomography with 18F-Fluorodeoxyglucose. J Neurosurg 82: 445–452
116. Lilja A, Bergstrom K, Hartvig P, Spannare B, Halldin C, Lundqvist H, Langstrom B (1985) Dynamic study of supratentorial gliomas with L-methyl 11C-methionine and positron emission tomography. AJNR 6: 505–514
117. Magistretti PL (1983) Functional radionuclide imaging of the brain. Serono Symposia Publications 10d 5. Raven, New York
118. Martiat P, Ferrant L, Labard, Cogneau M, Bol A, Michel A, Michaux JL, Sokal G (1988) In vivo measurement of carbon-11 thymidine uptake in non Hodgkin's lymphoma using positron emission tomography. J Nucl Med 19: 1633–1637
119. Martins AN, Johston JS, Henry JM, Stoffel TJ, Di Chiro J (1977) Delayed radiation necrosis of the brain. J Neurosurg 47: 336–345
120. Maublant JC, Gachon P, Moins N (1988) Hexakis (2-methoxy isobulisonitrile) technetium-99m and thallium-201 chloride: uptake and release in cultured myocardial cells. J Nucl Med 29: 48–54

121. McKenzie CG, Lenzi GL, Jones T, Moss S (1978) Radioactive oxygen ^{15}O studies in cerebral neoplasms. J R Soc Med 71: 417–425
122. Meyer GJ, Schober O, Hundeshagen H (1985) Uptake of 11C-L- and D-methionine in brain tumors. Eur J Nucl Med 10: 373–376
123. Meyer CJ, Schober O, Gaab MR, Kietz H, Hundeshagen H (1989) Multiparameter studies in brain tumors. In: Beckers C, Goffinet A, Bol A (eds) PET in clinical research and clinical diagnosis. Kluwer, Dordrecht, pp 229–248
124. Mineura K, Yasuda T, Kowada M, Shishido F, Ogawa T, Uemura K (1986) Positron emission tomographic evaluation of histological malignancy in gliomas using oxygen-15 and fluorine-18-fluorodeoxyglucose. Neurol Res 8: 164–168
125. Mineura K, Sasajima T, Kowada M, Uesaka Y, Shishido F (1991) Innovative approach in the diagnosis of gliomatosis cerebri using carbon-11-L-methionine positron emission tomography. J Nucl Med 32: 726–728
126. Mosskin M, Holt V, Bergstrom M, Collins VP, Erikson L, Johnstrom P, Noren G (1987) Positron emission tomography with ^{11}C-methionine and X-ray computed tomography of intracranial tumors compared with histopathologic observations in multiples biopsies. Acta Radiol Diag 28: 673–681
127. Moulinoux JP, Le Calve M, Quemener V, Quash G (1984a) In vitro studies of the entry of polyamines into normal red blood cells. Biochimie 66: 385–393
128. Moulinoux JP, Quemener V, Larzul JJ, Le Calve M, Roch M, Toujas L, Quash G (1984b) Red blood cell polyamines in mice bearing the Lewis lung carcinoma (3LL) and in patients with bronchopulmonary cancers. Int J Cancer 34: 277–281
129. Moulinoux JP, Quemener V, Le Calve M, Chatel M, Darcel F (1984c) Polyamines in human brain tumors. A correlative study between tumor, cerebrospinal fluid and red blood cell free polyamine levels. J Neurooncology 2: 153–158
130. Murakami M, Takahashi K, Kondo Y, Mizuzawa S, Nakamichi H, Sasaki H, Hagami E, Iida H, Kanno I, Miura S, Uemura K (1988) 2-18F-phenylaline and 3-18F-tyrosine. Synthesis and preliminary data of tracer kinetics. J Labelled Comp Radiopharmaceut 25: 773–782
131. Ogawa T, Uemura K, Kanno I, Shishido F, Inugami A, Yamaguchi T, Murakamin M, Hirata K, Kato T, Mineura K, Kowada M (1988a) Delayed radiation necrosis of brain evaluated by positron emission tomography. Tohoku J Exp 155: 247–260
132. Ogawa T, Uemura K, Shishido F, Yamaguchi T, Murakami M, Inugami A, Kanno I, Sasaki H, Kato T, Hirata K, Kowada M, Mineura K, Yasuda T (1988b) Changes of cerebral blood flow and oxygen and glucose metabolism following radiochemotherapy of gliomas: A PET study. J Comput Assist Tomogr 12: 290–297
133. Olson JM, McNeel W, Young AB, Mancini WR (1992) Localization of peripheral-type benzodiazepine binding site to mitochondria of human glioma cells. J Neurooncology 13: 35–42
134. O'Tuama LA, Travers ST, Larar JN, Packard AB, Kwan AJ, Barnes PD, Scott RM, Black P, Mcl, Madsen JR, Goumnerova LC, Sallan SE, Tarbell

S, Tarbell NJ (1993) Thallium-201 versus technetium-99m-MIBI SPECT in evaluation of chilhood brain tumors: a within-subject comparison. J Nucl Med 34: 1045–1051

135. Pantano P, Baron JC, Crouzel C, Collard P, Sirou P, Samson Y (1985) The ^{15}O continuous-inhalation method: correction for intravascular signal using $^{15}CO_2$. Eur J Nucl Med 10: 387–391
136. Pappata S, Cornu P, Samson Y, Prenant C, Benavides J, Scatton B, Crouzel C, Hauw JJ, Syrota A (1991) PET study of carbon 11 PK 11195 binding to peripheral type benzodiazepine sites in glioblastoma: a case report. J Nucl Med 32: 1608–1610
137. Patronas NJ, Di Chiro G, Brooks RA, De La Paz RL, Kornblith PL, Smith BH, Rizzoli HV, Kessler RM, Manning RG, Channing M, Wolf AP, O'Connor CM (1982) Work in progress: (^{18}F) fluorodeoxyglucose and positron emission tomography in the evaluation of radiation necrosis of the brain. Radiology 144: 885–889
138. Patronas NJ, Brooks RA, de la Paz RL, Smith BH, Kornblith PL, Di Chiro G (1983) Glycolytic rate (PET) and contrast enhancement (CT) in human cerebral gliomas. AJNR 4: 533–535
139. Patronas NJ, Di Chiro G, Kufta G, Bairamian D, Kornblith PL, Simon R, Larson SM (1985) Prediction of survival in glioma patients by means of positron emission tomography. J Neurosurg 62: 612–622
140. Pegg AE, McCann PP (1982) Polyamine memtabolism and function. Am J Physiol 243: C212–C221
141. Pegg AE (1988) Polyamine metabolism and its importance in neoplastic growth and as a target for chemotherapy. Cancer Res 48: 759–774
142. Phelps ME, Huang SC, Hoffman EJ, Selin C, Sokoloff L, Kuhl DE (1979) Tomographic memasurement of local cerebral glucose metabolic rate in humans with (F-18)2-fluoro-2-de'oxy-D-glucose: validation of method. Ann Neurol 6: 371–378
143. Phelps ME, Barrio JR, Huang SC, Keen RE, Chugani H, Mazziotta JC (1986) Measurement of cerebral protein synthesis in man with positron computerized tomography: model, assumptions and preliminary results. In: Phelps ME, Mazziotta JC, Schelbert HR (eds) The metabolism of the human brain studied with positron emission tomography. Raven, New York, pp 215–232
144. Phelps ME, Mazziotta JC, Schelbert HR (1986) Positron emission tomography and autoradiography: principles and applications for the brain and heart. In: Phelps ME, Mazziotta JC, Schelbert HR (eds) The metabolism of the human brain studied with positron emission tomography. Raven-Press, New York
145. Pirotte B, Goldman S, Brucher JM, Zomosa G, Balériaux D, Brotchi J, Levivier M (1994) PET in stereotactic conditions increases the diagnostic yield of brain therapy. Stereotact Funct Neurosurg 63: 144–149
146. Plate KH, Breier G, Weich HA, Risau W (1992) Vacular endothelial growth factor is a potential tumor angiogenesis factor in human gliomas. Nature 359: 845–848

147. Preul MC, Caramanos Z, Collins DL, Villemure JG, Leblanc R, Olivier A, Pokrupa R, Arnold DL (1996) Accurate noninvasive diagnosis of human brain by using proton magnetic resonance spectroscopy. Nature Med 2: 323–325
148. Quemener V, Darcel F, Chatel M, Moulinoux JP (1986) Can polyamines act as positron emitter in cerebral oncology? Preliminary results obtained in nude mice bearing human glioblastoma xenografts. In: Chatel M, Darcel F, Pecker J (eds) Brain oncology. Martinus Nijhoff, Dordrecht, pp 201–204
149. Reivich M, Alavi A (eds) (1985) Positron emission tomography. Liss, New York
150. Reivich M, Alavi A, Wolf A, Fowler J, Russell J, Arnett C, MacGregor RR, Shiue CY, Atkins H, Anand A, Dann R, Greenberg JH (1985) Glucose metabolic rate kinetic model parameter determination in humans: the lumped constants and rate constants for 18F-fluorodeoxyglucose and ^{11}C-deoxyglucose. J Cereb Blood Flow Metab 5: 179–192
151. Rhodes CG, Wise RJS, Gibbs M, Frackoviak RSJ, Hatazawa J, Palmer AJ, Thomas DJT, Jones T (1983) In vivo disturbance of the oxidative metabolism of glucose in human cerebral gliomas. Ann Neurol 14: 614–626
152. Richfield EK, Ciliax BJ, Starosta-Rubinstein SR, Keever PE, Penney JB, Young AB (1988) Comparison of (14C)-deoxyglucose metabolism and peripheral benzodiazepine receptor binding in rat C6 glioma. Neurology 38: 1255–1262
153. Roelcke U (1994) PET: Brain tumor biochemistry. J Neurooncology 22: 275–279
154. Rogers S, Robertson JT (1981) A method of studying metabolic variation between individual tumors. Nutr Cancer 2: 148–149
155. Rottenberg DA, Ginos JZ, Kearfott KJ, Junck L, Bigner DD (1984) In vivo measurement of regional brain tissue pH using positron emission tomography. Ann-Neurol 15 [Suppl]: S98–S102
156. Rottenberg DA, Ginos JZ, Kearfott KJ, Dhawan V, Jarden JO (1985) In vivo measurement of brain tumor pH using (^{11}C) DMO and positron emission tomography. Ann Neurol 17: 70–79
157. Röttinger EM, Mendouca BA (1980) Modification of pH induced cellular inactivation by irradiation-glial cells. Int J Radiat Oncol Biol Phys 6: 1659–1662
158. Rozental JM, Levine RL, Nickles RJ, Dobkin JA (1989) Glucose uptake by gliomas after treatment. Arch Neurol 46: 1302–1307
159. Rozental JM, Cohen JD, Mehta MP, Levine RL, Hanson JM, Nickles RJ (1993) Acute changes in glucose uptake after treatment: the effects of carmustine (BCNU) on human glioblastoma multiforme. J Neurooncology 15: 57–66
160. Rutten EHJ, Doesburg WH, Slooff JL (1992) Histologic factors in the grading and prognosis of astrocytoma grade I–IV. J Neurooncology 13: 223–230
161. Sasaki M, Ichiya Y, Kuwabara Y, Otsuka M, Tahara T, Fukumura T, Gunasekera R, Masuda K (1990) Ringlike uptake of 18F-FDG in brain abcess: a PET study. J Comput Assist Tomogr 14: 486–487

162. Sato K, Kameyama M, Ishiwata K, Katakura R, Yoshimoto Y (1992) Metabolic changes of glioma following chemotherapy: an experimental study using four PET tracers. J Neurooncology 14: 81–89
163. Schifter T, Hoffman JM, Hanson MW, Boyko OB, Beam C, Paine S, Schold SC, Burger PC, Coleman RE (1993) Serial FDG-PET studies in the prediction of survival in patients with primary brain tumors. J Comput Assist Tomogr 17: 509–516
164. Shields AF, Quackenbush RC, Coonrod DV (1986) Development of C-11 thymidine as a PET imaging agent: biochemistry of its synthesis, degradation, and reutilization (abstract). J Nucl Med 27: 1033
165. Shields A, Lim K, Grierson J, Link J, Krohn K (1990) Utilization of labeled thymidine in DNA synthesis: studies for PET. J Nucl Med 31: 337–342
166. Shweiki D, Itin A, Soffer D, Keshet E (1992) Vascular endothelial growth factor induced by hypoxia may mediate hypoxia-initiated angiogenesis. Nature 359: 843–845
167. Sokoloff L, Reivich M, Kennedy M, Des Rosiers MH, Patlak CS, Pettigrew KD, Sakurada O, Shinohara M (1977) The 14C-deoxyglucose method for the measurement of local cerebral glucose utilization: theory, procedure, and normal values in the conscious and anesthetized albino rat. J Neurochem 28: 897–913
168. Sokoloff L (ed) (1985) Brain imaging and brain function. Raven, New York
169. Tjuvajev J, Abrams D, Ginos J, Desai R, Finn R, Blasberg R (1993a) Iododeoxyruidine (IUdR) imaging for tumor proliferation: correlation with kinetic parameters of local tumor cell proliferation. Neurology 43: A399
170. Tjuvajev J, Muraki A, Ginos J, Berk J, Kourcher J, Ballon D, Beattie B, Finn R, Blasberg R (1993b) Iododeoxyuridine uptake and retention as a measure of tumor growth. J Nucl Med 34: 1152–1162
171. Tsurumi Y, Kameyama M, Ishiwata K, Katakura R, Monma M, Ido T, Suzuki J (1990) ^{18}F-fluoro-2 deoxyuridine as a tracer of nucleic acid metabolism in brain tumors. J Neurosurg 72: 110–113
172. Tyler JL, Yamamoto YL, Diksic M, Theron J, Villemure JG, Worsinghton C, Evans AC, Feindel W (1986) Pharmacokinetics of superselective intra-arterial and intravenous (^{11}C) BCNU evaluated by PET. J Nucl Med 27: 775–780
173. Tyler JL, Diksic M, Villemure JG, Evans AC, Meyer E, Yamamoto YL, Feindel W (1987) Metabolic and hemodynamic evaluation of glicomas using positron emission tomography. J Nucl Med 28: 1123–1133
174. Tyler JL, Strother S, Zatorre RJ, Alivisatos B, Worsley KJ, Diksic M, Yamamoto YL (1988) Stability of regional cerebral glucose metabolism in the normal brain measured by positron emission tomography. J Nucl Med 29: 631–642
175. Vander Borght T, Pauwels S, Lambotte L, Labar S, De Maeght S, Stroobandt G, Laterre C (1994) Brain tumor imaging with PET and 2-(carbon-11) thymidine. J Nucl Med 35: 974–982
176. Viader F, Derlon JM, Petit-Tavoué MC, Shishido F, Hubert P, Houtteville JP, Courtheoux P, Chapon F (1993) Recurrent oligodendroglioma diagnosed with ^{11}C-L-methionine and PET: a case report. Eur Neurol 33: 248–251

177. Volkow N, Goldman SS, Flamm ES, Cravioto H, Wolf AP, Brodie JD (1983) Labeled putrescine as a probe in brain tumors. Science 221: 673–675
178. Wackers F, Berman D, Maddahi J (1989) Technicium-99m hexakis 2-methoxyisobutyl isonitrile: human biodistribution, dosimetry, safety and preliminary comparison to thallium-201 for myocardial perfusion imaging. J Nucl Med 30: 301–311
179. Warburg O (1956) On the origin of cancer cells. Science 123: 309–314
180. Warnick RE, Pietronigro DD, Duncan D, Mc Bride Q, Flamm ES (1989) In vivo metabolism of radiolabeled putrescine in gliomas. Implications for positron emission tomography of brain tumors. Neurosurgery 23: 464–469
181. Weisberg LA (1980) Cerebral computed tomography in diagnosis of supratentorial astrocytoma. Computerized tomography, vd 4. Pergamon, Elunsford, NY, pp 87–105
182. Wike-Hooley JL, Van den Berg AP, Van der Zee J, Reinhold HS (1985) Human tumour pH and its variation. Eur J Cancer Clin Oncol 21: 785–791
183. Wilson MJ, Poirier LA (1987) An increased requirement for methionine by transformed rat liver epithelial cells in vitro. Exp Cell Res 111: 397–400
184. Yamaguchi T, Ssaski H, Ogawa T, Mineura K, Uemura K, Kanno I, Shishido F, Murakami M, Inugami A, Higano S (1986) Relation between tissue nature and (18F) fluorodeoxyglucose kinetics evaluated by dynamic positron emission tomography in human brain tumors. Acta Radiol [Suppl] 369: 415–418

Use of Surgical Wands in Neurosurgery

L. Zamorano, F. C. Vinas, Z. Jiang, and F. G. Diaz

Department of Neurosurgery, Wayne State University, Detroit, MI (U.S.A.)

With 18 Figures

Contents

Introduction

Recent technological developments in neuroimaging and surgical techniques, including the use of interactive image-guided surgical procedures, have opened new frontiers in neurosurgery. Advances in imaging techniques have created the need for more precise navigational assistance, in order to approach image-defined lesions. Several methods that transform coordinates from imaging studies to the surgical field have been developed and used in intraoperative guidance systems.

Interactive image-guided surgery implies a methodology that translates into accurate and reliable image-to-surgical space guidance. The methodology involves three components: image acquisition, with definition of coordinate space from one or several imaging modalities, planning or simulation of the surgical procedure, and intraoperative surgical procedures, which include the determination of the spatial relationship between the image and the surgical coordinate space.

The critical component in interactive image-guided surgery is the use of an intraoperative localizer system or a digitizer or "surgical wand", which ultimately provides the surgeon useful navigational information usually in the form of position and/or orientation of surgical instruments. Thus, the accuracy of a localizing system is limited to that of the digitizer being used (7). The other important component of interactive systems is the intraoperative computer system and display of the images to achieve surgical guidance.

This chapter will review the methodology for interactive image-guided surgery including the different strategies to achieve image-to-image and image-to-surgical space co-registration, the different digitizing technologies, and some of the clinical implementations that have been developed. Having reviewed the methodology and instrumentation, this chapter will look at the different clinical and future applications of these systems.

Image Acquisition and Registration

The advent of digital imaging such as computed tomography (CT), magnetic resonance imaging (MRI), and positron emission tomography (PET) has resulted in images with exquisite detail. In order for these images to be available for manipulation by the surgeon, the images need to be registered with one another (multi-modality image registration) and with physical space (image-to-surgical space registration). Registration is defined as the determination of one-to-one mapping between the coordinates in one space and those in another. There are several different registration techniques, including stereotactic frame systems, which involves the use of a headframe, and frameless methods such as point, curve and surface, moment and principal axes, correlation, interactive, and atlas methods. Because the registration process is one of the most important steps in interactive image guidance we will discuss it at length.

Registration Methods

Stereotactic Frame-based Methods

Stereotactic frames constitute a mechanical device used to accurately position an instrument such as a biopsy probe or an electrode in three-dimensional (3-D) space. Current stereotactic systems include those based on a stereotactic reference frame that provides rigid skull fixation using pins or screws and defines a stereotactic coordinate system in physical space, those derived from an image localizing system, and a system or arch for mechanical direction of a probe to a defined intracranial target. The problems with stereotactic headframes are many; attaching them to patients means some degree of invasiveness and they obstruct some areas of the skull where access is crucial, such as a combined supra-infratentorial approach used in skull base surgery. Also, using a headframe to register imaging studies logistically implies the acquisition of images the same day (although there are possibilities of relocation in almost all systems). Using a headframe means that the intraoperative procedure is not interactive (although there are exceptions as we will see later) and that their use is limited to surgery since they are invasive. Nevertheless they are an accurate and reliable registration method. To avoid invasiveness attempts have been made to use a "mask" fixation system, but of course this is not possible in many craniotomies.

The image localizing system consists in N-shaped (Brown-Robert Wells, BRW [6], Leksell [33], Todd-Wells [17]) or V-shaped bars (Riechert-Mundinger, Zamorano-Dujovny (Z-D) systems) that are attached to the base frame during image acquisition. The rods appear as fiducial markers arranged around the images; the positions of these fiducial points are used to calculate the position of any point on the image in the physical space coordinate system defined by the base frame. Thus, stereotactic frames provide a registration methodology for image-to-image and image-to-space.

It is important to understand that stereotactic frames can be used exclusively for image-image registration and a digitizer then used for image-to-space registration. The advantage of this approach is to bring in interactive image guidance but keep the accuracy and sometimes simplicity of placement of the stereotactic frame. The frame can be used also as the head-holder in many of the cases. We have currently worked with an open ring to facilitate combined supra-infratentorial approaches and/or decrease airway obstruction [63].

Frameless Methods

The most relevant frameless methods currently used with digitizers are the point method and the curve-surface method. *Point methods* involve the determination of the coordinates of corresponding points in different images and/or physical space and the estimation of the geometric transformation using these corresponding points (Fig. 1a). The points may be anatomical landmarks (intrinsic markers) [24] or external fiducials (extrinsic markers) [36] that may be used as non-invasive or invasive implantable markers. Registration based on anatomical landmarks is difficult and generally less accurate for image-to-space registration than extrinsic markers.

Extrinsic markers as temporary non-invasive markers can be used to register multi-modality images and for image-space registration. Of course, the major disadvantage to this method of registration is that if the patient moves or the markers attached to the skin move registration is not accurate. Further improvement is achieved with implantable markers that bring the accuracy of stereotactic frames to the registration process, but this also means reintroducing a level of invasiveness; for this reason we recommend this method only if surgery follows closely.

On the other hand, as we mentioned earlier, a stereotactic frame can be used as an extrinsic marker in conjunction with digitizers; the question then becomes which method is less cumbersome, i.e. implantable markers vs placement of the stereotactic frame; probably the answer depends more on the surgeon's preference and type of planned approach. The last is especially true if we consider that image-to-space registration with markers requires fixation of the patient's head.

Curve and Surface Methods

These methods involve the determination of the coordinates of corresponding curves or surfaces in different images and/or physical space and estimating the geometric transformation using these corresponding structures (Fig 1b). The curves or surfaces are derived from intrinsic structures such as skin surface that allows CT-MRI registration, or brain surface used to co-register MRI/PET scans. Pelizzari and Chen developed a surface-based approach for registering multi-modality images in which they fit a set of points ("hat") extracted from contours in one image, to a surface model ("head") extracted from contours in the other image [8, 41]. Several improvements of this registration technique have been reported by different authors in order to improve the accuracy of registration or optimize the time necessary to achieve those calculations [26]. This technique has been used to register MRI, CT, PET, and single photon emission computed tomography scans (SPECT). It has also been used to register image and physical space. It requires a 3-D digitizer: once one to two hundred points are acquired, this digitizer-derived surface is then registered to an image-derived surface using a surface matching algorithm. Levin was the first one to describe this approach using surface mapping of the skin created by touching it with a magnetic digitizer [34, 35]. We have used this approach with the infrared-based digitizer. In order to improve timing and accuracy we have used a combination of the point method and surface matching.

Other Methods

Other methods available are limited to image-to-image registration, and have not been used for intraoperative interactive image guidance. They are of limited use to the neurosurgeon and include moment and principal axes methods, which involves registering images by bringing the principal axes of corresponding objects in the images into coincidence [2]. This method uses the total volume of data, making registration accuracy very sensitive to missing data, since it requires that the entire object be present in both image sets. Also, the technique is very sensitive to pathology.

Another method is correlation [27], registering images by determining the transformation that optimizes a similar criterion between one image and the other transformed image. Correlation methods are primarily used for mono-modality image registration like the comparison of serial images for follow-up. The interactive method creates corresponding brain slices from multi-modality image volumes in individual patients. The method is

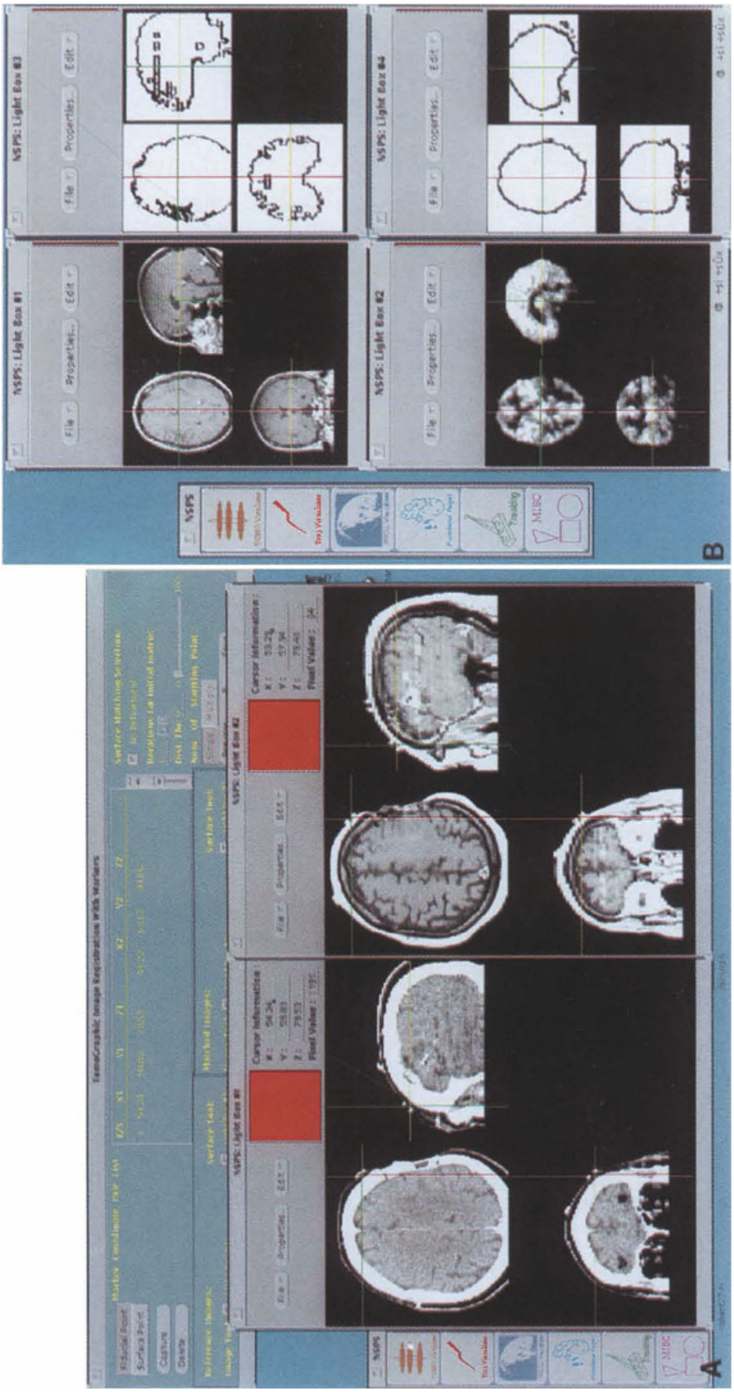

Fig. 1. Image to image registration. (A) Point to point registration. The cross section shows the fiducial marker in all three planes; in order to optimize the localization of the center, is necessary to match three fiducial markers. (B) Surface-based registration: in this case, an example of MRI-PET coregistration using surface matching is presented. Upper right image shows the computer-extracted surface of the brain based on the MRI (upper left). The lower right shows the computer-extracted brain surface from the PET data (lower left). A subsequent step will match both structured contours and from them, the MRI-PET data set will be coregistered

time-consuming, requires precise knowledge of the anatomy, and is less accurate.

The atlas method involves the registration of images with an anatomic atlas. One approach is to establish a brain coordinate reference system such as the AC-PC line in the Tailarach proportional grid system [52]. This technique may be useful to the neurosurgeon for surgical planning; the limitations include the variability of normal brains and the pathological processes. One approach to overcome the first is a technique to elastically deform a 3-D computerized brain atlas to match the individual image volume [3, 10].

The Surgical Planning Process: An Overview

By analyzing data for each patient the surgeon can begin to develop a plan for each part of the operative procedure, such as devising a route to approach a target, the size and location of the craniotomy, electrode placement, pedicle screw position and orientation, and other aspects of surgical treatment. The objectives of surgical planning include designing, evaluating, and optimizing the surgical approach, and anticipating any problems that may occur during the procedure.

The traditional method of surgical planning was based on two-dimensional (2-D) cross-sectional x-ray images, which required the surgeon to extrapolate the 3-D configuration of anatomy and tumor areas by deduction. This method was far from accurate and carried a potentially high degree of human error. With the development of 3-D medical imaging, pathological information can be viewed in 3-D using a variety of visualization methods [42]. Different image modalities (CT, MRI, SPECT, PET) and various correlation and fusion methods mean surgeons can get direct, accurate, and reliable 3-D information for different anatomical and physiological pathology (Fig. 2). It is the stereotactic technique that makes it possible for a surgeon to proceed with a plan that begins with precise definitions of tumor volumes and locations. Intraoperatively, real-time display of the procedure on the computer monitor helps guide the surgeon through the preplanned surgical approach. Computer digitized atlases are also used in conjunction with the patient's actual anatomy to locate critical structures and thus avoid collateral damage during the procedure.

Planning Applications

Many surgical planning systems have been developed for a variety of procedures. In neurosurgery, planning systems have been developed for brain surgery and spine surgery. All planning systems are some form of integration of visualization, manipulation, analysis, and database management tools.

Once basic imaging studies have been done and registered to each other and an anatomical atlas, the data set is ready for multi-planar reconstruction (MPR), 3-D surface and volume rendering, and manipulation using a variety of computer-based modules that conduct image segmentation, enhancement, and fusion.

Surgical plans are formulated specifically for different surgical purposes such as stereotactic open surgery (a stereotactic biopsy, stereotactic resection), epilepsy surgery, functional surgery, brachytherapy, and radiosurgery. To create routes for approaching targets, volume definition for resection, location and shape of craniotomy, and location and orientation of electrode grids, accurate geometric information is needed as the basis for calculations. Other contexts in which geometry is used includes deriving parameters for implanting radioactive seeds, parameters for functional stimulation, and setup parameters for various instruments such as stereotactic arcs and medical robots.

Planning the Surgical Approach

The planning process contains multiple cycles of consecutive steps: definition/modification, simulation, and evaluation. The cycle is complete when a surgical plan is constructed.

Planning Definition/Modification

In this step, the surgeon analyzes all available information about a specific patient and plans surgical approaches inside the virtual patient environment, which is comprised mainly of medical images such as CT, MRI, PET, SPECT, and X-ray.

Geometric analysis of patient data is crucial for this step. Segmentation tools are used, if necessary, to segment a lesion and other volumes of interest (VOI); these volumes help guide the resection process during surgery. Other VOIs can be used to highlight important anatomy and physiology. In addition to volume measurement, stereotactic position measurements, distance measurements, and area measurements are also basic components of geometric analysis.

Once a target has been defined, it can be approached in a simple straight line, or a curved line for more complex lesions. The straight line approaches are frequently used in stereotactic biopsies, and are defined by two points, an entry point and a target point. The target point can be defined somewhere in the lesion, in most cases the center. The entry point is used mainly to define the orientation of the approach. It may, but not necessarily so, be the real entry position on the skin, skull, or brain surfaces.

The curved approach is often used for more complicated procedures to approach deep targets with minimal damage to normal tissue. It can be defined by multiple points along the planned approach. Both straight line and curved approaches can be defined using computer visualization and manipulation tools. Positions of points can be digitized either from MPR, 3-D surface/volume rendering, or even projective image tools which contain cross-sectioned projected x-ray images. The MPR techniques can produce oblique and surgeon's perspective views; these will be discussed in further detail in the section about simulation.

Determining the size and shape of the craniotomy around the entry point is also part of the planning process. The benefit of craniotomy planning is that the surgeon can design an efficient opening to expose only as much brain as necessary, and reduce the chance of making an oversized opening, which happens sometimes using traditional surgical procedures. Craniotomy planning can be done either by shape parameters (side size for rectangular areas and diameters for circular shapes) or by arbitrarily drawing on a computer-imaged 3-D skull rendering. The planned shape can be executed intraoperatively during surgical procedures by tracking the movement of a marking pen.

For epilepsy surgery, electrode grids can be placed over suspicious brain surface areas during pre-planning, thereby defining their position and orientation. Doing so not only increases the chance of precise capture of lesion areas, but also helps to plan the craniotomy to avoid oversized openings. Steps for electrode planning proceed by locating suspicious areas in the virtual patient environment based on both the surgeon's knowledge and medical image studies like an activation study using PET. Once the suspicious area is located, the number of electrodes and the shape of grids are determined based on size and shape of the area. Currently all existing electrode grids are rectangular shaped; position and orientation of grids can be defined by digitizing three corner points of the rectangle on the 3-D brain surface rendering display.

For functional surgery, locating functional targets is still a challenge. Images such as functional MRI, PET, and SPECT scans reveal some, but not all, physiological information about the patient's brain activities. Computer digitized functional atlases can be warped to fit a specific patient's anatomical structure, which in turn help determine functional targets. However, determining warping algorithms used to make atlases for specific patients is still an uncertain science, due to random variations among individual anatomical and physiologic structures. Anatomical variation for a specific individual can be forecasted with a limited level of confidence. Methods for absolute accurate forecasting do not exist right now; that means a functional atlas can only be used as a reference. With functional targets localized, surgical approach planning is the same as general stereotactic open procedure planning.

For brachytherapy and radiosurgery, besides definition of target volume and designated surgical approaches, a radiation dosage has to be prescribed and analyzed during the planning process. For brachytherapy, catheters and seeds are defined and modified based on calculation of dosage distributions. The objective is to deliver prescribed dosages to cover as much of the target volume as possible and avoid surrounding areas. It is the same principle for Linax or Gamma knife radiosurgeries. The difference is that different parameters (number of shots, iso-centers, collimator size) are adjusted to accomplish the goal.

Modification or optimization of the plan can be done either automatically, semi-automically, or fully by surgeons. Automatic optimization is done by the computer system alone. The objective of the plan is translated into a cost function inside the computer; by minimizing cost functions, the system can generate an optimal plan that is more efficient and safe.

Planning Simulation

Once the plan is defined, the surgeon can view the simulation in the patient virtual environment. Simulation results help surgeons get the "look and feel" of their surgical strategies, crucial for planning evaluation and refinement. Simulation can be done on the virtual environment which is built upon medical images of the patient. The MPR is an efficient tool for simple surgical approach simulations. With MPR, several oblique reconstructed images along the planned trajectory can be created and viewed. Also, a series of surgeons' perspective views perpendicular to the trajectory and reconstructed at different depth locations along the trajectory can be constructed using MPR techniques. These views simulate the surgeons' view during the actual surgical procedure when approaching the target following the planned trajectory. Then, 3-D surface rendering and volume rendering techniques are used to simulate the surgical result based on the planned strategy. Displaying electrode grids over the suspicious area of the brain, the opened skull, and the brain surface under it to simulate the surgical view after craniotomy, offer surgeons rich 3-D information about the operative plan.

Evaluation

After simulation, surgeons have accurate information about possible surgical processes for the planned strategy. The plan then has to be evaluated based on possible surgical outcomes. Criteria such as effectiveness, efficiency, and safety are used to determine if the plan needs to be further refined. If the decision is further refinement, then the plan process restarts its cycle from the definition/modification step. Otherwise, the planning process is finished and planning reports that include instrument setting and other crucial parameters are printed for the actual surgery.

Issues Related to Surgical Planning

Preplanning and Intraoperative Planning

For general stereotactic surgery, strategies are planned before the actual surgery procedures. With the availability of intraoperative techniques, a surgical plan can be done right at the time of surgery in the operating room. Surgeons can plan approaches by directly positioning the intraoperatively tracked surgical instrument on the patient's head. Since the intra-operative tracking system offers immediate feedback, optimal position and orientation can be quickly achieved.

On-line Anatomical and Physiological Reference for Surgical Plan Optimization

Planning evaluation and optimization can also be based on digitized anatomical and physiological atlases embedded within the surgical planning system. Using digitized anatomical and physiological atlases as an on-line planning reference is an efficient way for planning optimization. Current research on virtual brain modelling enables planning systems to offer some crucial information for plan optimization. For example, once the functional areas are modelled and customized for a specific patient, given a surgical approach, the surgical planning system can tell surgeons which functional area the approach might pass through, and provide the accompanying geometry of measurements of the trajectory.

Human Interface Factors

Any computer application system designs are considered poor if they do not consider human interfaces. Human-machine communications are very important and often neglected issues. A high performance user interface system should be safe, efficient, and easy to use. Besides a computer mouse and keyboard, voice recognition, bio-sensors, and tracking devices are also introduced into an advanced surgical planning system. Information output devices include head-mounted display and holography.

Surgical Planning and Simulation

Wayne State University Surgical Planning System: Hardware and Software Configuration

At Wayne State University surgical pre-planning and simulation takes place on a SPARC 10 workstation (Sun Microsystems Inc, Mountain View, CA 94043) with 64 Mbyte memory space. This workstation is part of a complete local network system connected to all imaging systems available in the Medical Center, and is located in a control room overlooking the surgical suite, equipped with a complete video system for intraoperative image capturing and display (Fig. 2).

The main imaging modalities we use are CT, MRI, and digital angiography (DA). These modalities link digital images with real-world coordinates corresponding to the patient's actual anatomy in two ways, as previously discussed: a frame-based reference system, and a frameless system.

The NSPS Software

Once the imaging studies are completed and correlated through the registration process, the information is made available to the neurosurgeon for pre-planning and simulation through the use of software developed at Wayne State called the Neurosurgical Planning System (NSPS). The NSPS software runs under an "Open Windows" environment and consists of several modules able to interact and display at the same time. This feature is especially important for intraoperative localization where several image modalities are used simultaneously to track the position of surgical instruments on the computer monitor.

Data Manipulation Modules from the NSPS Software

These computer graphic modules include a patient database management module, a projective image visualization module, a tomographic image visualization module, a resident functional atlas, a three-dimensional (3-D) visualization module, and a position tracking module. During pre-planning, neurosurgeons first define volumes of interest (VOIs) such as lesions' ventricle, or tumors, in tomographic image visualization module, projective image visualization module, and/or the resident functional atlas module. The VOIs can be created from several different imaging studies, including CT, MRI, the resident atlas, or a combination of these. In 3-D visualization module, these studies can be projected together; the surgeon then defines an entry point and a target point which together comprise a trajectory for the surgical instrument. In NSPS, points can be digitized in slice

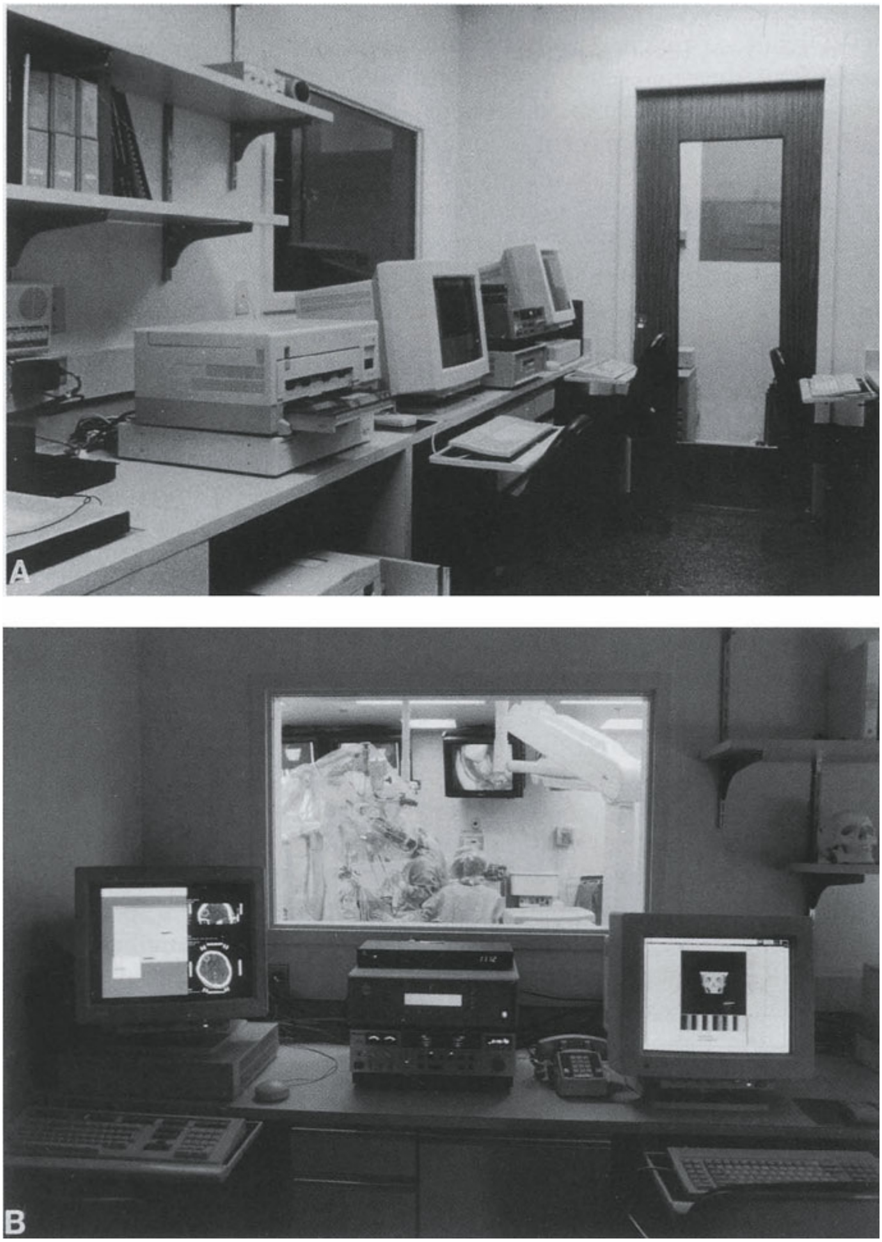

Fig. 2. (A) Computer workstations located next to the operating suite for preoperative planning and simulation. (B) The surgical suite, showing the planning room overlooking the operating room through a glass window. This room is also networked to other operating rooms. A workstation located in the operating room is used for intraoperative interactive guidance

images (CT, MRI, resident atlas), projective images (DA), or as images of the VOI surface area in 3-D visualization module.

Each module makes a unique contribution to the planning/simulation process. The patient database management module consists of three submodules that modify patient information through three channels: data input, data query, and data modify. In addition to tracking and organizing the files created during the preplanning study such as a patient's VOI file, lesion boundary file, surgeon's perspective file, and others created in the course of designing a patient's treatment protocol, this module is responsible for adding patients, scheduling surgery cases, and loading imaging data from pre-operative studies (CT, MRI, DA).

The projective image visualization module uses 2-D projective X-ray and angiography pictures to create 3-D data. It offers a way to digitize points, needles (trajectories), and VOIs that can then be displayed and used interactively with other modules for multi-modality image correlation.

Tomographic image visualization module is designed for viewing slice-based images from diagnostic modalities such as CT, MRI, and PET. Axial, sagittal, coronal, and oblique CT images generate information to neurosurgeons regarding tumor volumes through a series of surgeon's eye-view perspectives for each trajectory, which can be manipulated to focus on specific details of the tumor. More than one tomographic image visualization module can be opened at a time, each one containing a different image modality (CT, MRI). Each visualizer gives axial, sagittal, and coronal views passing through the intersection point. (Fig. 3A–C)

The resident functional atlas module displays and manipulates a functional neurological atlas. Since variations exists between a patient's brain structures and the standard atlas, a full scan of the standard functional atlas is used as a starting point to map certain points between the patient's brain and the atlas. Then it warps the standard atlas so that all points are matched. The result of the warping algorithm is a unique atlas for each patient. The NSPS superimposes the new atlas on any view of the brain constructed in tomographic image visualization module, and projects the structure on angiographic images in projective image visualization module. It also displays defined VOIs on the atlas in 3-D visualization module.

The 3-D visualization module manipulates VOIs by segregation, combination, and then projecting them in 3-D. Segmentation includes threshholding and tracing, gradient boundary detection, and region growing, among other functions. This feature can be used with different image modalities, creating from each modality several different VOIs. Using coordinate mapping, different VOIs are combined in the same display space with correct relative orientation and position. (Fig. 3D–E)

The display mechanisms in 3-D visualization module include surface rendering, volume rendering, projection rendering, and any combination of these three. Surface rendering treats each VOI as sets of polygons, and displays all the polygons with shading as well as transparency techniques on the screen. With volume rendering any necessary voxel values are displayed, offering detailed information for each VOI. In the projective rendering module, maximum intensity projections (MIPS) render the volume on the display by sets of projection beams passing through the volume and obtaining the maximum voxel value to be posted to the screen.

The position tracking module is used during surgery to display the position and orientation of the surgical instrument. We use three tracking devices: a Zamorano-Dujovny (Z-D) arc digitizer (Multipurpose Neurosurgical Localizing Unit, F.L. Fischer, Freiburg, Germany), an articulated arm, and an infrared digitizer. All these devices are connected on one end to surgical instruments and on the other end to a personal computer (PC), which in turn is connected with an NSPS workstation (Fig. 3E).

The position tracking module maps the tracking device coordinate system with an NSPS reference coordinate system. The mapping scheme varies depending upon whether a frame-based or frameless system of reference is used. After performing the calibration for either system a transformation matrix is obtained. When the NSPS receives position and orientation parameters, it transfers them into a reference coordinate system used by all the NSPS modules. Intraoperative display of the position and orientation of surgical instruments together with 2-D images and 3-D VOIs are presented to the surgeon through this module.

Intraoperative Display and Guidance

The intraoperative display provides the neurosurgeon with crucial information for localization and orientation. The information is presented in multiplanar views, 3-D views, 3-D views with cutaway planes, oblique views, surgeon's/instrument's perspective view, and with an instrument navigator to provide interactive target-trajectory guidance. The best way to display this information may vary according the type of procedure and the surgeon's preference.

Surgeon-Computer Interface

The majority of the currently available systems display information on computer screens, making the surgeon move her/his head to view the procedure. Heads-up displays have been used to show contour information in surgical microscopes. Much work needs to be done to provide the information in an easier way. The same is true in order to activate different portions of the registration and localization process; currently the

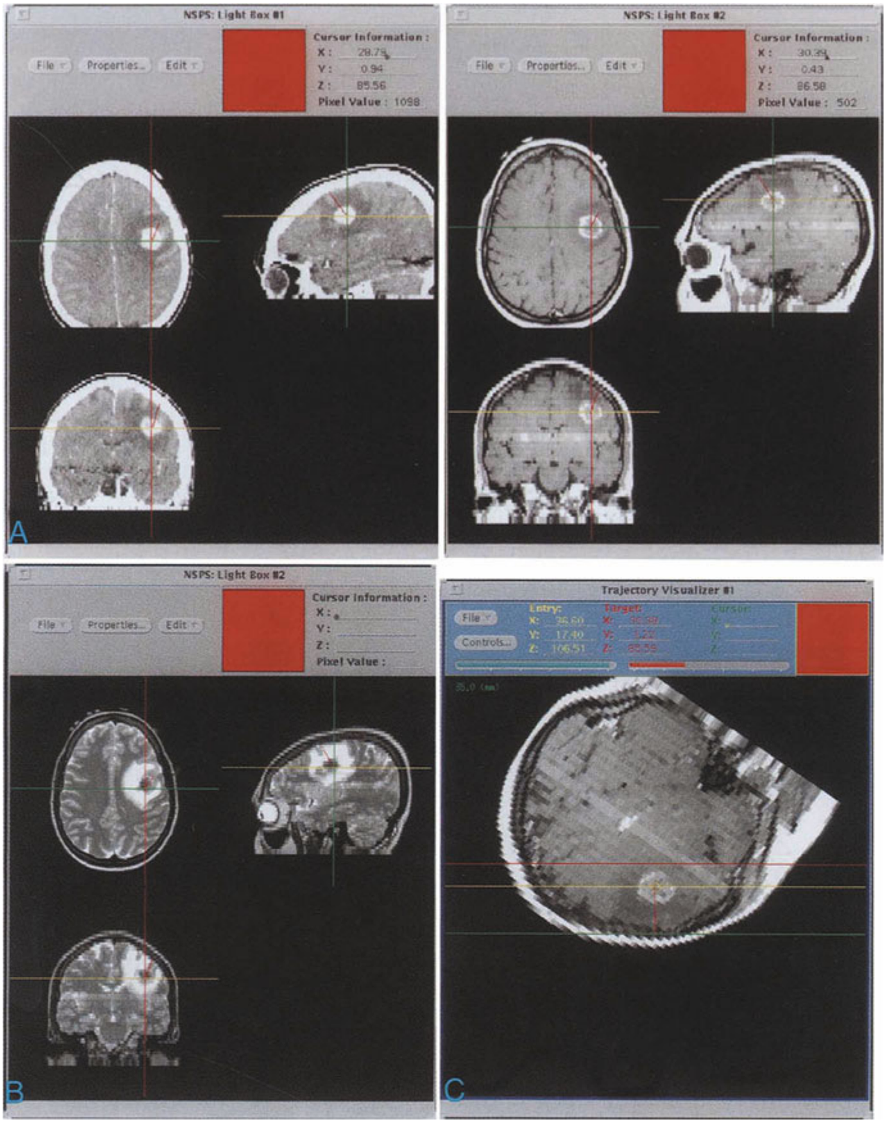

Fig. 3 (A–C)

Fig. 3. Surgical planning and intraoperative target/trajectory guidance. (A) Coregistered MRI-CT showing the surgical trajectory in multiplanar views. (B) The same lesion in T_2-weighted images. This example shows how the same image modality can be used in different acquisition modes to provide different types of information. (C) Oblique view reconstructed from the plane of the defined trajectory. The centered line indicates the chosen target level (level = 0) and the green and red lines defines the superficial and deeper defined limits for reconstruction of the surgeon's perspective views; (D) Surgeon's perspective view at the 0 level; (E) 3-D reconstruction from the surgeon's point of view with the defined trajectory; (F) Instrument navigator showing the point of the pointer at the different levels of the trajectory

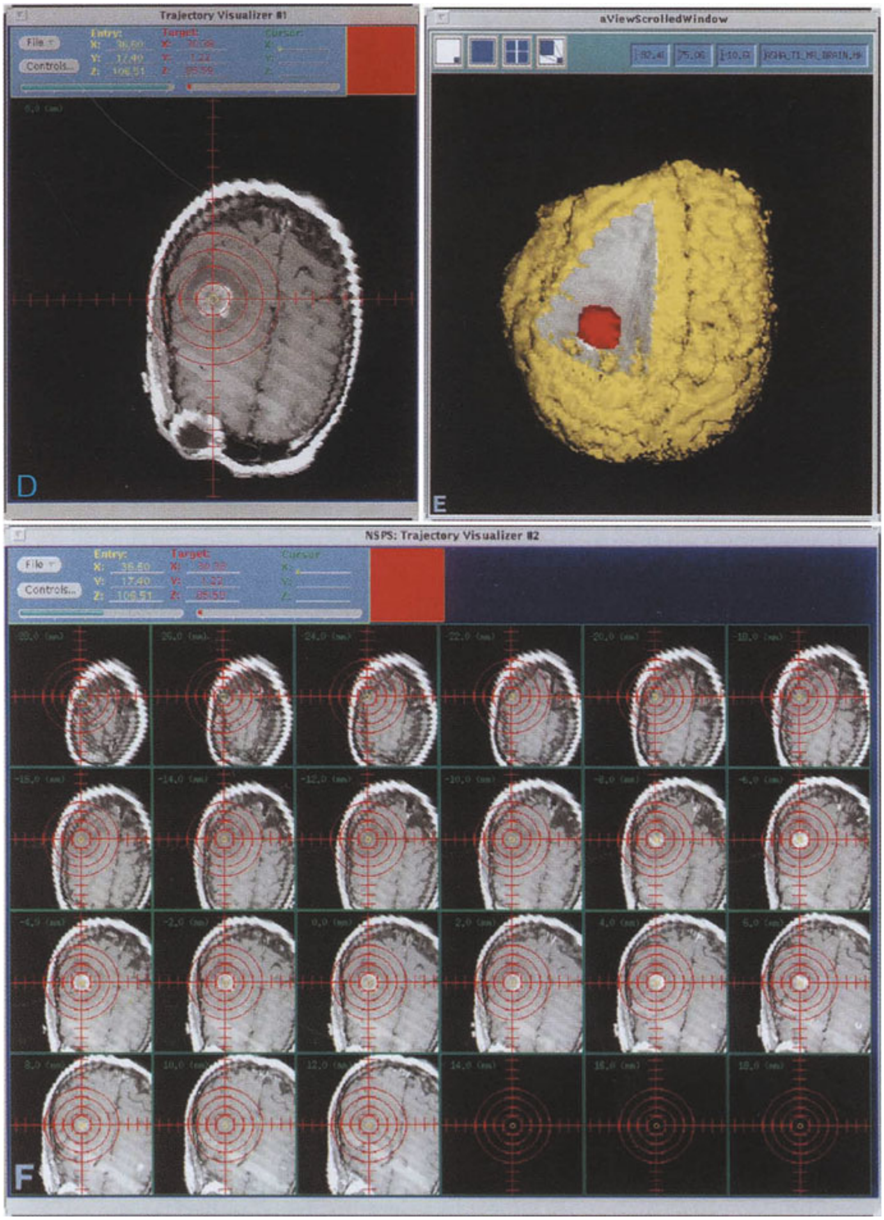

Fig. 3 (D–F)

majority of the systems require technical support to enter commands on computers. Newer technology using a "touchless" type of computer-surgeon interaction such as voice recognition is being developed and appears promising.

Intraoperative Digitization

The quest for accurate information during neurosurgical procedures has led to development of a number of different systems to provide intraoperative interactive image localization. The development of interactive image-guided neurosurgical techniques has revolutionized the diagnosis and surgical management of a wide range of intracranial disorders. A number of systems incorporate 3-D digitizers in the operating room and move easily between the coordinates of imaging studies and the operating field. It is important to understand that for a digitizer to become a useful surgical wand some requirements must be met. Systems for intraoperative localization require one or more registered image data sets, a pointing device, digitizer, or wand to be used in the operating room, a process to register these two coordinate systems (image-to-space registration), and a display to provide the surgeon with useful presentation of localizing information.

Localizing systems or digitizers allow the spatial registration of imaging data in the surgical field. In addition to locating small subcortical or deep lesions, this technology can provide volumetric information about the extent of the lesion or normal neighboring structures.

Passive and Active Digitizing Systems

Systems for intraoperative digitization can be broadly divided into two categories: passive and active systems. Passive systems provide sophisticated preoperative planning and intraoperative interactive localization on preacquired images. These provide constant feedback on the position of a surgical instrument in image space with continuous participation by the surgeon. Passive digitizers include the modified stereotactic frame, articulated arms, sonic digitizers, magnetic digitizers, and optical digitizers.

Passive digitizers can be classified into two groups: those that require a mechanical link between the pointer and the digitizing technology (linked systems), and those that do not (non-linked systems). Mechanical linked systems usually consist of articulated arms while non-linked systems rely upon the detection of signals generated by emitters attached to the surgical instrument and a receptor array. Such systems localize using magnetic, sonic, or optical emissions [7], while their pointing device can be either the surgical microscope or a surgical instrument.

Active systems are controlled by a computer, and consist of robotic systems adapted for stereotactic neurosurgery. We will review the different digitizing technologies and present the most used clinical implementations.

Passive Systems

Modified Stereotactic Frame (Arc Digitizer)

In this approach, we modified a conventional stereotactic arc by adding optical encoders (Z-D arc digitizer). The base ring and the image registration process follow the conventional stereotatic approaches.

During the surgical procedure, the Z-D arc digitizer provides accurate localization and steady fixation of surgical instruments (Fig. 4). This arc digitizer provides on-line trajectory setting and instrument position tracking by integrating the Z-D localizing unit with the computer system that presents the image display. The Z-D arc digitizer has three translational joints for position and two rotational joints for orientation. The three translational links are held fixed during surgery for any particular planned procedure. Therefore, these three positions can be read manually and fed to the computer system at the beginning of the procedure. The two rotations, however, along with a sixth degree-of-freedom (motion along the axis of the needle) can vary during the procedure. By calibrating these three variables with position transducers (i.e. optical encoders), the position and orientation of the needle can be tracked and transferred to the computer system, where it is displayed by the NSPS software as a superposition upon three different imaging views: axial, saggital, and coronal. This capability gives the neurosurgeon a real-time feedback tool, which allows easy changes in the direction of the predefined trajectory. It also provides a mechanism for conventional stereotactic procedures to use real-time image guidance in a safe maneuvering capacity [62].

Articulated Arms

Articulated arms rely on detectors (potentiometers or optical encoders) located in joints to determine position [50, 56]. By determining the angle of each joint and the length of each segment, the position of the tip can be calculated with reference to its base (Fig. 5).

This approach was first reported by Watanabe [55] who developed the "neuronavigator". The neuronavigator is a potentiometer-based frameless stereotactic guiding device that is computer-assisted and provides the neurosurgeon with real-time information about the location of the operating site. It consists of a personal computer (PC-9801RX), a multi-joint sensing arm, and an image scanner. The user interface is by way of a mouse with which one selects menu items and enters fiducial points on a screen that displays CT or MRI scans. Requirements for point input are announced by voice signal generated by a sound card, so that the neurosurgeon can continue maneuvers in the operating field without looking at the CRT prompt. The image monitor displays CT or MRI pictures in eight different grey

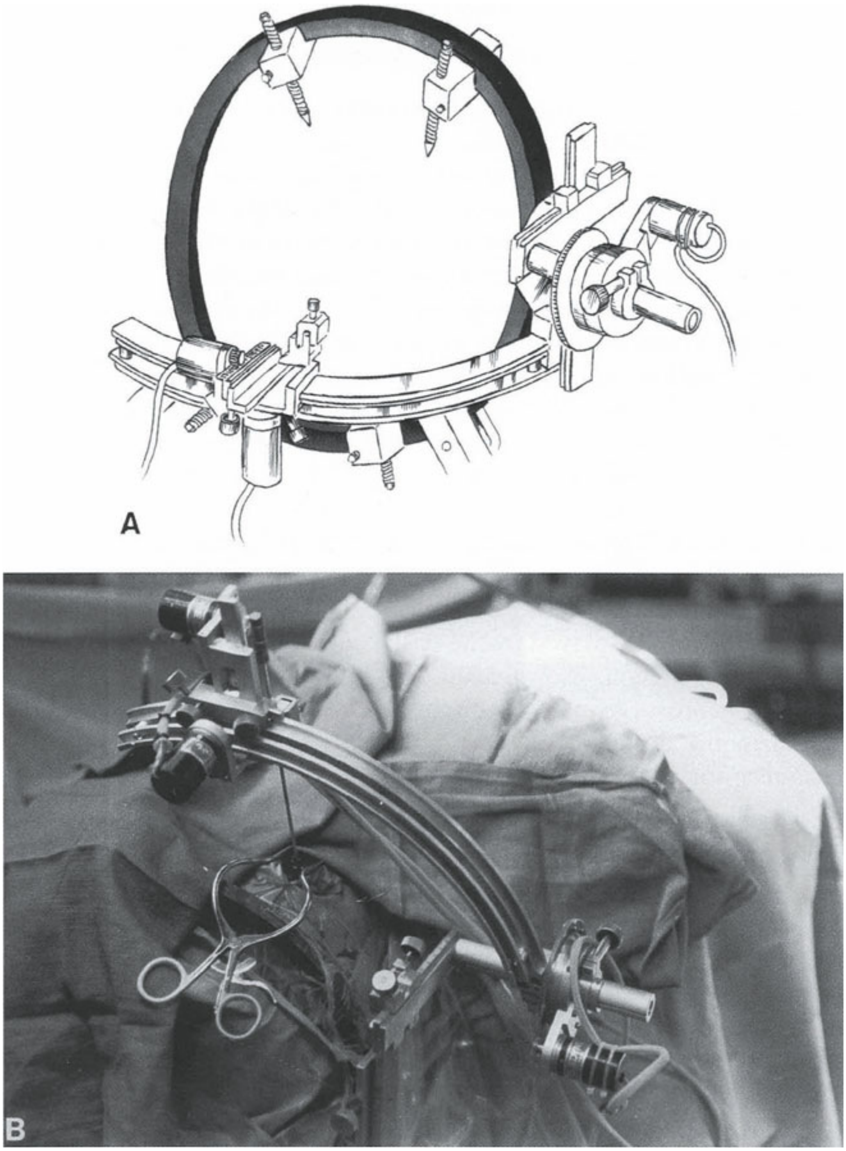

Fig. 4. The Z-D digitizer with optical encoders. Using three encoders fixed on joints D, E, and F, the target position of the needle (or any surgical instrument connected to the Z-D system) is tracked and displayed on the computer-generated 3-D images. (A) Artist drawing of the Z-D arc digitizer and optical encoders. (B) Intraoperative use of optical encoders during a stereotactic brain biopsy

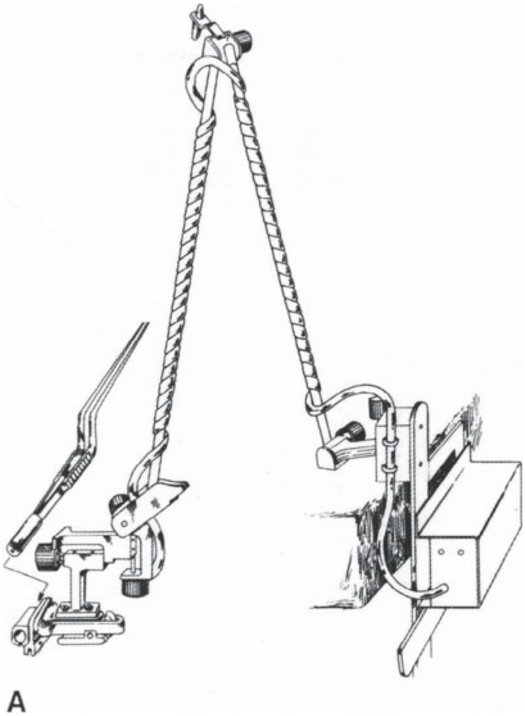

Fig. 5. Articulated arm developed at Wayne State University. (A) Different surgical instruments can be attached to the distal end of the arm. The tip localization and surgical trajectory are displayed on the computer generated images. (B) Intraoperative use of the articulated arm. Note that the stereotactic base-ring is used for registration

scales and a color cursor. The sensing arm has six joints, each of which is equipped with a high-resolution potentiometer (50 K Ohm, nonlinearity: 0.1%). A stabilized DC potential is loaded onto the potentiometer to obtain an angle-related output potential, which is sampled by the computer through an analog/digital converter. The 3-D coordinates of the arm tip are calculated using the angle of each joint and the length of each segment. The accuracy of this system has been evaluated by means of phantom simulation and clinical application. Evaluations include the linearity of the potentiometers, arm bending, and imaging distortion error. In a phantom model, the error measurement was 1.33 mm. During clinical applications, the error was studied with reference to skull base structures clearly identifiable both on CT and in the operating field; the edge of the anterior clinoid process and the sphenoid ridge were chosen. The maximum detection error during surgery was 2.5 mm, which was considered sufficient for open microsurgery [55, 56]. In open surgery, accuracy of less than 2 mm was

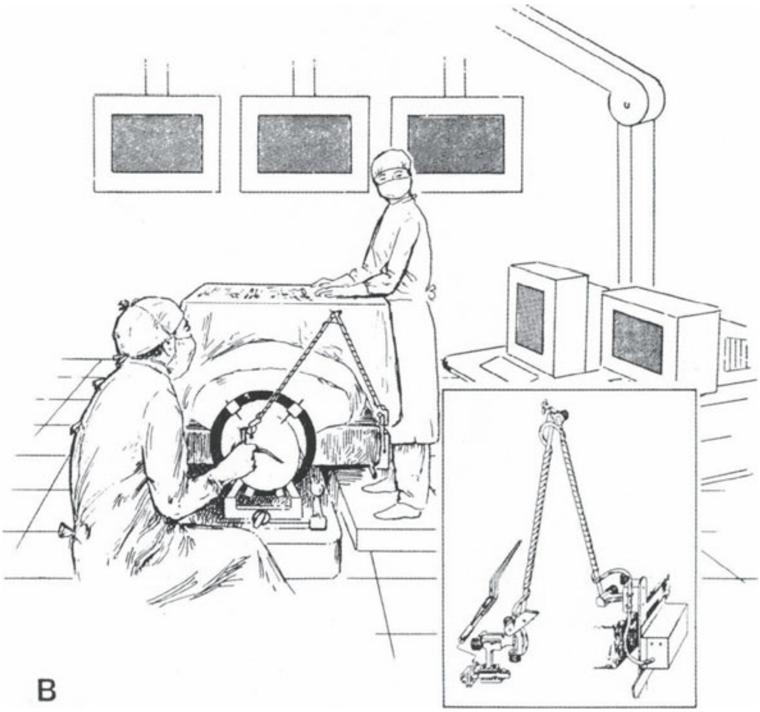

Fig. 5 (*continued*)

considered to give no practical benefit because of the movements of brain tissue and target after a craniotomy has been performed [55].

The neuronavigator has been followed by many other implementations by Mosges [38], Schlondorf [49], Adams [1], Leggett [32], Guthrie [20], Maciunas [14], Koivukangas [29], and others. A popular model has been the viewing wand.

The viewing wand system (ISG Technologies Inc, Mississagua, Ontario, Canada) is an arm-based frameless stereotactic system that uses the Surgicom articulated position sensing arm (Faro Technologies Inc, Lake Mary, FL), in conjunction with sophisticated 3-D imaging software. Analog-digital converters transfer the data from the sensors located in the three arm joints to an interface processor that calculates the position of the viewing wand tip. The tip position is updated 30 times per second. This information is then transferred to an image processor that displays the superposition of the viewing band tip on a 3-D reconstruction of the imaging studies.

The clinical accuracy reported has been 2.35 mm $\pm$ 1.18 mm (15) and 2–3 mm [18]. Articulated arms are without the line-of-sight constrains but

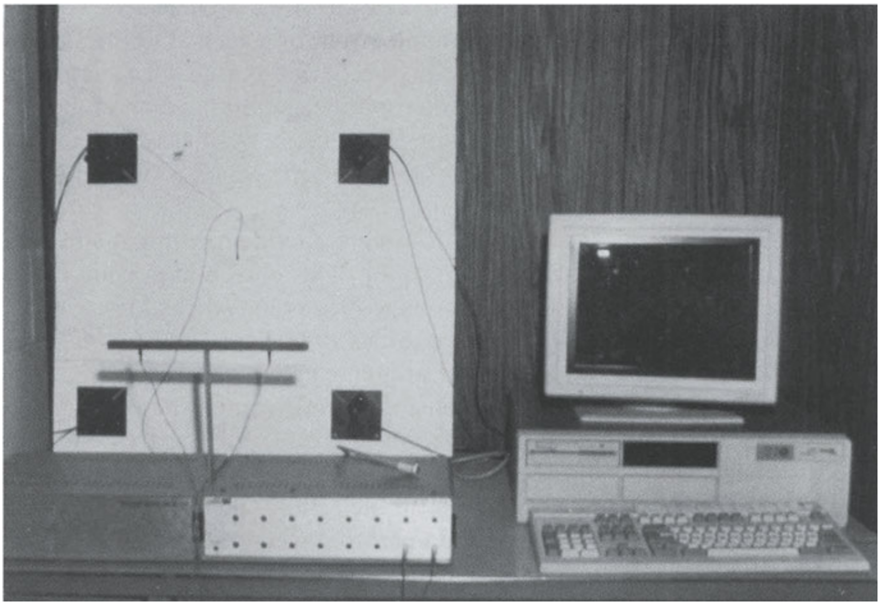

Fig. 6. Sonic digitizer used at Wayne State University. An array of four microphones detects and processes the ultrasound produced by a spark

all of them involve an additional mechanical instrument in the surgical field; they are also relatively cumbersome to use with the surgical microscope.

Sonic Digitizers

Sonic digitizers are based on the production of sound impulses at 24 kHz generated by a large voltage placed across two wires to produce a spark. The ultrasonic component of that spark is received by a series of microphones. This system works by determining the traveling time and frequency change of the sound, based on the trigonometry of the emitters and receivers (Fig. 6). Using an array of at least three microphones, the location of a spark gap in three dimensions can be determined. The optimal size for microphone array depends on the volume to be digitized, and the spacing of the emitters on the probe.

The main advantages of sonic digitizers are the technical simplicity and the possible miniaturization, whereas the main disadvantage is the sensitivity to reflected sound and environmental influences, such as temperature changes or air turbulence [7]. It is possible to improve the accuracy of these systems by modifications and software algorithms. These systems require line of sight between the emitter and the receivers.

The sonic digitizer GP8-3D (Scientific Accessories Co, Stratford, CT) is based on a frameless measuring system. For this sonic digitizer, the emitters consist of bare wires encased in a ceramic insulator attached to the surgical instrument. Critical to the accuracy of the device is that all four microphones must be in one plane. Each microphone should have an embedded emitter for temperature compensation. The accuracy of this digitizer increases with the physical separation of the emitters, which is limited by the size of instruments normally used [43].

One example of this technology is the stereotactic operating microscope developed at Dartmouth by Roberts [46]. The core component of the Dartmouth system is a Vicom-VME image processing workstation (Vicom Systems Inc, Fremont, CA), which consists of a Sun 3/160 workstation with monitor, an enhanced backplane of image processing hardware, and a high speed data bus [11]. It uses a sonic digitizer to track the position and orientation of a microscope to which an array of three sparks gaps has been attached. Modifications of the system included the movement of the microphone array originally mounted on the ceiling, then on a light track, to its current position attached to the operating room table itself.

Sonic digitizers have also been used as frameless systems by two main groups. Barnett and Kormos developed a sonic digitizing wand interfacing this technology first to a Sun SparcStation I (Sun Microsystems, Mountain View, CA) and lately to a Picker ViStar Medical Imaging Supercomputer (Picker International, Highland Heights, OH) [4, 5]. Using handheld instruments such as a bipolar to which two spark gaps have been attached and a table mounted microphone array, their reported mean error in localization is 3.1 mm $\pm$ 1.5 mm. Reinhardt has also developed a sonic-based system for localization of handheld instruments [25, 44]. They use the SAC GP8-3D digitizer and a 386 IBM-compatible personal computer. Their accuracy in the laboratory was 0.897 $\pm$ 0.635 mm. Our preliminary *in vitro* experience with the SAC digitizer at Wayne State gave us a digitizer accuracy of 3 $\pm$ 2 mm.

Electromagnetic Digitizers

Electromagnetic digitizers (also called the magnetic stereotaxis system (MSS)) are attractive because they are relatively inexpensive and do not require a "line of sight" between the transmitter and the receiver. The use of magnetic fields to guide small objects through the body for therapeutic purposes has been studied experimentally for many years [12]. Magnetic digitizers use a transmitter that generates an electromagnetic field upon the operative field. Position can then be determined by introducing a probe (receiver) that can detect gradients in the magnetic field in three dimensions [28, 53]. Because the many metals within the operating room environment could distort the electromagnetic field, such systems were not well suited for surgical use. A newer system, based upon pulsed direct current field, less susceptible to environmental materials, was developed (Ascension Technology Corp, Burlington, VT) and has been adapted for intraoperative use for at least two groups. Manwaring described its use for tracking of an endoscope [37] and Kelly has used it with a probe localization device [17].

These systems have gone through several generations of development, from the use of a primitive single wire neck loop to the use of multicoil superconducting systems [45]. Besides interactive image guidance, the potential applications of magnetic fields in stereotactic neurosurgery include the treatment of brain tumors with hyperthermia (dynamic boundary hyperthermia), and MSS-based drug delivery in, for example, the treatment of Parkinson's disease [45].

As mentioned earlier the method is without line-of-sight constraint, the system interferes minimally with the surgical field, and accuracy has been reported better than 2 mm. The repeatability error reported is of 3–4 mm, and the main disadvantage is the lack of compatibility with any iron metal device (i.e. surgical table, instruments).

Optical Digitizers

To counteract some disadvantages of sonic digitizers, such as distortion by extraneous ultrasonic noise and echoes in the operating room, 3-D digitizers based on optical tracking have become available for use in frameless stereotaxis. Pixsys, Inc. (Boulder, CO) and Northern Digital (Waterloo, Canada) have developed digitizers based on three cameras fitted with linear charged coupled devices (CCDs) and cylindrical lenses that detect the infrared light-emitting diodes (LEDs). The system implemented for surgical use consists of an array of CCD cameras that track instrument position by localizing LEDs located in the surgical instrument (infrared digitizers). Another means of optical digitizing used "ordinary" video cameras to monitor the movements of a wand, determining its differential position on 2-D video images viewed from two different angles ("machine vision" method).

Optical digitizers are attractive because they can be adapted for interactive tracking of surgical tools, and they are not significantly influenced by extraneous signals in the operating room. However, they require a clear line of sight between the LEDs and the cameras. This problem can be ameliorated by suspending the cameras over the surgical field and by using redundant cameras (more than three one-dimensional CCD detectors or more than two video cameras) in the operating suite.

Infrared-based systems have been implemented by Bucholz [7] (Stealth

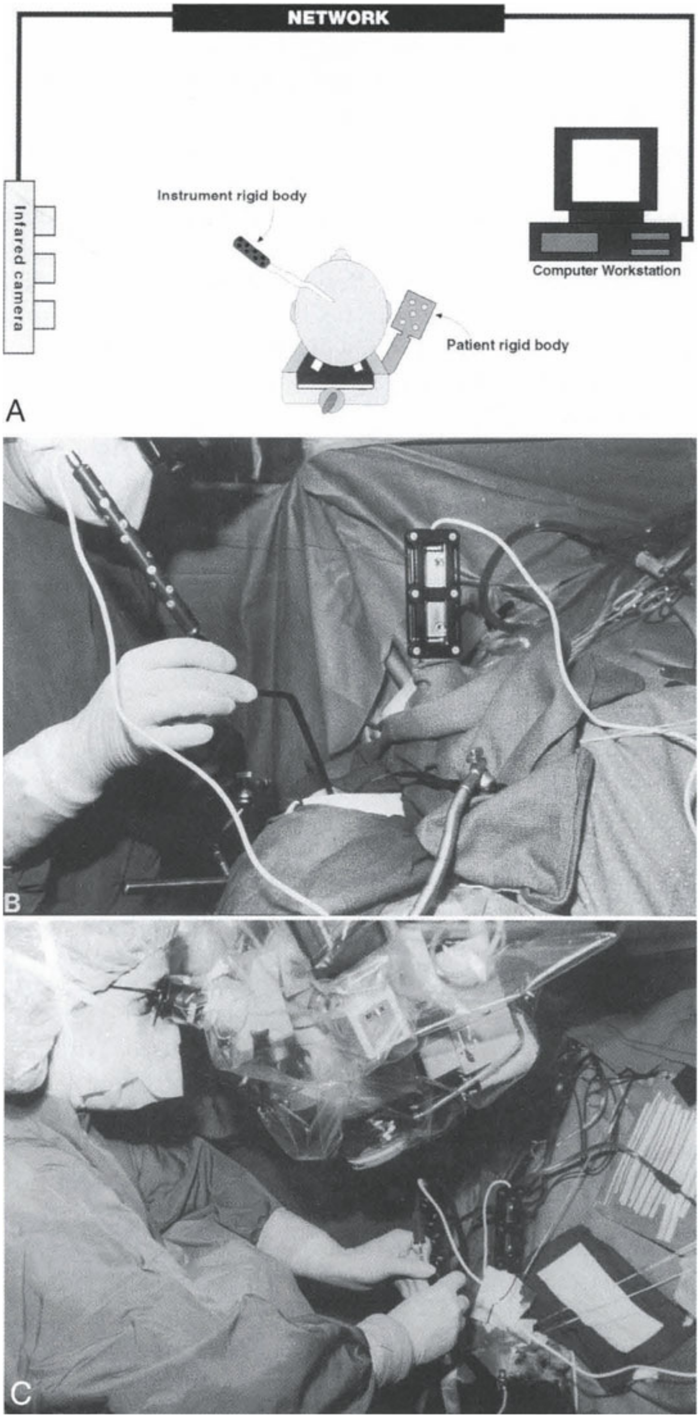
NETWORK
Instrument rigid body
Infared camera
Computer Workstation
Patient rigid body
A
B
C

Technology, St. Louis, MO) using a Pixys digitizer and by Zamorano (Wayne State University) using a Northern Digital digitizer [61]. Recently Codman Corporation (Randolph, MA) and Elekta (Atlanta, GA) have made commercially available systems using the Northern Digital digitizer. In terms of the approach with LEDs mounted on surgical instruments, two approaches have been used. Bucholz uses mounted LEDs on each surgical instrument [7]; Zamorano uses a redundant multiple LEDs piece that can be exchanged between different instruments or the surgical microscope. We believe the advantage of the latest approach is to have a redundant probe that decrease somehow the line-of view constraint; it may, though, make the system more expensive and cumbersome with the need to exchange the probe and calibrate the instrument.

Infrared-based Optical Digitizer: The Wayne State University System

As previously mentioned, intraoperative digitization through an infrared detecting system is based upon a 3-D opto-electronic motion analysis system (Optotrak 3-D Bar, Northern Digital, Waterloo, Canada) that uses LEDs. Three infrared sensors mounted in a series track target points defined by several miniature leads placed in the surgeon's instrument, in a predefined relationship, and referred to as a "surgical rigid body or pointer" (Fig. 7). A "rigid body" with several infrared emitters on it is attached to the patient's head and then mounted into the headholder or stereotactic frame (and comprises the patient's "rigid body"). Another similar rigid body is attached to the surgical instrument [58–62]. The first rigid body is used to tell the system where the patient is in relation to the other LEDs, and the second rigid body tells the system the position of the surgical instrument. With this information the system can combine the virtual patient and virtual instrument information and send the simulation to the neurosurgeon. Each time the surgeon moves the instrument, three monitors mounted in the room display the instrument position on the pre-acquired computer-generated images.

The surgical procedure starts by mapping the image studies with the intraoperative space (intraoperative registration). This is achieved by

Fig. 7. Infrared digitizer for intraoperative localization: (A) 3 infrared cameras detect continuously the position of multiple LED's mounted as a "patient rigid body" and as a "instrument rigid body or pointer". The computer workstation displays the position of the surgical instrument on the 3-D displayed images. (B) Intraoperative picture demonstrating the use of the "instrument rigid body" (pointer) and "patient rigid body" attached to the head holder. (C) Intraoperative view of interactive display using the surgical microscope

touching the pointer on at least three or four "real" points that can be easily located in the pre-acquired images. We use known points of the stereotactic frame or fiducial markers. Once this is accomplished, any time the pointer is used, its tip position and trajectory are simultaneously displayed on the computer images, giving real-time orientation.

Next a centered incision and craniotomy are performed according to the surgical pre-planning protocol. The infrared system confirms at all times the entry point, trajectory, and target localization.

Machine Vision-based Methods

Machine vision-based methods use 2-D images obtained from two different viewing angles and calculate the 3-D position of an object in that space. Once this position is established, localization and guidance can be accomplished by standard stereotactic calculations and techniques.

The first step of the machine vision technique entails digitizing two images of the operating room space that contain the operative field (surgical workspace). To calculate the coordinates of the surgical workspace, two video cameras located 3 feet apart are aimed at the surgical workspace. Both cameras are connected to a computer workstation, and focus on a "video localizer" that consists of eight fiducial markers in a box-like configuration of known dimensions. Thus, the 2-D positions of the fiducial markers projected on the digitized video images are measured. Those values are entered into a photogrammetric projection algorithm which defines the 3-D coordinates of any object seen in the field of view of the two cameras. Once this is accomplished, the video localizer can be removed from the operative field.

As long as the position and field of view of the video cameras remain unchanged, the 3-D position of any object in the surgical workspace can be determined and tracked. The spatial relationship between an object such as the patient's head and the CT, MRI, or angiogram image is established by calculations between a series of multiple Cartesian coordinates. Thus, the position of a surgical instrument within the operative field can be tracked.

Mechanical accuracy tests of this system were performed by comparing 3-D coordinates derived from the projection algorithm using the video localizer with 3-D coordinates obtained by physical measurements using a calibrated Brown-Robert-Wells (BRW) arc and phantom. Comparisons were made in multiple coordinates with measurement errors of less than 1.5 mm for each vector calculated using the machine vision system [22, 23].

Active Systems: Robotic Systems

Robotic manipulators are extensions of computer systems that allow programmed physical interaction with the environment. The Robotic Institute of America defines a robot as "a reprogrammable, multifunctional manipulator designed to move materials, parts, tools, or specialized devices through variable programmed motions for the performance of a variety of tasks" [9]. Recent years have seen an increased interest in the robot research community on the development of special-purpose designs for medical use. These manipulators are widely used today in many fields, from industrial production to the service sector and the military. Some industrial robots have a precision of up to ± 25 microns which clearly is superior to the accuracy obtained in stereotaxy or with any passive digitizer.

The special-purpose computer that interprets operator inputs controlling the manipulator motions is called robot controller. The principal component of a robotic system is the robot manipulator, which is composed of a base, links, actuators, and end-effector. The base, usually fixed to a supporting surface, provides a fixed reference system. The manipulator links are its movable segments. Links are numbered in ascending order, starting with the base (link 0). The motion of manipulators is made possible by joints that connect adjacent links, and correspond to the degree of freedom. Joints may be prismatic (allow relative translation of two links) or revolute (have rotation but not translation).

The first three joints are called major joints. Depending on the type of major joints (prismatic or revolutes), robotic systems are classified as Cartesian, cylindrical, spherical, or revolute. We briefly discuss these, as follows:

A *Cartesian*, or x, y, z joint; if a robot has a Cartesian work envelope it means all its major joints are prismatic. The robot manipulator moves on a 3-D slide system, which defines each of the axes x, y, and z.

A *cylindrical* arm joint means if one major joint is revolute, the robot is cylindrical. The robot arm is raised or lowered on a cylindrical shaft and rotates about that shaft.

A *spherical* joint is defined as when two major joints are revolute, the extendable arm can pivot or rotate about a base unit.

An *articulated* arm or revolute joint indicates that all the major joints are revolute. This device is the closest to the human anatomy and most consider it the preferred candidate for a surgical robot. The system has multiple flexion-extension-rotation articulations which provide six or seven degrees of freedom.

Actuators are used to move the manipulator to the desired position and orientation. Depending on the type of actuator used, a manipulator may be classified as hydraulic, electric, or pneumatic. Most robotic systems for surgery use electric actuators; they can handle small to medium loads, are clean, and easy to install and maintain. Thus, the movement at each joint is performed by servomotors and feed-back controlled by the host computer by means of optical encoders on each joint.

Operator inputs are sent to the controller through an operator interface. Use of external sensors gives robots a degree of flexibility and adaptability. Sensor noise and drift, however, can affect their accuracy.

Finally, actuators and end-effectors allow for a programmed effect. Their dexterity increases the overall system's complexity and costs. Currently, robot systems can be used surgically as an operating "hand" or as guidance for the operating microscope.

The use of robots offers potential advantages on stereotactic applications: their use eliminates human errors in transferring calculations to frame settings, offers no restrictions in access or proximity to the patient's skull, offers nearly unlimited operative angles to the brain, provides a steady motion system with the ability to remain poised in a fixed position, is able to react rapidly to changes in force level, allows for easier maneuverability of the robot in and out of the surgical field by push-button computer-assisted techniques, and similarly, allows adjustments to be made in the probe trajectory by push-button-controlled robotic movements (remote operation). To date the main disadvantage of robotic systems is their prohibitive cost. Different authors including Young [57], Kwoh [31], Glauser [16], and Drake [11] have initiated this approach.

Robots and the Surgical Microscope

A second utilization of robots in neurosurgery is related to the surgical microscope [14, 46]. A multi-articulated robot structure can be attached to a surgical microscope and guide its position during surgery according to preoperative planning. This means that the microscope will choose optimal positioning parallel to the surgical trajectory and on its own computer will display this position in relation to the skull and brain and to the previously chosen trajectory. Currently such a robotic stereotactic microscope has been developed by Zeiss (Zeiss MKM: Carl Zeiss Inc, Thornwood, New York) and is already in use in several centers in Europe, Japan, and the United States (Fig. 8). A similar system to this is the Grenoble system. All these systems are passively activated and are not yet able to reach alone a given position designated on the CT and or MRI images.

MKM Robotic Microscope

The Zeiss MKM Stereotactically-Guided Microscope System offers great flexibility for frame-based and frameless stereotactic surgery [64] (Fig. 8). It consists of a microscope mounted on an articulated robotic arm that moves the microscope on 6 axes. The microscope (Zeiss OPMI-ES, Carl Zeiss, New York) has an autofocus system with a digitally encoded zoom that selects the true focal plane, with a continuously variable focus length from

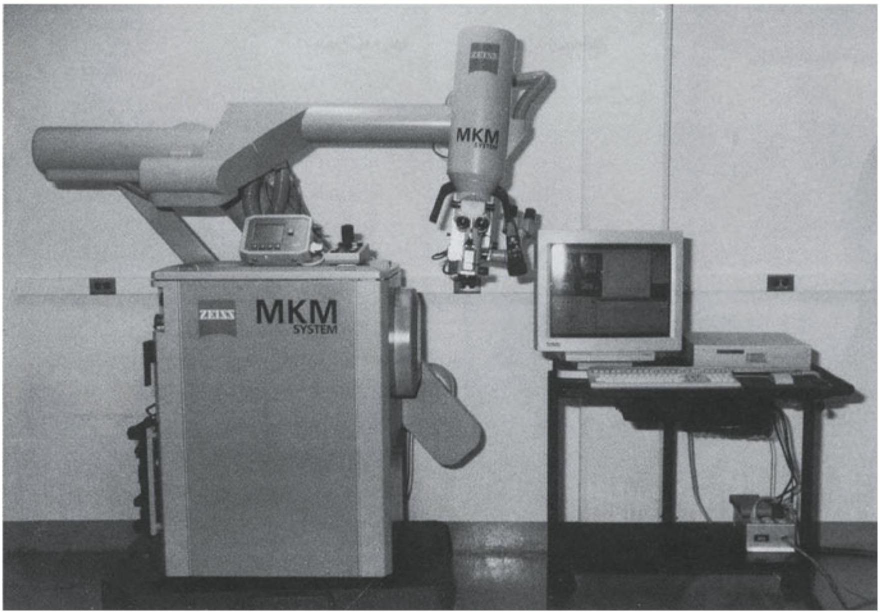

Fig. 8. Zeiss MKM stereotactically-guided microscope system and planning workstation in use at Wayne State University

200–400 mm. This system does not require the use of any external pointing device, since it utilizes the microscope's actual focal point as a virtual probe. The accuracy of the Zeiss MKM system has been estimated of 0.75 mm (bench studies).

The Grenoble Robotized Microscope Support System (MSS) and Surgiscope

This passive system consists of a robot-held microscope support system based on a triple-arm parallel system attached to the ceiling of the operating room. The system is a motorized support driven by servomotors activated by two lateral wands handled by the surgeon; as the systems knows the position of its joints they are fed into a computer. A recent development of the system (Surgiscope, Elekta) includes an infrared detection system coupled to the microscope as well as to the patient holder in order to continuously calculate the optical axis, focus, and display on the images.

Intraoperative Digitization: Clinical Applications

Intraoperative digitizers have proved to be reliable and accurate in clinical use treating brain tumors, vascular malformations, epilepsy and spine surgery. We will review its applications on those pathologies.

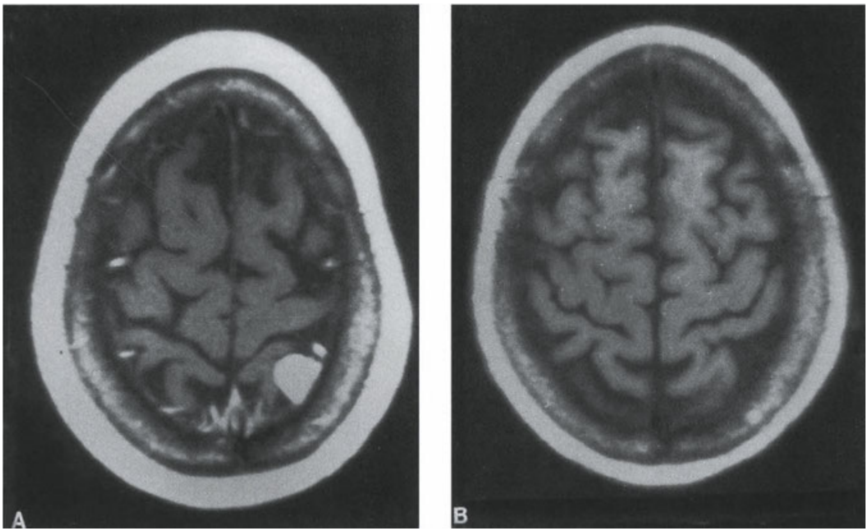

Fig. 9. Centered craniotomy. 59-year-old patient who presented with seizures. (A) Preoperative T_1-axial MRI after gadolinium infusion shows a left parietal mass. (B) Postoperative MRI shows complete resection. In this case, the intraoperative interactive infrared guidance allowed a minimally invasive craniectomy; the procedure was also performed under local anesthesia with mapping of motor and sensory function and continuous intraoperative monitoring

Brain tumors. Digitizers are useful during the resection of superficial, subcortical, and deep located tumors. Some cystic lesions such as arachnoidal cysts, colloid cysts, abscesses, intracerebral hematomas, and some intraventricular tumors can be successfully managed using a computer-assisted stereotactic endoscopic approach.

Superficial tumors. For the resection of cortical or subcortical tumors, we perform a centered craniotomy, which is a small craniotomy centered exactly above a cortical or subcortical lesion. In these cases, the digitizer allows to minimize the size of the craniotomy and decrease operative morbidity. Most lesions can be removed as intact specimens with minimal bleeding (Figs. 9, 10).

Deep tumors. Neurological complications in the surgical resection of deep-seated tumors located in the basal ganglia or thalamus are primarily related to problems of localization, exposure, and extent of resection [5, 11, 21, 48]. The surgical approach depends on the location of the tumor. For example, anterior thalamic tumors are approached transfrontally, while posterior dorsal thalamic lesions can be approached through the temporo-occipital junction. The surgeon should choose the surgical approach according to the location, size, and extent of the tumor, so that removal of

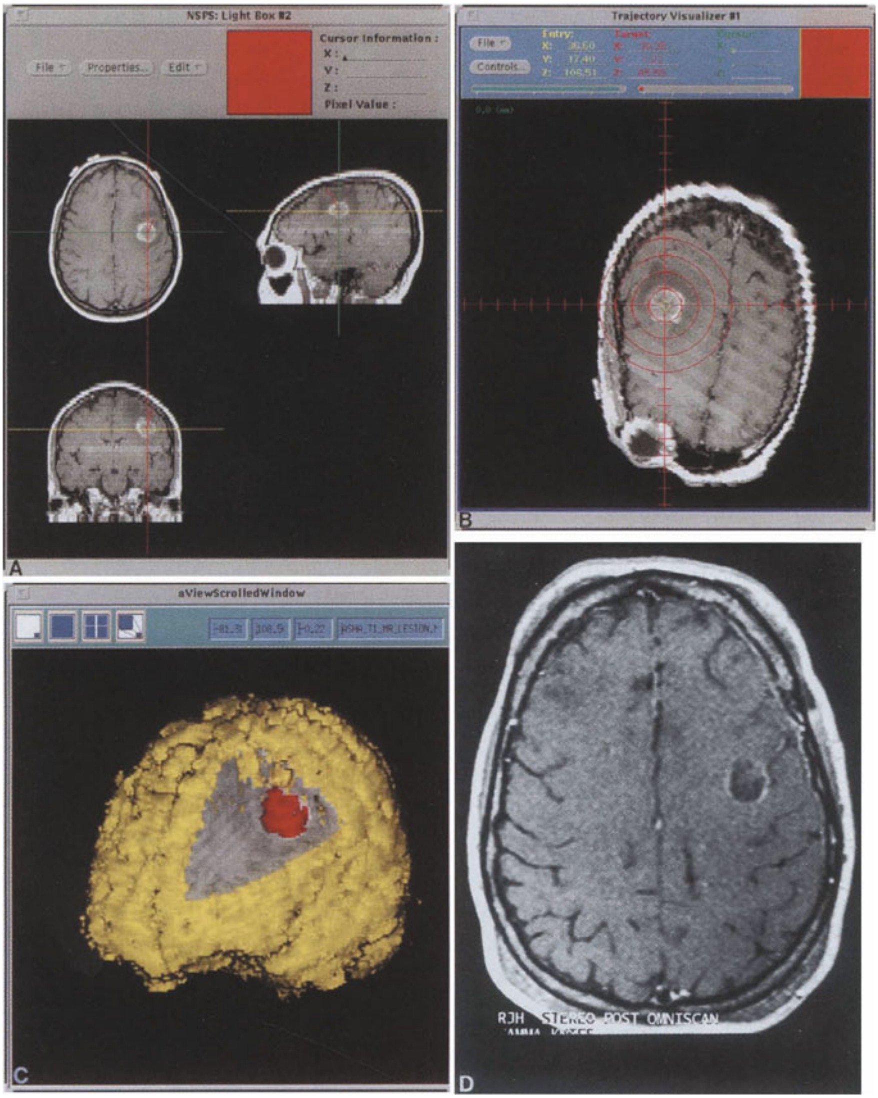

Fig. 10. 50-year-old woman with severe headaches. An awake craniotomy was performed with interactive intraoperative guidance and functional mapping. The patient underwent a complete resection of the mass. Intraoperative dysplay of the interactive image guidance showing (A) multiplanar T_1-weighted gadolinium-enhanced MRI, (B) 3-D reconstruction, (C) Surgeon's perspective. (D) Postoperative T_1-weighted MRI. The pathology was consistent with metastatic carcinoma. Postoperatively the patient remains without neurological deficits. In this case, the intraoperative interactive infrared guidance was useful for the intraoperative localization of a subcortical lesion as well as defining the margins of the resection

the tumor will be complete and damage to the normal brain will be minimal (Figs. 11, 12).

Computer assistance allows the surgeon to select the safest and most effective surgical approach for a deep lesion. Furthermore, during the resection, digitizers provide a constant display of the instrument position, tumor volume and geometry, and definition of tumor margins, surrounding normal brain, and vascular pedicles.

Intraventricular tumors. Mass lesions located in the ventricular system present a particular surgical challenge. They are deeply situated, surrounded by vital neurological and vascular structures, and often have irregular geometrical configurations, posing particular difficulty for the surgeon in maintaining orientation during surgery. The blood supply is particularly complex, including vessels from both anterior and posterior circulations. Frequently, conventional neurosurgical techniques lead to incomplete or suboptimal resection of these masses. Conversely, resection beyond desired margins can result in severe neurological complications.

During the resection of intraventricular tumors, digitizers provide an interactive display of the surgical instrument, which is useful in determining in real-time the geometry of the tumor, margins of the surgical resection, and the vascular structures. They also show the relationship of the tumor and surrounding brain structures, making it possible to optimize the surgical resection of intraventricular tumors [54] (Fig. 13).

Skull base tumors. Skull base lesions may originate from the neural, vascular, or meningeal structures of the nervous system, or can arise from bone, cartilage, or extracranial tissues. Even though many lesions are benign, surgical interventions of the skull base are known to be extremely difficult and dangerous, and have traditionally been associated with relatively high morbidity and mortality rates. The proximity of skull base tumors to vital areas of the brain, major blood vessels, and cranial nerves, pose a variety of obstacles. A skull base surgeon must have a 3-D understanding of these structures and be able to visualize their relationships from all angles [50] (Fig. 14).

During the surgical exposure and resection of skull base tumors, digitizers allow the intraoperative visualization of the tumor geometry, allowing the surgeon to maintain orientation during surgery, even with irregular geometrical configurations. Furthermore, during skull base surgery, digitizers show the position of blood vessels and cranial nerves, which often are displaced from their usual anatomical position.

Epilepsy Surgery

Recent technological advances in functional neuroimaging such as PET, SPECT, functional MRI, and magnetic resonance spectroscopy (MRS),

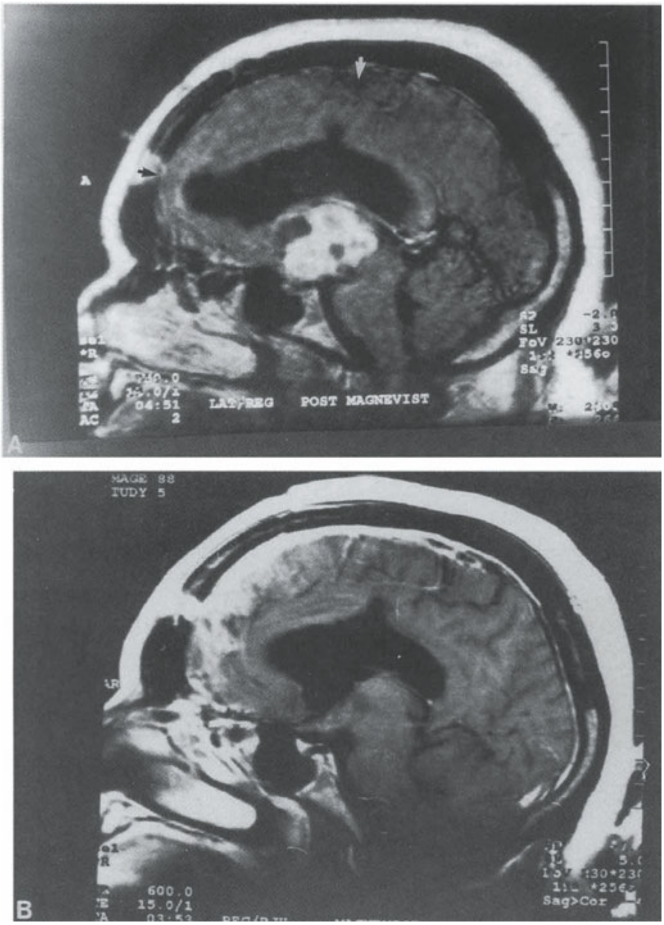

Fig. 11. 25-year-old patient with severe headaches and diabetes insipidus. He was diagnosed with a suprasellar mass and underwent two previous attempts at resection, via transcallosal and transventricular approaches (arrows). Subsequently he was referred to Wayne State University for image-guided resection. (A) Sagittal T_1-weighted image after infusion of gadolinium shows a large enhancing suprasellar mass. This lesion was approached via subfrontal-translamina terminalis using the infrared digitizer. (B) Postoperative sagittal T_1-weighted gadolinium-enhanced MRI shows only some postoperative changes without residual tumor. The pathology was consistent with craniopharyngioma. In this case, the intraoperative interactive infrared guidance was useful to localize the lesion and define the margins of the resection of an irregular mass, and to keep orientation with important surrounding anatomical structures such as optic chiasm, brainstem and blood vessels

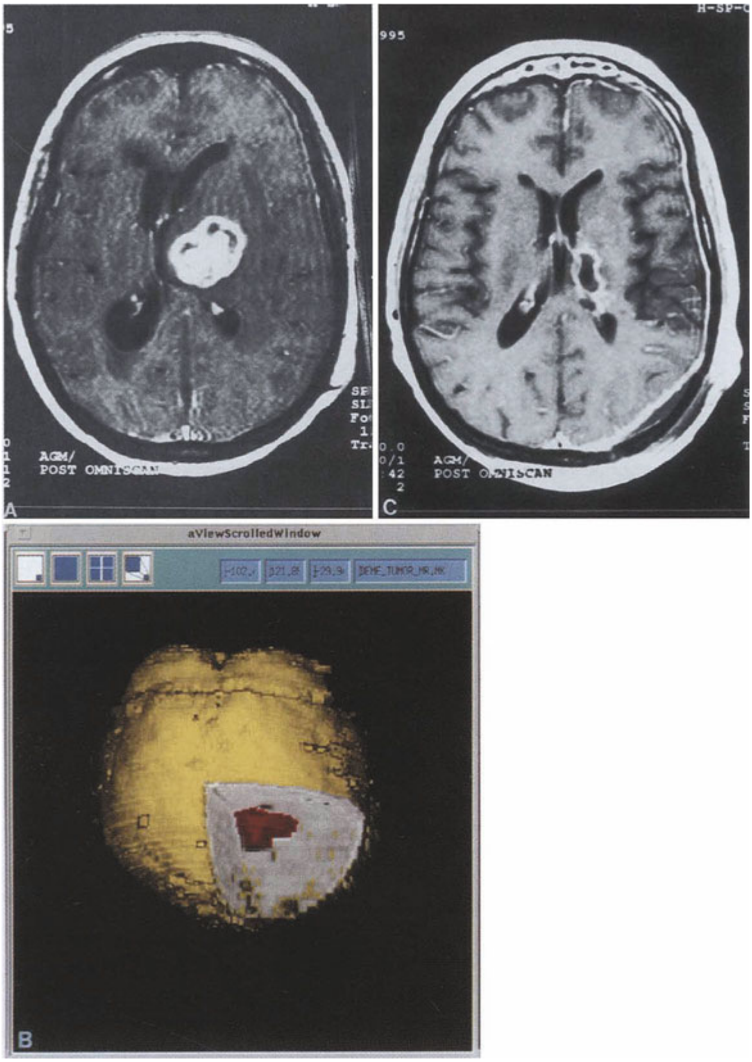

Fig. 12. 42-year-old patient who presented with right hemiparesis. (A) Preoperative gadolinium-enhanced T_1-weighted MRI that shows the presence of a large left thalamic mass with significant mass effect. (B) 3-D reconstruction, surgeon's perspective. The patient underwent image-guided stereotactic gross total resection of the mass with the use of the infrared digitizer. (C) Postoperative T_1-weighted MRI shows no residual tumor, and some postoperative changes. The pathology was consistent with anaplastic astrocytoma. This case shows the usefulness of the system in the localization and resection of a deep-seated lesion

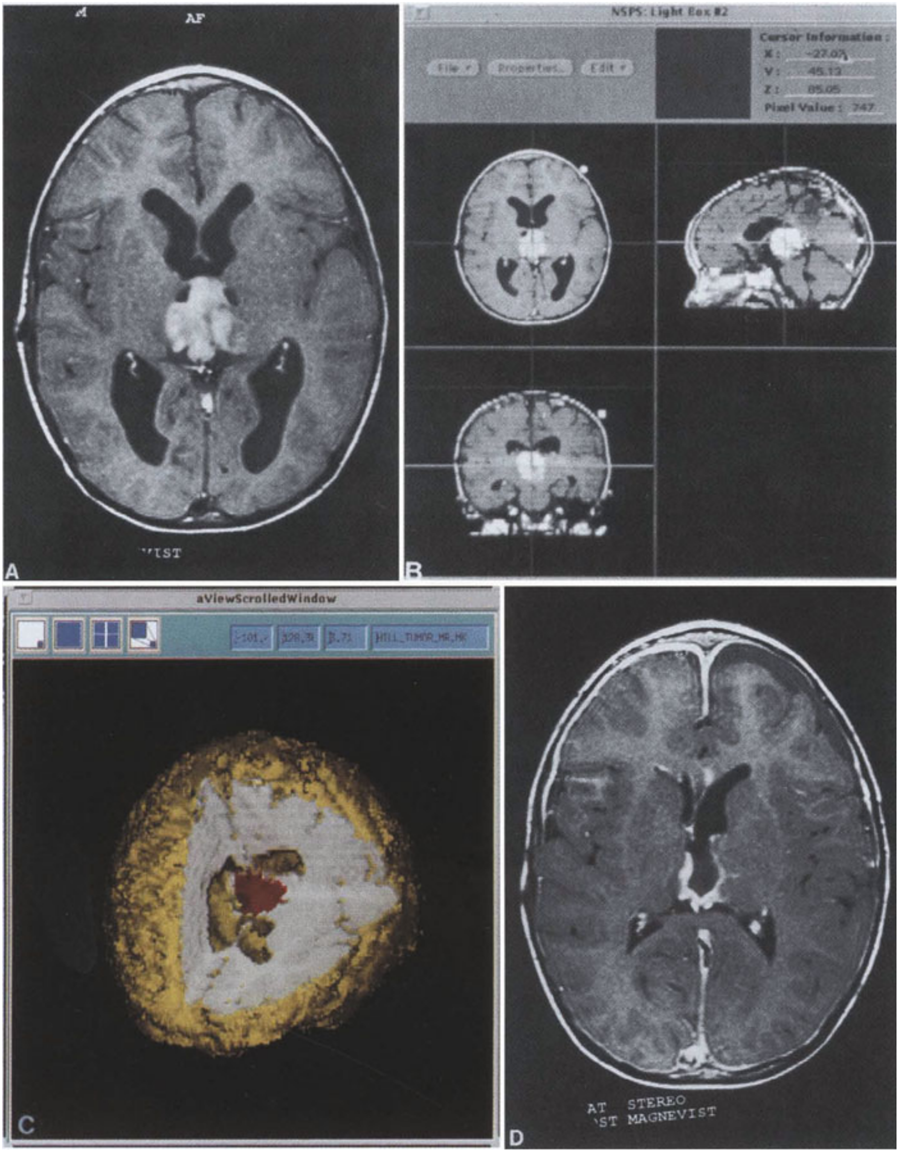

Fig. 13. 4-year-old patient with severe headaches and mental changes. (A) Preoperative T_1-weighted gadolinium-enhanced MRI shows the presence of a large intraventricular mass. (B) Intraoperative localization: multiplanar images. (C) 3-D reconstruction (D) Postoperative MRI showed gross total resection and postoperative changes. The pathology was reported as a low-grade astrocytoma. During resection of intraventricular tumors, the intraoperative infrared guidance helped to keep orientation and to locate the margins of the resection and vital surrounding structures

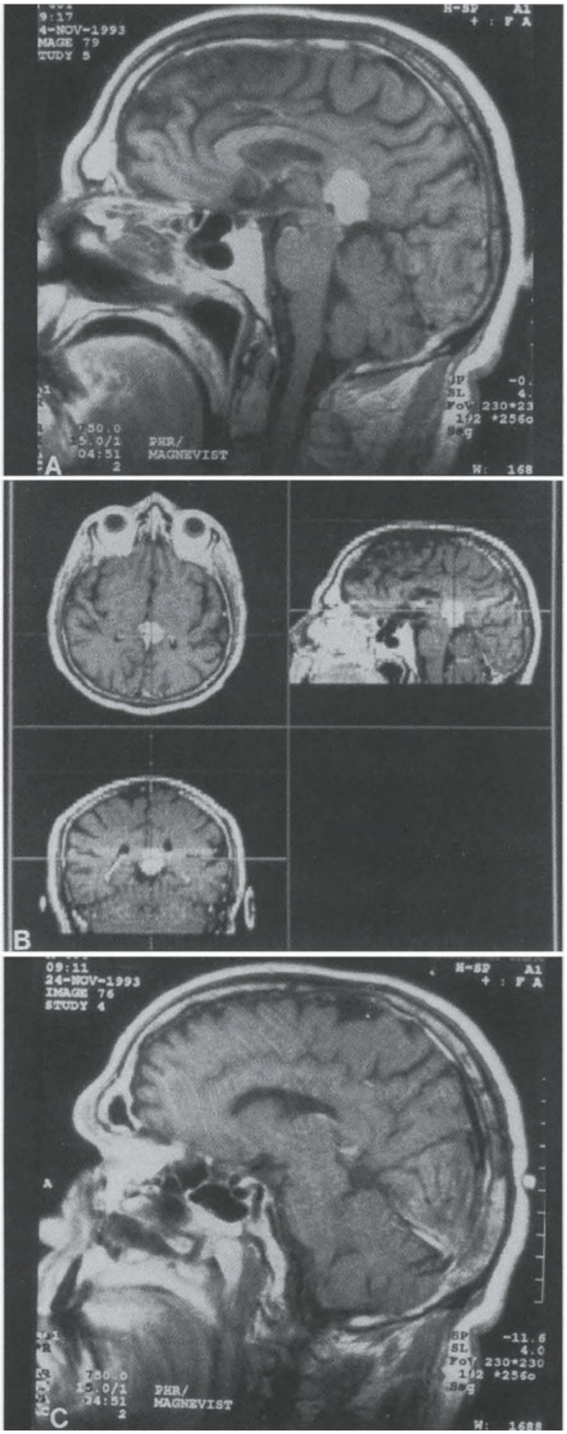
9:17
4-NOV-1993
MAGE 79
TUDY 5
PHR/
MAGNEVIST
A
B
09:11
24-NOV-1993
IMAGE 76
STUDY 4
PHR/
MAGNEVIST
C

together with new operative modalities such as computer-assisted surgery and new navigational devices, have revolutioned the treatment of epileptic patients regarding both seizure control and postoperative morbidity. During the surgical treatment of temporal and extra-temporal epilepsy, the use of a digitizing system allows localization of normal anatomical structures, and abnormalities defined by imaging studies (Fig. 15). For example, when the epileptic focus is located close to eloquent areas, digitized information can be gathered into the registered images for localization of sensory, motor, and language functions from intraoperative mapping (functional localization). During callosotomies, a digitizing system (i.e. optical infrared digitizer) defines the extent of the corpus callosum section. During the surgery of temporal lobe epilepsy, digitizers are useful in judging the posterior margin of anterior temporal lobe resection (Fig. 16). In conclusion, we believe that during the surgical treatment of epileptic patients, the integration of computer assistance with intraoperative electrocorticography and functional mapping, adds safety and accuracy to the procedure, contributing to its goal, which is to obtain seizure-free patients with minimal morbidity and thereby improve their quality of life.

Resection of Vascular Malformations

Management of vascular malformations located in deep or eloquent areas of the brain represents a therapeutic challenge. Digitizers are useful for making a centered craniotomy and to locate deep small lesions such as deep cavernous angiomas. During the resection of arteriovenous malformations, the use of digitizers may provide additional guidance for planning the surgical strategy, demonstrating the localization of feeders, nidus and draining veins, allowing a safer and more effective resection [59] (Fig. 17).

In vascular malformations close to eloquent areas, digitized functional information can be gathered into the registered images for localization of sensory, motor, and language functions derived from cortical and subcortical intraoperative mapping (functional localization).

Finally, interactive image guidance provides a constant display of surgical instrument position during the resection, demonstrating the relationships between the vascular malformation and surrounding vital structures, contributing to decreased surgical morbidity.

Fig. 14. 50-year-old patient with headaches and transitory diplopia, diagnosed with a pineal region mass. (A) Preoperative T_1-gadolinium enhanced MRI. (B) Intraoperative localization: multiplanar 2-D images. The patient underwent resection of the mass using the infrared digitizer. (C) Postoperative MRI shows a gross total resection. The patient did not develop any new neurological deficit. The pathology revealed a meningioma. This case demonstrates the application of infrared-based digitizers during the resection of pineal region tumors

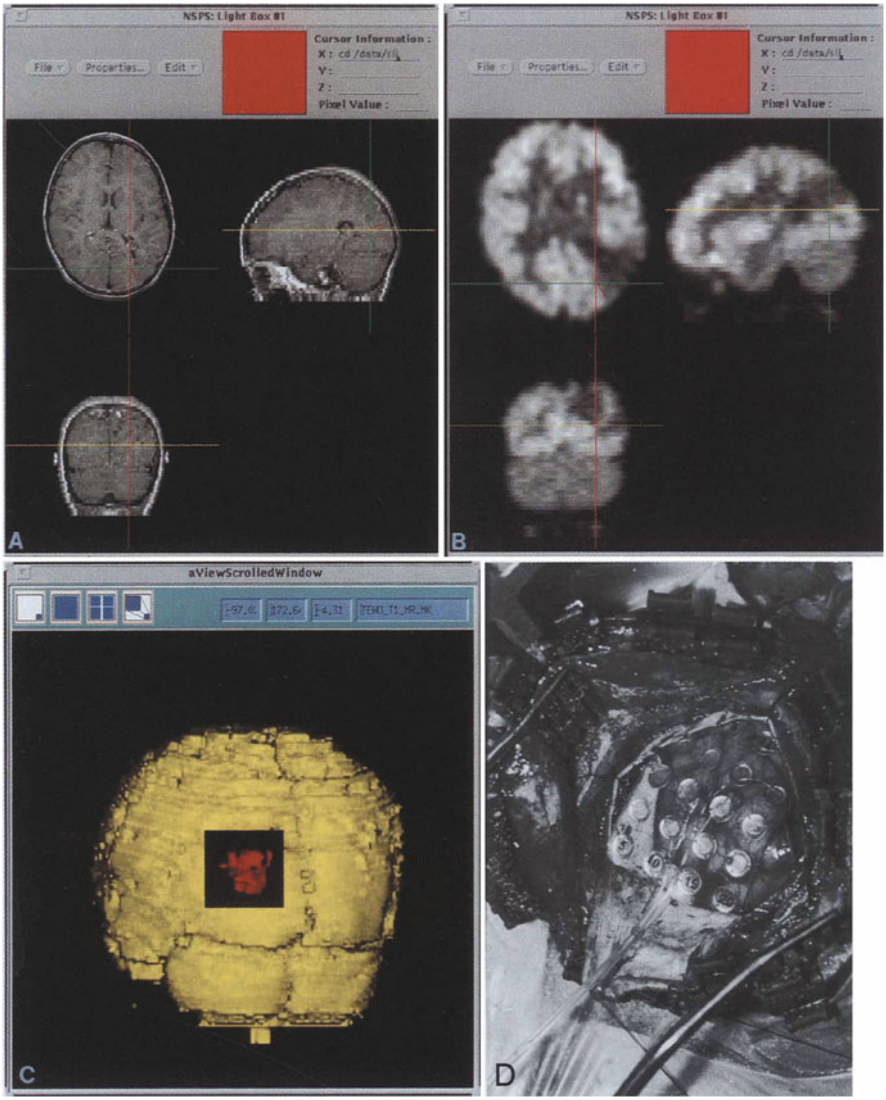

Fig. 15. 8-year-old patient with intractable generalized seizures. T_1-and T_2-weighted MRI did not show any abnormalities. (A) Axial, sagittal, and coronal MRI does not show any abnormality. (B) Interictal PET scan shows an area of hypometabolism in the left occipital lobe. (C) 3-D reconstruction of the PET abnormality superimposed to the MRI image. A craniotomy was performed with placement of a subdural grid of the surface of the PET abnormality. (D) The intraoperative recording revealed focal spikes. Subsequently, she underwent resection of this PET defined abnormality and postoperatively was seizure-free. In this case, the infrared digitizer was used to localize the PET-defined abnormality, and to position the subdural grid above it. Once the PET and electrophysiological information was concordant, the infrared digitizer was used to define the margins of the resection

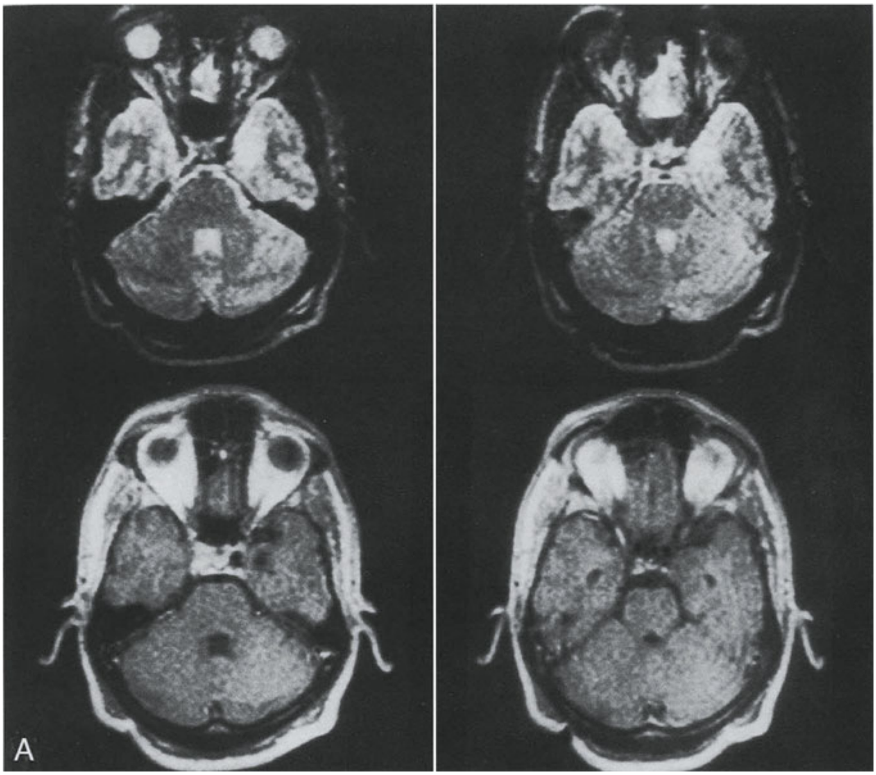

Fig. 16. 33-year-old patient with generalized intractable seizures. (A) Preoperative MRI shows a non-enhancing T_2-weighted hyperintense lesion on the left temporal lobe. The patient underwent functional mapping and computer-assisted resection of the seizure focus integrating anatomical and functional data. A limited resection confined to the margins of the lesion was perfomed. (B) Postoperative MRI shows the resection of the seizure focus. Currently, the patient remains seizure free without any neurological deficit. The pathology was consistent with ganglioglioma

Spinal Applications

Conventional means of intraoperative localization of spinal anatomy have historically been inaccurate. The position and dimensions of critical anatomic structures were inferred on the basis of their relationships with surgically exposed anatomic landmarks [13, 39]. For example, the location of a lumbar pedicle was determined from the position of a transverse process and the adjacent pars interarticularis. If these inferences were not made correctly, surgical procedures meant to alleviate pain and neurologic deficit were liable to result in undesirable outcomes. The spine is composed of rigid, independent bodies that remain anatomically constant, and has numerous

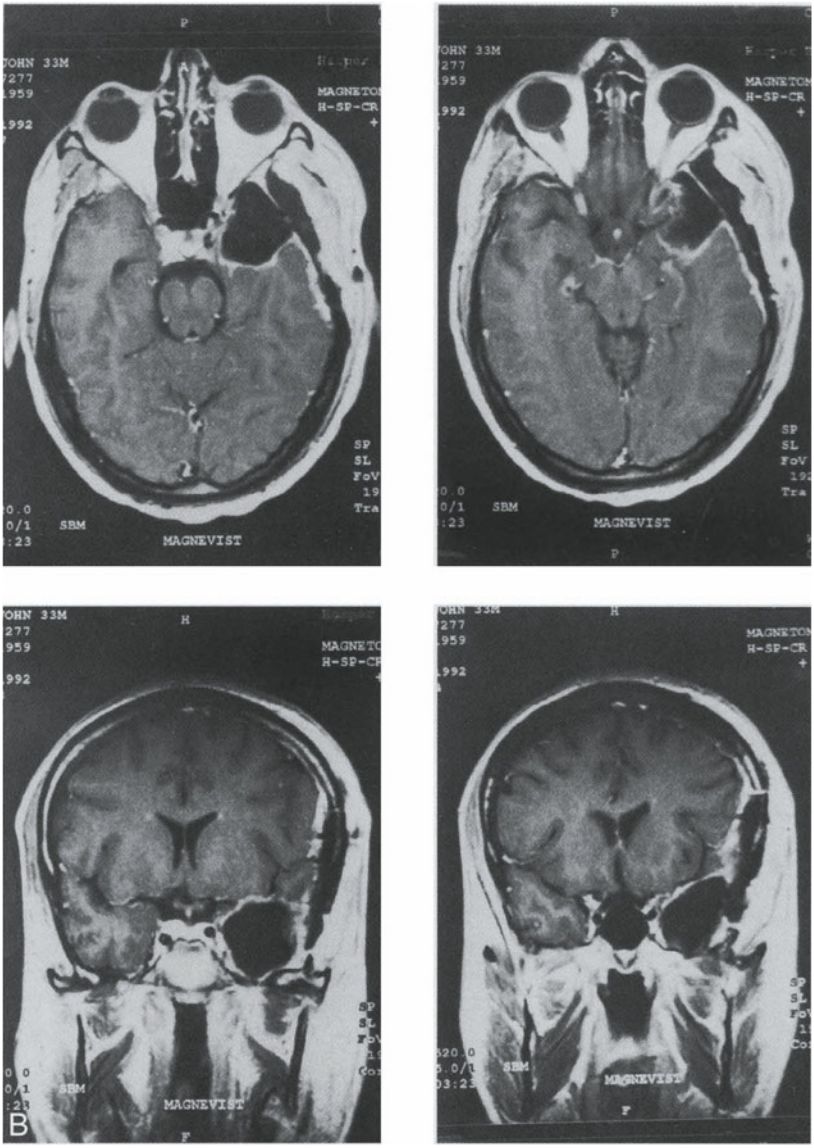

Fig. 16 (*continued*)

anatomical landmarks distinguishable in both image scans and the surgical field. For those reasons, the spine is ideally suited for image guidance.

Because image-guided spinal surgery involves separate registration of each spinal segment, intersegmental movement between the time of image acquisition and that of surgery is not a problem. In cases where anterior or posterior instrumental fixation is needed, digitizers provide the surgeon

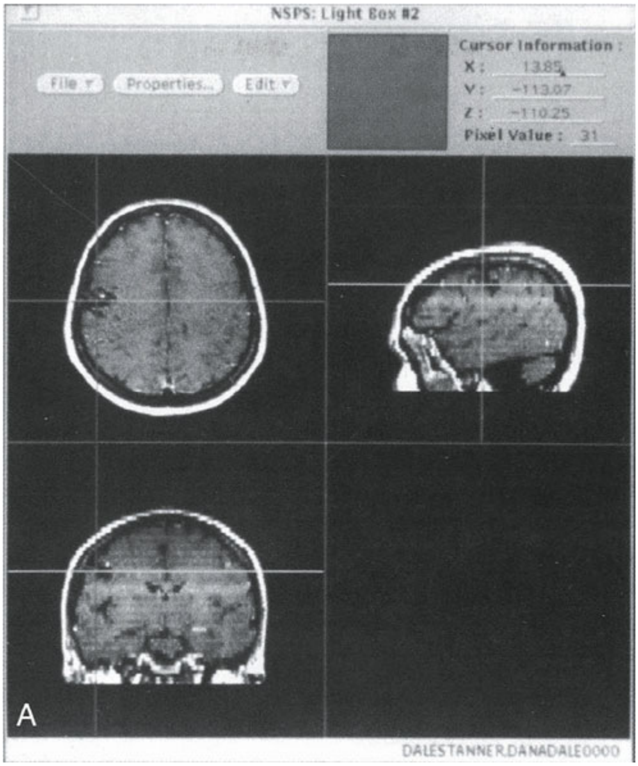

Fig. 17. 35-year-old patient with seizures had an arteriovenous malformation on the right side, close to the motor cortex, fed mainly by branches of the middle cerebral artery. She underwent preoperative embolization and computed-assisted awake craniotomy and resection of the AVM. (A) and (B) Surgical planning and intraoperative digitization: 2-D axial, sagittal, and coronal MRI images, lateral and AP angiographic views. (C and D) Postoperative angiogram shows no residual AVM. Postoperatively the patient had no neurological deficits. During the resection of vascular malformations, intraoperative interactive infrared digitization is useful to localize feeding vessels, remove the nidus, and preserve draining veins to be resected at the end of the procedure

with a method for safe and precise placement of implants. For example, the successful insertion of a pedicle screw relies on accurate definition of the pedicle. Optimally, the screw entry point is at the junction of the facet joint and transverse process and the screw must be angled to correspond to the orientation of the pedicle. In addition, the depth of insertion needs to be defined. Digitizers allow the surgeon to plan and simulate the procedure preoperatively and create an approximate axis for pedicle screw insertion (Fig. 18). During the placement of pedicle screws, software tools can be used to interactively optimize the screw trajectory and display the trajectory in 2-D and 3-D images. This decreases the patient's and surgeon's exposure to

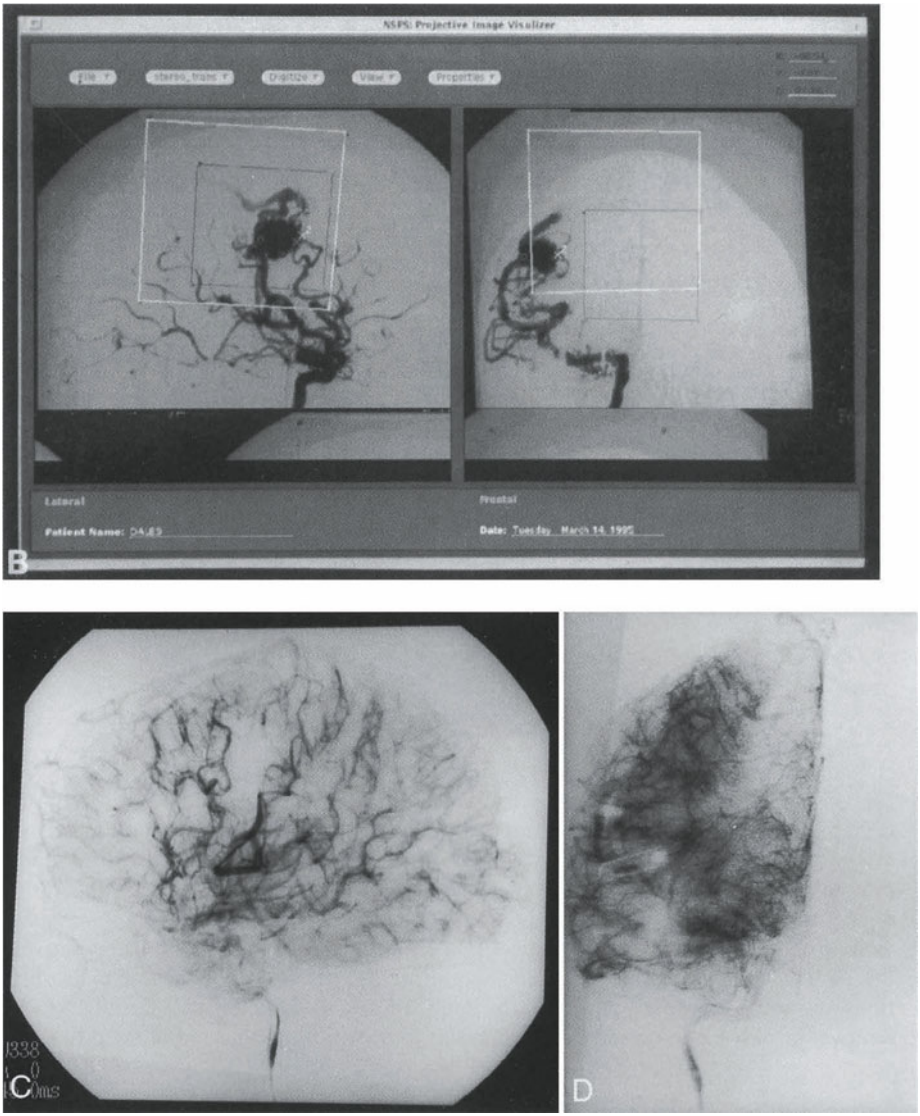

Fig. 17 (*continued*)

fluoroscopy, and the risk of neurological deficit due to an improper screw placement.

Another application of digitizers during spinal surgery is the treatment of patients with vertebral tumors. These patients usually appear with compression fractures, are unstable, and show neurological deficits. Immediate surgical goals include the resection of the pathological segment, restoration

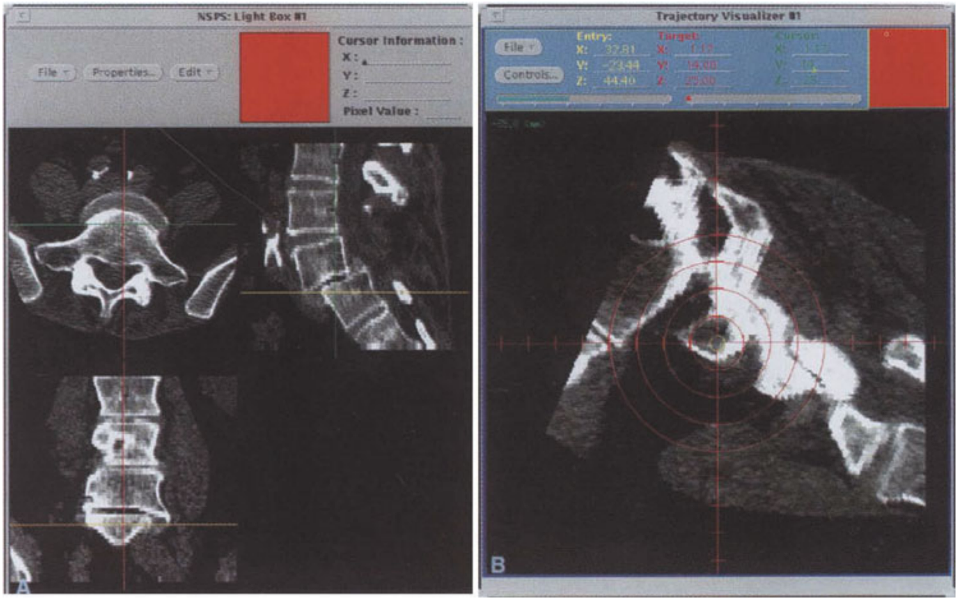

Fig. 18. Spinal applications. (A) Axial, saggital, and coronal CT reconstructions during planning for pedicle screw placement. (B) Screw perspective: Image reconstruction in a plane parallel to the screw trajectory

of the load-bearing capacity of the spine, and decompression of compromised neural structures in an attempt to increase the patient's quality of life. However, the surgical treatment of vertebral tumors has been associated with severe complications, including vascular injury, profuse hemorrhage, neurological deterioration, and postoperative instability leading to kyphosis.

During the surgical resection of a vertebral tumor and spinal reconstruction, the use of digitizers offers several advantages. The position of the instrument tip is displayed intraoperatively on the 2-D and 3-D images to determine in real-time the geometry of the tumor, margins of the surgical resection, and the position of the posterior longitudinal ligament and spinal canal. In cases where anterior instrument fixation is needed, digitizers enable measurement of the length of screw needed, and the interactive control of the drilling procedure, until the screw path is optimized.

Discussion

Localization is essential to the successful completion of a neurosurgical procedure. An error in surgical position can result in failure to remove a lesion or damage to normal functioning tissue, with severe and irreversible neurological deficit. The advent of CT and MRI has allowed the neurosurgeon to visualize preoperatively the anatomy, location, and margins of intracranial lesions with a high degree of spatial precision. This has developed into a new field of study in neurosurgery, that of computer image-guided pre-planning, simulation, and surgical procedures. In any image-guided surgical system, errors may arise from a number of factors: distortions in the imaging, mechanical maladjustment, or changes due to slipping frames or markers between image manipulation and surgery or during surgery. In addition, the ability of any imaging system to localize a single point in space is bound by the voxel size. Mechanical systems may be exactly adjusted, yet the location of the tip is not a point but a volume in space described by the device's mechanical resolution.

The first application of a microscope as a pointing device for frameless procedures was Robert's stereotactic microscope [11, 46]. Although an ideal localizing system should be compatible with a surgical microscope, the primary pointing device should not require the additional use of the surgical microscope [4]. The stereotactic microscope has several undesirable characteristics as a pointing device, but the main one is its long focal length that results in a "moment" arm that magnifies errors in localization. In addition optical focal length is not reliably constant in clinical use.

Stereotactic pointing devices based on the use of multi-articulated arms have been proposed. These articulated arms can be directed by different methods, including the use of precision potentiometers or optical encoders [19, 21]. These articulated arms can provide great precision, but are extremely complex, very expensive, occupy much room, and are not very portable. The use of a hand-free pointer, free of most mechanical constraints, has been proposed [4]. It offers high accuracy, the feel of a surgical instrument, may be adaptable to multiple surgical instruments, and would be unobtrusive.

Each of the above systems present some problems. The accuracy needed for surgical procedures is primarily dependent on the location of the lesion. Lesions near the midbrain, optic nerve, or major blood vessels require much more accuracy than other, more approachable convexity lesions. When localization is based on preoperative diagnostic images, the resolution of MRI is a limiting factor, depending on its voxel dimensions. Current MRI systems have an accuracy of 1–2 mm.

Another source of error could be the method of patient-image registration (surface matching, stereotactic frame, or fiducial markers). In order to minimize error, we utilize semi-permanent fiducial markers (Fisher-Leibinger, Freiburg, Germany) for frameless stereotaxis. Finally, registration could be skewed by a few millimeters if movement of the brain relative to the skull occurs, which can happen after the dura is incised, or if atrophy or osmotic agents are given (aggressive dehydration). These problems can be minimized by performing a small-size craniotomy and implanting marking threads into the tissue as soon as possible, after the brain is exposed.

Sonic digitizers have been introduced as a way of overcoming some of these problems [11, 43, 47]. Intraoperative use of ultrasound allows for continuous tracking of intracranial structures. However, ultrasound suffers from low resolution and the resulting difficulty in interpreting the images obtained. Because the speed of sound varies with temperature, temperature gradients between the surgical field and the instrument result in positional error [55]. Furthermore, sonic digitizers are also sensitive to echoes, as the sound may bounce off walls and other smooth surfaces. If the delayed echo is used for localization, the resultant positional error can be extreme [7]. All these problems can be solved, but high reliability is hard to achieve.

The use of a magnetic field sensor was also attempted, with a reported maximum 4 mm error. However, the use of surgical instruments can increase distortion [28]. Their accuracy depends on achieving a precise magnetic field. Ferromagnetic substances, aluminium, and electromagnetic radiation distort magnetic fields, impairing localization accuracy. This drawback limits their usefulness in the operating room.

An optically identifiable navigator can be localized by one or more video cameras. Reasonable accuracy could be achieved with such an approach, but there is a need for a very sophisticated custom-designed hardware and software. The cameras cannot detect rotation movements of the pointer, and the cameras need to be able to visualize the pointer [30].

Articulated arms are extremely precise, but offer a series of disadvantages. They are usually bulky, clumsy, heavy, and interfere with the course of surgery. Usually the pointer needs to be rigidly attached to the arm, making it difficult to change instruments during surgery. Active robots are programmed to move near the treatment area, but they may make unpredictable, dangerous moves in case of failure in the control software, image calibration, or hardware [40]. Passive systems are moved only by the neurosurgeon, so failures of the system can be better controlled. With the exception of magnetic digitizers, all non-linked systems require an unobstructed path from the emitters to the detector array.

Finally, none of the existing systems currently employed allows imaging of the brain during the course of surgery. We believe that the most versatile digitizing technology is provided by optical trackers, utilizing CCD cameras. This system has proven to be safe, reliable, and very accurate, is a hands-free system that can be used with multiple instruments, and does not interfere with any of the standard neurosurgical techniques [60, 61]. Any surgical instrument, including the operative microscope, can be used with this system. We have used an infrared digitizer in more than 700 cases of intracranial surgery including intraaxial and skull base tumors, vascular malformations, and epilepsy [58, 59, 62].

Conclusion

Much work remains to be done to make the intraoperative display more convenient for the neurosurgeon, including the use of virtual or augmented reality displays (overlay of real video images and MR-derived 3-D models of the patient), or imaging studies projected directly on the patient or in the operative microscope. Also additional work is necessary on the surgeon-computer interface to make it more intuitive and transparent. In the future, intraoperative CT/MRI scans and software simulation of brain distortion may help solve these problems.

References

1. Adams L, Krybus W, Meyer-Ebrecht D, *et al* (1990) Computer assisted surgery. IEEE Computer Graph Appl 10: 43–51
2. Alpert NM, Bradshaw JF, Kennedy D, Correia JA (1990) The principal axes transformation: A method for image registration. J Nucl Med 31: 1717–1722
3. Bajcsy R, Lieberson R, Reivich M (1983) A computerized system for the elastic matching of deformed radiographic images to idealized atlas images. J Comput Assist Tomogr 7: 618–625
4. Barnett GH, Kormos DW, Steiner CP, Piraino D, Weisenberger J, Hajjar F, Wood Chris, McNally J (1993) Frameless stereotaxy using a sonic digitizing wand. Development and adaptation to the Picker ViStar Medical Imaging System. In: Maciunas RJ (ed) Interactive image-guided neurosurgery. AANS, Park Ridge, pp 113–119
5. Barnett GH, Kormos DW, Steiner CP, Weisenberger J (1993) Use of a frameless, armless stereotactic wand for brain tumor localization with 2-D and 3-D neuroimaging. Neurosurgery 33: 674–678
6. Brown RA, Roberts TS, Osborn AG (1980) Stereotaxic frame and computer software for CT-directed neurosurgical localization. Invest Radiol 15: 308–312
7. Bucholz RD, Smith KR (1993) A comparision of sonic digitizers versus light emitting diode-based location. In: Maciunas RJ (ed) Interactive image-guided neurosurgery. AANS Publications Committee, Park Ridge, pp 179–200
8. Chen CT, Pelizzari CA, Chen GTY, *et al* (1988) Image analysis of PET data with the aid of CT and MR images. In: de Graaf CN, Viergever MA, (eds) Information processing in medical imaging, 10th ed. Plenum, New York, pp 601–611
9. Critchlow AJ (1985) Introduction to robotics. MacMillan, New York
10. Dann R, Hoford J, Kovacic S, *et al* (1988) Three-dimensional computerized brain atlas for elastic matching: Creation, and initial evaluation. Medical imaging II: Image formation, detection, processing, and interpretation. Proc SPIE 914: 600–608
11. Drake JM, Joy M, Goldenberg A, Kreindler D (1991) Computer and robot-assisted resection of thalamic astrocytomas in children. Neurosurgery 29: 27–33

12. Driller J, Frei EH (1987) A review of medical applications of magnet attraction and detection. J Med Eng Technol 11: 271–277
13. Foley KT, Smith MM (1996) Image-guided spine surgery. Neurosurg Clin N Am 7: 171–186
14. Friets EM, Strohbehn JW, Hatch JF, Roberts DW (1989) A frameless stereotaxic operating microscope for neurosurgery. IEEE Trans Biomed Eng 36: 608–617
15. Galloway RL Jr, Maciunas RJ (1993) An articulated arm for neurosurgical use. In: Maciunas RJ (ed) Interactive imaged-guided surgery. AANS, Park Ridge, pp 159–168
16. Glauser D, Flurry P, Piguet Y, Epitaux M, Favre J, Meuli RA, Frankhauser H, (1994) Robot CT guided stereotactic neurosurgery. Stereotact Funct Neurosurg 63: 93–98
17. Goerss SJ, Kelly PJ, Kall BA, Alker GJ (1982) A computed tomographic stereotactic adaptation system. Neurosurgery 10: 375–379
18. Golfinos JC, Fitzpatrick BC, Smith LR, Spetzler R (1995) Clinical use of a frameless stereotactic arm: Results of 325 cases. J Neurosurg 83: 197–205
19. Guthrie BL, Adler JR (1991) Frameless stereotaxy: Computer interactive neurosurgery. In: Barrow DL (ed) Perspectives in neurological surgery. Quality Medical Publishing, St Louis, pp 1–19
20. Guthrie BL, Kaplan R, Florek D (1992) Stereotactic neurosurgical operating arm system. Stereotact Funct Neurosurg 58: 144–145
21. Hassenbusch SJ, Anderson JS, Pillay PK (1991) Brain tumor resection aided with markers placed using stereotaxis guided by magnetic resonance imaging and computed tomography. Neurosurgery 28: 801–806
22. Heilbrun PM, Koehler S, McDonald P, Peters W, Sieminov Y, Wiker C (1993) Implementation of a machine vision method for stereotactic localization and guidance. In: Maciunas RJ (ed) Interactive image-guided neurosurgery. AANS, Park Ridge, pp 169–177
23. Heilbrun MP, Mc Donald P, Wiker C, Koehler S, Peters W (1992) Stereotactic localization and guidance using a machine vision technique. Stereotact Func Neurosurg 58: 94–98
24. Hill DLG, Hawkes DJ, Crossman JE, Gleeson MJ, Cox TC, Braley EE, Strong AJ, Graves P (1991) Registration of MR and CT images for skull base surgery using point like anatomical features. Br J Radiol 64: 1030–1035
25. Horstmann GA, Reinhardt HF (1994) Ranging accuracy test of the sonic microstereometric system. Neurosurgery 34: 754–755
26. Jiang H, Robb RA, Holton KS (1992) A new approach to 3-D registration of multimodality medical images by surface matching. Visualization in biomedical computing. Proc SPIE 1808: 196–213
27. Junck L, Moen JG, Hutchins GD, Brown MB, Kuhl DE (1990) Correlation methods for the centering, rotation, and alignment of functional brain images. J Nucl Med 31:1220–1226
28. Kato A, Yoshimine T, Hayakawa T, Hayakawa T, Tomita Y, Ikeda T, Mitomo M, Harada K, Mogami H (1991) A frameless, armless navigational system for computer-assisted neurosurgery. J Neurosurg 74: 845–849

29. Koivukangas J, Louhisalmi Y, Alakuijala J, Oikarinen J (1993) Ultrasound controlled neuronavigator-guided brain surgery. J Neurosurg 79: 36–42
30. Krybus W, Knepper A, Adams L, *et al* (1991) Navigation support for surgery by means of optical position detection. Proceedings of the International Symposium CAR91 Computer Assisted radiology. Springer, Berlin Heidelberg New York Tokyo, pp 362–366
31. Kwoh YS, Hou J, Jonckheere EA, Hayati S (1988) A robot with improved absolute positioning accuracy for CT guided stereotactic brain surgery. IEEE Trans Biomed Eng 35: 153–160
32. Leggett WB, Greenberg MM, Gannon WE, *et al* (1991) The viewing wand—a new system for three-dimensional CT correlated intraoperative localization. Curr Surg 48: 674–678
33. Leksell L, Jernberg B (1980) Stereotaxis and tomography: A technical note. Acta Neurochir (Wien) 52: 1–7
34. Levin DN, Hu XP, Tan KK, Galhotra S, Pelizzari CA, Chen GT, Beck RN, Chen CT, Cooper MD (1989) The brain: integrated three dimensional display of MR and PET images. Rad 172: 783–789
35. Levin DN, Pelizzari CA, Chen GTY, Chen CT, Cooper MD (1988) Retrospective geometric correlation of MR, CT, and PET images. Radiology 169: 817–823
36. Mandava VR, Fitzpatrick JM, Maurer CR Jr, *et al* (1992) Registration of multimodal volume head images via attached markers. Medical imaging VI: Image processing. Proc SPIE 1652: 271–282
37. Manwaring KH (1993) Intraoperative microendoscopy. In: Maciunas RJ (ed) Interactive imaged-guided surgery. AANS, Park Ridge, pp 217–232
38. Mosges R, Schlondorff G (1988) A new imaging method for intraoperative therapy control in skull base surgery. Neurosurg Rev 11: 245–247
39. Nolte LP, Zamorano L, Jiang Z, Wang Q, Langlotz F, Berlemann U (1995) Image guided insertion of transpedicular screws: A laboratory set-up. Spine 20: 497–500
40. Oikarinen J, Alakuijala J, Louhisalmi Y, *et al* (1993) The oulu neuronavigator system: Intraoperative ultrasonography in the verification of neurosurgical localization and visualization. In: Maciunas RJ (ed) Interactive image-guided neurosurgery. AANS, Park Ridge, pp 233–246
41. Pelizzari CA, Chen GTY, Spelbring DR, *et al* (1989) Accurate three-dimensional registration of CT, PET, and/or MR images of the brain. J Comput Assist Tomogr 13: 20–26
42. Pelizzari CA, Tan KK, Levin DN, *et al* (1991) Interactive 3-D patient-image registration. In Colchester ACF, Hawkes DJ (eds) Information processing in medical imaging, 12th ed. New York, pp 132–141
43. Reinhardt H, Meyer H, Amrein E (1988) A computer assisted device for the intraoperative CT correlated localization of brain tumors. Eur Surg Res 20: 51–58
44. Reinhardt HF, Horstmann GA, Gratzl O (1993) Sonic stereometry in microsurgical procedures for deep-seated brain tumors and vascular malformations. Neurosurgery 32: 51–57

45. Ritter RC, Grady MS, Howard III MA, Gillies GT (1996) Magnetic stereotaxis: Computer-assisted image-guided remote movements of implants in the brain. In: Taylor RH, Lavalle S, Burdea GC (eds) Computer integrated surgery. Cambridge, MIT, pp 365–369
46. Roberts DW, Strohbehn JW, Friets EM, Kettenberger J, Hartov A (1989) The stereotactic operating microscope: Accuracy, refinement, and clinical experience. Acta Neurochir (Wien) [Suppl] 46: 112–114
47. Roberts DW, Strohbehn JW, Hatch JF, Murray W, Kettenberger H (1986) A frameless stereotaxic integration of computerized tomographic imaging and the operating microscope. J Neurosurg 65: 545–549
48. Salcman M (1993) Intrinsic cerebral neoplasms. In: Apuzzo M (ed) Brain surgery complication avoidance and management. Churchill Livingstone, New York, pp 379–461
49. Schlondorff G, Mosges R, Meyer-Ebrecht D, Krybus W, Adams L (1989) CAS-computer-assisted surgery. HNO 37: 187–190
50. Sekhar LN, Goel A (1993) General considerations on skull base surgery. In: Apuzzo M (ed) Brain surgery complication: Avoidance and management. Churchill Livingstone, New York, pp 2167–2174
51. Takizawa T (1993) Neurosurgical navigation using a noninvasive stereoadapter. Surg Neurol 40: 1–6
52. Talairach J, Tournoux P (1988) Co-planar stereotactic atlas of the human brain. Thieme, New York
53. Tan KK, Grzeszuk R, Levin DN, Pelizzari CA, Chen GT, Erickson RK, Johnson D, Dohrmann GJ (1993) A frameless stereotactic approach to neurosurgical planning based on retrospective patient-image registration. J Neurosurg 79: 296–303
54. Vinas FC, Zamorano L, Lis-Planells M, Buciuc R, Diaz FG (1997) Interactive intraoperative localization during the resection of intraventricular lesions. Min Invas Neurosurg 39: 65–70
55. Watanabe E (1993) The neuronavigator: A potentiometer-based localizing arm system. In: Maciunas RJ (ed) Interactive image-guided neurosurgery. AANS, Park Ridge, pp 135–147
56. Watanabe E, Mayanagi Y, Kosugi Y, Manaka S, Takakura K (1991) Open surgery assisted by the neuronavigator, a stereotactic, articulated, sensitive arm. Neurosurgery 28: 792–800
57. Young RF (1987) Application of robotics to stereotactic surgery. Neurol Res 9: 123–128
58. Zamorano L, Nolte LP, Kadi AM, Jiang Z (1994) Interactive intraoperative localization using an infrared-based system. Stereotact Funct Neurosurg 63: 84–88
59. Zamorano L, Lis-Planells M, Jiang Z, Nolte LP, Kadi AM, Diaz FG (1996) Vascular malformations of the brain: Surgical management using interactive image guidance. Neurosurg Clin North Am 7: 201–214
60. Zamorano L, Nolte L, Jiang C, Kadi M (1993) Image-guided neurosurgery: frame based versus frameless approaches. Neurosurgical Operative Atlas 3: 402–422

61. Zamorano L, Nolte L, Kadi M, Jiang Z (1993) Interactive intraoperative localization using an infrared-based system. Neuro Res 15: 290–298
62. Zamorano L, Nolte L, Kadi M, Jiang Z (1993) Modification of stereotactic frame guidance arcs using optical encoder verniers. In: Maciunas RJ (ed) Interactive image-guided neurosurgery. AANS, Park Ridge, pp 97–103
63. Zamorano L, Vinas FC, Buciuc R, Jiang Z, Li H, Diaz FG (1997) Use of an open stereotactic ring for neurosurgery procedures. Min Invas Neurosurg 40: 79–82
64. Zamorano L, Vinas FC, Buciuc R, Diaz FG (1997) Advanced neurosurgical navigation using a robotic microscope integrated with an infrared-based system. In: Trmaki N, Ehrra K (eds) Computer-assisted neurosurgery. Springer Tokyo

Editorial Comment

Dr. Zamorano has made major contributions to the field of neuronavigation, and the Editorial Board is pleased to be able to publish this paper. The preoperative imaging, registration, and pointer-tracking technologies are certain to become cheaper, more user-friendly, and hence more accessible to a broader market. Surgeons will therefore need to develop robust performance criteria on which to assess competing systems, and manufacturers will need to agree on standard interfaces which permit easy data transfers between components from different sources. Dr. Zamorano's suggestion that 2 mm is an appropriate accuracy to be expected from navigation systems is supported by a wide body of opinion, and in open surgery there is probably little to be gained from accuracies greater than this. However, the problem of tissue movement and deformation from the anatomy imaged preoperatively, following, for example, ventricular drainage, brain retraction, or resection of a mass lesion is a very significant one; intraoperative MRI is unlikely to provide a *general* solution, and tracked ultrasound probes may be a possible alternative.

The Editorial Board

B. Technical Standards

The Endovascular Treatment of Brain Arteriovenous Malformations

A. Valavanis and M. G. Yaşargil

Institute of Neuroradiology, University Hospital of Zurich, Zurich (Switzerland)

With 5 Figures and 10 Tables

Contents

1. Introduction and Historical Perspective

Brain AVMs are angioarchitecturally and hemodynamically complex systems of arteriovenous shunts with specific neurovascular relationships, a variable and unpredictable clinical presentation and a dynamic and only partially understood natural history, associated with a significant morbidity and mortality.

Brain AVMs are generally regarded as congenital lesions representing inborn errors of embryonic vascular morphogenesis caused by a defect or malfunction of the embryonal capillary maturation process and resulting in the formation or persistence of arteriovenous shunts (Kaplan *et al.* 1961).

There is increasing evidence that the majority of brain AVMs, with the exception of aneurysmal malformations of the Galenic vein, develop postnatally and represent a complex endothelial cell dysfunction, triggered by still unknown factors (Lasjaunias, personal communication). In favour of this hypothesis are recent immuno-histochemical studies performed on surgically obtained specimens of human brain AVMs which demonstrated, that the preproendothelin-1 gene is locally repressed in brain AVMs (Rhoten *et al.* 1997). The repression of this gene is an intrinsic phenotype of endothelial cells of brain AVMs and is not due to factors in the microenvironment of the AVM (Rhoten *et al.* 1997). In addition, other recent studies demonstrated expression of vascular endothelial growth factor predominantly in the subendothelial layer and in perivascular spaces of vessels composing brain AVMs (Rothbart *et al.* 1996).

Embolization represents one of the modalities currently available for the treatment of brain AVMs, the others being microneurosurgical removal and radiosurgical obliteration. The theoretical advantage of the endovascular approach is, that it avoids any direct interference with the brain parenchyma, such as cortical incisions, brain retraction, cranial nerve manipulations. The limitations are mainly technical and include the inaccessibility of certain AVMs or parts of AVMs with the currently available microcatheters and the occasional unpredictability of behaviour of the injected embolic agent within the vascular spaces of the AVM.

During the years, embolization advanced from a simple technique initially conceived to block feeding arteries of AVMs to a sophisticated one with the aim to use the feeding arteries as vascular routes to reach and obliterate the core, so called nidus, of the AVM.

The endovascular approach to brain AVMs dates back to Brooks

(1930), who injected muscle particles into the surgically exposed internal carotid artery in order to occlude endovascularly carotid-cavernous fistulas. Luessenhop and Spence (1960) were the first to use this concept introduced thirty years earlier by Brooks to treat brain AVM's. They used steel particles (spheres) covered with methyl methacrylate introduced into the surgically exposed internal carotid artery in order to block feeding arteries supplying a brain AVM, and called this technique "artificial embolization" (Luessenhop and Spence, 1960). This technique was subsequently refined by using barium-impregnated Silastic spheres introduced into the cerebral circulation through a catheter inserted surgically into the common carotid artery and advanced manually into the internal carotid artery (Luessenhop and Velasquez 1964, Luessenhop *et al.* 1962, Luessenhop *et al.* 1965).

In 1964 Dolce reported on the first superselective catheterization of the cerebral arteries using a self-constructed 1.5 mm thin microcatheter tapering at its tip to 0.7 mm, inserted percutaneously with the Seldinger technique into the internal carotid artery and advanced into the proximal anterior and middle cerebral arteries.

In the late sixties, Yodh *et al.* (1968) and Hilal (1969) in an attempt to improve intravascular navigation developed and applied independently magnetic control systems used with Silastic catheters, but without success regarding distal microcatheterization.

In the early seventies, Kricheff *et al.* developed the percutaneous transfemoral catheter embolization technique which enabled either the anterior or the posterior cerebral circulation to be approached (Kricheff *et al.* 1972). This nonselective endovascular technique using flow-directed particles was applied palliatively for embolization of large brain AVMs or preoperatively (Kricheff *et al.* 1972, Hilal and Michelsen 1975).

A major technical breakthrough in endovascular techniques occurred in 1974, when Serbinenko reported for the first time on the introduction of detachable balloons mounted on the tip of microcatheters and used for flow-guided intracranial navigation beyond the circle of Willis and for occlusion of major cerebral arteries as well as occlusion of feeding arteries related to brain AVMs and AV-fistulae (Serbinenko 1974). Serbinenko's technique had a major impact on the further refinement of cerebral endovascular techniques leading to the modern era of superselective microcatheterization and embolization, pioneered by Djindjian (1975) in Europe and Kerber (1976) and Pevsner (1977) in the United States.

Kerber (1976) introduced flow-guided, calibrated-leak microballon catheter systems consisting of very flexible and soft Silastic, permitting superselective microcatheterization of brain AVM feeding arteries and embolization with acrylics. Pevsner (1977) introduced a pressure chamber to enhance the propulsion of the calibrated-leak microballoon-catheter and Berenstein (1981) and Debrun *et al.* (1982) introduced calibrated-leak latex balloons to improve small vessel microcatheterization and acrylic delivery. This technique was in routine use until 1986/87, when a new era of superselective cerebral vascular navigation began with the introduction of the newest generation of variable stiffness microcatheters, used either in conjunction with microguidewires (Kikuchi *et al.* 1987) or as flow-guided systems (Dion *et al.* 1989) and permitting safer and more controllable superselective catheterization.

2. Epidemiology, Clinical Presentation and Natural History of Brain AVMs

Brain AVMs exhibit a wide variability in size, location, vascular composition, and clinical presentation so that accurate determination of the natural history of an individual case is difficult and may even be impossible.

The prevalence of brain AVMs in the general population is uncertain and is probably influenced by geographical and racial factors. Jellinger (1986) reported a prevalence of 0.11% calculated from general autopsy series on 41'395 cases and Karhunen (1990) estimated the prevalence to be 0.06% based on a material of 8'038 consecutive medico-legal autopsies. In North America the prevalence has been estimated to be between 0.02% and 0.08% (Berenstein and Lasjaunias 1991). The incidence, i.e. the frequency of newly diagnosed brain AVMs per year, has been estimated to be 0.01%–0.001% (Ondra *et al.* 1990, Crawford *et al.* 1986, Wikholm 1995).

Hemorrhage is the most common presenting symptom of a brain AVM, being reported to occur as the initial manifestation of the disease in approximately 50% of patients with an AVM (Perini *et al.* 1995, Perret and Nishioka 1966, Waltimo 1973). There is increasing evidence, that the incidence of hemorrhage is higher. It is not unusual to find old hemorrhagic areas on MR images or to observe small chronic hemorrhage during microsurgical removal of AVMs in patients, in whom these events have not been detected clinically (Berenstein *et al.* 1993, Stein and Wolpert 1980, Yamada 1982, Yaşargil 1988). It has been postulated, that episodes of acute headaches, seizures or other acute neurologic symptoms may represent hemorrhages.

In a prospective study of 166 patients with untreated symptomatic cerebral AVMs, Ondra *et al.* reported an annual bleeding rate of 4% regardless of the initial clinical presentation (Ondra *et al.* 1990). This annual bleeding rate remained constant throughout the follow-up period of 24 years. The first hemorrhage is associated with a mortality of 10% reaching up to 20% for subsequent recurrent hemorrhages (Wilkins 1985). In the prospective study of Ondra *et al.* (1990), the annual rate of mortality was 1% and that of severe morbidity 1.7%, this rates being constant over the course of the study. 85% of the patients who bled, corresponding to 34% of the patient population of the study, either died or suffered severe morbidity during the 24 years of the study.

Several studies correlate the angiographic features with the clinical presentation of patients with brain AVMs (Albert *et al.* 1990, Berenstein and Lasjaunias 1991, Brown *et al.* 1990, Kader *et al.* 1994, Marks *et al.* 1990, Miyasaka *et al.* 1994, Miyasaka *et al.* 1992, Okamoto *et al.* 1984, Norbash *et al.* 1994, Patel *et al.* 1995, Turjman *et al.* 1995a, Turjman *et al.* 1995b, Willinsky *et al.* 1988, Nataf *et al.* 1997). These studies clearly showed, that there is a statistically significant increased incidence of hemorrhage in AVMs that are associated with flow-related aneurysms, stenoses or occlusion of draining veins, or that are located in the deep parts of the brain and in the posterior fossa. It has been repeatedly postulated, that small and micro-AVMs are at higher risk of hemorrhage than larger AVMs because the pressures in the feeders and the nidus of small AVMs were found to be significantly higher than in larger AVMs (Graf *et al.* 1983, Spetzler *et al.* 1992). Recent reports suggest, that there is no direct correlation between the size of the AVM and the incidence of hemorrhage (Berenstein and Lasjaunias 1991, Crawford *et al.* 1986a, Marks *et al.* 1990, Ondra *et al.* 1990, Willinsky *et al.* 1988). Small AVMs are usually asymptomatic before hemorrhage and their most frequent manifestation is due to rupture. This in contrast to larger AVMs which more often present with seizures or neurological deficits.

Seizures are the second most frequent presenting symptom of cerebral AVMs following hemorrhage reported to occur in 28% to 67% of patients with an AVM (Berenstein and Lasjaunias 1991, Perret and Nishioka 1966). The incidence of seizures is particularly high in AVMs of the temporal lobe and in those involving the motor-sensory strip (Crawford *et al.* 1986b). Retrospective analysis of angiographic data of patients with AVM presenting with epilepsy suggests, that rerouting of venous drainage from the AVM through a vein that previously drained normal brain and the associated venous hypertension may be a major cause of epilepsy (Berenstein and Lasjaunias 1991, Turjman *et al.* 1995). This evidence is further substantiated by the fact, that AVMs located in non-epileptogenic areas, such as the basal ganglia and the cerebellum, may cause seizures following venous thrombosis and rerouting of venous drainage (Berenstein and Lasjaunias 1991). Seizures may also be a clinical manifestation of minor hemorrhage. The risk of hemorrhage in patients experiencing seizures related to their AVMs is lower than in those with previous hemorrhage, but higher than in patients without a history of epilepsy (Crawford *et al.* 1986b, Graf *et al.* 1983). In the prospective study of Ondra *et al.* (1990), patients with AVM-related hemorrhage and patients with epilepsy had similar long-term morbidity and mortality.

Neurologic deficits not associated with previous hemorrhage occur less frequently than seizures or bleeding and may be caused by several mechanisms including steal effect of the AVM, decreased perfusion because of associated arterial stenoses, venous hypertension or mass-effect caused by compression of brain parenchyma by venous ectasias or varices (Berenstein and Lasjaunias 1991).

Headache not associated with an acute hemorrhage is a relatively frequent complaint of patients with AVMs. Angiographic-clinical correlations have shown, that dilated feeding arteries and draining veins, in topographic relationship with the meninges and the tentorium, may be responsible for chronic headaches in patients with brain AVMs. Furthermore, the incidence of headaches is particularly high in patients with additional dural supply of their AVM and in those with an occipital location of the lesion (Berenstein and Lasjaunias 1991).

3. Patients and Methods

This series consists of 387 patients with a brain AVM, which underwent endovascular treatment between November 1986 and July 1996 and refers to patients treated after the introduction of variable stiffness microcatheters, thus excluding all patients treated before November 1986 either with calibrated leak balloons in conjunction with a propulsion chamber or with non-selective free flow techniques.

236 patients were male and 151 female, 50 patients being children below the age of 16 years. The age ranged between 1 and 74 years, with a mean age of 32 years. 158 patients (41%) presented with intracranial hemorrhage or had a history of previous hemorrhage. 119 patients (30.7%) presented with epilepsy, 31 (8%) with focal neurological deficits, 27 (7%) with chronic headache, 4 (1%) with tinnitus, 2 (0.5%) with signs of increased intracranial pressure, 4 (1%) with congestive cardiac failure, and 4 (1%) with psychomotoric retardation. In 38 patients (9.8%) the AVM was detected incidentally by CT or MR performed for non-specific or vague complaints. 17 patients had received previously radiosurgical treatment without success, 13 patients have been operated upon at other institutions and two patients had been treated previously by surgery and radiosurgery.

A total of 710 embolization sessions were performed in the 387 patients, with an average of 1.7 sessions per patient. 195 patients received one session, 106 patients two sessions, 52 patients three sessions, 26 patients four sessions, 6 patients five sessions, one patient six sessions and one further patient seven sessions. 292 patients underwent endovascular treatment on a monoplane DSA unit and 95 patients were treated on a biplane DSA unit with high-resolution live roadmapping capability.

With the exception of four patients, which underwent emergency embolization in the presence of an acute hematoma, all other patients underwent preembolization MR and MR-angiography (MRA). Triplanar T1-weighted MR was performed for topographic assessment of the AVM and axial T2-weighted MR was performed for evaluation of brain parenchyma. MRA was performed with 3D phase contrast and 3D time-of-flight techniques.

In the time period between 1986 to 1993 the majority of embolizations were performed under neuroleptic analgesia. Children under the age of 15 years were embolized under general anaesthesia. Since the end of 1993 the great majority of embolizations (90%) were performed under general anaesthesia.

All procedures were performed via the transfemoral route using the Seldinger technique. In 46 patients a bifemoral approach for simultaneous catheterization of two feeding arteries was used. The guiding catheters used during the procedure were continuously flushed with heparinized saline (2000 units/L) but no systemic heparinization was used throughout this series.

A total of 3550 superselective catheterizations and 2985 embolic injections were performed, using exclusively variable stiffness microcatheters of either the over-the-wire type (Tracker microcatheters) or more rarely the flow-guided type (Magic microcatheters).

Functional evaluation following superselective injection of amytal (Rauch *et al.* 1992a, b) has not been performed in this series. Decisions regarding injection of embolic material were taken following anatomic evaluation of superselective angiograms and preembolization MR and with the conviction that all brain areas are "eloquent".

Cyanoacrylate was the embolic material of choice used throughout this series. Isobutyl-2-cyanoacrylate (IBCA) was employed between 1986 and 1991. It was replaced by n-butyl-cyanoacrylate (NBCA) in 1991. Cyanoacrylates were used as the sole embolic material in 261 (67%) cases of this series. Polyvinyl-alcohol foam (PVA) in the form of microparticles was used as a supplementary embolic material following either IBCA or NBCA in 103 (27%) of cases. In nine cases (2%) with high-flow fistulae either platinum microcoils or Guglielmi-Detachable Coils (GDC) were used prior to cyanoacrylate embolization. Finally, in fourteen cases (4%) PVA was used exclusively for embolization, because of angioarchitectural reasons.

The techniques of catheterization and embolization used throughout this series are described in detail further below.

With the exception of four patients who suffered an intracerebral hematoma and died, and seven further patients who either refused MR or in whom MR was contraindicated, all other patients had postembolization MR follow-up. Patients with AVM's, in which a complete obliteration was achieved, had follow-up MR and angiography at 6 months following the last embolization session and at variable intervals ranging between 1 and 9 years, with a mean follow-up period of 3.8 years.

4. Topographic Classification of Brain AVMs

Based on the concept of Ask-Upmark formulated in 1938 to localize gliomas and cerebral angiomas on the basis of evolution of the brain and its vascular system, Yaşargil (1988) introduced a refined classification of brain AVMs taking also in consideration the intrinsic arterial supply and the pattern of the venous drainage and incorporating the surgical approaches used for removal of brain AVMs. According to this topographic classification, brain AVMs are divided into two main groups, *i.e.* convexity or pallial AVMs with supra- and infratentorial subgroups and in deep central AVMs with supra- and infratentorial subgroups. The convexial (pallial) group includes the cortical and subcortical areas of the frontal, temporal, insular, parietal, occipital and cerebellar regions. The central or deep system includes the grey matter nuclei of the diencephalon, mesencephalon, metencephalon, connecting white matter fibers, the entire limbic system (amygdala and hippocampus, cingulate gyrus, corpus callosum, parasplenial area and fornix) and the choroid plexus of the lateral, 3rd and 4th ventricles (Yaşargil 1988). From the perspective of endovascular treatment of brain AVMs this classification system, although useful to a certain extent, fails to correlate the type of feeding arteries with the specific location of the AVM. For that purpose, a more detailed vascular anatomic-topographic subdivision of brain AVMs was necessary. This was achieved with the routine application of MR imaging in the pretherapeutic evaluation of brain AVMs. MR imaging proved essential for a precise localization and topographic evaluation of brain AVMs. T1-weighted, triplanar MR imaging allows the evaluation of the AVM nidus with respect to adjacent gyri, sulci and subcortical white matter in cases of convexial or pallial (so-called cortical) AVMs—and with respect to basal fissures, cisterns, the ventricular system, the deep grey matter nuclei and the white matter tracts in cases of deep or central AVMs. Correlation of the topographic information derived from MR imaging with the angioarchitectural information derived from cerebral angiography provides a better understanding of the particular vascularization and drainage of each AVM in relation to its specific location.

Based on MR imaging, both convexial and deep AVMs can be further and more precisely classified into distinct subtypes. Knowledge of the sulcal and gyral anatomy of the brain and application of MR criteria to correctly identify individual sulci, gyri and other structures are essential when analyzing an AVM with regard to location and topography (Naidich *et al.* 1995, Ono *et al.* 1990, Yaşargil 1994).

Convexity or so-called cortical AVMs. Within the group of convexity or so-called cortical AVMs three main types can be distinguished by MR imaging: 1) sulcal AVMs, 2) gyral AVMs and 3) mixed, sulco-gyral AVMs

(Valavanis 1996). To understand the arterial supply of the sulcal and gyral AVMs and analyze superselective angiograms of these types of AVMs, knowledge of the vascularization of the cerebral surface is essential. The arterial vascularization of the pial surface of the brain, the cortex and the subcortical white matter has been extensively studied by several authors (Courville 1958, De Reuck 1972, Duvernoy *et al.* 1981, Forbes 1928, Gillilan 1974, Lang and Schäfer 1980, Lazorthes 1976, Pfeifer 1930, Salamon 1973, Van den Berg and Van der Eecken 1968, Wollschläger and Wollschläger 1978).

Sulcal AVMs. Sulcal AVMs are primarily located within a specific sulcus. As was shown by Hutchings and Weller (1986) with electron microscopic studies, the pial arteries on the surface of gyri and sulci are located in the subpial space, which forms an intrinsic compartment of the subarachnoid space. Therefore, the nidus of sulcal AVMs occupies the subpial space of the sulcus and, depending on its size, it compresses the adjacent gyri to various degrees. Sulcal AVMs may be confined to a sulcus or may extend into the depths of the sulcus, through underlying cortex into the subcortical white matter and even to the ventricular wall. Depending on their size and extension, sulcal AVMs are therefore further classified into three subtypes: (1) pure sulcal, (2) sulcal with subcortical extension and (3) sulcal with subcortical and ventricular extension.

The nidus of sulcal AVMs adapts to the geometric space of the sulcus and assumes a pyramidal or conical shape. The base is covered by the dura-arachnoid layer whereas the apex is located in the depth of the sulcus, the subcortical white matter or in the ventricular wall, depending on the in depth extension of the AVM. The supply to sulcal AVMs is mainly provided by pial arteries. The pial feeders end directly in the nidus after giving off cortical, medullary and cortico-medullary branches to the adjacent gyrus. Therefore, the main supply of sulcal AVMs is provided by direct type of feeders terminating into the sulcally located nidus and not participating into the supply of normal brain distal to the AVM. This angioarchitectural feature has significant importance regarding the endovascular treatment of sulcal AVMs. Deeper portions of larger sulcal AVMs located into the subcortical white matter or near the ventricular wall receive additional supply from short or long medullary and cortico-medullary arteries arising from the pial arterial system as well as from basal perforating arteries. Unlike short and long medullary feeding arteries, the cortico-medullary as well as the perforating arteries always participate in the supply of normal brain. In sulcal AVMs, these feeding arteries provide supplementary supply to the AVM, the dominant supply being provided by the pial feeding arteries. The base of the pyramidally shaped sulcal AVMs is covered by dura-arachnoid layers and not by brain. This explains the frequent participation of additional supply of the more superficial portions of sulcal AVMs from meningeal arteries.

Gyral AVMs. Gyral AVMs are located within a specific gyrus. In contrast to sulcal AVMs, gyral AVMs are covered by cortex and have usually a round shape. Larger gyral AVMs expand the involved gyrus, compress the adjacent sulci and may extend into the subcortical white matter and toward the ventricular wall. The supply of gyral AVMs is provided by dilated cortical, cortico-medullary and medullary branches of the pial arteries of the involved gyrus that continue their course to supply normal brain distal to the AVM. Paraventricular extensions of gyral AVMs receive additional supply from basal perforating arteries. Since gyral AVMs are covered by cortex and, therefore, have no direct contact with the dura-arachnoid layer, they lack additional meningeal supply.

Mixed sulcal and gyral AVMs. Mixed sulcal and gyral AVMs are usually larger lesions than the pure sulcal or gyral type. They involve adjacent sulci and gyri and extend usually into the subcortical white matter and the ventricular wall. Their pattern of arterial supply combines the features of sulcal and gyral AVMs, i.e. the sulcal components of mixed AVMs are supplied by direct and terminal type pial arteries and in addition frequently by meningeal arteries whereas the gyral and subcortical components are supplied by cortico-medullary or medullary branches of pial arteries as well as in a supplementary fashion from basal perforating arteries.

"Diffuse cortical AVMs". A particular type of AVM within the group of so-called "cortical" or convexity AVMs is the rare "diffuse" AVM. These lesions are characterized by numerous, only slightly dilated feeding arteries belonging to the pial-cortical arterial system, a moderately shortened shunt transit time and by numerous cortical draining veins of almost normal caliber. A nidus in the strictest sense cannot be identified angiographically and appears to be intermingled with normal brain tissue. The lesions are typically located cortico-subcortically and may involve small or large areas of a lobe, more than one lobe or even the surface of an entire cerebral hemisphere. Clinically, they present commonly with seizures. They most probably correspond to a proliferative type of angiopathy of yet unknown ethiology and not to a true AVM (Berenstein and Lasjaunias 1991).

Subcortical AVMs. The term subcortical AVMs has been introduced to characterize a topographically distinct type of AVM. These lesions have been always grouped together with the deep brain AVMs. These AVMs are located in the deeper parts of the subcortical white matter, which represents the arterial territory of the long medullary and corticomedullary arteries arising from the pial arterial system and the venous territory of the deep transcerebral veins joining the subependymal venous system. Accordingly, subcortical AVMs receive their dominant supply from long medullary and corticomedullary arteries but may have supplementary supply from deep perforating arteries. The main venous drainage is towards the deep subependymal venous system through transcerebral veins but accessory veins may drain towards the cortical venous system. Subcortical AVMs are extremely rare and were found in 2% of cases in this series.

Deep (central) brain AVMs. The topographic classification principle described above can also be used for further topographic classification of deep cerebral AVMs. Based on MR imaging and its correlation with angiography, deep brain AVMs are further subdivided into (1) subarachnoid AVMs (corresponding to the sulcal AVMs of the convexity), (2) parenchymal AVMs (corresponding to the gyral AVMs of the convexity), (3) plexal or intraventricular AVMs and (4) mixed deep AVMs.

Subarachnoid AVMs are located outside the brain parenchyma within basal cisterns and fissures. Their supply is provided by dilated branches of the proximal subarachnoid segment of perforating and choroidal arteries, which are more readily accessible for micro-catheterization than the distal parenchymal segments of these arteries.

Deep parenchymal AVMs are located within the deep brain structures such as basal ganglia, thalamus, hypothalamus, septum pellucidum, corpus callosum, limbic system, internal capsule or other deep white matter tracts and nuclei. They are supplied in a dominant fashion by basal perforators, choroidal and basal circumferential arteries and in a supplementary fashion by transcortical long medullary or corticomedullary branches of the pial arterial system.

Plexal AVMs arise from the vasculature of the choroid plexus and are therefore extracerebral, intraventricular AVMs. They are primarily and dominantly supplied by choroidal arteries in a direct, terminal fashion. Larger plexal AVMs in contact with the ventricular wall receive additional supply from the subependymal arteries arising from the circle of Willis.

Mixed type deep brain AVMs are usually large lesions and have angioarchitectural features of the subarachnoid, parenchymal and even plexal types.

Deep cerebral AVMs drain primarily and mainly into the venous collectors of the deep venous system, but may also use transcerebral veins joining the superficial venous system for drainage.

The topographic classification of brain AVMs presented here is summarized in Table 1.

5. Angioarchitecture of Brain AVMs

The term "angioarchitecture" refers to the angiographically demonstrable vascular elements composing a brain AVM and includes the feeding arteries, the nidus, the draining veins, any associated vascular anomalies and secondary vascular changes induced by the inherent high-flow of the AVM, subsumized under the term high-flow angiopathy.

Table 1. *Topographic Classification of Brain AVMs*

A.	*Convexity or superficial AVMs (72%)*[a]
	(so-called "cortical" AVMs)
	(1) Sulcal AVMs (28%)[a]
	(a) pure sulcal
	(b) sulcal-subcortical
	(c) sulcal-subcortical-ventricular
	(2) Gyral AVMs (12%)[a]
	(a) pure gyral
	(b) gyral-subcortical
	(c) gyral-subcortical-ventricular
	(3) Mixed sulco-gyral AVMs (29%)[a]
	(a) sulco-gyral
	(b) sulco-gyral-subcortical
	(c) sulco-gyral-subcortical-ventricular
	(4) Diffuse AVMs (= proliferative angiopathy) (3%)[a]
B.	*Subcortical AVMs (2%)*[a]
C.	*Deep or central AVMs (26%)*[a]
	(1) Subarachnoid (fissural, cisternal) (12%)[a]
	(2) Parenchymal (intrinsic) (7%)[a]
	(3) Plexal (intraventricular) (1%)[a]
	(4) Mixed (6%)[a]

[a] Data derived from the MR and angiographic evaluation of the 387 cases of this series.

5.1 Feeding Arteries

Proper angiographic analysis of the arteries supplying an AVM is essential for both understanding the individual construction of a given AVM and for treatment planning. The success of endovascular treatment of brain AVMs with respect to nidus obliteration and patient outcome clearly depends on the ability to superselectively catheterize the distal (prenidal) segments of feeding arteries and on the identification of their relationship with the nidus, their concomitant or absent participation into the supply of normal brain and of any associated high-flow angiopathic changes.

Regarding the endovascular treatment of brain AVMs a classification system incorporating hemodynamic, geometric and anatomic criteria for each feeding artery proved useful in the authors' experience (Table 2).

Hemodynamic Types of Feeding Arteries

Hemodynamically, the feeding arteries of an AVM may be classified according to their contribution to nidus supply. Feeding arteries supplying a

Table 2. *Classification System of Feeding Arteries of Brain AVMs*

A. Direct types of feeding arteries
- (1) Monoterminal
  - (a) dominant
  - (b) supplementary
- (2) Multiterminal
  - (a) dominant
  - (b) supplementary
- (3) Pseudoterminal
  - (a) with flow reversal distally
    - (a.1) dominant
    - (a.2) supplementary
  - (b) induced by wedged catheter

B. Indirect types of feeding arteries
- (1) Transit arteries
  - (a) with single or multiple supplementary feeding branches
  - (b) rarely, with dominant feeding branches
- (2) Retrograde collateral feeding arteries
  - (a) leptomeningeal
    - (a.1) usually supplementary
    - (a.2) dominant following proximal occlusions of dominant feeders
  - (b) subependymal
    - (b.1) usually supplementary
    - (b.2) dominant following proximal occlusions of dominant feeders

large portion or vascular compartment of the nidus are called dominant, whereas feeding arteries supplying a small portion or compartment are called supplementary. Dominant type feeding arteries usually have a significantly larger diameter and higher flow than supplementary type feeding arteries (Fig. 1).

Most AVMs, 82% in this series, were supplied by both dominant and supplementary type of feeders, in various combinations. In the majority of cases with dominant and supplementary supply, multiple dominant and multiple supplementary type of feeding arteries are identified. The next frequently observed combination is that of a single dominant and multiple supplementary feeding arteries. Single or multiple dominant feeding arteries in combination with a single supplementary artery is rarely observed.

Some AVMs, 13% in this series, were supplied exclusively by multiple supplementary type feeding arteries. This mode of supply is particularly observed with insular, some gyral and brain stem AVMs.

Finally, a few AVMs, 5% in this series, were exclusively supplied by one or few dominant type feeding arteries. This pattern of supply is mainly

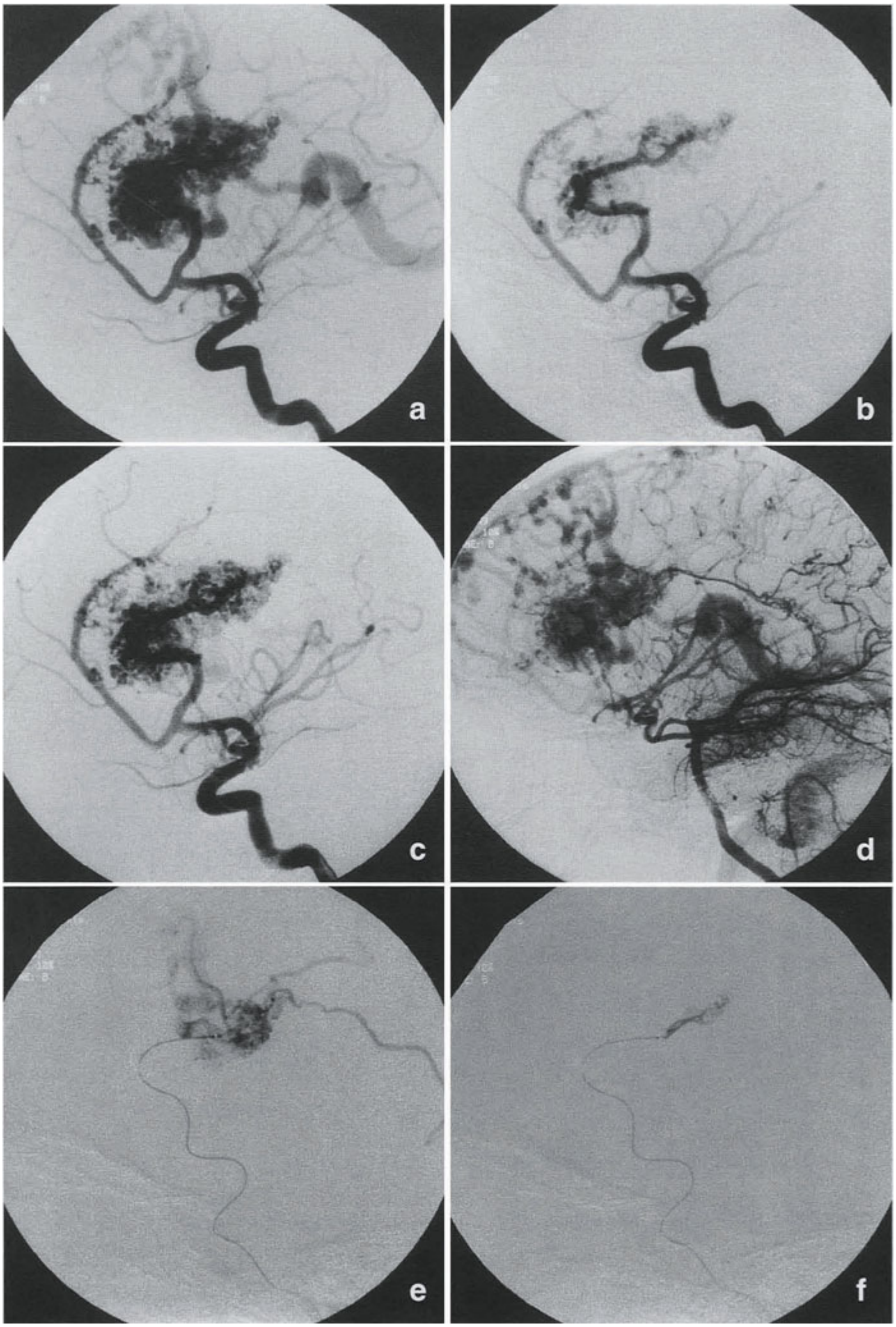

Fig. 1 (a–f)

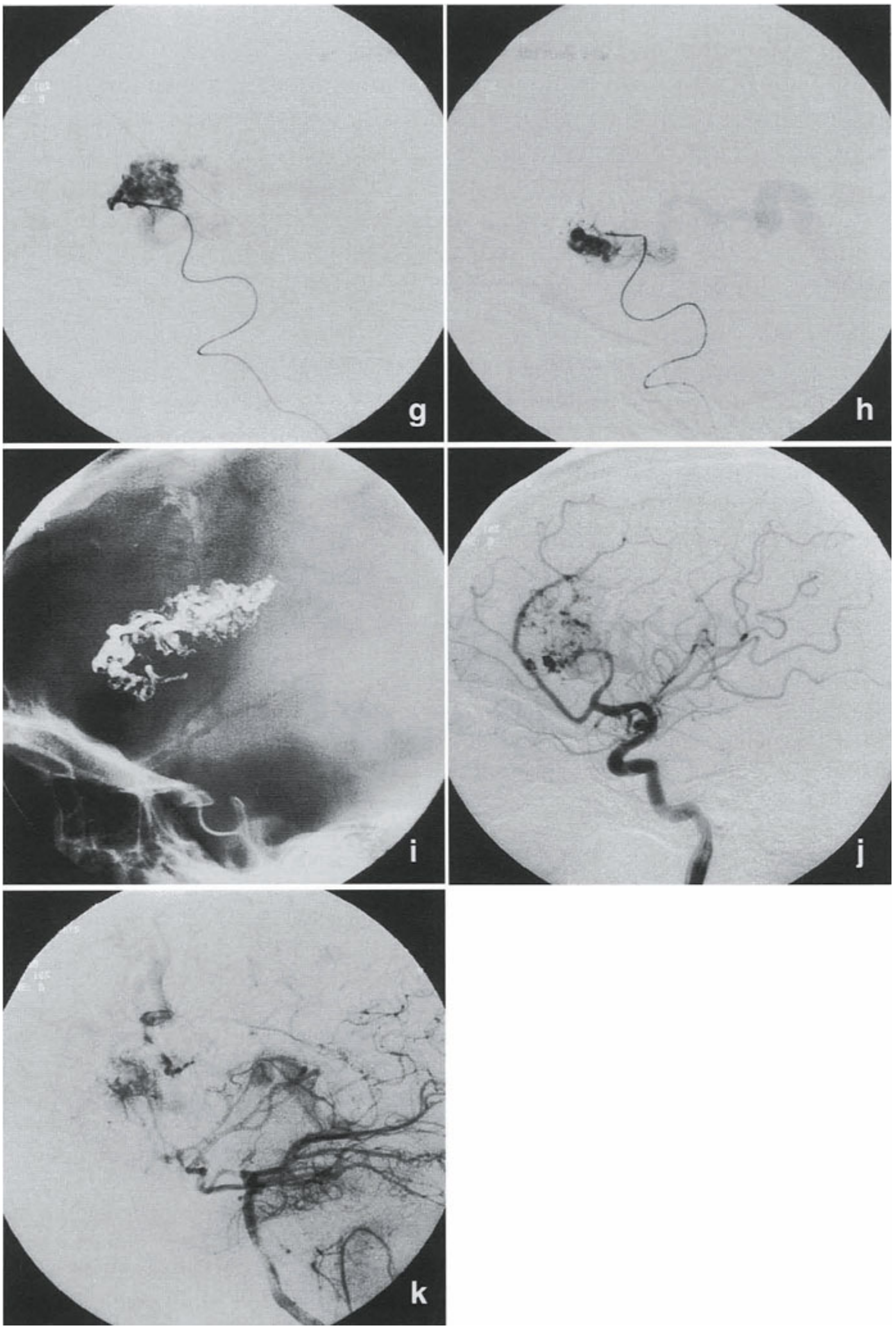

Fig. 1 (g–k)

seen with purely fistulous AVMs, such as pial AVFs and some vein of Galen aneurysmal malformations.

Obviously, the participation of dominant and/or supplementary type of feeding arteries and their relative number in a given AVM influence the achievable degree of obliteration. As a general rule, AVMs supplied either exclusively by dominant feeding arteries or by more dominant than supplementary feeding arteries have a higher chance for complete or subtotal obliteration, than AVMs supplied either exclusively by supplementary or by more supplementary than dominant feeding arteries.

Geometric Types of Feeding Arteries

The term "geometric" refers to the angiographically demonstrable relationship between a feeding artery with the nidus and the supply of normal brain parenchyma. This relationship is primarily guided by the underlying normal vascular anatomy and arterial disposition of the area involved by the nidus of the AVM. Generally, two types of supply of an AVM can be distinguished, *i.e.* direct and indirect.

Fig. 1. Cingulo-callosal AVM with multifocal nidus in a 21 years old female patient presenting with small ventricular hemorrhage. (a) Left internal carotid angiography in lateral projection shows large cingulo-callosal AVM, fed by (obscured) branches of the pericallosal artery and multiple, small branches of the callosomarginal artery. It is draining into an ascending interhemispheric and into the internal cerebral vein. The AVM appears to be composed of two nidi. (b) Very early and (c) early arterial phase of the same injection as in (a) showing the beginning opacification of two distinct nidi, one in the genu and the second in the trunk of the corpus callosum. (d) Vertebral angiography in lateral view showing retrograde filling of the distal pericallosal artery from the posterior callosal artery through an angiogenic collateral pericallosal network. (e) Superselective angiogram of the pericallosal artery showing the posterior compartment of the second nidus. Its single draining vein divides early into a main ascending interhemispheric vein and into two accessory posterior interhemispheric veins. (f) Very early arterial phase of the same superselective injection as in (e) shows that the direct type of feeder divides into two terminal branches before entering the compartment (multiterminal type). (g) Superselective angiogram of an anterior callosal branch of the pericallosal artery showing a plexiform compartment of the first nidus draining exclusively into the internal cerebral vein. (h) Superselective angiogram of a subcallosal branch of the pericallosal artery showing intranidal aneurysm and another plexiform compartment. This aneurysm most probably represents the source of the intraventricular hemorrhage. (i) Plain x-ray of the acrylic cast following one embolization session. Note also the embolized intranidal aneurysm. (j) Left internal carotid angiogram at the end of the embolization session showing residual supply through indirect feeders arising from the callosomarginal artery. (k) Vertebral angiography after embolization showing no supply of the posterior nidus from the retrograde pericallosal artery and significant regression of the posterior pericallosal angiogenic collateral network (compare with (d))

Direct Type

Direct type of feeding arteries end directly in the nidus without continuation towards normal brain distal to it. This type of feeder has been called "*terminal artery*" by Yaşargil (1987). The main trunk of a direct type feeding artery may terminate in the nidus either as a single artery, i.e. monoterminal type or may divide into two or even more branches all terminating in the nidus, i.e. multiterminal type (Fig. 1). Regardless of their termination pattern, direct type feeding arteries give off branches to normal brain before entering the nidus and therefore participate into the supply of normal brain proximal to the AVM. Because of the high-flow within direct type feeders and the concomitant sump effect of the nidus, these normal branches are usually not opacified on selective angiography carried out from the internal carotid or vertebral arteries but may become visible on superselective studies.

Fig. 2. Medium-sized left frontal sulcal AVM with subcortical extension in a 32-year-old male presenting with seizures. (a) Coronal MR shows left frontal AVM located within the superior frontal sulcus compressing the superior frontal gyrus and the precentral gyrus and extending in the depth of the superior frontal sulcus into the subcortical white matter. (b) Bilateral internal carotid angiography in frontal projection shows the medium sized nidus supplied by feeding branches of the dilated middle and posterior internal frontal arteries arising from the pericallosal artery and of the precentral, central and anterior parietal arteries of the middle cerebral artery. The nidus appears compact, without evidence of perinidal angiogenesis. Venous drainage is exclusively superficial through the dilated superior frontal cerebral vein in the superior sagittal sinus. (c) Simultaneous superselective angiograms of the posterior internal frontal artery (from the pericallosal artery) and of the precentral artery (from the middle cerebral artery) opacifying two larger plexiform compartments of the nidus. Both feeding arteries represent direct and terminal type of feeders. (d) Superselective angiogram of the distal precentral artery opacifying an anterior lateral plexiform compartment of the nidus. Note a normal branch arising from this direct terminal type of feeder. For embolization the catheter tip must be advanced beyond the origin of this normal branch. (e) Superselective angiogram of the distal central artery opacifying a posterior lateral compartment of the nidus. Note the dilated medullary branch arising from the deep sulcal segment of the pial artery and supplying the deep subcortical extension of the AVM. (f) Superselective angiogram of the distal anterior parietal artery, demonstrating dilated medullary arteries coursing through the normal postcentral gyrus to supply the posterior deep subcortical extension of the AVM. Note two isolated compartmental veins joining the main nidal draining vein. (g) Superselective angiogram of the distal middle internal frontal artery supplying with its distal sulcal segment in a multiterminal pattern the medial compartment of the nidus. Note the dilated compartmental vien. (h) Bilateral internal carotid angiography following complete obliteration of the AVM in one session. Note normal caliber of previously feeding arteries (compare with (b)). (i) Coronal MR at 1 year follow-up showing persisting complete obliteration of the AVM

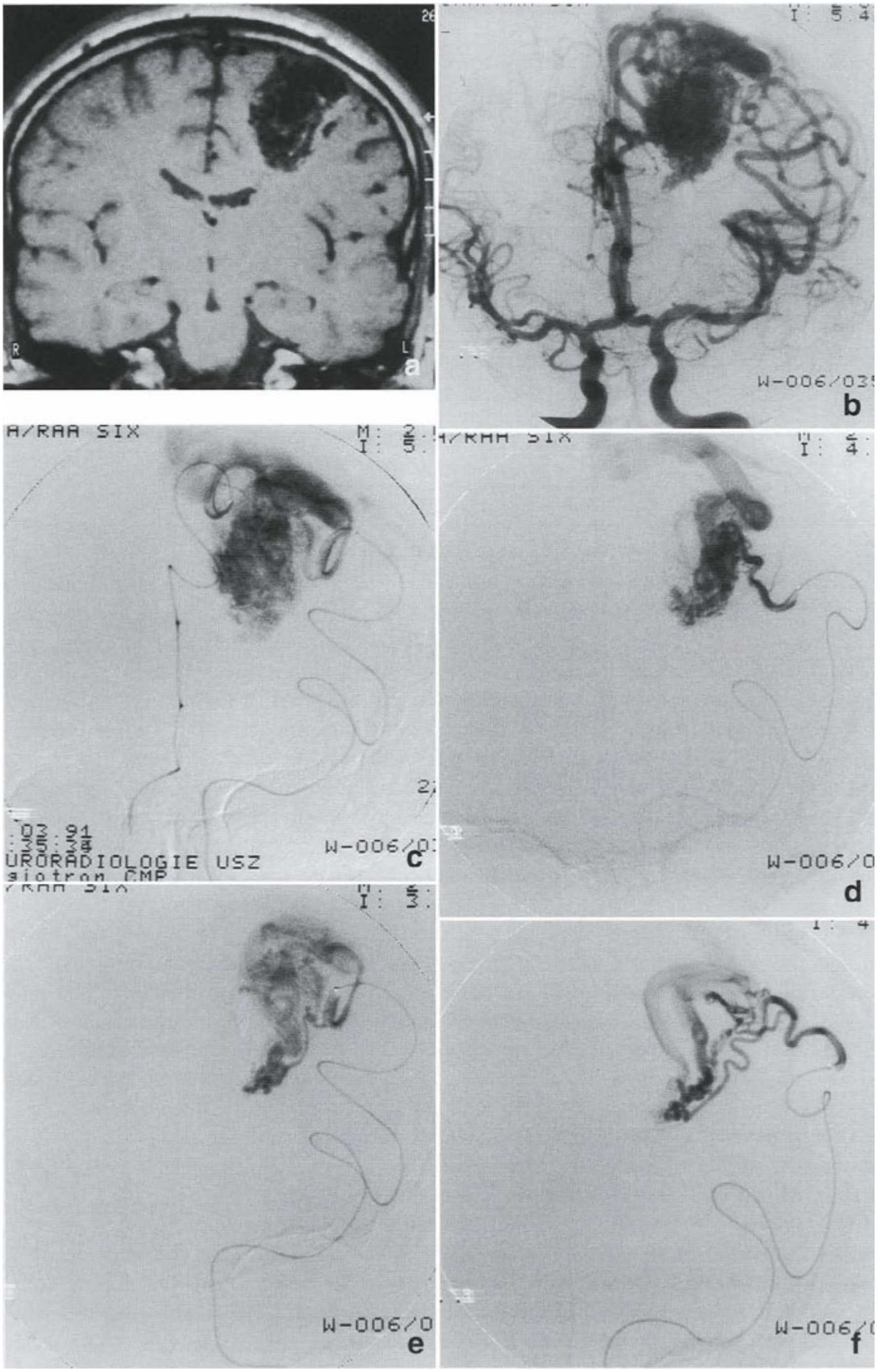

Fig. 2 (a–f)

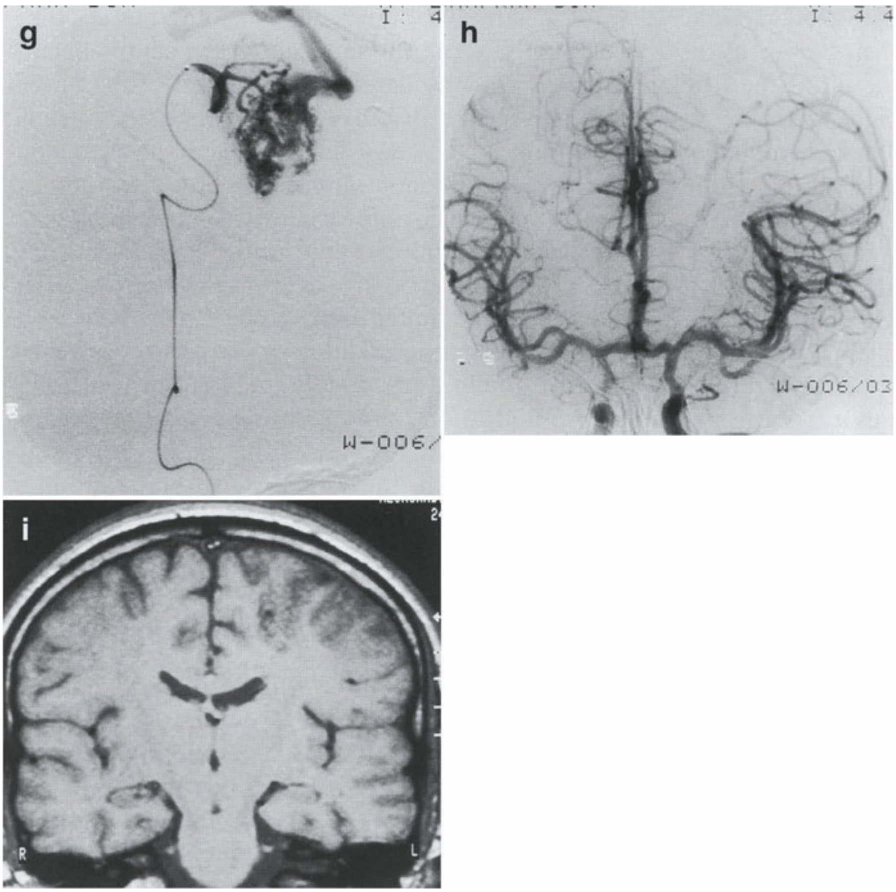

Fig. 2 (g–i)

On their course towards the nidus, direct type feeding arteries may give off other direct or indirect feeding branches to the nidus (Fig. 2d).

Depending on their contribution to nidus supply, direct type feeding arteries may be hemodynamically either dominant or supplementary. According to the authors' observation direct, multiterminal type feeding arteries are usually dominant feeders, whereas direct, monoterminal type feeding arteries may be either dominant or supplementary feeders.

Pseudoterminal type. The term "pseudoterminal feeder" is introduced to describe particular types of feeders, which angiographically appear to end directly in the nidus but because of their known anatomic disposition a continuation of their course distal to the nidus must be assumed. The angiographic nonvisualization of their distal portion is caused by the sump effect of the nidus. This particular pattern of AVM supply is encountered with feeders, which give off a terminal branch to the AVM but continue their course distal to it to supply normal brain. Due to the sump effect of the nidus the feeding terminal branch dilates up to the size of the parent trunk and flow reversal occurs in the distal portion of the parent trunk. These hemodynamic, flow-induced changes finally create the erroneous angiographic impression of a direct, monoterminal type of feeder.

A pseudoterminal feeder appearance may be caused by a microcatheter wedged into the main trunk. The pseudoterminal feeder appearance may also be induced by spasm of the main trunk caused by the microcatheter. These iatrogenically induced pseudoterminal feeder appearances have to be distinguished from the naturally occuring pseudoterminal type of feeders.

Embolization performed through a pseudoterminal type of feeder carries a risk for an ischemic complication occuring in the brain parenchyma located immediately distal to the AVM. Because of the changing hemodynamic conditions taking place during the injection of NBCA, migration of the embolic material into the invisible distal segment of the feeding artery may occur. Obviously, this situation cannot be simulated with amobarbital injection, thus making functional testing of pseudoterminal type of feeders highly unreliable.

Indirect Types of Feeding Arteries

The term "indirect" supply refers to the main participation of the feeding artery into the supply of normal brain and to its secondary participation into the supply of the nidus of the AVM. Two types of indirect supply of an AVM can be distinguished, i.e. transit arteries with feeding branches to the nidus and collateral arteries feeding the nidus in a retrograde fashion.

Transit arteries. The term "*transit*" artery refers to an arterial trunk coursing in close topographic proximity to the nidus of an AVM, giving off one or several branches to the nidus, but continuing its course distal to the nidus to supply normal brain parenchyma. This arrangement of supply to an AVM has been called "feeder en passage", "indirect feeder", "transit artery with participation", and "perforating type" (Yaşargil 1987, Berenstein and Lasjaunias 1991, Valavanis 1996). Feeding branches arising from a transit artery are usually smaller and shorter than direct type of feeding arteries and they usually originate in a right or sharp angle from the parent artery (Fig. 1). Depending on their origin from the transit artery in relation to the nidus, they may have either a short, more or less direct course ending in the nidus or, if they arise more distally from the transit artery, they have a recurrent, rather long course toward the nidus. Typically, the transit artery is usually moderately dilated up to the point of origin of the most distal feeding branch and assumes distal to it a normal size. The majority of transit type feeding arteries provide supplementary supply to an AVM. Some AVMs are exclusively supplied by supplementary feeding arteries arising from transit arteries.

The anatomic characteristics of feeding branches arising from transit arteries make superselective catheterization difficult and represent an important limiting factor regarding complete obliteration of brain AVMs. The recent introduction of hydrophilically coated microcatheters and the ability to appropriately preshape the tip of the microcatheter (FasTracker 10 or Magic) made it recently possible to safely catheterize and embolize such feeders in several cases (Fig. 3d, e).

Retrograde collateral feeding arteries. This type of feeding arteries is observed with AVMs located proximal to a watershed area between two or three arterial territories. Anatomically, these feeding arteries belong to the distal arterial system of the vascular territory, within which the AVM is located. Their anterograde perfusion distal to the AVM is compromised by the sump effect of the nidus. Reconstitution of flow is provided through compensatory recruitment of leptomeningeal collaterals developing at the watershed area and being supplied by the distal branches of the adjacent vascular territory. Therefore, flow in the artery or arteries distal to the AVM is reversed. This phenomenon has been called "watershed transfer" by Berenstein and Lasjaunias (1991) and represents one of the manifestations of the high-flow angiopathy occuring with brain AVMs.

Watershed transfer and the retrograde supply of the nidus is observed with both superficial (cortical and subcortical) (Fig. 3) and with deep brain AVMs (Fig. 1). In the superficial AVMs retrograde supply is provided by the leptomeningeal arterial system while in deep brain AVMs and in paraventricular extensions of corticosubcortical AVMs retrograde supply is provided by the subependymal arterial system. Obviously, watershed transfer cannot occur with AVMs located in a watershed area.

Anatomic Types of Feeding Arteries

The anatomic types of arteries participating into the supply of AVMs depend primarily on the specific location, the topography and the vascular territory or territories of the AVM. Anatomically, the following types of feeding arteries can be distinguished:

1. Pial Feeding Arteries

The pial arteries participate in the supply of AVMs either by their extracortical subpial trunks or by their cortical, medullary or cortico-medullary branches.

(a) The pial artery trunks typically supply in a dominant fashion so called pial arteriovenous fistulae (AVFs) and distal pial arteries of the pericallosal

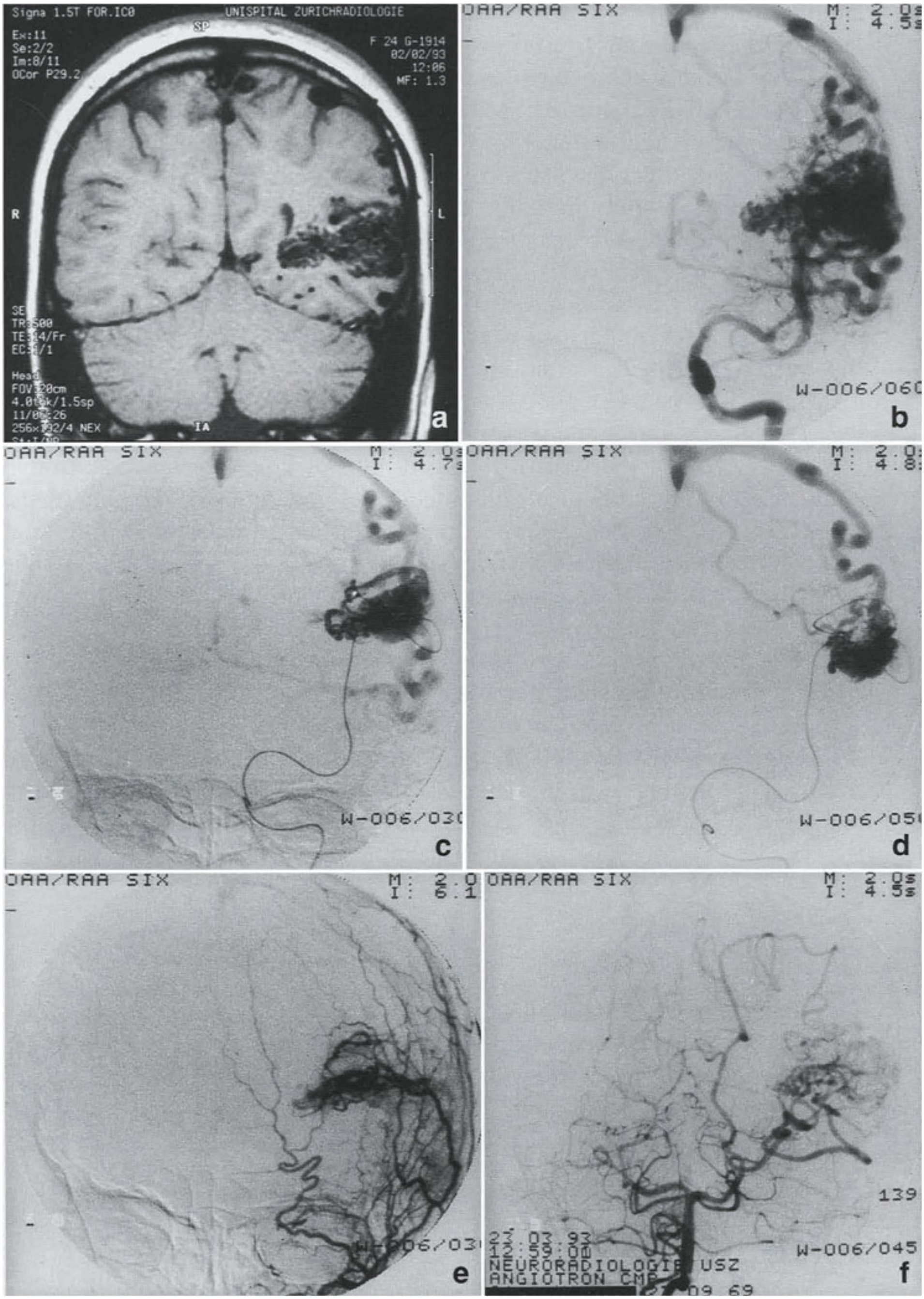
Signa 1.5T FOR.IC0
UNISPITAL ZURICHRADIOLOGIE
a
OAA/RAA SIX
W-006/060
b
W-006/030
c
W-006/050
d
e
W-006/045
NEURORADIOLOGIE USZ
ANGIOTRON CMP
f

Fig. 3 (a–f)

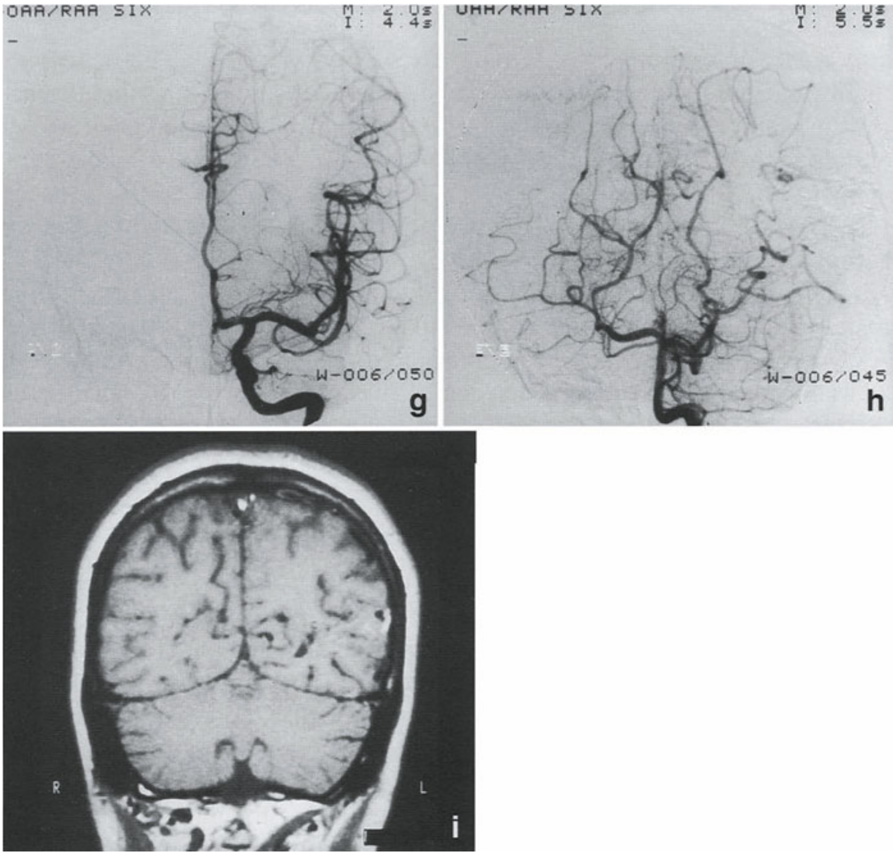

Fig. 3 (g–i)

Fig. 3. Left temporooccipital, sulcal AVM with subcortical extension in a 24-years-old female patient presenting with epilepsy. (a) Coronal MR showing the typically pyramidal nidus within the temporooccipital sulcus with compressed adjacent gyri, and subcortical-ventricular extension. (b) Left internal carotid artery angiography in frontal projection showing the pyramidal shape of the nidus. The individual feeding arteries of the dilated temporooccipital, posterior temporal and angular branches of the middle cerebral artery cannot be discerned. (c) Superselective angiogram of the direct terminal feeding artery arising from the temporooccipital trunk and supplying the plexiform, compact superior, sulcal compartment. (d) Superselective angiogram of another direct-terminal feeding artery arising from the temporooccipital trunk and supplying an inferior sulcal compartment. (e) Ipsilateral external carotid angiogram in frontal projection showing supplementary supply of the sulcal portion of the nidus by the middle meningeal artery. (f) Vertebral artery angiography in frontal projection showing supplementary supply of the nidus by dilated branches of the posterior temporal artery and indirect retrograde supply through leptomeningeal collaterals between the distal calcarine and the distal temporooccipital artery. (g) Left internal carotid angiogram following complete obliteration of the AVM with NBCA embolization in one session. (h) Vertebral angiogram also confirming complete obliteration of the AVM and showing regressing indirect retrograde collateral supply. (i) Postembolization coronal MR at 1 year follow-up showing the completely obliterated and shrinked nidus of the AVM

and posterior cerebral arteries typically supply vein of Galen aneurysmal malformations. The trunks of the pial arteries coursing in the subpial space over gyri and within sulci supply in a dominant fashion sulcal type of AVMs and in either a dominant or supplementary fashion mixed sulcal-gyral AVMs (Fig. 2).
(b) The cortical branches of the pial arteries may become involved in the supply of purely gyral AVMs.
(c) The medullary and the corticomedullary branches of the pial arteries may be dominant feeders of gyral, mixed gyral-sulcal and of subcortical AVMs (Fig. 4). They may be supplementary feeders of deep brain AVMs as well as of the subcortical extension of sulcal, gyral or mixed sulcal-gyral AVMs.

2. *Dural (Meningeal) Feeding Arteries*

Three instances of participation of the meningeal arterial system into the supply of AVMs can be recognized.
(a) Direct supply of the nidus in a supplementary fashion (Fig. 3e). Such direct nidus supply is reported to occur in approximately 30% of cases (Newton and Cronqvist 1969, Willinsky *et al.* 1988). Direct dural supply is observed with AVMs being in contact with the dural-arachnoid-pial layers, as with sulcal, mixed sulcal and gyral but also some deep but subarachnoidally located AVMs with direct contact to the tentorium.
(b) Transdural anastomoses with normal pial arteries distal to the AVM. This, most probably represents an angiogenic reaction to brain tissue ischemia distal to the AVM (Russell and Berenstein 1981).
(c) An associated secondarily induced, dural sinus arteriovenous shunt. Such acquired, secondary arteriovenous shunts are not related to the AVM and should not be confused with a second AVM. They arise from the high sump effect of the dural sinus downstream to the AVM on dural arteries, are asymptomatic, represent incidental angiographic findings, and regress spontaneously following treatment of the AVM.

It seems, that subarachnoid hemorrhage represents an additional factor that may secondarily increase dural supply to an AVM (Faria and Fleischer 1980).

3. *Retrograde Collateral Feeding Arteries*

These types of feeding arteries involve the leptomeningeal and rarely the subependymal systems, develop in association with watershed transfer as described earlier and provide supplementary supply to the nidus of the AVM (Figs. 1 and 3).

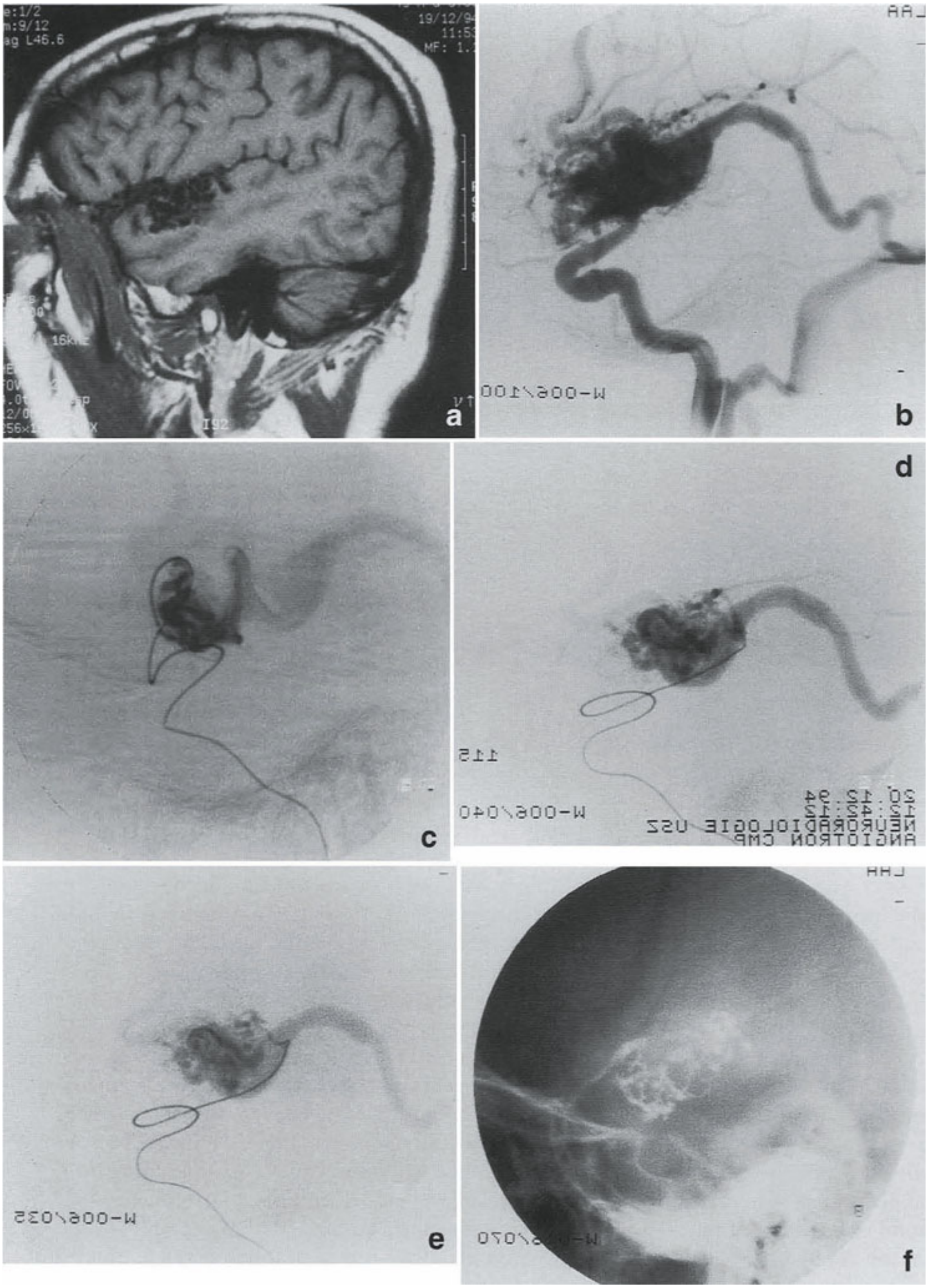

Fig. 4 (a–f)

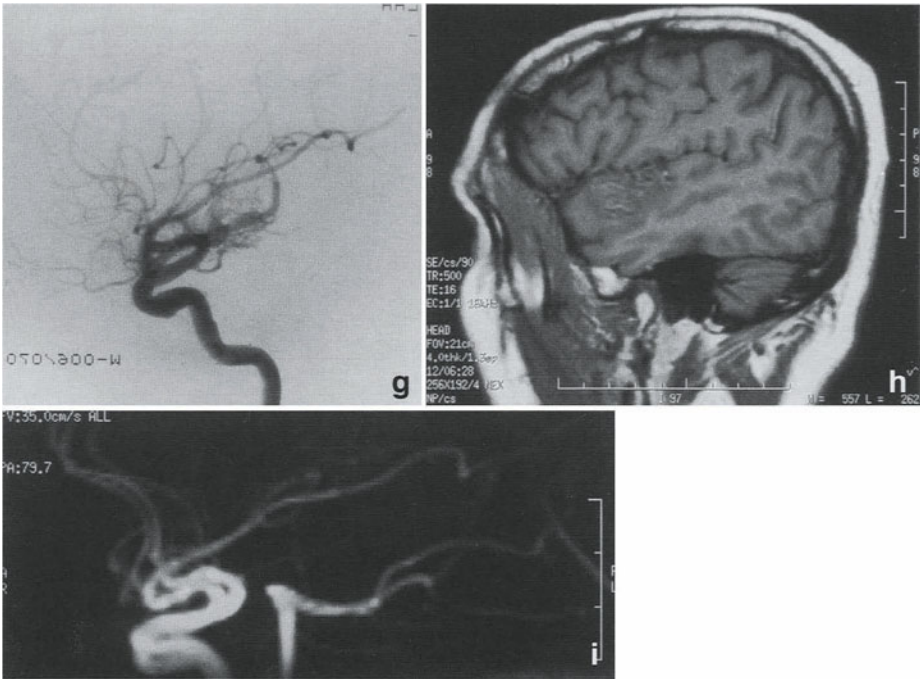

Fig. 4 (g–i)

Fig. 4. Left sided, medium-sized temporal gyral AVM in a 49-years-old male presenting with episodes of dysphasia. (a) Sagittal MR showing location of nidus within left superior temporal gyrus. (b) Left internal carotid angiography in lateral projection, not allowing for identification of the individual feeding arteries. The AVM seems to drain into two superficial veins, i.e. the vein of Labbé and an ascending frontal vein. Note moderate signs of venous high-flow angiopathy with stenosis at the junction between the Vein of Labbé and the transverse sinus as well as at the junction between sigmoid sinus and jugular bulb. (c) Superselective angiogram of a dilated medullary branch of the middle temporal artery, supplying as a dominant and direct monoterminal feeder the anterior compartment of the nidus. (d) Superselective angiogram of the angular artery, supplying with an indirect type of feeder the posterior compartment of the AVM. (e) Superselective angiogram of the indirect feeding branch arising from the angular artery. Note intranidal micoaneurysms and the early division of the compartmental vein in the well opacified vein of Labbé and the faintly seen ascending frontal vein. (f) Plain x-ray showing cast of NBCA within nidus. Note that the indirect feeder arising from the angular artery has been embolized with NBCA. (g) Internal carotid angiography in lateral projection at the end of the embolization session showing subtotal obliteration of the AVM. (h) Post-embolization sagittal-MR showing obliteration of the AVM. (i) Follow-up MR-angiogram at 1 year demonstrating complete obliteration of the AVM

4. Perforating Arteries

The perforating arteries provide the main supply to the majority of deep brain AVMs (Fig. 5). Depending on the size and location of a deep brain AVM, perforating type feeding arteries may provide supply in a dominant, combined dominant and supplementary or exclusively supplementary fashion. Perforating type arteries and particularly lenticulostriate arteries provide supplementary supply to the subcortical and paraventricular extensions of superficial AVMs.

5. Choroidal Feeding Arteries

The anterior, posterior medial and posterior lateral choroidal arteries participate into the supply of deep brain AVMs, deep brain AVMs with intraventricular extensions or purely intraventricular (plexal) AVMs. Parenchymal and intraventricular branches of the choroidal arteries supply in a dominant or supplementary fashion these AVMs (Fig. 5). Intraventricular AVMs are supplied in a dominant way by the choroidal arteries.

5.2 Arterial High-Flow Angiopathy in Brain AVMs

The term "high-flow angiopathy" describes secondary changes of the arterial and venous circulation developing over a period of time and being induced by the avshunt of the AVM. The concept of high-flow angiopathy has been proven experimentally (Pile-Spellman *et al.* 1986) and is best explained as the response of endothelial cells of the proximal arterial and distal venous system upon stress-triggers generated by the av-shunt and acting upon the normal functioning endothelial cells. The arterial high-flow angiopathy includes the following:

1. Arterial Enlargements and Variations

Development of extra- and intracranial dolichoarteries is a relatively frequent observation in brain AVMs. Such dolichovessels and loops, if intracranial, may cause cranial nerve symptoms or focal neurological deficits due to mechanical compression.

Arterial variations are reported to occur more frequently in patients with brain AVMs than in patients evaluated for other pathology or in autopsy series (Willinsky *et al.* 1988). Anatomical variations of the internal carotid and vertebral arteries such as persistence of the trigeminal or hypoglossal arteries, are only moderately increased in patients with brain AVMs. More frequently, anatomical variations are observed in the circle

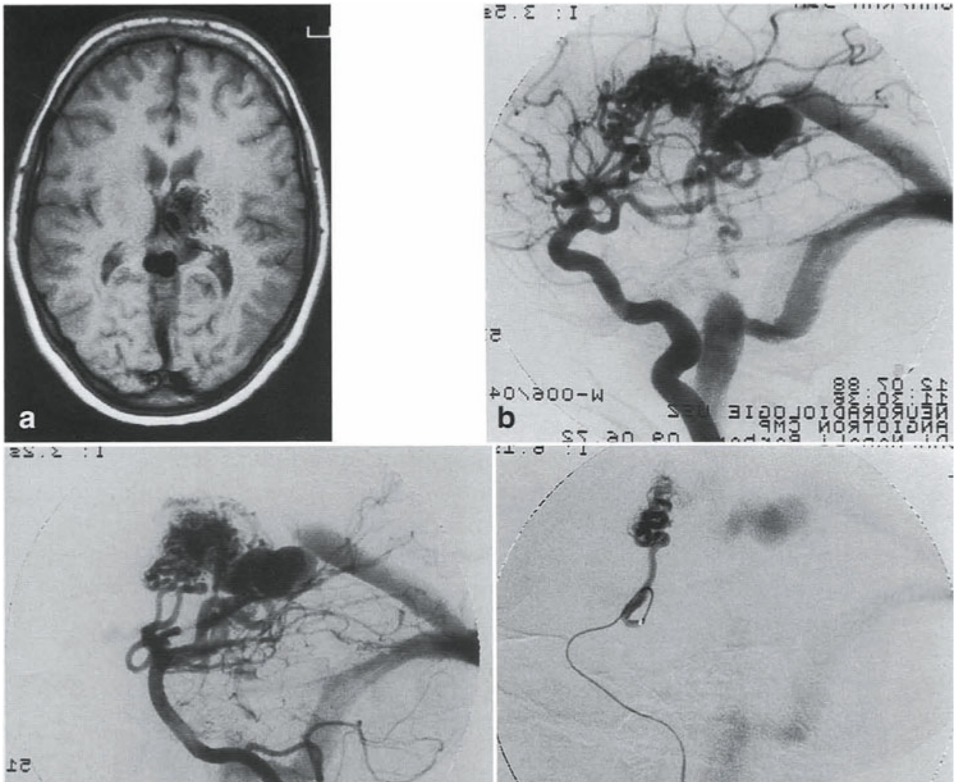

Fig. 5 (a–f)

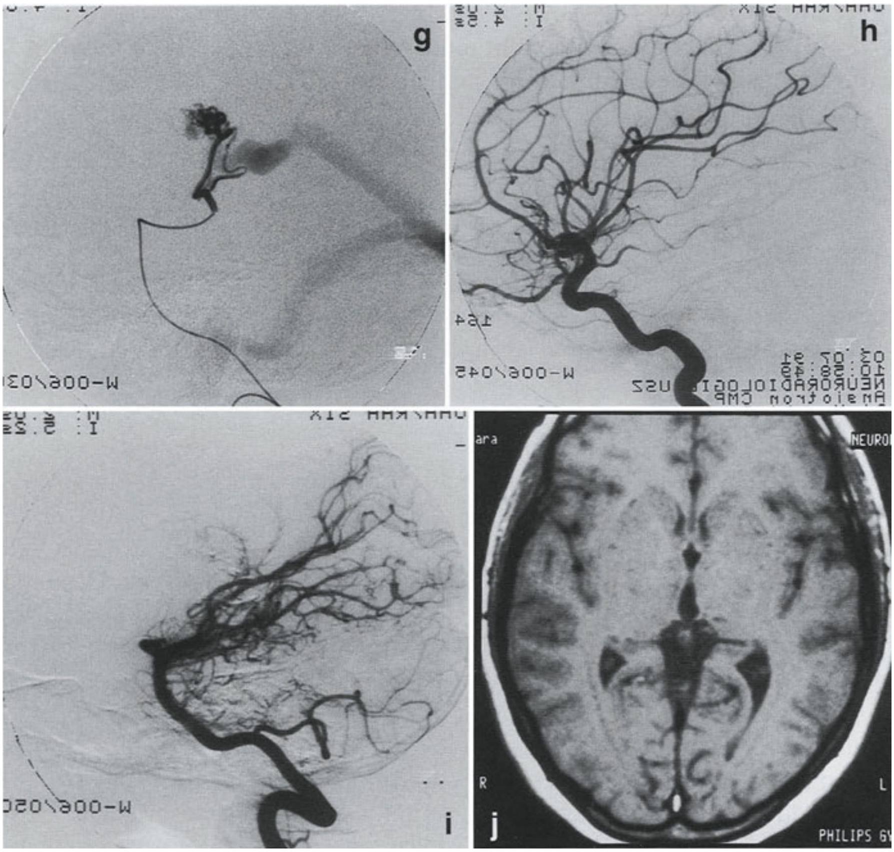

Fig. 5 (g–j)

Fig. 5. Deep parenchymal brain AVM within the left thalamus in a 13-years-old girl presenting with a history of subarachnoid hemorrhage. (a) Axial MR showing the location of the AVM within the left thalamus. Note varicose dilatation of galenic vein. (b) Internal carotid and (c) vertebral artery angiograms showing compact nidus within thalamus, fed by thalamo-perforating branches of Pcom, by P1-perforators, thalamo-geniculate branch of P2 and by medial and lateral posterior choroidal arteries. Note stenosis at the junction of the galenic vein with straight sinus and varicose dilatation of galenic vein. (d) Superselective angiogram of thalamo-perforating feeding artery opacifying the anterior compartment of the nidus. (e) Superselective angiogram of thalamo-geniculate artery opacifying a small superior fistulous compartment. (f) Superselective angiogram of lateral, posterior choroidal artery opacifying a posterior plexiform compartment. (g) Superselective angiogram of the medial posterior choroidal artery opacifying a posterior compartment. Note, that each compartmental draining vein in (c–f) converges towards the single nidal draining galenic vein. (h) Complete obliteration with IBCA in two embolization sessions was achieved in 1988. Follow up internal carotid angiography in 1991 (3 years) confirms persisting obliteration of the AVM. (i) Follow-up vertebral angiography in 1991 confirms complete and persisting obliteration. (j) Follow-up axial MR at 3 years shows complete disappearance of the lesion

of Willis and include such rare variations as an accessory middle cerebral artery, a duplicated posterior communicating artery, an artery of the corpus callosum, etc. (Berenstein and Lasjaunias 1991).

2. *Arterial Stenoses*

Angiographically detectable stenotic changes in the feeding arteries or in the more proximal arteries of the vascular territory, in which the AVM is located, are reported to occur in up to 20% of cases. Angiographically, such stenoses may be isolated or multifocal.

3. *Associated Aneurysms*

The overall incidence of arterial aneurysms associated with brain AVMs has been reported to vary from 2.7% to 23% (Azzam 1987, Batjer *et al.* 1986, Berenstein and Lasjaunias 1991, Hayashi *et al.* 1981, Kondziolka *et al.* 1988, Miyasaka *et al.* 1982, Okamoto *et al.* 1984, Suzuki and Onuma 1971, Yaşargil 1987). The rate of detection of such AVM-associated arterial aneurysms depends on complete, high-quality selective angiography for visualization of more proximally located aneurysms, and superselective angiography of the feeding arteries for detection of more distally located aneurysms. Unfortunately, this data are derived from angiographic studies varying in their degree of selectivity and completeness. In recent studies using additional superselective angiography, the incidence of such aneurysms has been reported to be 58% (Turjman *et al.* 1994), a rate closer to that found in pathologic specimens, reported as 55.5% (Paterson and Blackwood 1959).

Angiographically, two types of aneurysms can be distinguished in patients with AVMs: (1) those occurring on the arteries related hemodynamically to the supply of the AVM, so-called flow-related aneurysms and, (2) those located on arteries not related hemodynamically to the supply of the AVM that are called remote, dysplastic, or not flow-related aneurysms (Table 3).

Flow-related aneurysms represent 37% to 69% of all aneurysms associated with brain AVMs (Cronqvist and Troupp 1966, Hayashi *et al.* 1981, Perret and Nishioka 1966, Suzuki and Onuma 1971). Depending on their location with respect to the nidus of the AVM, flow-related aneurysms are classified into proximal and distal types. Distal flow-related aneurysms may be located on the distal segments of feeding arteries (extranidal type) or may be located within the nidus itself (intranidal type). Each type of flow-related aneurysm may occur singly or with additional flow-related or not flow-related aneurysms.

Table 3. *Types of Associated Aneurysms in Brain AVMs (50–70%)*

A. Flow-related aneurysms (40–70%)
(1) Proximal
(a) single
(b) multiple
(2) Distal-extranidal
(a) single
(b) multiple
(3) Distal-intranidal
(a) single
(b) multiple
B. Not flow-related aneurysms (10–20%)
(remote or dysplastic aneurysms)
(a) single
(b) multiple

In a recent report based on superselective angiographic evaluation of brain AVMs, intranidal aneurysms have been found in 42% and multiple flow-related aneurysms in 57% of patients (Turjman 1994). In previous reports based mainly on selective and not on superselective angiographic studies, intranidal aneurysms were reported in 12% to 90% (Marks *et al.* 1992, Lasjaunias *et al.* 1988) and multiple aneurysms in 12% to 84% of patients (Turjman 1994, Lasjaunias *et al.* 1988).

The angiographic demonstration and the number of identified flow-related aneurysms correlate significantly with a clinical presentation or history of hemorrhage (Fig. 1). In patients with AVMs presenting with hemorrhage, 75% to 80% are found to harbour an aneurysm (Turjamn *et al.* 1994, Willinsky *et al.* 1988). This association appears to be even stronger in the presence of multiple aneurysms (Turjman *et al.* 1994). Therefore, angiographic demonstration of a flow-related aneurysm in a patient with a brain AVM worsens the overall prognosis of that AVM (Berenstein and Lasjaunias 1991, Brown *et al.* 1990).

The angiographic visualization of a flow-related aneurysm significantly influences the therapeutic endovascular approach to the brain AVM. As a general rule, the primary endovascular target is the AVM, since it represents the causative factor of the flow-related aneurysms. Distal intra- and extranidal aneurysms will usually be obliterated together with the obliteration of the brain AVM. More proximally located aneurysms frequently regress spontaneously following successful obliteration of the AVM. If, on follow-up angiograms performed after 6 months no regression of the aneurysm is visible, then surgical clipping must be considered.

Endovascular navigation in the presence of an associated aneurysm carries a certain risk for microcatheter- or microguidewire induced aneurysm perforation and hemorrhage. Such a complication has been occasionally reported (Debrun *et al.* 1997). The use of biplane roadmapping technique is of critical importance, when navigating through an artery carrying an associated aneurysm.

4. *Watershed Transfer*

The phenomenon of "watershed-transfer" as one of the angiographically demonstrable manifestations of arterial high-flow angiopathy, refers to compensatory recruitment of leptomeningeal collaterals and associated pial arteries to reconstitute the arterial territory distal to an AVM (Berenstein and Lasjaunias 1991, Valavanis 1996). This may occur as a congenital disposition to provide supply of brain distal to the nidus or secondarily to provide also supply to the nidus. This secondary watershed transfer may be associated with non-sprouting angiogenesis developing as a response to brain tissue ischemia (see above).

5.3 The Nidus of Brain AVMs and Its Angioarchitecture

The term "nidus" was introduced by Doppman (1971) based upon his angiographic observations on spinal cord arteriovenous malformations. The term nidus is derived from latin (plural nidi) and means a nest. Other terms which could also be used include epicenter, nucleus, or focus of the AVM. The nidus of an AVM represents that area of the entire AVM angioarchitecture, interposed between the readily identifiable distal segments of feeding arteries and emerging proximal segments of draining veins, where arteriovenous shunting occurs (Doppman 1971, Yaşargil 1987, Berenstein and Lasjaunias 1991, Houdart *et al.* 1993, Valavanis 1996). The nidus is the source of all hemodynamic changes observed up- and downstream of the AVM, of the secondarily induced high-flow-angiopathy and of the majority of hemorrhages occurring with AVMs. It represents the actual target of any therapeutic approach because its radical elimination or complete obliteration results in cure of the AVM.

Size of Nidus

The size of the nidus of brain AVMs varies from very small to giant. Various systems of size classification of brain AVMs have been introduced, varying in sophistication from simple to complex. The practical importance of size determination of a nidus of an AVM lies mainly in its surgical resectability or radiosurgical accessibility. From the perspective of endovascular treatment, size is not a parameter of major or critical importance as it does not affect directly neither the endovascular accessibility nor the degree of achievable obliteration of the AVM. The primary practical importance of size determination from the endovascular view point lies primarily in the estimation of the length of a procedure, its technical complexity and the number of sessions to be performed.

Size of the nidus represents a major component of most surgical AVM grading systems (Luessenhop and Rosa 1984, Pasqualin *et al.* 1991, Pelletieri *et al.* 1979, Shi and Chen 1986, Spetzler and Martin 1986). Based on the angiographically measured maximum diameter of the nidus, AVMs are classified according to Yaşargil (1987) into micro-AVMs (0.5–1.0 cm), small (1–2 cm), moderate (2–4 cm), large (4–6 cm) and giant AVMs (more than 6 cm).

Shape of Nidus

Correlation of MR-imaging with cerebral angiography has shown that the shape of an AVM nidus is primarily determined by the anatomic structure or space within which it is located. AVMs located within a sulcus, cistern or fissure tend to adapt their shape to the overall geometry of that particular space. This explains why a sulcal AVM exhibits a pyramidal shape (Fig. 3) or a fissural AVM a more linear, elongated shape. In AVMs located within the brain parenchyma, the shape of the nidus is determined by the intrinsic parenchymal structure involved and its anatomic boundaries. A subcortical white matter AVM typically exhibits a spherical shape whereas a callosal AVM adapts to the shape of that part of the corpus callosum involved by the nidus (Fig. 1). Obviously, larger AVMs involving several structures and spaces exhibit complex or even undefinible shapes.

Vascular Composition of Nidus

Hamby (1958) in examining grossly and histopathologically brain specimens containing AVMs, considered the nidus to be a complex vascular system of coiling and intercommunicating vascular channels that empty into thin-walled tortuous veins. The vascular composition and intrinsic angioarchitecture of the nidus cannot be evaluated adequately by selective internal carotid or vertebral angiography. Simultaneous visualization of different, hemodynamically independent compartments, overprojection of large venous structures of the nidus and flow- or pressure-related poor or non-visualization of various vascular elements limit precise nidus evaluation. This information, however, often may be obtained from superselective angiography of the individual feeding arteries that enables architectural and compositional mapping of the nidus. Based on the experience obtained from routine application and systematic interpretation of superselective feeder injections performed before or during the course of embolization procedures of brain AVMs (3'550 individual injections in this series), new insights and concepts regarding the nidus of the AVM have been developed and progressively incorporated in the endovascular treatment.

Angiographically, three main patterns of arteriovenous shunting can be distinguished within an AVM. The nidus may consist of arteriovenous shunting across a plexiform network of vascular channels (i.e. pure plexiform nidus) (Fig. 1), large arteriovenous fistulae (i.e. pure fistulous nidus), or of both plexiform and fistulous parts (i.e. mixed plexiform and fistulous nidus) (Fig. 5). In this series pure plexiform nidi were observed in 36% of cases, mixed plexiform and fistulous nidi in 53% of cases and pure fistulous nidi in 11% of cases.

In the plexiform type of nidus, one or several arterial feeders end in a vascular conglomerate of multiple arteriovenous microcommunications from which one or multiple venous channels emerge as draining veins. In the mixed plexiform and fistulous type of nidus additional single or multiple direct arteriovenous communications (fistulae) are observed. In some of the mixed plexiform nidi, the plexiform portion may clearly dominate, in others there may be an even distribution of plexiform and fistulous parts and in still others there may be clear dominance of the fistulous components. In the pure fistulous type of nidus, dilated feeding arteries end directly into dilated venous channels. Such direct fistulous communications may be composed of single or multiple feeding arteries ending directly either in an end to end or in an end to side fashion along a draining vein or veins (Table 4).

In the majority of cases, the nidus of the AVMs appears angiographically as a single, compact, vascular structure. Rarely, multiple but compact

Table 4. *Nidus Composition According to the Type of Arteriovenous Shunts*

1. *Pure plexiform (36%)*[a]
2. *Mixed plexiform and fistulous (53%)*[a]
(a) plexiform > fistulous
(b) plexiform ~ fistulous
(c) plexiform < fistulous
3. *Pure fistulous (11%)*[a]
(a) monofistulous
(b) multifistulous

[a]Data derived from the analysis of the 387 cases of brain AVM reported here.

nidi are observed (2% in this series) (Fig. 1a–c). These multifocal nidi are observed mainly in children and may be distinct with interposed normal brain tissue or be adjacent without interposed normal brain tissue simulating a larger single nidus. Also rarely (3% in this series) the nidus may have a diffuse appearance without clearly defined borders, characterized by a nidus-like network of vessels and only slightly enlarged draining veins. The nidus-like network does not have a compact and homogenous appearance, as it contains normal brain tissue. There is increasing evidence, that this "diffuse type of AVM" most probably represents a proliferative form angiopathy. It can be localized involving only one or a few gyri or be extensive, involving one or more lobes or even an entire hemisphere. While in the majority of cases of single compact nidi there are clearly discernible boundaries, in approximately 23% of cases, the nidus is surrounded by perinidal angiogenesis. This perinidal angiogenesis most probably represents a secondary angiogenic response to chronic hypoperfusion or ischemia induced by the arteriovenous shunt of the nidus. Morphologically it can be localized, moderate or even extensive, simulating a diffuse nidus (pseudo-diffuse nidus). Failure of recognition of perinidal angiogenesis may lead to overestimation of the true size of the nidus of the AVM (Table 5).

The nidus may be composed of a single or multiple vascular compartments. The concept of vascular compartments was introduced by Moret *et al.* in 1980 to describe the vascular composition of glomus tumors as seen on selective angiography. Applied to the nidus of the AVM, a com-

Table 5. *General Angiographic Appearance of Nidus*

*A. Single, compact nidus (95%)**
1. Without perinidal angiogenesis (77%)*
2. With perinidal angiogenesis (23%)*
   (a) localized
   (b) moderate ⎤ = "pseudodiffuse nidus"
   (c) extensive ⎦

*B. Multifocal, compact nidus (2%)**
(1) Without perinidal angiogenesis
(2) With perinidal angiogenesis

*C. Diffuse nidus (3%)**
(proliferative angiopathy)
(a) localized
(b) extensive (lobar or hemispheric)

*Data derived from the analysis of the 387 cases of brain AVM reported here.

partment is a purely angiographic term, defined as an intranidal vascular unit, characterized by one or more feeding arteries, arteriovenous shunting and a draining vein (i.e. compartmental vein). In monocompartmental nidi, this compartmental vein is the draining vein of the AVM (i.e. nidal draining vein). It can exit the nidus as a solitary draining vein or can divide early into two or more veins, sometimes simulating the presence of multiple draining veins emerging from a single compartment. In multicompartmental AVMs, compartmental veins may converge towards one or more nidal draining veins or exit the nidus individually (Figs. 2–5). Excluding the 42 direct fistulous AVMs and the 11 diffuse AVMs (proliferative angiopathy), the vascular composition of the nidus in the remaining 334 AVMs of this series was monocompartmental in 49 (14%) and multicompartmental in 285 (86%) (Table 6).

Based on superselective angiographic observations, it can be concluded that the compartments of the AVM nidus are not rigid, well-defined anatomic vascular units, but rather hemodynamic units that may even intercommunicate. The feature of communication between compartments

Table 6. *Compartmental Composition of Nidus*

A. Monocompartmental nidus (14%)
- (1) (a) mono-pedicular
  - or
  - (b) multipedicular
- (2) (a) not dividing, single draining compartmental vein (= nidal draining vein)
  - or
  - (b) early dividing, draining compartmental vein (nidal vein)

B. Multicompartmental nidus (86%)
- (1) With
  - (a) monopedicular compartments
  - (b) multipedicular compartments
- (2) (a) converging compartmental veins
  - (b) isolated compartmental veins
  - (c) converging and isolated compartmental veins
- (3) With
  - (a) uniform appearance
  - (b) arterial dominance
  - (c) venous dominance
- (4) (a) with intercompartmental communications (= communicating compartments)
  - (b) without intercompartmental communications (= isolated compartments)

becomes evident following occlusion of a compartmental feeder without obliteration of its compartment. This compartment may still be perfused through communication with a neighbouring compartment or through collateral supply. The feature of intercompartmental communication may be used to reach otherwise inaccessible compartments of nidi during embolization of AVMs.

Intranidal Vascular Cavities

Superselective angiography may demonstrate intranidal vascular cavities (Berenstein and Lasjaunias, 1991). Such vascular cavities or pouches represent focal, aneurysmal dilatations originating from intranidal vascular channels. They may be small and hardly discernible, medium-sized or even rarely large. Intranidal vascular cavities may be located anywhere within the nidus, involving the arterial inlet, the central or peripheral part of the nidus or the venous outlet. They may be single or multiple and may be categorized as (1) intranidal arterial aneurysms, (2) arterial pseudoaneurysms, (3) venous pseudoaneurysms and (4) intranidal venous ectasias (Table 7). Intranidal aneurysms represent the most common type of an intranidal vascular cavity and are reported to occur in 12%–42% of cases (Turjman *et al.* 1994, Valavanis 1996). On superselective angiograms, arterial intranidal aneurysms are visualized in the early phase and are located on the nidal ramifications of the feeding arteries (Fig. 4d, e). They may be

Table 7. *Intranidal Vascular Cavities*

A. *Arterial intranidal cavities*
   (1) Arterial aneurysms (12–42%)
      (a) single
      (b) multiple
   (2) Arterial (posthemorrhagic) pseudoaneurysms (5%)
      (a) single
      (b) multiple
   (3) Arterial loop (simulating an aneurysm)
      (a) single
      (b) multiple

B. *Venous intranidal cavities*
   1. Venous (posthemorrhagic) pseudoaneurysms (3%)
      (a) single
      (b) multiple
   2. Venous intranidal ectasias / varices (34%)
      (a) with an open exit (proximal to mechanical venous kinking or stenosis)
      (b) with closed exit (proximal to venous thrombosis—posthemorrhagic)

single or more frequently multiple and are usually small (less than 4 mm in size). Coiled intranidal arterial segments and closed intranidal arterial loops may simulate the presence of an intranidal arterial aneurysm. Therefore, multiple projections may be needed to reliably differentiate a true intranidal aneurysm from an arterial loop.

Intranidal arterial aneurysms represent a weak angioarchitectural element of AVMs and an angioarchitectural risk factor for AVM rupture. Recent studies have confirmed a statistically significant correlation between prior hemorrhage and the frequency of intranidal aneurysms in patients with AVMs. The association of intranidal aneurysms and hemorrhage has been found in 41% to 100% of patients (Marks *et al.* 1992, Turjman *et al.* 1994, Willinsky *et al.* 1988). Two mechanisms are probably implicated in rupture of intranidal aneurysms. First, intranidal aneurysms are exposed to nearly the same arterial pressures as the arterial components of the AVM. Because intranidal aneurysms have a thinner and weaker wall than the other arterial elements of the AVM, they represent the most likely site of rupture following intraarterial pressure rise, particularly if it occurs suddenly. Following embolization of a nidus compartment, a sudden increase in intraarterial pressure involving the non-occluded vessels supplying the remaining AVM may occur predisposing unprotected intranidal aneurysms to rupture. Therefore, embolization of AVMs should be first performed through feeding arteries either carrying flow-related aneurysms or supplying compartments containing intranidal arterial aneurysms (Marks *et al.* 1992, Turjman 1994). Second, venous hypertension, as it occurs with stenosis or obstruction of the venous drainage, if severe enough may cause retrograde propagation of increased pressure towards the arterial side of the nidus and lead to rupture of intranidal arterial aneurysms (Berenstein and Lasjaunias 1991, Marks *et al.* 1992).

Intranidal pseudoaneurysms develop following nidus rupture and result from the unclotted portion of the hematoma that still communicates with the lumen of the ruptured vessel (Garcia-Monaco *et al.* 1993). Intranidal pseudoaneurysms are usually irregularly shaped, vascular cavities lacking true walls. They are located within or at the margin of a recent hematoma and originate from the arterial or venous part of the nidus, depending on the site of the ruptured vessel. Pseudoaneurysms represent an important angioarchitectural characteristic of an AVM because their angiographic demonstration indicates the exact site of AVM rupture and bleeding. They must be differentiated from intranidal arterial aneurysms. Angiographically, pseudoaneurysms appear as irregular, oval or round aneurysmal cavities frequently associated with some stagnation of contrast material. Arterial pseudoaneurysms usually fill before any visualization of draining veins and can be related to an arterial pedicle, whereas venous pseudoaneurysms usually fill simultaneously with the draining veins. Because intranidal pseudoaneurysms represent an acquired angioarchitectural feature encountered only in the posthemorrhagic period, the most pathognomonic diagnostic sign is their absence on previous angiograms or MR-images, if available for comparison.

The incidence of angiographically detected intranidal pseudoaneurysms in patients presenting clinically with a recent AVM rupture and bleeding has been reported to be approximately 8%, the majority of which were of arterial origin (60%) with the remaining involving the venous side the nidus (Garcia-Monaco *et al.* 1993).

Because intranidal pseudoaneurysms have only recently been recognized as a specific entity of ruptured AVMs and because they are usually not studied by repeated angiography, their natural history is not yet known. Based on data from small series of patients, three outcomes for pseudoaneurysms have been already identified. Intranidal pseudoaneurysms may undergo (1) spontaneous thrombosis, observed in most cases, (2) incorporation into a draining vein producing an intranidal eccentric venous ectasia not necessarily associated with distal stenosis or obstruction of the draining vein, observed in approximately 20% of cases, and (3) progressive enlargement and rupture responsible for rebleeding of the AVM, observed in approximately 10% of cases (Garcia-Monaco *et al.* 1993). Evidence of an enlarging pseudoaneurysm on repeat angiography in a patient with an acutely ruptured AVM represents a rare indication for emergency microsurgical or endovascular treatment of an AVM. Embolization of an AVM in the presence of an intranidal pseudoaneurysm should be performed under special precautions to avoid perprocedural rupture of the fragile pseudoaneurysm.

Intranidal venous ectasias or varices represent a separate entity of intranidal vascular pouches. In most cases, such venous ectasias are observed extranidally on a draining vein. However, venous ectasias may occur intranidally on the emerging segment of the draining vein. Their pathogenesis is identical to the extranidal venous ectasias in that they are produced following a distal stenosis or obstruction of a draining vein and indicate venous hypertension within the nidus. Two types of intranidal venous ectasias can be distinguished by superselective angiography, namely those with an open exit and those with a closed exit. Venous ectasias with an open distal exit occur more frequently than the closed exit variant and are almost constantly located proximal to a mechanical obstruction such as a kinking or a stenosis of the draining vein. Venous ectasias with a closed exit are caused by thrombosis of a draining vein and occur in association with an acute hemorrhage. They therefore indicate clinically relevant intranidal hypertension and may also represent one of the few indications for emergency microsurgical or endovascular treatment (Berenstein and Lasjaunias 1991).

5.4 Draining Veins

The anatomic type of veins draining an AVM can usually be predicted from the location of the lesion. Superficial AVMs drain through cortical veins into the adjacent dural sinus. Superficial AVMs with subcortical or ventricular extensions usually drain into both superficial cortical and deep subependymal veins. Deep brain AVMs usually drain into the subependymal venous system. In up to 30% of cases, however, an unexpected venous drainage pattern is observed angiographically. A deep brain AVM or the deep paraventricular extension of a superficial AVM may not drain ventriculopetally into the subependymal venous system as would be expected from nidus location, but unexpectedly through a dilated transcerebral vein in a vetriculofugal direction toward the cortical venous system. Inversely, a superficial AVM without subcortical extension may not drain exclusively through cortical veins, but empty unexpectedly either in addition or exclusively through one or several transcerebral veins in a ventriculopetal direction towards the subependymal venous system. Angiographic evidence of unexpected venous drainage most probably represents a secondary event following thrombosis of the anatomically expected draining vein and, therefore, corresponds to the development of venous collateral circulation (Berenstein and Lasjaunias 1991). Selective angiographic studies, however, have several limitations regarding the precise analysis of the draining veins of AVMs. Small, so-called accessory draining veins may be missed on selective angiography, but become visible upon superselective angiography of individual feeders (Fig. 1). Furthermore, because of superimposition of various venous channels, both the actual number and the relationship of the draining veins to the nidus may be obscured or even impossible to depict. On the other hand, selective angiography is essential in providing information on the venous drainage of normal brain parenchyma and its relation to the draining veins of the AVM. For precise evaluation of the nidal draining veins, superselective angiography of the individual feeding arteries is mandatory. Based on such studies, several observations on the architecture and arrangement of nidal draining veins have been made.

The draining veins of AVMs may be single or multiple. A single short draining vein may sometimes divide early into several channels simulating the presence of multiple draining veins (Fig. 2).

Hemodynamically, the draining veins may be classified into main and accessory types. Main draining veins are characterized angiographically by larger caliber and usually higher flow than accessory draining veins. A high variability in the venous drainage of individual intranidal compartments have been observed on superselective angiographic studies. Typically, an individual compartment has a single draining vein. This compartmental vein may exit the nidus as a single isolated vein corresponding to either a main or an accessory nidal draining vein. Larger compartments drain usually into main veins, whereas small compartments usually drain into accessory veins. However, separate compartmental veins may converge intranidally into a single, main nidal draining vein. Larger AVMs may show both draining patterns with isolated compartmental veins and converging compartmental veins. The incidence of these draining patterns of AVMs has not been yet elaborated.

5.5 Associated Venous Findings and Venous High-Flow Angiopathy

Important features regarding the venous drainage of an AVM are the presence of anatomic variations, the development of high-flow angiopathic changes resulting in stenoses or ectasias, the development of collateral venous circulation and competition between the venous drainage of the AVM and the normal brain. Angiographic recognition of these associated venous findings is important because they help to understand the clinical symptomatology, as well as the natural history of a particular AVM and contribute to decision making regarding treatment and its risks (Berenstein and Lasjaunias 1991, Yaşargil 1987).

Anatomic variations of the venous system occur in 30%–32% of cases of cerebral AVMs (Lasjaunias *et al.* 1986, Willinsky *et al.* 1988, Yaşargil 1987). They are of developmental origin and represent a morphologic reaction to the initial hemodynamic disturbance caused by the venous hypertension associated with the arteriovenous shunt. They include anatomic variations of the cerebral veins, the dural sinuses (such as persistence of the occipital or falcine sinus) as well as persistence of embryonic veins (Vidyasagar 1979, Berenstein and Lasjaunias 1991). Presence of venous obstacles or obstructions represent an important angiographic finding, because they indicate increased venous pressure proximally. Such a venous obstacle or obstruction may have several causes that may be identified angiographically and include extramural, mural and intraluminal causes. Venous obstacles of extramural origin include a) mechanical compression of the dilated draining vein by rigid extracerebral structures such as the tentorial edge, the sphenoid ridge or the falcotentorial junction and b) compression by pial arteries bridging over draining cortical veins. Venous obstacles of mural origin are focal stenoses of the wall of the draining vein occuring as an endothelial reaction and wall remodelling because of high flow. Venous obstructions of intraluminal origin are caused by spontaneous thrombosis of the venous lumen. Irrespective of the cause, such obstructions and obstacles increase the venous pressure proximally and induce collateral circulation to bypass the venous hyperpressure. Therefore, venous collateral circulation represents an acquired, secondary response of the venous system aimed to distribute the increased pressure of the veins draining the AVM into normal veins. Depending on the location of the AVM with respect to the venous system, such collateral rerouting may occur by way of ipsilateral, contralateral or transcerebral veins (Berenstein and Lasjaunias 1991, Lasjaunias *et al.* 1986). Sufficient venous collateralization decreases the risk of rupture and prevents the development of neurologic symptoms. Angiographically, it is recognized by the redistribution of venous flow in the ipsilateral, contralateral, or transcerebral veins without evidence of venous congestion of the brain and by the absence of significant venous ectasia or varix formation proximal to the obstacle (Berenstein and Lasjaunias 1991, Vinuela *et al.* 1987, Vinuela *et al.* 1985).

Failure of the venous collateral circulation to compensate for the venous hyperpressure results in the formation of a focal venous ectasia or varix proximal to the obstacle and in the development of acute or progressive, transient or permanent clinical symptoms (Fig. 5). The clinical manifestations of an insufficient or failing venous collateral circulation include (1) symptoms of mass effect or cranial nerve palsies caused by direct, mechanical compression of the brain or cranial nerves by the venous varix, (2) seizures or progressive neurologic deficits caused by venous congestion of normal brain parenchyma, (3) hemorrhage because of AVM rupture. AVM rupture caused by venous hypertension may occur at the venous side of the nidus, at the veno-nidal junction or from rupture of intranidal or distal extranidal arterial aneurysms due to retrograde propagation of the increased pressure. Therefore, such venous ectasias or varices represent weak elements of AVM angioarchitecture and their angiographic demonstration indicates an increased risk for hemorrhage.

Venous thrombosis may cause congestion of pial veins that may lead to a focal cerebral ischemia or infarction. Over time, focal ischemia will cause focal cortical atrophy that may be associated clinically with seizures or a neurologic deficit. Venous infarction will create a porencephalic cavity that may also be associated with a neurologic deficit.

An extreme high-flow condition in a dural sinus or major cerebral vein (such as the Galenic Vein) down-stream from an AVM may exert a sump effect on a remote pial vein or on adjacent dural arteries, which in turn may induce a secondary arteriovenous shunt. Such acquired, secondary arteriovenous shunts are not related to the AVM and should not be confused with a second AVM. They are asymptomatic and have been shown to regress spontaneously following treatment of the AVM and normalization of flow in the involved dural sinus or major draining vein (Berenstein and Lasjaunias 1991, Valavanis 1996).

Hydrovenous Disorders

In infants and children with AVMs, dural sinus high-flow may impair cerebrospinal fluid reabsorbtion leading to macrocrania, hydrocephalus or tonsillar herniation. If long lasting, such a hydrovenous disorder leads to subependymal artrophy with exvacuo hydrocephalus, subcortical atrophy, white matter calcifications or syringomyelia. Clinically, these patients develop mental retardation, complex neurologic deficits or epilepsy. The hydrovenous disorders induced by brain AVMs in the pediatric population have been extensively studied by Lasjaunias (Berenstein and Lasjaunias 1991).

6. Indications for Endovascular Treatment

The primary goal of treatment of a brain AVM is to prevent new or recurrent hemorrhage. Other goals may include to improve or stabilize neurological deficits, to treat intractable epilepsy or to reduce the severity and frequency of chronic headaches. An incidentally detected brain AVM does not automatically represent an indication for treatment. In general, the indication for active versus conservative treatment is derived from the estimated natural history of a given AVM, the anticipated risks of the various treatment modalities, the patient's neurologic and general condition, the patient's past history, the age and the patient's attitude toward conservative or active treatment (Aminoff 1987, Yaşargil 1988, Forster *et al.* 1972, Heros and Tu 1986). In the attempt to improve selection criteria for active treatment various decision analysis schemes (Fischer 1989, Steinmeier *et al.* 1989), classification systems (Pasqualin *et al.* 1991) and grading systems (Luessenhop and Gennarelli 1977, Pelletierri *et al.* 1979, Luessenhop and Rosa 1984, Garretson 1985, Shi and Chen 1986, Spetzler and Martin 1986) have been introduced and applied. These systems use various criteria, such as the number of feeding arteries, the size, the age, the sex, neurological deficits, the location, eloquence of adjacent brain, pattern of venous drainage and they range in complexity from simple and easy to apply to complex and difficult to use. The scope of these grading systems is to predict the risk of neurological morbidity resulting from treatment, especially surgery. They, therefore, are based mainly on criteria directly related to anticipated surgical difficulties, like deep venous drainage, large size or close proximity to so-called "eloquent" brain tissue (Spetzler and Martin 1986).

In a retrospective comparative study of the grading systems introduced to predict postoperative morbidity and mortality, the Spetzler and Martin system showed the highest overall correlation with surgical difficulty and postoperative neurological outcome (Steinmeier *et al.* 1989). This system is currently in wide use for prediction of surgical risk and for operative decision making in patients with AVMs. This system is based on only three graded variables derived from cerebral angiography, CT, or MR, i.e. (1) size of nidus (small <3 cm $= 1$ score / medium 3–6 cm $= 2$ scores / large >6 cm $= 3$ scores), (2) eloquence of adjacent brain (no $= 0$ score / yes $= 1$

score) and (3) deep venous drainage (no = 0 score / yes = 1 score). The sum of the three scores provides the AVM grade, which may range between Grade I and V (Spetzler and Martin, 1986). In addition, large AVMs that involve extensive areas of eloquent cortex or smaller AVMs located within the brain stem or hypothalamus are classified as Grade VI and are regarded as inoperable (Martin and Vinters 1990). Regarding the endovascular treatment of brain AVMs, these grading systems fail to take into consideration the specific angioarchitecture of the AVM, including high-flow angiopathic changes, the intrinsic angioarchitecture of the nidus and the relationship between topography of the lesion and its vascular supply and drainage. In contrast to surgical morbidity, morbidity of the endovascular approach is directly related to the capacity of reaching safely and superselectively the nidus and remaining strictly within it. Therefore, the specific indications for endovascular treatment and the particular goals of endovascular treatment in a given case, are derived from comprehensive MR and angiographic evaluation of the lesion including precise topographic evaluation, identification of the type of feeding arteries, depiction of the angioarchitecture of the nidus and its particular vascular composition, delineation of the venous drainage, detection of any associated lesions (flow related aneurysms, venous stenoses, venous varix, venous hypertension, pseudoaneurysms) and evaluation of the status of collateral circulation and of the circulation of the remaining brain.

For these reasons, the Spetzler-Martin grading system does not correlate with the difficulty of treating patients with AVMs by the endovascular approach and cannot be applied to predict the risk of neurological impairment resulting from endovascular treatment.

In the majority of cases, the specific goal of endovascular treatment in a particular patient with brain AVM can be defined from the above mentioned parameters. These goals include the curative application of embolization aiming at complete obliteration, the preoperative or preradiosurgical application of embolization aiming at size reduction and hemodynamic improvement and the palliative application of embolization aiming at partial and targeted elimination of angioarchitecturally weak elements or at elimination of vascular elements responsible for venous hypertension or tissue hypoperfusion. In some cases, however, a predefined goal of endovascular treatment has to be changed respectively adapted to the observations made during the initial endovascular procedure. For example, during preoperative embolization it may become clear to the interventional neuroradiologist, that complete obliteration of the AVM is possible without an increase of the predetermined risks of the combined embolization and surgical treatment. During embolization of an AVM with the goal of complete obliteration it may become evident, that subtotal obliteration followed by radiosurgery is preferable. Ideally, a multidisciplinary approach, including a neurosurgeon, an interventional neuroradiologist, a radiotherapist and a neuroanaesthesiologist should be adopted for therapeutic decision making (Berenstein *et al.* 1993, Yaşargil *et al.* 1990).

In the majority of cases, endovascular treatment of brain AVMs is carried out electively under optimal clinical conditions and after adequate neuroradiologic evaluation. In contrast to spontaneous intracerebral hematomas, patients presenting with even large acute hematomas following rupture of an AVM usually recover rapidly and spontaneously or in response to steroid and diuretic therapy without the need of early decompressive surgery (Yaşargil 1988). Emergency surgery is obviously required in patients with acute hematomas with rapid clinical deterioration. If possible, emergency operation should aim at removing the hematoma and not eliminating the AVM. CT is the imaging modality of choice to detect acute intracranial hemorrhage from a ruptured cerebral AVM. Most commonly, this occurs in the brain parenchyma adjacent to the AVM, with subarachnoid or intraventricular hemorrhage observed less frequently. In patients with AVMs subarachnoid hemorrhage is most probably caused by rupture of an associated proximal aneurysm and not by AVM rupture. In the acute phase of parenchymal hemorrhage, the hematoma compresses the nidus of the AVM. Cerebral angiography performed early may therefore not demonstrate the entire AVM giving the incorrect impression of reduced flow through the AVM or a small AVM as a result of vessel and nidus compression. Depending on the relative sizes of the hematoma and the AVM, the nidus may be fully compressed by the hematoma in the early acute phase of hemorrhage and be undetectable angiographically. Exceptionally, nidus compression by an acute hematoma may lead to thrombosis and spontaneous obliteration of the AVM. Unless there is an indication for emergency, surgical evacuation of the hematoma in the acute phase, cerebral angiography should be repeated after hematoma resorption to demonstrate the true size, extension and flow conditions of the AVM (Berenstein *et al.* 1993, Willinsky *et al.* 1993). Emergency embolization in a patient being investigated angiographically in the acute phase of intracerebral hemorrhage is indicated if a pseudoaneurysm is being identified. Pseudoaneurysms carry a relatively high risk of early rerupture of the AVM (Garcia-Monaco *et al.* 1993). Otherwise, the incidence of early rebleeding of an AVM is considered to be far less than that for aneurysms, so that it is preferable to delay definitive treatment until the patient has fully recovered and the lesion has been comprehensively investigated (Yaşargil 1988).

The incidence of angiographically visible vasospasm following subarachnoid hemorrhage from a ruptured AVM is very low and symptomatic vasospasm because of ischemia is extremely rare in patients with ruptured AVM (Kothbauer *et al.* 1995).

7. Technical Aspects

7.1 Patient Preparation

All patients scheduled for endovascular treatment are placed on corticosteroids, beginning the day before the procedure with a dose of 4×4 mg decadron per day. The dose is tapered off after the 3rd day following the embolization.

Antiepileptic medication is used in patients who have had previous seizures and in those patients already on antiepileptic therapy or with a recent intracranial haemorrhage. The endovascular treatment neither induces seizures nor increases their frequency.

7.2 General Versus Local Anaesthesia

In the initial period of the application of embolization techniques the great majority of patients with brain AVMs were treated under local anaesthesia, sedation and continuous monitoring of ECG, blood pressure and oxygen saturation. General anaesthesia was reserved for children up to 16 years, uncooperative adult patients and in a few patients with intracerebral hematoma. It was thought, that repeated neurological examination during the procedure with or without functional testing was essential in detecting beginning deficits and discontinuing the procedure before the establishment of major deficits.

With increasing experience in the application of endovascular techniques and with an improved understanding of the angioarchitecture and topography of brain AVMs it became apparent that local anaesthesia was an important limiting factor regarding the degree of AVM obliteration achievable in one session. Since 1993 the majority of patients with a brain AVM underwent embolization under general anaesthesia.

The advantages of general over local anaesthesia in the embolization of brain AVMs include:

(1) better working conditions for the interventional neuroradiologist. There is no distraction of the interventional neuroradiologist by the patient and there is no need to communicate verbally with the patient during the procedure, if it is performed under general anaesthesia.

Selection of microcatheters for catheterization of individual feeders, the fluoroscopically guided superselective catheterization itself, performance of superselective angiograms and their immediate analysis, decisions regarding choice, amount and rate of injection of embolic material, the fluoroscopically guided deposition of the embolic agent as well as the immediate fluoroscopic or angiographic recognition of any technical complication occuring during catheterization or embolization require the full concentration and undistracted attention of the interventional neuroradiologist in a

quite environment. These conditions are better achieved with general than local anaesthesia.
(2) General anaesthesia is also preferable for the patient, because it eliminates any patient anxiety and its associated cardiovascular and neurovegetative reactions.
(3) In case of a major complication occuring during the procedure, such as hemorrhage or occlusion of a normal cerebral artery, immediate endovascular treatment, or patient transfer to the CT unit and performance of an emergency CT with optimal quality or, if indicated, immediate transfer of the patient to the operation room for hematoma evacuation and/or ventricular drainage having the patient already under general anaesthesia obviates the need for intubation under difficult conditions, saves important time and may be life saving.

Because of these significant advantages of general over local anaesthesia both the total number of sessions required to complete endovascular treatment of larger AVMs can be reduced and the rate of complete obliteration of smaller and medium-sized AVMs achievable in one or two sessions can be increased.

Obviously, this benefit is achieved by prolonging the duration of individual sessions, because general anaesthesia eliminates patient discomfort, which usually increases in relation to the length of the procedure.

Premedication is performed approximately 45 to 60 minutes before induction of general anaesthesia, with a hypnotic, preferably benzodiazepin (Midazolam). General anaesthesia is induced with Thiopental. For muscle relaxation Pancuronium or a short acting non-depolarizing relaxant is used. For analgesia and maintaining narcosis, Fentanyl is administered. Ventilation is performed with a mixture of nitrous oxide and oxygen. The use of nitrous oxide is contraindicated in patients with increased intracranial pressure.

During the procedure there is routine continuous monitoring of systemic blood pressure, oxygen saturation and ECG.

If induced hypotension is required for better penetration of the nidus with an acrylic embolic agent or for occlusion of larger, high-flow fistulas, this is usually achieved with a nitroprussid drip infusion.

7.3 Neuroangiography Suite and Equipment

The neuroangiographic investigation and embolization of brain AVMs is carried out in the neuroendovascular therapy suite on biplane digital subtraction angiography (DSA) equipment with improved resolution capabilities, live high-quality subtraction roadmapping, magnification and high frame rate capabilities.

Advantages of the biplane DSA system include improved contrast sensitivity, reduced volume of contrast agent used throughout the procedure, reduction of radiation exposure and reduced study time.

Non-ionic iodinated contrast agents are used exclusively for the endovascular investigation and treatment of brain AVMs because of their decreased neurotoxicity compared with ionic agents. A 30% iodine concentration is usually used for DSA of brain AVMs. On average, a volume of 8 ml is injected for selective internal carotid artery, 6 ml for selective vertebral artery, 4 ml for selective external carotid artery and 1 to 2 ml for superselective AVM feeder angiography. Furthermore, these newer generation DSA systems provide the ability to rapidly acquire and continually interpret DSA images while endovascular treatment is in progress. Additional postprocessing capabilities of this neuroangiographic equipment such as delayed masking techniques, pixel shift, zooming techniques, etc. further enhance overall AVM and nidus visualization.

7.4 Neuroangiographic Investigation

Usually, the procedure is started with a complete neuroangiographic investigation guided by the location and extension of the AVM as derived from MRI and MRA with the goal to reveal the complete angioarchitecture of the AVM and the circulation of the brain.

Since this initial angiographic work-up is followed by superselective catheterization and embolization of the AVM nidus, an angiographic catheter which will be subsequently used as a guiding catheter is selected for the neuroangiographic investigation. The author routinely uses a 5.5 French polyethylene catheter (Valavanis cerebral catheter, Cook) for that purpose.

This initial comprehensive neuroangiographic investigation of a brain AVM should provide the following information (Valavanis 1987):

(1) The arterial territory or territories involved into the supply of the AVM.

(2) The individual feeding arteries.

(3) The arterial supply of normal brain proximal, around and distal to the AVM.

(4) Arterial high-flow angiopathic changes: (a) arterial enlargement, dolicho-ectatic arteries, loops and kinking; extra-and/or intracranial; (b) isolated or multiple arterial stenoses, moya-moya-like changes; (c) proximal and/or distal flow-related aneurysms.

(5) Gross assessment of the AVM nidus: (a) size and shape; (b) compact or diffuse; (c) plexiform and/or fistulous composition; (d) intranidal vascular cavities; (e) flow conditions.

(6) Venous territory or territories involved in the drainage of the AVM.

(7) Individual draining veins.

(8) Venous high-flow angiopathic changes. (a) venous stenosis with or without venous collateral circulation; (b) venous varix; (c) venous occlusion; (d) dural sinus high-flow with secondary cortical arteriovenous shunt.
(9) Venous anatomic variations; persisting embryonic veins.
(10) Venous drainage of the normal brain.

Despite the limitations inherent to selective neuroangiographic investigation of brain AVMs regarding the reliable depiction of intrinsic angioarchitectural details of the AVM as opposed to superselective neuroangiography, this information is essential in planning the superselective endovascular exploration and embolization of the AVM.

7.5 Selection of Cervical Artery or Arteries for Intracranial Navigation

Based on the information obtained from the preliminary neuroangiographic investigation on the anatomy and geometry of the involved and not-involved extra- and intracranial arteries in relation to the vascular territory or territories of the AVM and on the type, number and contribution of the feeding arteries, the cervical artery or arteries through which the endovascular microcatheter approach to the nidus of the AVM will be performed is selected. Selection of the best suited cervical artery and in case of involvement of more than one vascular territories into the supply of the AVM, determination of the sequence of the multiple approaches through the most appropriate cervical arteries is essential for the successful microcatheterization of the AVM nidus.

AVMs located fully or partially in the territory of one anterior cerebral artery may be approached through either the ipsilateral or contralateral internal carotid artery, depending on the angulation of the carotid siphon, on the angulation of the A1-segment in relation to the distal internal carotid artery and on the patency of anterior communicating artery.

In AVMs located in the vascular territory of both anterior cerebral arteries, such as is frequently the case with callosal AVMs, the approach to both anterior cerebral arteries may be performed through one internal carotid artery, or through each ipsilateral internal carotid artery or even through each contralateral internal carotid artery, depending on the siphon angulation, A1-segment angulation in relation to the distal internal carotid artery and on the presence or absence of loops or kinkings in the internal carotid arteries.

In AVMs located fully or in part in the middle cerebral artery territory, the approach is usually through the ipsilateral internal carotid artery. Rarely, in cases with extreme looping or kinking of the ipsilateral extracranial internal carotid artery or in cases with associated high-grade stenoses or occlusions of the ipsilateral internal carotid artery, an approach through the contralateral internal carotid artery and through anterior communicating artery has to be selected. In these cases a special, long microcatheter version has to be used.

In AVMs located in the posterior cerebral artery territory (perforator, choroidal or pial posterior cerebral artery branches), the approach is usually through the dominant vertebral artery. In several cases, however, with a dilated Pcom artery, an approach through the ipsilateral internal carotid artery proved very useful.

In AVMs located in the vascular territory of the anterior choroidal artery the approach is through the ipsilateral internal carotid artery.

In AVMs located in the vascular territory of the posterior communicating artery-perforators the approach is through the ipsilateral internal carotid artery or through the dominant vertebral artery, depending on the angle and orientation of the proximal segments of these perforators in relation to the posterior communicating artery and on flow-direction.

In AVMs supplied by proximal and/or distal M1-perforators the approach is usually through the ipsilateral internal carotid artery.

In AVMs supplied by A1-perforators and particularly by Heubner's artery the optimal approach in the majority of cases proved to be through the contralateral internal carotid artery, because of the recurrent orientation of the origin of these arteries with respect to the A1-segment.

AVMs supplied by anterior communicating artery-perforators are approached through one of the internal carotid arteries depending on the most suitable geometry.

Posterior fossa AVMs supplied by posterior inferior (PICA), anterior inferior (AICA) or superior cerebellar arteries (SCA) uni- or bilaterally are usually approached through the dominant vertebral artery. However, PICA catheterization is usually performed through the ipsilateral vertebral artery. In rare instances, with extreme tortuosity of the vertebral arteries a retrograde approach through one of the internal carotid artery's and through posterior communicating artery has to be performed.

In AVMs supplied by feeding arteries arising from two or three vascular territories and depending on vascular geometry two guiding catheters inserted through a bifemoral approach may be placed in the appropriate cervical arteries for simultaneous microcatheterization of two feeding arteries with two microcatheters (see 7.6).

7.6 Endovascular Microinstrumentation for Catheterization of Brain AVMs

The current generation of microcatheter systems available and applied in the superselective endovascular exploration and embolization of brain AVMs consists exclusively of the variable stiffness microcatheters. The shaft of these microcatheters consists of a more rigid proximal segment, a flexible mid segment, and a soft distal part including the microcatheter tip. Usually, a radiopaque marker is positioned at the distal tip for fluoroscopic visualization. This tapered design of the microcatheter diameter is a key design component of all currently available microcatheter systems used for distal superselective cerebral catheterizations. The stiffness of the proximal part of the microcatheter improves the ability to push and advance the catheter, while the softer distal segment prevents trauma to the vessel wall, catheter induced arterial vasospasm or vessel wall perforation.

Two types of variable stiffness microcatheters are available and used in brain AVM embolization. The first type is used exclusively in combination with steerable microguidewires allowing for distal catheterization by torque control (Kikuchi *et al.* 1987). Several types of variable stiffness microguidewires are available to assist in catheter advancement and guiding direction into the desired arteries or veins. The second type are flow guided microcatheters which have a slightly dilated radiopaque tip and a softer distal segment permitting distal catheterization of tortuous vessels (Dion *et al.* 1989).

7.7 Superselective Exploration of Brain AVMs

Despite its usefulness in demonstrating the general vascular features of an AVM, selective angiography of the internal carotid, external carotid, and vertebral arteries has significant limitations. Overprojection of early draining veins on arterial feeders may obscure visualization of small feeding arteries as well as small flow-related aneurysms located in proximity to the nidus. The nidus itself frequently obscures the origin of the draining veins and particularly intranidal division of a single draining vein into multiple veins. Frequently, the intranidal angioarchitecture can not be reliably recognized and important angioarchitectural features such as intranidal aneurysms, pseudoaneurysms or smaller direct arteriovenous fistulae may remain undetected on selective angiographic studies. In addition, because of different hemodynamic conditions in different parts (compartments) of an AVM, some small accessory draining veins may not be visualized at all. Most of the currently used classification and grading systems for brain AVMs as well as the available statistical data on the angioarchitecture and vascular characteristics of brain AVMs are mainly based on selective angiographic studies. Obviously, this data will differ from similar data derived from superselective angiographic studies.

Selective angiographic studies are used for planning the superselective endovascular microcatheterization of the nidus of a given AVM. Usually, several feeding arteries are superselectively catheterized and embolized in one session. Appropriate selection of feeding arteries for superselective microcatheterization and the microcatheterization sequence of several feeding arteries in a single session are important factors for successful embolization of a given brain AVM.

Superselective angiographic exploration of an AVM should provide the following information:

(1) Distal, prenidal, segments of feeding arteries: (a) anatomic type; (b) geometric features; (c) hemodynamic characteristics.

(2) Arterio-nidal junction.

(3) Assessment of nidus: (a) compartmental composition; (b) intercompartmental communications; (c) intranidal vascular composition (plexiform and/or fistulous); (d) intranidal vascular cavities or ectasias (aneurysms, pseudoaneurysms, venous varices); (e) arteriovenous transit time.

(4) Veno-nidal junction.

(5) Proximal segments of individual draining veins.

This information influences the final decision on proceeding with embolization, the selection of the appropriate embolic material, its amount, mixture and mode of injection.

The sequence of superselective microcatheterization and subsequent embolization of individual feeding arteries in the usual multipedicular AVM is mainly determined by the hemodynamic and geometric types of feeding arteries in relation to the major arterial territories involved into the supply of the AVM. If several feeding arteries in a single arterial territory supply the AVM, then catheterization and embolization starts with the dominant and direct type of feeder(s) and proceeds with the supplementary and direct feeder(s) and finally with the indirect type of feeders, if present and technically accessible. If more than one arterial territories participate in the supply of the AVM, the territory providing the dominant supply is being catheterized first. If dominant feeding arteries arise from two or three arterial territories, as is the case with larger AVMs located directly within a watershed area, catheterization usually starts with that feeding artery supplying the larger compartment of the nidus. Obviously this approach has to be adapted to the predefined goals of the embolization procedure, i.e. complete versus partial obliteration or embolization targeted to a particular component or weak angioarchitectural element.

In AVMs receiving supply from more than one arterial territories simultaneous catheterization of two feeding arteries arising from two territories through a bifemoral approach proved very useful in terms of nidus evaluation and embolization (Fig. 2). Simultaneous and alternate superselective angiograms obtained during injection of contrast material through both microcatheters allows a better evaluation of two adjacent nidus compartments and their individual draining veins and permits immediate continuation with acrylic embolization of the second compartment following the glue deposition in the first compartment. This technique was successfully used in 46 cases (12%) of this series and seems to improve the achievable obliteration rate. Of the 151 cases in which a complete obliteration was achieved in this series, 31 cases (20.5%) were approached and embolized with this technique.

7.8 Embolic Materials Used for Embolization of Brain AVMs

A wide variety of embolic materials, including particulate and liquid agents, have been used for the embolization of brain AVMs. Although the ideal material for endovascular therapy of brain AVMs has yet to be discovered, cyanoacrylates represent currently the primary material used in the endovascular management of brain AVMs.

Cyanoacrylates

Cyanoacrylates have been used for embolization of brain AVMs for more than 15 years. The exposure of the cyanoacrylate monomer solution to an ionic environment, such as blood, initiates the process of polymerization by adding a negative ion to open the carbon-double-bond. Among the cyanoacrylates, isobutyl cyanoacrylate (IBCA) and n-butyl cyanoacrylate (NBCA) have been used for embolization of brain AVMs. Presently, NBCA (Histoacryl or Avacryl, Tripoint Medical, Braun Melsungen, Germany) is the preferred embolic agent as it has significant advantages over IBCA (Brothers *et al.* 1989, Berenstein and Lasjaunias 1991, Debrun *et al.* 1997). NBCA has a lower bonding strength, higher surface tension and higher viscosity than IBCA. Its lower bonding strength significantly reduces the possibility of gluing the catheter tip in the arterial feeder immediately after embolization. Thanks to its higher surface tension and viscosity, NBCA produces a more uniform column and respectively a more compact cast of the nidus with less fragmentation. To prevent recanalization of the embolized nidus a complete, homogeneous and compact acrylic cast is necessary. If blood clot is left within or around the cast, this can be reabsorbed resulting in partial recanalization of the nidus. This phenomenon occurs in less than 2% of cases.

In order to permit fluoroscopic visualization it is essential to add opacifying agents to the acrylic mixture. As opacifying agent Tantalum powder is being added to the mixture. Tantalum is a biocompatible and inert metal with an atomic number of 73 and is used in powder form with particle sizes of 1 to 2 μm in size. Addition of Tantalum powder slightly increases the viscosity of the mixture. High resolution subtraction fluoroscopy increases the visibility of the mixture at lower concentrations of Tantalum powder. Usually, 0.5–1 g/1 ml NBCA mixture are used. The polymerization time of the cyanoacrylate must be adjusted to the flow conditions by the addition of Pantopaque. Pantopaque retards polymerization time and allows better penetration of plexiform nidi. Before injection of the acrylic, the microcatheter is irrigated with a non-ionic solution such as 5% dextrose. Contact of the acrylic mixture with an ionic solution will initiate the polymerization process. Therefore, precautions must be taken to avoid premature occurrance of polymerization. In order to determine the appropriate polymerization time, the transit time of the AVM nidus is assessed by determining the time from injection to the appearance of the earliest nidal draining vein or veins.

NBCA embolization was shown to facilitate the technical aspects of surgical resection. Vessels and niduses embolized with NBCA are found to be spongy and easily compressible during surgery. They can be easily cut with microscissors because they are softer and more pliable than those embolized with IBCA. In addition, the NBCA-embolized vessels are easily distinguished from arteries supplying normal parenchyma, which therefore can be readily spared (Jafar *et al.* 1993, Fournier *et al.* 1991).

Histologically, NBCA was shown to provoke a moderately intense foreign body reaction over the first weeks followed by a lymphocytic infiltration. After 4 weeks, focal necrosis of the vessel wall (angionecrosis) and occasional migration of the NBCA into the extravascular space have been observed histologically (Brothers *et al.* 1989, Vinters *et al.* 1981).

Polyvinyl Alcohol Foam

Polyvinyl alcohol foam (PVA) is a particulate embolic material used extensively in brain AVM embolization (Scialfa and Scotti 1985, Schumacher and Horton 1991). PVA is available in particle sizes ranging from 45–1250 μm. They are injected in a suspension of contrast material. PVA has been used extensively for preoperative embolization of brain AVMs. The main advantage of preoperative PVA embolization is that the AVM is easily compressed and retracted at surgery (Purdy *et al.* 1990). However, the main disadvantage of PVA embolization is its high recanalization rate. PVA produces vessel occlusion by mixing with stagnant blood that coagulates. This explains the high recanalization rate of vessels embolized with PVA. Histologically, a moderate foreign body reaction with areas of focal angionecrosis are observed following PVA embolization (Germano *et al.* 1992). Recent studies demonstrated the superiority of NBCA over PVA as embolic agent in the endovascular treatment of brain AVMs (Wallace *et al.* 1995, DeMeritt *et al.* 1995). In this series, PVA proved useful as a supplementary embolic material to complete obliteration of the AVM following embolization of the main part of the nidus with NBCA.

Coils

Soft platinum microcoils are available in different sizes and configurations and with or without Dacron fibers attached. Their application is restricted to certain high-flow arteriovenous fistulae, such as vein of Galen aneurysmal malformations, pial arteriovenous fistulae, or larger av-fistulas within plexiform AVMs in order to degrease flow prior to injection of NBCA, thus avoiding distal migration of NBCA. Coils can also be used through the transvenous approache to obliterate venous pouches of large arteriovenous fistulae. Similar results are achieved with Guglielmi detachable microcoils (GDC) in the obliteration of venous pouches of arteriovenous fistulae, through either the arterial or venous route.

No other embolic materials such as silicon sphere (Hilal 1984), silk (Benati *et al.* 1987), ethylene vinyl alcohol copolymer (Taki *et al.* 1990) or estrogen-alcohol and polyvinyl acetate (Su *et al.* 1991) have been used in this series.

8. Applications and Goals of Endovascular Treatment of Brain AVMs

8.1 Preoperative Embolization

Preoperative embolization represents one of the most important applications of this technique in the treatment of brain AVMs. According to the data available in the literature, it appears that preoperative embolization is the most frequently applied form of embolization in the overall treatment of brain AVMs. Preoperative embolization is performed in order to facilitate surgical removal of large, or angioarchitecturally complex but operable AVMs or in order to convert an inoperable into an operable AVM (Pelz *et al.* 1988, Viñuela *et al.* 1991).

In order to be efficient, preoperative embolization must be appropriately planned taking into consideration the particular surgical approach and the anticipated potential difficulties to be encountered during dissection and removal.

The specific goals of preoperative embolization include (1) the size reduction of the nidus, (2) the occlusion of deep feeding arteries such as perforators or choroidal supply, (3) the obliteration of intranidal aneurysms or other intranidal vascular cavities representing weak angioarchitectural elements, and (4) the occlusion of intranidal arteriovenous fistulae.

To have a favourable impact upon subsequent microsurgical removal in terms of radicality and postoperative morbidity, preoperative embolization should efficiently and significantly decrease the size of the nidus and the degree of arteriovenous shunting by intranidal deposition of the embolic material. For that purpose, an appropriate mixture of NBCA and Pantopaque instead of PVA particles should be used, because NBCA has a superior nidal penetration capacity and a significantly lower, if not absent, recanalization rate compared to PVA.

Preoperative embolization with NBCA was shown not to interfere with or adversely affect the technical aspects of microneurosurgical resection of partially or subtotally embolized brain AVMs. NBCA-embolized vessels and nidi are rather soft and therefore easily compressible and can be easily cut with microscissors, without any or with only minimal bleeding occurring from the transected vessels. This in turn minimizes peroperative blood loss and reduces overall operative time by decreasing the use of bipolar coagulation. Jafar *et al.* 1993 showed that the achieved results of microneurosurgical removal and the observed long-term outcome in their 20 patients with larger-sized (mean size 3.9 cm), higher-grade (mean Spetzler-Martin grade 3.2) AVMs who received preoperative transfemoral embolization with NBCA were comparable to those for previously nonembolized 13 patients with smaller-sized (mean size 2.3 cm), lower-grade (mean Spetzler-Martin grade 2.5) AVMs.

Occlusion of feeding arteries without concomitant nidus obliteration or with insufficient nidus obliteration will rapidly induce collateral supply creating significant technical difficulties during subsequent surgical removal of the AVM. This is particularly true for large cortico-subcortical or cortico-ventricular AVMs, where occlusion of the dominant superficial, pial feeders without sufficient nidus obliteration will lead to compensatory recruitment and enlargement of deep, perforating feeding arteries, either directly or through subependymal collaterals. These deep, perforating feeding arteries which lie on the far side of the nidus, can only be reached after coagulation and mobilization of the main, more superficial part of the AVM, are burried in the brain parenchyma, have a different consistency and higher fragility than pial feeders and their elimination may be associated with extreme operative difficulties.

Proximal occlusion of pial feeding arteries may also lead to early post-embolization development of leptomeningeal collateral arteries on the surface of the brain. Such superficial collateral neovascularity represents non-sprouting angiogenesis and may mask the plane of cleavage between the nidus and the adjacent brain and may also be the source of significant bleeding (Vinuela *et al.* 1991). Therefore, feeding artery occlusion without nidus obliteration, with the exception of av-fistulae, should be regarded as technical failure of embolization and the neurosurgeon should be made aware of the anticipated surgical difficulties expected to arise from either recruitment of deep perforating arteries and/or the development of collateral leptomeningeal vessels.

In order to achieve significant size reduction and diminution of the degree of AV-shunting, one or more embolization sessions may be required preoperatively, depending on the size, number of feeders and angioarchitectural complexity of a given AVM. The multiple session, staged reduction in size of large or giant and complex AVMs was shown to allow their complete microsugical removal in a single procedure with a relatively low incidence of morbidity and almost no mortality (Vinuela *et al.* 1991). Preoperative embolization was shown to be of particular assistance in the subsequent microsurgical removal of operable deep brain AVMs. Using a multimodality treatment approach, including preoperative and preradiosurgical embolization, Lawton *et al.* (1995) achieved a 72% elimination rate for deep brain AVMs, with no mortality and a morbidity rate of 9%, in a series of 32 patients.

The optimal timing of surgery following preoperative embolization is still controversial. Considering the time course of histopathological phenomena of acrylic embolization and the known phenomenon of progressive postembolization thrombosis a time interval of one to three weeks between embolization and surgery appears appropriate.

Complications of preoperative embolization leading to morbidity and mortality are reported to be similar to other applications of embolization, with severe morbidity rates between 1.5% and 8% and mortality rates between 0.5% and 4% (Jafar *et al.* 1993, Vinuela *et al.* 1991). However, since embolization has its own morbidity and mortality rates, patients with AVMs should be exposed to the risks of preoperative embolization only if it can be anticipated that it will reduce the risks of the overall, combined management. The experience obtained so far with technically optimal NBCA-embolization in carefully selected patients clearly shows that preoperative embolization does not adversely affect postoperative surgical complications and in many cases is even beneficial. In fact, a recent study comparing the outcome of a group of 30 patients who underwent embolization with NBCA and surgery with a group of 41 patients who underwent surgery only, demonstrated, that 1 week after surgery, the surgery and embolization group displayed a significantly better outcome evaluation (70% with Glasgow Outcome Scale score of 5) than the surgery only group (41% with Glasgow Outcome Scale score of 5), and the long-term evaluation continued to favor the surgery and embolization group (86% versus 66% with Glasgow Outcome Scale score of 5) (DeMeritt *et al.* 1995).

Regarding the important issue of the impact of preoperative embolization on health care costs, it has been argued that the cost of preoperative embolization is usually added to an already costly surgical procedure, thus increasing significantly the overall costs of the combined treatment of brain AVMs (Nelson *et al.* 1991). In a recent study designed to assess the cost and efficacy of embolization in the surgical management of brain AVMs and including both the direct costs associated with the procedure itself and the indirect costs resulting from morbidity and mortality, it was shown that endovascular therapy in conjunction with surgery resulted in 9%–34% savings per treated patient as compared to patients treated with surgery alone (Jordan *et al.* 1996).

8.2 Preradiosurgical Embolization

The role of embolization as a preradiosurgical modality found little attention in the literature, as opposed to its role as a preoperative method, which has been extensively covered and discussed. Only since 1990 reports addressing specifically the role and efficacy of preradiosurgically applied embolization and the obliteration rates achieved by radiosurgery of previously embolized AVMs appeared in the literature (Davson *et al.* 1990, Lemme-Plaghos *et al.* 1992, Dion and Mathis 1994, Mathis *et al.* 1995, Gobin *et al.* 1996). In the most recent study on the subject including 125 patients who underwent embolization to reduce the size of the AVM and subsequently underwent radiosurgery total occlusion of the AVM by embolization alone was achieved in 11.2% of the cases obviating the need for radiosurgery and by radiosurgery in 65% of the remaining, partially embolized AVMs (Gobin *et al.* 1996). This study also concludes that the risk of hemorrhage following partial embolization with NBCA is comparable to the natural history of the AVMs and that the results of radiosurgery of the residual nidus are almost as good as for previously untreated AVMs of the same size (Gobin *et al.* 1996).

The main goals of preradiosurgical embolization are:

(1) to decrease the target size to less than 3 cm in diameter or the residual nidus volume to less than 10 cm^3, because all radiosurgical series using either the gamma unit or the linear accelerator show a strong correlation between the size/volume of the AVM and the achieved rate of complete obliteration with a significant drop in the radiosurgical cure rate in AVMs exceeding a nidus volume of 10 cm^3 (Friedman *et al.* 1995, Lunsford *et al.* 1991, Luxton *et al.* 1993, Steiner *et al.* 1992).

(2) to occlude selectively angioarchitectural weak elements, particularly intranidal aneurysms and venous pouches in order to reduce the risk of bleeding in the latency period between radiosurgery and AVM thrombosis, which may last up to 24 months.

(3) to occlude large arteriovenous fistulae located within an otherwise plexiform nidus, because it is believed that these high-flow, rather large diameter intranidal channels are less sensitive to radiosurgery than the small diameter, slower-flow coiled and intermingled vascular channels of the plexiform part of the nidus, which are more prone to develop endothelial proliferation and subsequent thrombosis following application of appropriate radiosurgical dosages.

(4) to obliterate large AVMs in such a way that multiple compact smaller

targets, each one less than 10 cm^3 in volume are left, so that each of which can be treated individually by radiosurgery.
(5) to occlude the dural supply of an AVM, if present, because this represents a limitation of radiosurgery due to the proximity of the meningeal feeding arteries to the bone and the scalp (Berenstein and Lasjaunias 1991).

Preradiosurgical embolization with microparticles of PVA is less effective than NBCA embolization, because of the high recanalization rate of PVA and its inability to effectively occlude intranidal aneurysms and large arteriovenous fistulae. Therefore, for preradiosurgical embolization the best results in terms of stability of obliteration until radiosurgical obliteration is reached are achieved with the use of NBCA as an embolic material (Gobin *et al.* 1996, Berenstein and Lasjaunias 1991, Hurst *et al.* 1995).

Preradiosurgical embolization does not have any influence on the incidence of postradiosurgical complications, other than contributing to a smaller radiation field by reducing overall nidus size. The incidence of symptomatic radiation necrosis usually observed between 4 and 56 months is reported to be 3.5% to 12.5% (Steiner *et al.* 1992, Lunsford *et al.* 1991, Friedman *et al.* 1995, Colombo *et al.* 1994, Loeffler *et al.* 1990). In addition, Yamamoto *et al.* 1996, reported a delayed morbidity of 5.2% and delayed asymptomatic cyst formation in 7.8% of cases, occuring more than five and up to ten years following radiosurgery.

Since the long-term effects on the brain following radiosurgical treatment of brain AVMs, with or without previous embolization is not known, we follow a cautious policy regarding the indication for radiosurgery, particularly in children and young adult patients.

8.3 Palliative Embolization

The role of embolization as a palliatively applied technique in the management of brain AVMs has been underestimated in the literature. Palliative embolization is reserved for large or giant AVMs, which are regarded as inoperable and which because of their extensive arterial supply and complex angioarchitecture cannot be completely obliterated by embolization. The goals of palliative embolization include
(1) the targeted endovascular elimination of weak elements of angioarchitecture associated with a known increased risk for hemorrhage or rehemorrhage, such as flow-related extra- and/or intranidal aneurysms, intranidal venous varix proximal to an obvious obstruction of the venous drainage, or the presence of an arterial or venous intranidal pseudoaneurysm.
In these cases, catheterization and embolization is restricted to the feeder or feeders carrying the distal flow-related aneurysm or supplying a compartment containing the above mentioned weak angioarchitectural ele-

ments. In order to achieve a complete and permanent occlusion, NBCA is used in these cases.

(2) targeted endovascular occlusion of large AV-fistulae in large or giant AVMs, with or without associated venous varices, venous outflow restriction and venous congestion of surrounding brain. These patients usually present clinically with signs and symptoms of mass effect, cranial nerve palsies, seizure disorders or progressive neurologic deficits. Embolization is restricted to the AV-fistula or fistulae and is performed with NBCA in order to achieve permanent obliteration. Dramatic improvements of the clinical neurologic condition of such patients have been observed following such targeted palliative embolization.

(3) the targeted obliteration of compartments draining into the subependymal venous system and having an intraventricularly prolapsing venous varix. This may represent a significant risk factor for intraventricular bleeding and is observed with large corticoventricular as well as with deep, mainly strio-capsulo-thalamic AVMs. Targeted obliteration of the compartment draining into the subependymal varicously dilated vein, will usually result in flow and pressure decrease as well as shrinkage of the venous varix, eventually eliminating the risk of future intraventricular hemorrhage.

(4) partial embolization of extensive "convexity" AVMs in patients presenting with severe epilepsy resistant to antiepileptic medication. Such AVMs are usually large and located in two or three vascular territories (MCA, ACA and/or PCA), drain into both the superficial and deep venous system and are associated with regional hypoperfusion and various degrees of venous congestion. Significant improvement of the frequency and severity of seizures may require multiple sessions of embolization.

(5) the relief or amelioration of chronic headaches in patients with large AVMs and additional supply by dural arteries. Selective embolization of the dural supply proved to be very effective as a palliative treatment of severe, chronic headache, in an otherwise large, unresectable AVM.

8.4 Postoperative and Postradiosurgical Embolization

Postoperative embolization is rarely being performed, because surgery in well selected cases usually results in complete AVM removal.

Postoperative embolization is considered in the following situations:

(1) Following emergency surgical evacuation of hematoma, caused by rupture of an underlying AVM. Unless the underlying AVM is small and readily accessible and removable with the hematoma, larger AVMs are usually not manipulated and not removed. Embolization or other treatment is being performed following patient recovery and after repeat postoperative angiography has demonstrated the full size and construction of the AVM.

(2) Following incomplete surgical removal of an AVM. If following surgery of an AVM, a residual portion has been left intentionally or unintentionally, embolization or radiosurgery in order to obliterate this residual part may be performed. Obviously, endovascular accessibility will depend on the location of the residual nidus and the type of feeding arteries involved. Proximal clips on feeding arteries may render embolization technically impossible.

Embolization can be also applied after radiosurgery either to treat or to assist in the multimodality management of those brain AVMs that have not responded to initial radiosurgical treatment. If there has been no change in AVM size and angioarchitecture at the 24 months angiographic follow-up, or if obliteration has not been observed at 36 months, then the radiosurgical treatment should be regarded as having failed (Marks *et al.* 1993). Theoretically, embolization performed after radiosurgery may be associated with an increased risk of arterial dissection caused by microcatheter manipulations, because of radiation induced vessel wall changes such as fissuring and endothelial cell necrosis (Marks *et al.* 1993). However, in none of the 15 cases of postradiosurgical embolization of this series did such a complication occur.

8.5 Curative Embolization

Curative embolization refers to the complete and persisting endovascular obliteration of brain AVMs. Unfortunately, the application of endovascular techniques with the defined goal of achieving a complete obliteration of brain AVMs has not found up to now wide acceptance and in most series reported in the literature, curative embolization represents the least frequent type of application of endovascular techniques in the overall treatment of brain AVMs.

This limited role of embolization as a single modality curative method for brain AVMs is clearly reflected in the literature, where reports addressing specifically the issue of complete obliteration of brain AVMs are scanty and most data presented on achieved complete obliteration of brain AVMs form a part of data on the application of embolization as a preoperative or preradiosurgical adjunct.

Therefore, it seems that in most series reporting on embolization results in brain AVMs, complete obliteration was neither the intention nor the primary goal of the endovascular treatment in the majority of cases. This might explain the reportedly low rate of achievable complete obliteration of brain AVMs, which is reported to range between 10% and 20%, with the discrepancies between individual series being mainly related to different referral patterns and patient selection criteria. Retrospective analysis of the characteristics of the AVMs in which a complete obliteration was achieved shows a relation with the size, number of feeding arteries and Spetzler-Martin grade. In the series of Wickholm *et al.* (1996) complete obliteration was achieved in 10 out of 14 AVMs (71%) with a volume less than 4cc, but in only 3 out of 20 lesions (15%) with a volume of 4 to 8 cc for an overall complete obliteration rate of 13.3% in their series of 150 cases.

In the series of Gobin *et al.* (1996) a complete obliteration by embolization alone was achieved in 42% of grade II AVMs, in 15% of grade III AVMs, in 5% of grade IV AVMs and in 3% of grade V to VI AVMs. Relating the complete obliteration rate with the maximum diameter of the AVM, showed a 31% complete obliteration rate in AVMs with a size of 2 to 3 cm, 7% in AVMs 3 to 4 cm in size, 13% in AVMs 4 to 6 cm in size and 0% in AVMs larger than 6 cm. The complete obliteration rate was 16% in AVMs with a volume of 4 to 10 cc, 8% in AVMs with a volume of 10 to 50 cc and 0% in AVMs exceeding 50 cc. Finally, the complete obliteration rate was 33% in AVMs with one feeding artery, 24% in AVMs with two feeding arteries, 9% with three feeding arteries and 3% in AVMs with more than three feeding arteries. The overall complete obliteration rate in their series of 125 patients with a brain AVM was 11.2% (Gobin *et al.* 1996).

To similar results arrive Vinuela *et al.* (1995) in their retrospective analysis of 405 patients, with a reported long-term complete obliteration by embolization alone in 40 patients (9.9%) with small and medium-sized AVMs and with fewer than four feeding arteries.

Although both size of the AVM and number of feeders certainly may have an impact on the achievable obliteration rate they didn't prove to be the major determinants for achieving a complete obliteration in a given case of AVM in this series. With the exception of some large AV-fistulae, size and number of feeders are closely interrelated in plexiform and mixed plexiform and fistulous AVMs, with larger lesions usually having a higher number of feeding arteries. Both parameters were shown to influence more the technical challenge and complexity of the endovascular procedure, the number of required superselective microcatheterizations, the number of sessions and the length of sessions but not necessarily the achieved degree of obliteration.

In this series, with a clearly predefined subgroup of patients undergoing embolization with the goal of complete obliteration, several other parameters were identified, which proved to be more important than size of nidus and total number of feeding arteries in influencing in a positive or negative manner the obliteration rate. In addition, parameters were identified, which didn't seem to have a major influence on obliteration rate.

Complete obliteration rate was clearly related to the topography of the AVM as derived from preembolization multiplanar MRI, according to the classification described above. Since the topography of AVMs is related to the type of feeding arteries, it becomes evident that AVMs supplied by direct and dominant types of feeding arteries, as is the case with sulcal and mixed sulcal-gyral convexity supratentorial and infratentorial AVMs, pial AV-fistulae and mainly extrinsic deep brain AVMs and AVFs have a significantly higher chance of complete obliteration than AVMs supplied mainly or exclusively by indirect and supplementary types of feeders, as is the case with many gyral convexity, with deep parenchymal and especially with diffuse AVMs.

Accordingly, in this series, a complete obliteration was achieved in 60% of sulcal type AVMs, in 55.5% of deep, extrinsic AVMs, in 50% of plexal AVMs but in only 12.5% of gyral AVMs, 20.5% of mixed sulcal-gyral AVMs and in 0% of diffuse AVMs.

The type of feeding arteries supplying a given AVM is far more important in determining the possibility for complete obliteration than their total number. Pial, choroidal or perforating direct and dominant type feeding arteries, direct and supplementary type feeding arteries and in some cases transit arteries with dominant feeding branches have a positive influence on achieving a complete obliteration than transit type arteries with supplementary feeding branches and retrograde collateral type feeding arteries.

The type or types of av-shunt constituting the nidus is another important factor, determining the degree of achievable nidus obliteration. Pure fistulous niduses have a higher chance of complete obliteration, than mixed plexiform and fistulous or pure plexiform nidues. The presence of intranidal av-fistulae is frequently associated with dominant type feeding arteries, thus facilitating the endovascular access and the deposition of NBCA. In this series, a complete obliteration was achieved in 69% of pure fistulous AVMs (pial and subependymal AVFs and vein of Galen aneurysmal malformations), in 39% of mixed fistulous and plexiform AVMs and in 30% of purely plexiform AVMs.

Angiographic evidence of secondary perinidal angiogenesis was found to be an angioarchitectural feature influencing strongly and negatively the degree of achievable nidus obliteration. This phenomenon was very frequently associated with transit type arteries giving off multiple supplementary feeding branches but also branches connected with the perinidal angiogenic zone, making differentiation difficult and superselective catheterization impossible. Out of 90 cases associated with significant secondary perinidal angiogenesis complete obliteration was achieved in only 6 cases (6.6%) as opposed to a complete obliteration rate of 48.8% (145 cases) in the AVMs without evidence of perinidal angiogenesis (297 cases). However, in the six cases with complete obliteration of the AVM, spontaneous regression of the angiogenic zone was observed on follow-up angiograms, testifying to the reversible nature of this phenomenon.

The compartmental composition of the nidus also influences the

Table 8. *Angioarchitectural Features with Positive Influence on Complete Obliteration*

Direct and dominant feeders
Transit arteries with dominant feeding branches
Absence of perinidal angiogenesis
Pure fistulous nidus
Mixed plexiform-fistulous nidus
Monocompartmental nidus
Communicating compartments
Converging compartmental veins
Single, nidal draining vein

obliteration rate. As can be expected, the probability of achieving a complete obliteration is higher with monocompartmentally than with multicompartmentally composed niduses. In this series a complete obliteration was achieved in 88% of the 49 cases with a monocompartmental composition and in 28% of the 285 cases with a multicompartmental composition. The remaining cases of monocompartmental AVMs, although small in size and supplied by only one or two feeders, could not be completely obliterated because they were exclusively supplied by transit arteries with supplementary type feeding branches.

In several instances, penetration of the NBCA through intercompartmental communicating channels was observed fluoroscopically resulting in additional obliteration of that compartment and thus obviating the need of a subsequent separate catheterization and embolization. Although precise statistical data on the incidence of intercompartmental communications in multicompartmental AVMs are still lacking, it seems that their presence influences positively the degree of achievable obliteration rate, provided that the embolization is carried out with NBCA.

The pattern of venous drainage rather than the anatomic type of draining veins (cortical, subependymal, both) is an additional parameter influencing the obliteration rate. In this series, a complete obliteration was more frequently achieved in AVMs with converging compartmental draining veins or single draining nidal veins than in AVMs with isolated compartmental draining veins or mixed isolated and converging compartmental draining veins.

It is the overall constellation and the relative representation of these parameters in a given case of brain AVM, which influences positively, negatively or not essentially the achievable degree of obliteration (see Tables 8–10) (Figs. 2–5).

Based merely on the evaluation of these parameters the intention for

Table 9. *Angioarchitectural Features with Negative Influence on Complete Obliteration*

Transit arteries with supplementary feeding branches
Retrograde collateral feeders
Watershed transfer
Perinidal angiogenesis
Multicompartmental nidus
Purely plexiform nidus
"Diffuse AVM"
Isolated compartments
Multiple isolated compartmental veins

Table 10. *Angioarchitectural Features without (Significant) Influence on Complete Obliteration*

Number of feeding arteries
Flow-related aneurysms
Size/Volume of nidus
Intranidal vascular cavities
Anatomic type of draining veins (cortical, deep, mixed)
Venous high-flow angiopathy (stenosis, varix, venous collaterals)

complete obliteration was formulated in 182 of the 387 cases (i.e. in 47% of the cases) but it could be achieved in 136 cases, i.e. in 74.7%, for a failure rate of 25.3%. Of the remaining 46 cases, 37 had a subtotal obliteration (>90% nidus occlusion) as seen on the immediate postembolization angiogram and 9 cases had a partial obliteration (50% to 90% nidus occlusion).

Depending on the complexity of the AVMs, their size and the total number of feeding arteries, complete obliteration was achieved in one to five sessions, as follows: 91 AVMs (60%) were completely obliterated in one session, 41 AVMs (27%) in two sessions, 15 AVMs (10%) in three sessions, 3 AVMs (2%) in four sessions and 1 AVM (1%) in five sessions.

Both, the number of AVMs treated in one session and the complete obliteration rate increased significantly with the routine introduction of general anaesthesia in 1993 for all cases undergoing curative embolization in our institution.

A complete obliteration could be achieved in an additional 15 cases of the patient groups undergoing preoperative or preradiosurgical embolization. Therefore, the complete obliteration rate in relation to the total number of cases, which underwent endovascular treatment (387 cases) was 39% (151/387).

Many of the completely obliterated AVMs in this series were surgically well accessible and removable, even without preoperative embolization. Such cases included pure sulcal AVMs (20 cases), sulcal AVMs with some subcortical extension (25 cases) and single pedicle convexity pial AVFs (6 cases). The indication for embolization in these cases was influenced either by the patients themselves, explicitly wishing the endovascular treatment or by the referring neurosurgeon. Similarly, some small deep parenchymal, subarachnoid or mixed AVMs could have been treated either by radiosurgery or by microsurgery alone (8 cases), but the patients or their relatives preferred the endovascular treatment.

Follow-up angiograms performed either at 6 or at 12 months showed partial recanalization in 6 of the 151 initially completely obliterated AVMs, for a recurrence rate of 3.9%. Of the 37 subtotally obliterated AVMs, 13 progressed to complete obliteration, 7 showed further recanalization and 17 remained subtotally obliterated. The phenomenon of progressive thrombosis following embolization has also been observed previously by Viñuela *et al.* (1983).

The mechanisms underlying the recurrence of an obliterated brain AVM are recanalization and revascularization. Recurrence through recanalization refers to the restoration of the lumen in a feeding artery and/or in vascular channels of the nidus. The use of a reabsorbable material, like PVA, predisposes for recanalization of the occluded channels. Such a recanalization may occur as early as a few weeks following embolization. Recanalization may also occur with permanently occluding agents, such as NBCA. If the cast produced is incomplete, thrombus will form in the residual lumen, leading initially to compete occlusion. In the process of thrombus organization, new channels lined with endothelium may form reconstituting flow to the nidus (Lasjaunias and Berenstein 1987, Rao *et al.* 1989).

Recurrence through revascularization refers to the reestablishment of blood supply to the nidus of the AVM through development of collateral feeding arteries. Such revascularization will occur following proximal occlusion of feeding arteries without appropriate obliteration of the nidus and represents the vascular response to a technical failure. Angiographically, the venous drainage of the revascularized AVM is always identical to the initial venous drainage of the AVM, emphasizing the need to include the emerging segment of the draining vein in the nidus obliteration. Depending on the arterial territories involved in the supply of the AVM and the pattern of its arterial supply, the following types of collateral revascularization following proximal occlusion may develop, singly or in combination:

(1) Development of newly formed collateral supply: (a) leptomeningeal; (b) subependymal; (c) indirect retrograde, leptomeningeal or subependymal; (d) transdural.

(2) Accentuation of preexisting (not embolized) supply with transformation of supplementary into dominant supply.

Fournier *et al.* (1990) reported on two occipital AVMs out of a series of 52 brain AVMs embolized with cyanoacrylate, which showed revascularization at 6 months and two years respectively and suggested, that the occipital lobe, because of its rich vascularity, is more prone than other parts of the brain to produce intense collateralization leading indirectly to resupply of embolized AVMs.

Recanalization with formation of capillary structures within the lumen of vessels embolized with NBCA, has been shown histologically to occur later than 3 months in partially embolized AVMs (Gruber *et al.* 1996).

9. Results of Endovascular Treatment of Brain AVMs

Of the 387 AVMs, 158 (40.8%) were shown to be completely obliterated on the first 6 months follow-up angiography and MR. No hemorrhage occurred in any of these patients during the follow-up period ranging between 6 months and 10 years with a mean of 3.8 years, and no evidence for recanalization or recurrence was observed in the follow-up period.

19 AVMs were shown to be subtotally obliterated on the first follow-up angiography and MR, performed at six months following the last embolization session. Of these, 4 underwent radiosurgery, 12 microsurgical removal and 3 are scheduled for further treatment.

In 177 cases, partial obliteration ranging between 50% and 90% of the original nidus size, was achieved. Of these patients 21 underwent radiosurgery and 59 microsurgical removal. Of the remaining 97 patients in this group partial embolization was performed as a palliative treatment in 38 patients and 59 wait for further treatment.

In 33 cases only minimal obliteration could be achieved, either because of angioarchitectural reasons (25 cases) or because the patients refused further embolization sessions (6 cases).

Of the 387 patients in this series, 256 (66%) are cured (158 by embolization alone, 73 by embolization followed by surgical removal and 25 by embolization and radiosurgery).

In 62 patients treatment is not yet completed and in 69 patients with mainly large and angioarchitecturally complex AVMs or with diffuse type of nidus only palliative embolization either targeted on weak angioarchitectural elements or to palliate chronic severe headaches was performed.

Of the 131 up to now partially treated patients, 8 (6%) suffered a hemorrhage during the follow-up period. Of these, 3 died due to massive hemorrhage. Four platients recovered completely from the hemorrhage. In all four cases repeat angiography demonstrated intranidal aneurysms. Three underwent reembolization with aneurysm obliteration and one underwent radiosurgery. One further patient is moderately disabled but refused any further treatment.

10. Complications of Endovascular Treatment of Brain AVMs

Each step of the endovascular treatment of a brain AVM, *i.e.* transfemoral placement of the guiding catheter, initial angiographic work-up, superselective catheterization, superselective angiography, injection or delivery of embolic agents, microcatheter withdrawal, guiding catheter withdrawal and femoral artery compression may be the source of a complication. Clinically, the most serious complications related to the endovascular treatment of brain AVMs are cerebral ischemia and hemorrhage.

Ischemic complications of embolization may occur either during catheterization and navigation or following injection of embolic material. Ischemic complications due to catheterization and navigation represent technical failures and include dissections of major arteries, formation of blood clot around catheters or inadvertent injection of blood clot. The chance for such complications is higher with small than with larger, multipedicular, high-flow AVMs. Use of meticulous technique, full and constant attention during fluoroscopically guided catheterization and careful manipulation of microcatheters and microguidewires are essential for the endovascular treatment of brain AVMs.

Ischemic complications occurring in conjunction with the embolization, i.e. following the injection of the embolic material, are invariably due to occlusion of normal arteries. Two mechanisms of normal artery occlusion due to embolization of brain AVMs are distinguished, i.e. anterograde and retrograde (due to reflux). Anterograde occlusion of normal arteries may occur in the presence of a pseudoterminal type of feeding artery. Pressure rise in the pseudoterminal feeder occurring during the injection of the embolic material may suddenly open its anatomically present but angiographically invisible connection to its distal part with consecutive entrance of the embolic material leading to its occlusion and causing ischemia of normal brain parenchyma distal to the nidus. Anterograde occlusion of normal arteries may also occur, if injection of the embolic material is performed from a proximal position of the catheter tip, within a direct type of feeding artery. Failure to distinguish between an angiogenic zone in relation to watershed transfer and nidus of the AVM, may be another cause of occlusion of arteries supplying normal brain. Retrograde occlusion of normal arteries is caused by reflux of embolic material proximal to the tip of the microcatheter. This may occur either within a direct type of feeder with occlusion of normal branches proximal to the nidus or within a feeding branch of an indirect feeder with reflux into the trunk of the indirect feeder and occlusion of normal arteries distal to the AVM.

Ischemic complications occurred in 36 patients (9.3%). In five of these patients a focal infarction or ischemic zone was detected on postembolization MR as an oval or round hyperintensity on T2-weighted MR and was clinically asymptomatic. In all five patients, this clinically silent ischemia was localized either in the head of the caudate nucleus (3 cases) or in the thalamus (2 cases) and was detected following embolization of a deep brain AVM. It had resolved on follow-up MR performed either six months or one year later.

In an additional 18 patients a transient neurological deficit lasting between 24 hours and several weeks was observed. Postembolization MR demonstrated an ischemic lesion in 14 cases. In four cases no abnormality was seen on repeat postembolization MR examinations. Ten of these patients had a convexity AVM of the gyral or mixed (sulco-gyral) type and eight had a deep brain AVM (one callosal, one deep cerebellar and five strio-capsulo-thalamic).

A permanent neurological deficit occurred in thirteen patients (3.3%). In all of these patients an infarction was demonstrated on postembolization MR. Neurologically, an aggravation of preexisting deficits occurred in five patients and new deficits occurred in eight patients. Nine AVMs in this group of patients with permanent neurological deficits were larger convexity AVMs of either the mixed (sulco-gyral) type (five cases) or the gyral (2 cases) respectively sulcal type (1 case) or the diffuse type (one case) and four were deep brain AVMs.

One of these patients with a ventral mesencephalic AVM was lethargic following embolization and died several weeks later due to pulmonary and urinary infection. The neurological deficits in the remaining twelve cases were classified as severe in two, moderate in four and mild in six.

The other type of serious complication of endovascular treatment of brain AVMs is hemorrhage, occurring either during the procedure (perprocedural hemorrhage) or during the early (<72 hours) postembolization period. Perprocedural hemorrhage may be caused by mechanical perforation of a cerebral artery during microcatheterization or due to hemodynamic changes induced by partial embolization of the nidus. Early postembolization hemorrhage is invariably caused by hemodynamic changes occurring in the hours following partial or subtotal embolization of the AVM.

Before the advent of variable stiffness microcatheters, overdistention of an artery by a calibrated leak balloon was the most common cause of intraprocedural hemorrhage (Berenstein and Lasjaunias 1991, Berenstein 1980, Khangure and ApSimon 1989). With the newer generation variable stiffness microcatheters used for brain AVM embolization, mechanically induced hemorrhage became a rare complication of microcatheterization. Perforation of an artery by a microguidewire or microcatheter has been reported by Halbach *et al.* 1991, Purdy *et al.* 1990 and anectodically by others (Lundqvist *et al.* 1996). Immediate recognition of arterial perforation is crucial in avoiding morbidity. Perforation of flow-related aneurysms during microcatheter navigation or placement has also been occasionally reported (Debrun *et al.* 1997). Arterial perforation is diagnosed by contrast material extravasation. Depending on the type of artery perforated, this extravasation will occur either into the subarachnoid space or into the brain parenchyma. It is imperative not to withdraw or pull back the microcatheter, once extravasation of contrast material and thus an arterial perforation has been recognized. The spasm induced by the trauma to the arterial wall may lead to cessation of bleeding, if the microcatheter is left in place and thus blocks blood flow. If bleeding does not stop rapidly, then it is advisable to proceed with occlusion of the rupture area using either coils or cyanoacrylate. In this series, arterial perforation occurred in three cases, i.e. in 0.7% of the 387 cases or in 0.4% of the 710 embolization sessions. The perforation occurred during the attempt to pass an acutely angulated segment of a feeding artery. In all three cases bleeding stopped spontaneously. Two patients experienced headache lasting for approximately 48 hours, none of the patients had a neurologic deficit and all three patients had an excellent outcome.

Perprocedural hemorrhage not associated with mechanical arterial perforation and early postprocedural hemorrhage occurring within 72 hours following embolization is usually caused by compromise of the venous drainage of the AVM, but in some cases no obvious cause can be identified. In this series, perprocedural hemorrhage occurred in five cases, *i.e.* in 1.3% of cases and early postprocedural hemorrhage in seven cases, *i.e.* in 1.8% of cases. In an additional four cases, a small clinically asymptomatic hematoma in the region of the embolized nidus was seen on regular early postembolization MR (1% of cases). Therefore, a hemorrhagic complication related to nidus embolization occurred in a total of 16 cases, *i.e.* in 4.1% of cases. Three of these patients died because of massive hemorrhage. Six patients underwent emergency surgical removal of the hematoma because of rapidly progressing clinical deterioration. Of these, two had a good outcome, three a moderate and one a poor outcome (vegetative state), according to the Yaşargil classification of outcome assessment of operated AVMs (Yaşargil 1988).

When a patient demonstrates rapid neurologic deterioration following embolization of an AVM or if AVM rupture occurs during the procedure, an emergency CT should be immediately performed. If a cerebral hematoma with mass effect, intraventricular extension and/or CT signs of herniation is diagnosed, immediate intubation, hyperventilation and administration of an intravenous bolus of 100 mg mannitol should be performed and the patient transferred to the operating room for emergency craniotomy and hematoma evacuation under barbiturate anaesthesia. Following hematoma evacuation, the patient preferably remains in a pentobarbital-induced coma, with continuous monitoring of blood pressure, pulmonary capillary wedge pressure, central venous pressure and cardiac output through arterial and pulmonary artery catheters, until the intracranial pressure returns to normal, i.e. less than 15 mmHg for 24 hours. This policy proved life saving for the six patients in whom emergency craniotomy was indicated with results comparable to those reported by Purdy *et al.* 1991 and Jafar and Rezai, 1994. The only poor outcome was most probably caused by a delay of more than one hour between beginning of clinical deterioration and surgery, while in the remaining five patients with moderate and good outcome surgery was performed within 30 to 45 minutes from the beginning of clinical deterioration.

Seven patients were treated conservatively, because of a stable neurologic condition without or with only slight decline of the level of consciousness. Of these, six had a good and one a moderate outcome. The overall outcome in this group of 19 patients with a hemorrhagic complication was 11 good (57.8%), 4 moderate (21.1%), 1 poor (5.3%) with a mortality of 3 cases (15.8%).

Twelve of the ruptured AVMs were subtotally and four partially obliterated. Retrospective evaluation of these 16 cases with per- or early post-procedural hemorrhage not associated with mechanical arterial perforation revealed the following causes:

(1) Embolization of an intranidal AV-fistula including its draining vein in a mixed plexiform-fistulous AVM, in which the plexiform portion drains also through the same vein.

(2) Compromise of drainage of a main nidal draining vein in the presence of multiple converging compartmental draining veins.

(3) Occlusion of the main nidal draining cortical vein in a convexity AVM with paraventricular extension, in which the deep, paraventricular portion does not drain as would be expected into the subependymal venous system, but unexpectedly into the cortical, superficial draining vein through transcerebral veins.

(4) Passage of cyanoacrylate into the venous side with occlusion of already stenotic veins at a distance from the nidus, in AVMs with a nidal vein dividing early into multiple draining veins and associated with significant venous high-flow angiopathic changes.

(5) Presence of intranidal or distal extranidal arterial flow-related aneurysms in the residual (not embolized) portion of the AVM.

(6) Progressive thrombosis leading to delayed occlusion of draining veins (Duckwiler *et al.* 1992).

In no instance could the phenomenon of normal perfusion pressure breakthrough, as described by Spetzler *et al.* (1978), be identified as a cause of a hemorrhagic complication. Maintaining the mean arterial blood pressure at approximately 10 to 15% below baseline for 24 hours after embolization may minimize the risk of hemorrhage in cases in which partial occlusion of the major venous outlet occurred (Debrun *et al.* 1997).

The overall morbidity in this series of 387 patients with brain AVMs, which underwent a total of 710 sessions of embolization treatement, was 5.1% (20 patients). Five of these permanent neurological deficits were severe (1.3%), six were moderate (1.5%) and nine were mild (2.3%).

The overall mortality rate was 1.3% (5 patients). Three patients died of a massive postembolization hematoma, one of the consequences of brain stem ischemia and one of massive rupture of a basal ganglionic AVM at the beginning of a first embolization session during the angiographic evaluation.

11. Summary and Conclusions

Advances in superselective microcatheterization techniques, which took place in the past decade, established superselective endovascular exploration as an integral and indispensable tool in the pretherapeutic evaluation of brain AVMs. The strict and routine application of superselective angiography furthered our knowledge on the angioarchitecture of brain AVMs, including vascular composition of the nidus, types of feeding arteries and types and patterns of venous drainage. In addition, various types of weak angioarchitectural elements, such as flow-related aneurysms, intranidal vascular cavities and varix formation proximal to high-grade stenosis of draining veins, could be identified as factors predisposing for AVM rupture. A wide spectrum of secondary angiomorphological changes induced by the arteriovenous shunt of the nidus and occurring up- and downstream of the nidus have been identified as manifestations of high-flow angiopathy. These data help to better predict the natural history, understand the widely variable clinical presentation and to define therapeutic targets of brain AVMs.

Correlation of the topography of the AVM as demonstrated by MR with the angioarchitecture as demonstrated by superselective angiography provided a system for topographic-vascular classification of brain AVMs, which proved very useful for patient selection and definition of therapeutic goals.

This study showed, that 40% of patients with brain AVMs can be cured by embolization alone with a severe morbidity of 1.3% and a mortality of 1.3%. Part of theses patients can, however, be cured equally effective by microsurgery or radiosurgery. Which modality will be chosen for a particular patient will mainly depend on the locally available expertise and experience, but also on the preference of the patient following its comprehensive information about the chances for cure and the risks associated with each of these therapeutic modalities.

Embolization has a significant role in the multimodality treatment of brain AVMs, by either enabling or facilitating subsequent microsurgical or radiosurgical treatment. Appropriately targeted embolization in otherwise untreatable AVMs represents a reasonable form of palliative treatment of either ameliorating the clinical condition of the patient or reducing the potential risk of hemorrhage.

Regarding the practical aspects of the endovascular treatment the following conclusions could be drawn from the experience obtained with this series of 387 patients with a brain AVM:

(1) The goal of endovascular treatment should be defined prior to the procedure. This does not preclude a change in the goal, if additional information obtained during the procedure make this necessary.

(2) The result of endovascular treatment of a brain AVM in terms of the degree of obliteration achieved and complication rate depends mainly on the endovascular strategy developed and the technique applied. These depend on the specific angioarchitecture and topography of the individual AVM, on the past history and clinical presentation of the patient and on the predefined goal of embolization. The strategy should include the definition of embolization targets, the selection of the most appropriate approach for endovascular navigation, the determination of the sequence of catheterization of individual feeding arteries, the selection of the type of catheters and microcatheters, the selection of the appropriate embolic materials as well as the site and mode of their delivery. Thereafter, every endovascular move should be, as in a chess game, the result of a logical plan.

(3) Atraumatic superselective microcatheterization is a key point in the endovascular treatment of brain AVMs. It requires manual skills, knowledge of anatomy and respect for the vascular wall.

(4) All locations of brain AVMs should be regarded as eloquent, and no distinction should be made between eloquent and non-eloquent areas of the brain when deciding on the execution of embolization or the selection of embolic materials.

(5) Embolization should be performed only after the particular angioarchitecture has been fully appreciated and the particular compartment to be embolized has been precisely localized with angiographic-MR-correlation.

(6) The technical goal of embolization is the stable obliteration of the nidus of the AVM with preservation of the normal arterial supply to the adjacent and remote brain parenchyma and without compromise of the venous drainage of the brain. Cyanoacrylate is, currently, the best available embolic agent to achieve that goal. It is not more dangerous than the other available embolic materials, but its use requires appropriate training. Other embolic materials can be used in selected cases with particular angioarchi-

tectural features, either to enable appropriate delivery of cyanoacrylate (e.g. use of coils in large intranidal arterio-venous fistulae to slow down the flow before injecting the cyanoacrylate) or to enhance progressive nidus obliteration following cyanoacrylate embolization (e.g. supplementary embolization of a small remaining part of nidus fed by indirect type of feeders with microparticles of PVA, following subtotal nidus obliteration with cyanoacrylate).

(7) Performing the endovascular treatment of brain AVMs under general anaesthesia was shown in this series to improve the working conditions for the interventional neuroradiologist and its team, to increase the obliteration rate, to improve the overall patient outcome and to decrease the number of sessions required to achieve the defined goal of treatment.

Our understanding of the topographic-vascular relationships and of the angioarchitecture of brain AVMs as well as our ability to resolve angiographically small feeding arteries and intranidal vascular microchannels are more advanced than the currently available endovascular microinstrumentation in safely entering these vessels and precisely obliterating them. Unless smaller, less traumatic microcatheter-microguidewire systems and additional endovascular obliteration techniques will be developed, it is hardly expectable that the currently achievable complete obliteration rate will significantly increase.

12. Acknowledgements

The authors wish to thank Mrs Irene De Bastiani and Miss Romina Bottari for their expert secretarial work and Miss Manuela Keller, vascular radiology technician, for her invaluable help in the preparation of the manuscript.

13. References

1. Albert P, Salgado H, Polaina M, *et al* (1990) A study on the venous drainage of 150 cerebral arteriovenous malformations as related to hemorrhagic risks and size of the lesion. Acta Neurochir (Wien) 103: 30
2. Aminoff MJ (1987) Treatment of unruptured cerebral arteriovenous malformations. Neurology 37: 815–819
3. Ask-Upmark E (1938) On the localization of gliomas and angiomas of the cerebral hemisphere with special regard to evolutionary conditions. Acta Med Scand 94: 392–406
4. Azzam CJ (1987) Growth of multiple peripheral high-flow aneurysms of the posterior inferior cerebellar artery associated with a cerebellar arteriovenous malformation. Neurosurgery 21: 934–940
5. Batjer H, Suss RA, Samson D (1986) Intracranial arteriovenous malformations associated with aneurysms. Neurosurgery 18: 29–35
6. Benati A, Beltramello A, Maschio A, Perini S, Rosta L, Piovan E (1987)

Combined embolization of intracranial AVMs with multipurpose mobile-wing microcatheter system; indications and results in 71 cases. AJRN 8: 938
7. Berenstein A (1980) Transvascular fracture and repair of a cerebral artery. AJNR 1: 358 (abstract)
8. Berenstein A (1981) Technique for catheterization and embolization of the lenticulostriate arteries. J Neurosurg 54: 783–789
9. Berenstein A, Lasjaunias P, Choi IS (1993) Endovascular treatment of arteriovenous malformations of the brain. In: Valavanis A (ed) Interventional neuroradiology. Springer, Berlin Heidelberg New York Tokyo, pp 93
10. Berenstein A, Lasjaunias P (1991) Surgical neuroangiography, vol 4. Springer, Berlin Heidelberg New York Tokyo
11. Brooks B (1930) The treatment of traumatic arteriovenous fistula. South Med J 23: 100
12. Brothers MF, Kaufmann JCE, Fox AJ, *et al* (1989) N-butyl-2-cyanoacrylate —substitute for IBCA in interventional neuroradiology: Histopathologic and polymerization time studies. AJNR 10: 777–786
13. Brown RD, Wiebers DO, Forbes GS (1990) Unruptured intracranial aneurysms and arteriovenous malformations: Frequency of intracranial hemorrhage and relationship of lesions. J Neurosurg 73: 859–863
14. Colombo F, Pozza F, Chierego G, Casentint L, DeLuca G, Francescon P (1994) Linear accelerator radiosurgery of cerebral arteriovenous malformations: An update. Neurosurgery 34: 14–21
15. Courville CB (1958) Vascular patterns of the encephalic gray matter in man. Bull Los Angeles Neurol Soc 23: 30
16. Crawford PM, West CR, Chadwick DW, Shaw MD (1986a) Arteriovenous malformations of the brain: natural history in unoperated patients. J Neurol Neurosurg Psychiatry 49: 1–10
17. Crawford PM, West CR, Shaw MD, Chadwick DW (1986b) Cerebral arteriovenous malformations and epilepsy: factors in the development of epilepsy. Epilepsia 27: 270–275
18. Cronqvist S, Troupp H (1966) Intracranial arteriovenous malformation and arterial aneurysms in the same patient. Arch Neurol Scand 42: 307–316
19. Davson RC III, Tarr RW, Hecht ST, *et al* (1990) Treatment of arteriovenous malformations of the brain with combined embolization and stereotactic radiosurgery: Results after 1 and 2 years. AJNR 11: 857–864
20. De Reuck T (1972) The cortico-subcortical arterial angioarchitecture in the human brain. Acta Neurol Belg 72: 323
21. Debrun GM, Vinuela FV, Fox AJ, Kan S (1982) Two different calibrated leak balloons: Experimental work and application in human. AJNR 3: 407
22. Debrun GM, Aletich V, Ansman JI, Charbel F, Dujovny M (1997) Embolization of the nidus of brain arteriovenous malformations with n-butyl cyanoacrylate. Neurosurgery 40: 112–121
23. DeMeritt JS, Pile-Spellman J, Mast H, Moohan N, Lu DC, Young WL, Hacein-Bey L, Mohr JP, Stein BM (1995) Outcome analysis of preoperative embolization with n-Butyl cyanoacrylate in cerebral arteriovenous malformations. AJNR 16: 1801–1807

24. Dion JE, Duckwiler GR, Lylyk P, Viñuela F, Bentson J (1989) Progressive suppleness pursil catheter: A new tool for superselective angiography and embolization. AJNR Am J Neuroradiol 10: 1068–1070
25. Dion JE, Mathis JM (1994) Cranial arteriovenous malformations: the role of embolization and stereotactic surgery. Neurosurg Clin N Am 5: 459–474
26. Djindjian R, Houdart R (1975) Arteriographie supersélective de la carotide interne et embolisation. Rev Neurologique 131: 829–846
27. Dolce G (1964) Über eine neue Methode: Der Arterien-Katheterismus des Gehirns. Psychopharmacologia 5: 313–316
28. Doppman JL (1971) The nidus concept of spinal cord arteriovenous malformations. A surgical recommendation based upon angiographic observations. Br J Radiol 44: 758–763
29. Duckwiler GR, Dion JE, Vinuela R, Reichman A (1992) Delayed venous occlusion following embolotherapy of vascular malformations in the brain. AJNR 13: 1571–1579
30. Duvernoy HM, Delon S, Vannson JL (1981) Cortical blood vessels of the human brain. Brain Res Bull 7: 519
31. Faria MA, Fleischer AS (1980) Dual cerebral and meningeal supply to giant arteriovenous malformations of the posterior cerebral hemisphere. J Neurosurg 52: 153–161
32. Fischer WS (1989) Decision analysis: A tool of the future: an application to unruptured arteriovenous malformations. Neurosurgery 24: 129–136
33. Forbes HS (1928) The cerebral circulation. 1: Observation and measurement of pial vessels. Archs Neurol Psychiat 19: 751
34. Forster DMC, Steiner L, Hakanson S (1972) Arteriovenous malformations of the brain. A long-term clinical study. J Neurosurg 37: 562–570
35. Fournier D, Terbrugge K, Rodesch G, Lasjaunias P (1990) Revascularization of brain arteriovenous malformations after embolization with bucrylate. Neuroradiology 32: 497–501
36. Fournier D, TerBrugge KG, Willinsky R, Lasjaunias P, Montanera W (1991) Endovascular treatment of intracerebral arteriovenous malformations: experience in 49 cases. J Neurosurg 75: 228–233
37. Friedman WA, Bova FJ, Mendenhall WM (1995) Linear accelerator radiosurgery for arteriovenous malformations: The relationship of size to outcome. J. Neurosurg 82: 180–189
38. Garcia-Monaco R, Rodesch G, Alvarez H, *et al* (1993) Pseudoaneurysms within ruptured intracranial arteriovenous malformations: diagnosis and early endovascular management. AJNR 14: 315
39. Garretson HD (1985) Intracranial arteriovenous malformations. In: Wilkins RH, Rengachary SS (eds) Neurosurgery. McGraw-Hill, New York, pp 1448–1458
40. Germano IM, Davis RL, Wilson CB, *et al* (1992) Histopathological follow-up study of 66 cerebral arteriovenous malformations after therapeutic embolization with polyvinyl alcohol. J Neurosurg 76: 607–614
41. Gillilan LA (1974) Potential collateral circulation to the human cerebral cortex. Neurology 24: 941

42. Gobin YP, Laurent A, Merienne L, Schlienger M, Aymard A, Houdart E, Casasco A, Lefkopoulos D, George B, Merland JJ (1996) Treatment of brain arteriovenous malformations by embolization and radiosurgery. J Neurosurg 85: 19–28
43. Graf CJ, Perret GE, Torner JC (1983) Bleeding from cerebral arteriovenous malformations as part of their natural history. J Neurosurg 37: 331–337
44. Gruber A, Mazal PR, Bavinzski G, Killer M, Budka H, Richling B (1996) Repermeation of partially embolized cerebral arteriovenous malformations: A clinical, radiologic, and histologic study. JANR 17: 1323–1331
45. Halbach V, Higashida R, Dowd C, *et al* (1991) Management of vascular performations that occur during neurointerventional procedures. AJNR 12: 319–327
46. Hamby W (1958) The pathology of supratentorial angiomas. J Neurosurg 15: 65
47. Hamilton MG, Spetzler RF (1994) The prospective application of a grading system for arteriovenous malformations. Neurosurgery 34: 2–7
48. Hayashi S, Arimoto T, Itakura T, Fiji T, Nishiguchi T, Komai N (1981) The association of intracranial aneurysms and arteriovenous malformation of the brain: case report. J Neurosurg 55: 971–975
49. Heros RC, Tu YK (1986) Unruptured arteriovenous malformations: A dilemma in surgical decison making. Clin Neurosurg 33: 187–236
50. Hilal SK (1969) Catheter with a magnetic tip for cerebral angiography. Med Tribune 2: 1
51. Hilal SK, Michelsen JW (1975) Therapeutic percutaneous embolization for extraaxial vascular lesions of head, neck and spine. J Neurosurg 43: 275–287
52. Hilal SK (1984) Endovascular treatment of AVMs of CNS. In: Wilson CB, Stein BN (eds) Intracranial arteriovenous malformations. Williams and Wilkins, Baltimore, pp 259–273
53. Hurst R, Berenstein A, Kupersmith MJ, Madrid M, Flamm ES (1995) Deep central arteriovenous malformations of the brain: the role of endovascular treatment. J Neurosurg 82: 190–195
54. Houdart E, Gobin YP, Casasco AE, *et al* (1993) Proposed angiographic classification of intracranial arteriovenous fistulae and malformations. Neuroradiology 35: 81
55. Hutchings M, Weller RO (1986) Anatomical relationships of the pia mater to cerebral blood vessels in man. J Neurosurg 65: 316
56. Jafar JJ, Davis AJ, Berenstein A, Choi IS, Kupersmith MJ (1993) The effect of embolization with N-butyl cyanoacrylate prior to surgical resection of cerebral arteriovenous malformations. J Neurosurg 78: 60–69
57. Jafar JJ, Rezai AR (1994) Acute surgical management of intracranial arteriovenous malformations. Neurosurgery 34: 8–13
58. Jellinger K (1986) Vascular malformations of the central nervous system: A morphological overview. Neurosurg Rev 9: 177–216
59. Jordan JE, Marks M, Lane B, Steinberg GK (1996) Cost-effectiveness of endovascular therapy in the surgical management of cerebral arteriovenous malformations. AJNR 17: 247–254

60. Kader A, Young WL, Pile-Spellman J, *et al* (1994) The influence of hemodynamic and anatomic factors on hemorrhage from cerebral arteriovenous malformations. Neurosurgery 34: 801
61. Kaplan HA, Aronson SM, Browder EJ (1961) Vascular malformations of the brain. An anatomical study. J Neurosurg 18: 630–635
62. Karhunen PJ, Penttila A, Erkinjuntti T (1990) Arteriovenous malformation of the brain: imaging by posmortem angiography. Forensic Sci Int 48: 9–19
63. Kerber C (1976) Balloon catheter with a calibrated leak. A new system for superselective angiography and occlusive catheter therapy. Radiology 120: 547–550
64. Khangure MS, ApSimon HT (1989) Vessel rupture during calibrated-leak balloon AVM embolization — some additional mechanisms. AJNR 8: 970 (abstract)
65. Kikuchi T, Strother CM, Boyer M (1987) New catheter for endovascular interventional procedures. Radiology 165: 870–871
66. Kondziolka D, Nixon BJ, Lasjaunias P, Tucker WS, TerBrugge K, Spiegel SM (1988) Cerebral arteriovenous malformations with associated arterial aneurysms: Hemodynamic and therapeutic considerations. Can J Neurol Sci 15: 130–134
67. Kothbauer K, Schroth G, Seiler RW, *et al* (1995) Severe symptomatic vasospasm after rupture of an arteriovenous malformation. AJNR 16: 1073
68. Kricheff II, Madayag M, Braunstein P (1972) Transfemoral catheter embolization of cerebral and posterior fossa arteriovenous malformations. Radiology 103: 107–111
69. Lang J, Schäfer K (1980) The angioarchitectonics of the cortical arterial vessels of the human telencephalon. Z Hirnforschung 21: 665
70. Lasjaunias P, Manelfe C, Chiu M (1986) Angiographic architecture of intracranial AVMs and fistulas: pretherapeutic aspects. Neurosurg Rev 9: 253
71. Lasjaunias P, Berenstein A (1987) Surgical neuroangiography, vol 2. Endovascular treatment of craniofacial lesions. Springer, Berlin Heidelberg New York Tokyo
72. Lasjaunias P, Piske R, Terbrugge K, Willinsky R (1988) Cerebral arteriovenous malformations and associated arterial aneurysms. Acta Neurochir (Wien) 91: 29–36
73. Lawton MT, Hamilton MG, Spetzler RF (1995) Multimodality treatment of deep arteriovenous malformations: thalamus, basal ganglia, and brain stem. Neurosurgery 37: 29–36
74. Lazorthes G, Gouaze A, Salamon G (1976) Vascularization et circulation de l'encéphale. Tome 1. Masson, Paris
75. Lemme-Plaghos L, Schönholz C, Willis R, *et al* (1992) Combination of embolization and radiosurgery in the treatment of arteriovenous malformations. In: Steiner L (ed) Radiosurgery. Baseline and trends. Raven, New York, pp 195–208
76. Loeffler JS, Rossitch EJr, Siddon R, Moore MR, Rockoff MA, Alexander EIII (1990) Role of stereotactic radiosurgery with a linear accelerator in

treatment of intracranial arteriovenous malformations and tumors in children. Pediatrics 85: 774–784
77. Luessenhop AJ, Spence WT (1960) Artificial embolization of cerebral arteries. Report of use in a case of arteriovenous malformation. JAMA 172: 11 153–1155
78. Luessenhop AJ, Gibbs M, Velasquez AC (1962) Cerebrovascular response to emboli. Arch Neurol 7: 264
79. Luessenhop AJ, Velasquez AC (1964) Observations on the tolerance of the intracranial arteries to catheterization. J Neurosurg 21: 85
80. Luessenhop AJ, Kachmann R, Shevlin W, *et al* (1965) Clinical evaluation of artificial embolization in the management of large cerebral arteriovenous malformations. J Neurosurg 23: 400–417
81. Luessenhop AJ, Gennarelli TA (1977) Anatomial grading of supratentorial arteriovenous malformations for determining operability. Neurosurgery 1: 30–35
82. Luessenhop AJ, Rosa L (1984) Cerebral arteriovenous malformations. Indications for and results of surgery, and the role of intravascular techniques. J Neurosurg 60: 14–22
83. Lundqvist C, Wikhom G, Svendsen P (1996) Embolization of cerebral arteriovenous malformations: Part II—Aspects of complications and late outcome. Neurosurgery 39: 460–469
84. Lunsford LD, Kondziolka D, Flickinger JC, *et al* (1991) Stereotactic radiosurgery for arteriovenous malformations of the brain. J Neurosurg 75: 512–524
85. Luxton G, Petrovich Z, Jozsef G, *et al* (1993) Stereotactic radiosurgery: principles and comparison of treatment methods. Neurosurgery 32: 241–259
86. Marks MP, Lane B, Steinberg G, Chay P (1990) Hemorrhage in intracerebral AVMs: Angiographic determinants. Radiology 176: 807–813
87. Marks MP, Lane B, Steinberg GK, *et al* (1992) Intranidal aneurysms in cerebral arteriovenous malformations evaluation and endovascular treatment. Radiology 183: 355–360
88. Marks MP, Lane B, Steinberg GK, Fabrikant JI, Levy R-P, Frankel KA, Phillips MH (1993) Endovascular treatment of cerebral arteriovenous malformations following radiosurgery. AJNR 14: 297–303
89. Martin N, Vinters H (1990) Pathology and grading of intracranial vascular malformations. In: Barrow DL (ed) Intracranial vascular malformations. Neurosurgical topics. American Association of Neurological Surgeons, Park Ridge, Illinois, pp 1–30
90. Mathis JA, Barr JD, Horton JA, *et al* (1995) The efficacy of particulate embolization combined with stereotactic radiosurgery for treatment of large arteriovenous malformations of the brain. AJNR 16: 299–306
91. McCormick WF (1966) The pathology of vascular ("arteriovenous") malformations. J Neurosurg 24: 807
92. Miyasaka K, Wopert SM, Prager PJ (1982) The association of cerebral aneurysms, infundibula and intracranial arteriovenous malformations. Stroke 13: 196–203

93. Miyasaka Y, Yada K, Ohwada T, *et al* (1992) An analysis of the venous drainage system as a factor in hemorrhage from arteriovenous malformations. J Neurosurg 76: 239
94. Miyasaka Y, Yada K, Kurate A, *et al* (1994) Unruptured arteriovenous malformations with edema. AJNR 15: 385
95. Moret J, Lasjaunias P, Theron J (1980) Vascular compartments and territories of tympano-jugular tumors. J Belg Radiol 63: 321–377
96. Naidich TP, Valavanis AG, Kubik S (1995) Anatomic relationships along the low-middle convexity: Part I—normal specimens and magnetic resonance imaging. Neurosurgery 36: 517
97. Nataf F, Meder JF, Roux FX, Blustajn J, Merienne L, Merland JJ, Schlienger M, Chodkiewicz JP (1997) Angioarchitecture associated with haemorrhage in cerebral arteriovenous malformations: A prognostic statistical model. Neuroradiology 39: 52–58
98. Nelson M, Bonsor G, Lamb JT (1991) Cost implications of different policies for the treatment of AVMs of the brain. Neuroradiology 33: 203–205
99. Newton TH, Cronqvist S (1969) Involvement of dural arteries in intracranial arteriovenous malformations. Radiology 93: 1071–1078
100. Norbash AM, Marks MP, Lane B (1994) Correlation of pressure measurements with angiographic characteristics predisposing to hemorrhage and steal in cerebral arteriovenous malformations. AJNR 15: 809
101. Okamoto S, Handa H, Hashimoto N (1984) Location of intracranial aneurysms associated with cerebral arterio-venous malformations: Statistical analysis. Surg Neurol 22: 335–340
102. Ondra SL, Trouppp H, George ED, Schwab K (1990) The natural history of symptomatic arteriovenous malformations of the brain: a 24 year follow up assessment. J Neurosurg 73: 387–392
103. Ono M, Kubik S, Abernathy CD (1990) Atlas of the cerebral sulci. Thieme, New York
104. Pasqualin A, Barone G, Cioffi F, Rosta L, Scienza R, Da Pian R (1991) The relevance of anatomic and hemodynamic factors to a classification of cerebral arteriovenous malformations. Neurosurgery 28: 370–379
105. Patel C, Burke T, Chundi V, *et al* (1995) Venous restrictive disease in cerebral arteriovenous malformations. Neuroradiology [Suppl] 37: 118
106. Paterson RMcD, Blackwood W (1959) The association of arteriovenous angioma and saccular aneurysm of the arteries of the brain. J Pathol Bacteriol 77: 101–110
107. Pelletieri L, Carlsson CA, Grevsten SS, *et al* (1979) Surgical versus conservative treatment of intracranial arteriovenous malformations: A study in surgical decison making. Acta Neurochir (Wien) [Suppl] 29: 1–86
108. Pelz DM, Fox AJ, Vinuela F, *et al* (1988) Preoperative embolization of brain AVM's with isobutyl-2 cyanoacrylate. AJNR 9: 757–764
109. Perini S, Talamini G, Pasqualin A, *et al* (1995) Arteriovenous malformations of the brain: risk of first bleeding, rebleeding and related risk factors in 168 untreated patients. Neuroradiology [Suppl] 37: 120
110. Perret G, Nishioka H (1966) Report on the cooperative study of intracranial

aneurysms and subarachnoid hemorrhage. Section VI. Arteriovenous malformations. An analysis of 545 cases of cranio-cerebral arteriovenous malformations and fistulae reported to the cooperative study. Neurosurgery 25: 467–490
111. Pevsner PH (1977) Microballoon catheter for superselective angiography and therapeutic occlusion. AJR 128: 225–230
112. Pfeifer RA (1930) Grundlegende Untersuchungen für die Angioarchitektonik des menschlichen Gehirns. Springer, Berlin
113. Pile-Spellman JMD, Baker KF, Liszczak TM, *et al* (1986) High flow angiopathy: cerebral blood vessel changes in experimental chronic arteriovenous fistula. AJNR Am J Neuroradiol 7: 811–815
114. Purdy PD, Samson D, Batjer HH, *et al* (1990) Preoperative embolization of cerebral arteriovenous malformations with polyvinyl alcohol particles: experience in 51 adults. AJNR 11: 501–510
115. Purdy P, Batjer HH, Samson D (1991) Management of hemorrhagic complications from preoperative embolization of arteriovenous malformations. J Neurosurg 74: 205–211
116. Rao VRK, Mandalam KR, Gupta AK, Kumar S (1989) Dissolution of isobutyl 2-cyanoacrylate on long-term follow-up. AJNR 10: 135–141
117. Rauch RA, Vinuela F, Dion J, Duckwiler G, Amos ED, Jordan SE, Martin N, Jensen ME, Bentson J, Thibault L (1992a) Preembolization functional evaluation in brain arteriovenous malformations: The superselective amytal test. AJNR 13: 303–308
118. Rauch RA, Vinuela F, Dion J, Duchwiler G, Amos ED, Jordan SE, Martin N, Jensen ME, Bentson J (1992b) Preembolization functional evaluation in brain arteriovenous malformations: The ability of superselective amytal test to predict neurologic dysfunction before embolization. AJRN 13: 309–314
119. Rhoten RLP, Comair YG, Shedid D, Cyatte D, Simonson MS (1997) Specific repression of the preproendothelin-1 gene in intracranial arteriovenous malformations. J Neurosurg 86: 101–108
120. Rothbart D, Awad I, Lee J, Kim J, Harbaugh R, Criscuolo GR (1996) Expression of angiogenic factors and structural proteins in central nervous system vascular malformations. Neurosurgery 38: 915–925
121. Russell EJ, Berenstein A (1981) Meningeal collateralization to normal cerebral vessels associated with intracerebral arteriovenous malformations: A functional angiographic study. Radiology 139: 617–622
122. Salamon G (1973) Atlas of the arteries of the human brain. Asclepios, Paris
123. Schumacher , Horton JA (1991) Treatment of cerebral arteriovenous malformations with PVA. Results and analsis of complications. Neuroradiology 33: 101–105
124. Scialfa G, Scotti G (1985) Superselective injection of polyvinyl alcohol microemboli for the treatment of cerebral arteriovenous malformations. AJNR 6: 957–960
125. Serbinenko FA (1974) Balloon catheterization and occlusion of major cerebral vessels. J Neurosurg 41: 125–145
126. Shi Y, Chen X (1986) A proposed scheme for grading intracranial AVMs. J Neurosurg 65: 484–489

127. Spetzler RF, Wilson CB, Weinstein P, Mehdorn M, Townsend J, Telled D (1978) Normal perfusion pressure breakthrough theory. Clin Neurosurg 25: 651–672
128. Spetzler RF, Martin NA (1986) A proposed grading system for arteriovenous malformations. J Neurosurg 65: 476–83
129. Spetzler RF, Martin NA, Carter LP, *et al* (1987) Surgical management of large AVM's by staged embolization and operative excision. J Neurosurg 67: 17–28
130. Spetzler RF, Hargraves RW, McCormick PW, Zabramski JM, Flom RA, Zimmerman RS (1992) Relationship of perfusion pressure and size to risk of hemorrhage from arteriovenous malformations. J Neurosurg 76: 918–923
131. Stein BM, Wolpert SM (1980) Arteriovenous malformations of the brain II: Current concepts and treatment. Arch Neurol 37: 69–75
132. Steiner L, Lindquist C, Adler J, *et al* (1992a) Clinical outcome of radiosurgery for cerebral arteriovenous malformations. J Neurosurg 77: 1–8
133. Steiner L, Lindquist C, Steiner M (1992b) Radiosurgery. In: Symon L, *et al* (ed) Advances and technical standards in neurosurgery. Springer, Wien New York, pp 18–102
134. Steinmeier R, Schramm J, Muller HG, Fahlbusch R (1989) Evaluation of prognostic factors in cerebral arteriovenous malformations. Neurosurgery 24: 193–200
135. Su CC, Takahashi A, Yoshimoto T, *et al* (1991) Histopathological studies of a new liquid embolization methods using estrogen-alcohol and polivinyl acetate. Experimental evaluations with a model of cortical arterial cannulation in the canine brain. Surg Neurol 36: 4–11
136. Suzuki J, Onuma T (1971) Intracranial aneurysms associated with arteriovenous malformations. J Neurosurg 34: 225–228
137. Taki W, Yonekawa Y, Iwata H, *et al* (1990) A new liquid material for embolization of arteriovenous malformations. AJNR 11: 163–168
138. Turjman F, Massoud TF, Vinuela F, Sayre JW, Guglielmi G, Duckwiler G (1994) Aneurysms related to cerebral arteriovenous malformations: superselective angiographic assessment in 58 patients. AJNR 15: 1601–1605
139. Turjman F, Massoud TF, Vinuela F, Sayre W, Guglielmi G, Duckwiler G (1995a) Correlation of the angioarchitectural features of cerebral arteriovenous malformations with clinical presentation of hemorrhage. Neurosurgery 37: 856–862
140. Turjman F, Massoud TF, Sayre JW, *et al* (1995b) Epilepsy associated with cerebral arteriovenous malformations: Multivariate analysis of angioarchitectural characteristics. AJNR 16: 345
141. Valavanis A (1987) Neuroradiological evaluation. In: Yaşargil MG (ed) Microneurosurgery III A: AVM of the brain, history, embryology, pathological considerations, hemodynamics, diagnostic studies, mircosurgical anatomy. Thieme, New York, pp 250–283
142. Valavanis A, Müller-Forell W (1991) Diagnostic and interventional neuroradiology of brain arteriovenous malformations: implications of angioarchi-

tecture for embolization. Advances in neurosurgery, vol 18. Springer, Berlin Heidelberg New York Tokyo, pp 35–40
143. Valavanis A (1996) The role of angiography in the evaluation of cerebral vascular malformations. Neuroimaging Clin N AM 6(3): 679–704
144. Van den Berg R, Van der Eecken H (1968) Anatomy and embryology of cerebral circulation. Prog Brain Res 30: 20
145. Vidyasagar C (1979) Persistent embryonic veins in arteriovenous malformations of the posterior fossa. Acta Neurochir (Wien) 48: 67–82
146. Vinters H, Debrun G, Kaufmann J, Drake C (1981) Pathology of arteriovenous malformations embolized with isobutyl-2-cyanoacrylate (bucrylate). J Neurosurg 55: 819–825
147. Viñuela F, Fox A, Debrun G, Drake CG, Peerless SJ, Girriin JP (1983) Progressive thrombosis of brain arteriovenous malformations after embolization with isobuty 2-cyanoacrylate. AJNR 4: 1233–1238
148. Viñuela F, Nombela F, Roach MR, *et al* (1985) Stenotic and occlusive disease of the venous drainage system of deep brain AVM's. J Neurosurg 63: 180
149. Viñuela F, Drake CG, Fox AJ, *et al* (1987) Giant intracranial varices secondary to high-flow arteriovenous fistulae. J Neurosurg 66: 198
150. Viñuela F, Dion JE, Duckwiler G, *et al* (1991) Combined endovascular embolization and surgery in the management of cerebral arteriovenous malformations: experience with 101 cases. J Neurosurg 75: 856–864
151. Viñuela F, Duckwiler G, Guglielmi G (1995) Intravascular embolization of brain arteriovenous malformations. In: Maciunas RJ (ed) Endovascular neurological intervention. The American Association of Neurological Surgeons, pp 189–199
152. Wallace RC, Flom RA, Khayata MH, Dean BL, McKenzie J, Rand C, Obuchowski NA, Zepp RC, Zabramski JM, Spetzler RF (1995) The safety and effectivencess of brain arteriovenous malformation using acrylic and particles: the experience of a single institution. Neurosurgery 37: 606–618
153. Waltimo O (1973) The relationship of size, density and localization of intracranial arteriovenous malformations to the type of initial symptom. J Neurol Sci 19: 13–19
154. Wikholm G (1995) Occlusion of cerebral arteriovenous malformations with N-butyl cyanoacrylate is permanent. AJNR Am J Neuroradiol 16: 479–482
155. Wickholm G, Lundqvist C, Svendsen P (1996) Embolization of cerebral arteriovenous malformations: Part I—technique, morphology, and complications. Neurosurgery 3: 448–459
156. Wilkins RH (1985) Natural history of intracranial vascular malformations. A review. Neurosurgery 16: 421–430
157. Willinsky R, Lasjaunias P, TerBrugge K, *et al* (1988) Brain arteriovenous malformations. Analysis of the angio-architecture in relationship to hemorrhage. J Neuroradiol 15: 225–237
158. Willinsky RA, Fitzgerald M, TerBrugge K, *et al* (1993) Delayed angiography in the investigation of intracerebral hematomas caused by small arteriovenous malformations. Neuroradiology 35: 37

159. Wollschläger G, Wollschläger PB (1978) The transcerebral arteries. A post-mortem arteriographic study. Neuroradiology 16: 249
160. Yamamoto M, Jimbo M, Hara M, Saito I, Mori K (1996) Gamma knife radiosurgery for arteriovenous malformations: Long term follow-up results focusing on complications occuring more than 5 years after irradiation. Neurosurgery 38: 906–914
161. Yaşargil MG (1987) Microneurosurgery IIIA. Thieme, New York
162. Yaşargil MG (1988) Microneurosurgery IIIB. Thieme, New York
163. Yaşargil MG, Valavanis A, Adamson TE (1990) The respective indications of endovascular or surgical treatment in the AV-Malformations of the brain. In: Bigot JM, *et al* (ed) Radiology. Elsevier, Amsterdam, pp 541–552
164. Yaşargil MG (1994) Anatomy of the sulci. In: Microneurosurgery Vol IVA. Thieme, New York, p 19
165. Yodh S, Perce NT, Weggel RJ, Montgomery DB (1968) A new system for intravascular navigation. Med Biol Eng 6: 143

The Interventional Neuroradiological Treatment of Intracranial Aneurysms

G. GUGLIELMI

Los Angeles Medical School, University of California, Los Angeles, CA (USA)

With 20 Figures

Contents

Cerebral Arteries

Normal arteries of the brain are thinner and stiffer than extracranial arteries. They are composed of four layers: adventitia, media, internal elastic lamina, and intima. An external elastic lamina is absent. Intracranial arteries have no support from surrounding tissue while they pass through the subarachnoid space [60].

True Aneurysms

An intracranial aneurysm is a balloon-like dilatation of a portion of the circumference of a cerebral artery (saccular aneurysms). The dilated portion of saccular aneurysms is constituted by intima and adventitia only; the muscular layer and internal elastic lamina are absent. If the entire circumference of the arterial wall is dilated, the aneurysm is called fusiform.

The opening (orifice or neck) of a saccular aneurysm can be small (1 to 3 mm) or large (4 to 10 mm) [77]. With the possible exception of 1 to 2 mm orifices, it seems reasonable to believe that the orifice is oval in shape [7]. Small aneurysms often have a small orifice. Small neck size is quite unusual for larger aneurysms [22, 79]. Large and giant lesions have, in general, large orifices that may involve the entire arterial wall and, at times, incorporate the inflowing and outflowing arteries. This is not infrequently the case with giant or large lesions involving the basilar artery apex [20], the internal carotid artery bifurcation [25] (Fig. 1), the anterior communicating artery complex, or the middle cerebral artery bitrifurcation (Fig. 2).

Pseudo-Aneurysms

These "false aneurysms" are a result of traumatic damage to the entire arterial wall. They constitute a recanalization of periarterial hematomas. Surgical damage (i.e. internal carotid artery damage during trans-sphenoidal pituitary surgery), skull fractures, and penetrating foreign bodies can be the cause of such lesions.

Mycotic aneurysms, due to bacterial emboli that cause necrosis of the arterial wall, might be considered fusiform false aneurysms.

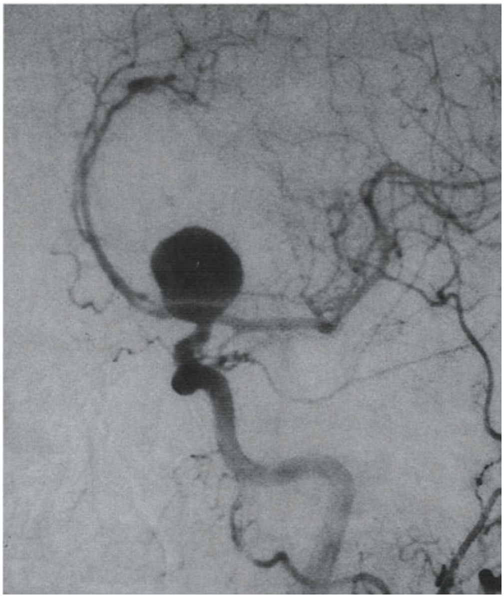

Fig. 1. Left common carotid angiogram, antero-posterior oblique view. The base of this giant aneurysm of the internal carotid artery bifurcation incorporates the origin of the middle cerebral artery and of the anterior cerebral artery. Only incomplete occlusion can be achieved in this kind of aneurysm, with the GDC technique. Partial GDC treatment was performed. This possibly prevented early rebleeding. Subsequent unsuccessful surgical exploration was followed by left ICA occlusion, extra-intracranial by-pass and trapping of the lesion, with excellent outcome

Dissecting Aneurysms

A dissection of the wall of the artery may be spontaneous or post-traumatic. A breach in the endothelium is the initial event. The blood column then enters and separates the layers of the arterial wall. The blood may collect between the internal elastic lamina and the media (with possible consequent ischemic symptomatology), or between the media and the adventitia. If the adventitia is disrupted, an SAH may result. Most dissecting aneurysms causing SAH are vertebral or basilar in location.

From the point of view of endovascular therapy with Guglielmi detectable coils (GDCs), and as a general rule, true saccular aneurysms (these represent the vast majority of all intracranial aneurysms) are amenable to endovascular occlusion with preservation of the parent vessel (Fig. 3). Fusiform aneurysms can be cured by occlusion of the arterial axis, if tolerated (Fig. 4). Pseudoaneurysms and dissecting aneurysms (Fig. 5) should be treated with occlusion of the aneurysm and of the parent artery. In fact these aneurysms, even when they have a saccular appearance, do

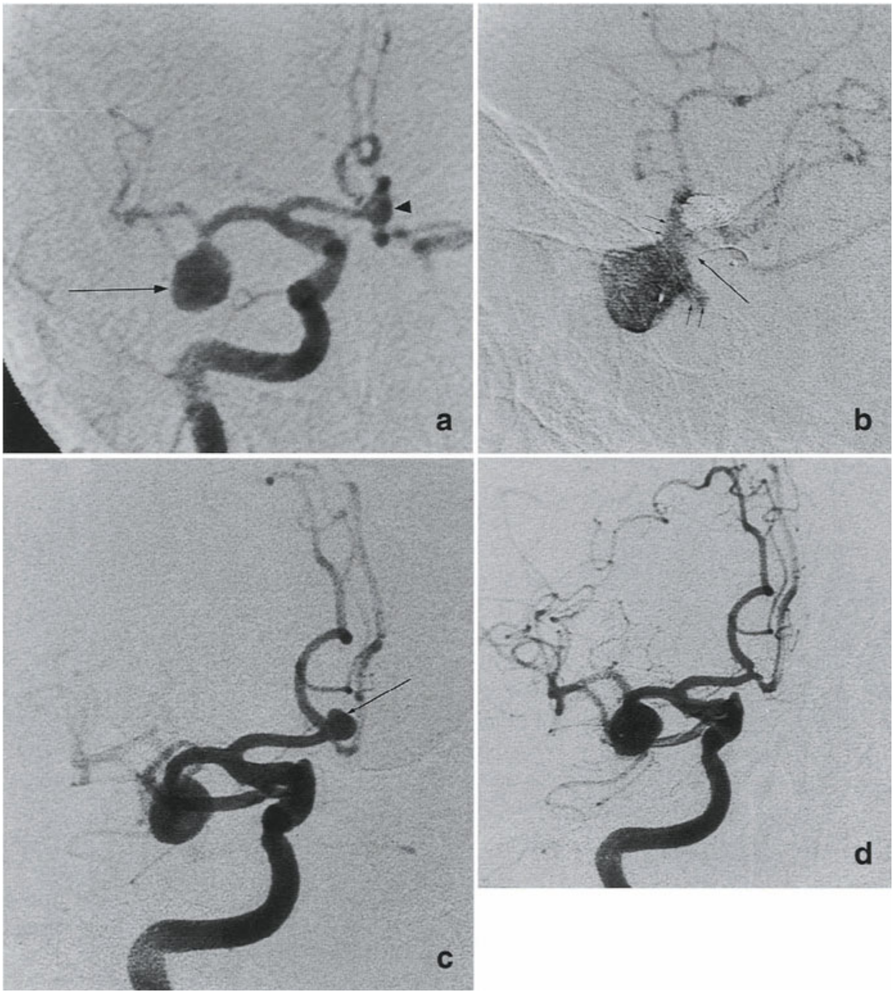

Fig. 2. (a) Sixty year old woman with two incidental aneurysms. Anteroposterior view. The large aneurysm (arrow) arising from the right middle cerebral artery appeared to have a small neck. A small anterior communicating artery aneurysm is also present (arrowhead). Additional angiographic studies were performed to discern the anatomical configuration of both lesions. (b) Intra-aneurysmal injection of the large MCA aneurysm, lateral view. The injection shows the fusiform configuration of the aneurysm. The inflowing artery is depicted by the microcatheter (arrow), and the two separate outflowing arteries are clearly visible (double arrows). This aneurysm is not treatable by the GDC technique. (c) This oblique antero-posterior view allows clear separation of the ACom aneurysm (arrow) from the normal arteries: "working projection". (d) Complete occlusion of the ACom aneurysm with six GDC-10. The normal arteries have been preserved

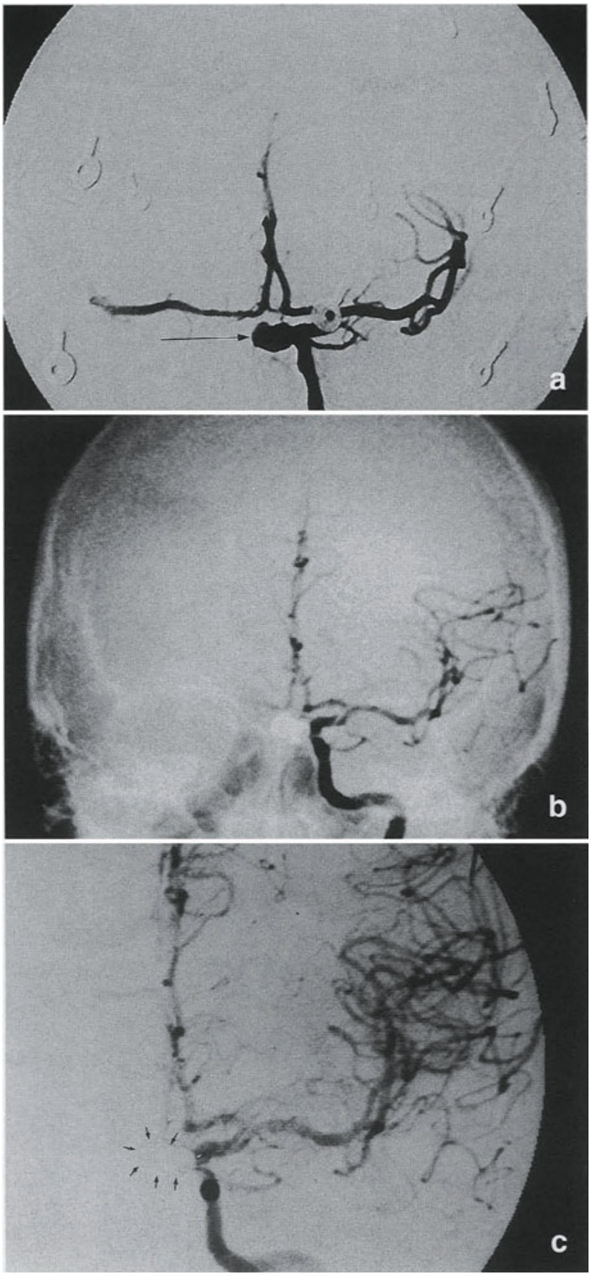

Fig. 3. (a) Left internal carotid artery angiogram on a 32 y. o. woman with a ruptured para-ophthalmic (superior hypophyseal) aneurysm (arrow). This aneurysm was treated 7 days post-SAH with the GDC-10 system (six coils for a total length of 130 cm). (b) The 2 year angiogram confirms persistent complete aneurysm occlusion of this small-necked, lateral type, aneurysm. (c) The 5 year angiogram shows occlusion of the aneurysm with no deformation and no compaction of the coil mesh (arrows)

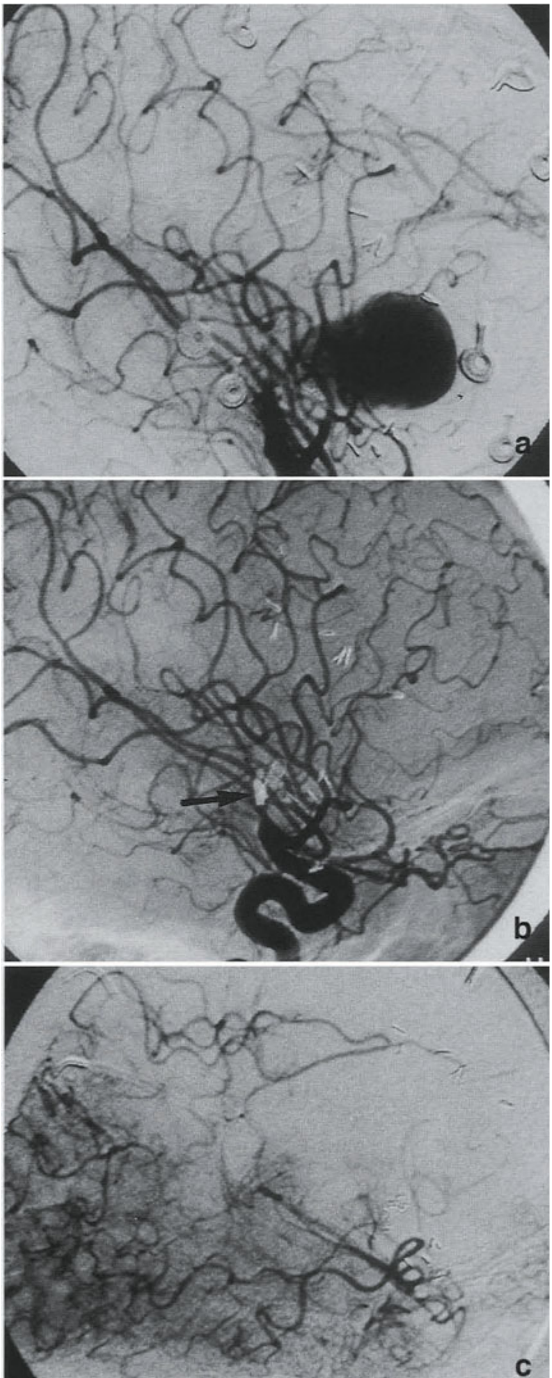
a
b
c

not have a wall that can hold in place any occlusive agent. In the future, endovascular stents might allow treatment of these lesions, with preservation of the arterial axis.

Dimensions and Measurements of Intracranial Aneurysms

For practical purposes the size of the sac of an aneurysm is commonly classified as small (up to 15 mm), large (15–25 mm), or giant (larger than 25 mm). It is the author's opinion, however, that the Yasargil classification should be utilized. According to Yasargil [77], aneurysms can be classified as "baby" (less than 2 mm), small (2 to 6 mm), medium sized (6 to 15 mm), large (15 to 25 mm), and giant (larger than 25 mm). From the Cooperative Study on ruptured aneurysms [61] the size distribution was: small aneurysms—78%; large aneurysms—20%; giant aneurysms—2%.

Aneurysms can be small-necked (less than 4 mm) or wide-necked (4 mm or more) [22]. Small aneurysm necks can be found almost exclusively in small aneurysms, whereas large and giant lesions possess, with rare exceptions, wide necks. The method for measuring aneurysm dimensions on the diagnostic angiogram has been previously published [79]. It consists in comparing the (known) size of the internal carotid or basilar artery with the size of the aneurysm or aneurysm neck. Aneurysms can be rounded, bilobular, trilobular, oval, elongated, irregular, etc.

From the endovascular perspective, a) the size of the aneurysm neck; b) the shape of the aneurysm; c) the dimension of the neck compared to the size and shape of the aneurysm, and d) the dimension of the aneurysm neck compared to the size of the parent vessel are of great importance in predicting whether the treatment will result in a complete occlusion, in a neck remnant, or in a subtotal occlusion. As an example, two aneurysms having both a 4 mm neck have to be considered two completely different entities if the sac of the first is 4 mm and the sac of the second is 8 mm (vide infra).

Fig. 4. (a) Patient presenting with a frontal lobe syndrome from this giant, partially thrombosed, fusiform aneurysm arising from the proximal A2 segment of the left anterior cerebral artery. Temporary balloon occlusion of the A2 segment proximal to the aneurysm was first performed and was tolerated. (b) Two GCD-10 were detached immediately proximal to the aneurysm (arrow) excluding the lesion from the blood circulation, with no untoward complications. (c) The collateral circulation fills the left anterior cerebral artery territory. The aneurysm was subsequently surgically removed, with no blood loss, as an attempt to reverse the compression on the frontal lobe. This patient is gradually improving

Fig. 5. (a) Patient presenting with a subarachnoid hemorrhage from this dissecting aneurysm of the right intracranial vertebral artery (arrows). (b) Several GDC-10 were delivered and detached into the aneurysm (arrows) and between the aneurysm and the posterior inferior cerebellar artery (arrowhead), occluding the arterial axis. Motion artifact is present. (c) Injection of the contralateral vertebral artery shows filling of the posterior circulation and no filling of the dissecting aneurysm. The patient had an excellent outcome

Location

All the possible different locations of intracranial aneurysms have been extensively described in the neurosurgical literature. Surgery necessitates the manipulation of tissues (bone, brain) other than vessels, that need to be removed or retracted to reach the vascular lesion. From the neurosurgical perspective, therefore, the accurate assessment of the location of aneurysms with many subdivisions in the same territory is of utmost importance in planning the operation. From the endovascular perspective this is less important, as the aneurysm is approached from the inside and is clearly visible in the diagnostic angiogram and during road-mapping fluoroscopy. The angle of origin of the aneurysm from the parent artery is more important in that it will determine the angiographic ("working") projection and the type (degrees) of the distal curve to be given to the microcatheter.

Comparing classic neurosurgical treatment with endovascular treatment, one could consider the steps of craniotomy, brain retraction, and aneurysm neck exposure as equivalent to femoral puncture, carotid or vertebral artery negotiation, and aneurysm catheterization, respectively.

The relationship of the aneurysm neck with surrounding normal small arterial branches (i.e. posterior communicating artery, anterior choroidal artery, thalamoperforators arising from the basilar apex or from the P1 segments of the posterior cerebral arteries, lateral lenticulostriate arteries arising as a single trunk from the middle cerebral artery, anterior temporal artery, ophthalmic artery etc.) should be carefully analyzed in order plan a safe endovascular treatment. As a general rule, however, and with the exception of fusiform dilatation of bifurcations, saccular aneurysms do not incorporate normal arteries.

From the endovascular point of view, aneurysms arising from the vertebrobasilar system are simpler to treat, due to easier catheterization of the aneurysm.

The presence of the carotid syphon objectively makes the catheterization of anterior circulation aneurysms less facile.

Clinical Presentation and Incidence

In regard to clinical presentation, there are 5 main categories of aneurysms: 1) Aneurysms that present with an hemorrhage (generally a subarachnoid hemorrhage-SAH). 2) Aneurysms that present with symptoms due to compression of neural structures. 3) True incidental aneurysms (asymptomatic aneurysms). 4) Incidental aneurysms in patients presenting with an SAH from another aneurysm. 5) Aneurysms that cause ischemia in the distal vascular territory.

The worst possible sequela of aneurysmal SAH is rebleeding. This is prevented by early aneurysm treatment (see Indications for Treatment). Patients presenting with SAH may also develop vasospasm, usually between day 4 and 12 after the hemorrhage. Vasospasm is the leading cause of death and morbidity in patients admitted to a health care facility with a ruptured intracranial aneurysm [76]. Vasospasm can be symptomatic or asymptomatic. Symptomatic vasospasm can be recognized when an alteration in level of consciousness or a new focal neurological deficit is detected.

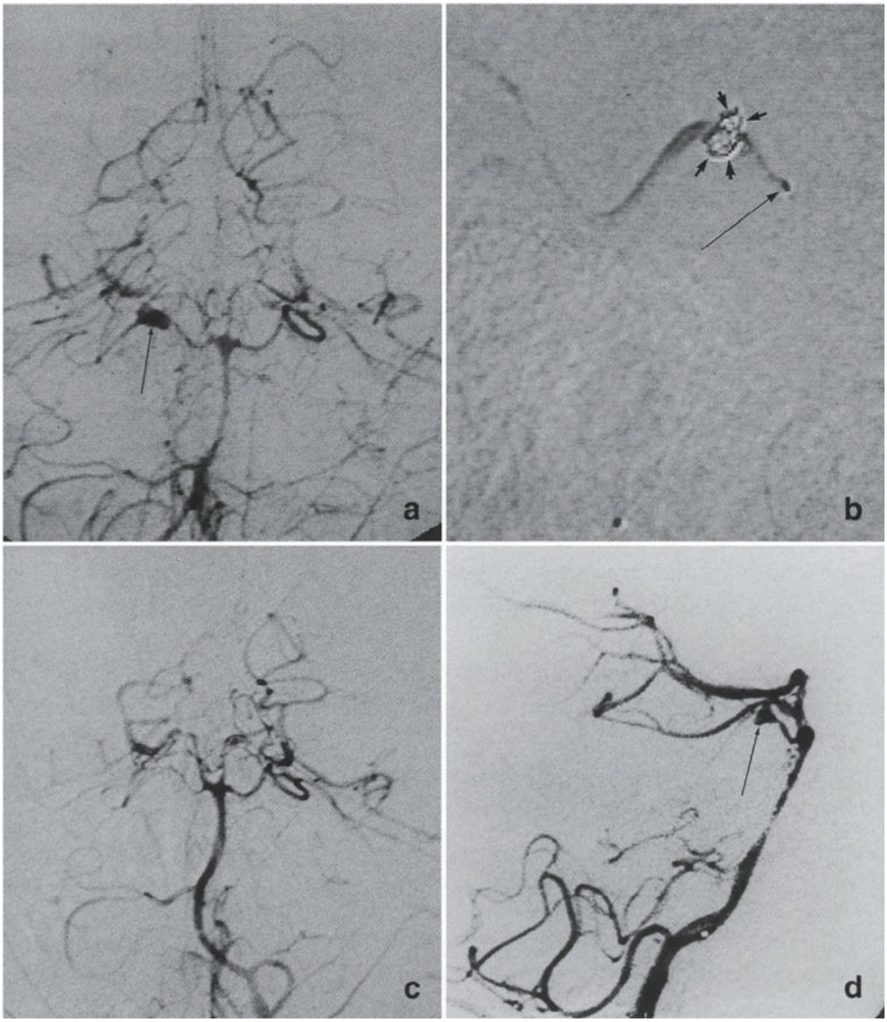

Fig. 6 (a–d)

Fig. 6. (a) This thirty-five year old woman presented with acute SAH and basilar artery vasospasm from a small, fusiform "peripheral" aneurysm of the superior cerebellar artery (arrow). In spite of the fusiform configuration of the aneurysm, the treatment aimed at the preservation of the parent vessel. (b) Superselective angiogram of the superior cerebellar artery (arrow points at microcatheter tip). A Tracker-10 microcatheter had been previously positioned into the aneurysm and two GDCs (2 × 4) had been detached (arrows). The aneurysm is occluded and the arterial axis is preserved. (c) Subsequently, balloon angioplasty of the basilar artery was performed, utilizing a silicon balloon (Interventional Therapeutics Corporation). The angiogram shows the post-angioplasty increased caliber of the basilar artery, non filling of the aneurysm, and filling of the superior cerebellar artery. The patient recovered fully. (d) Same as "a",

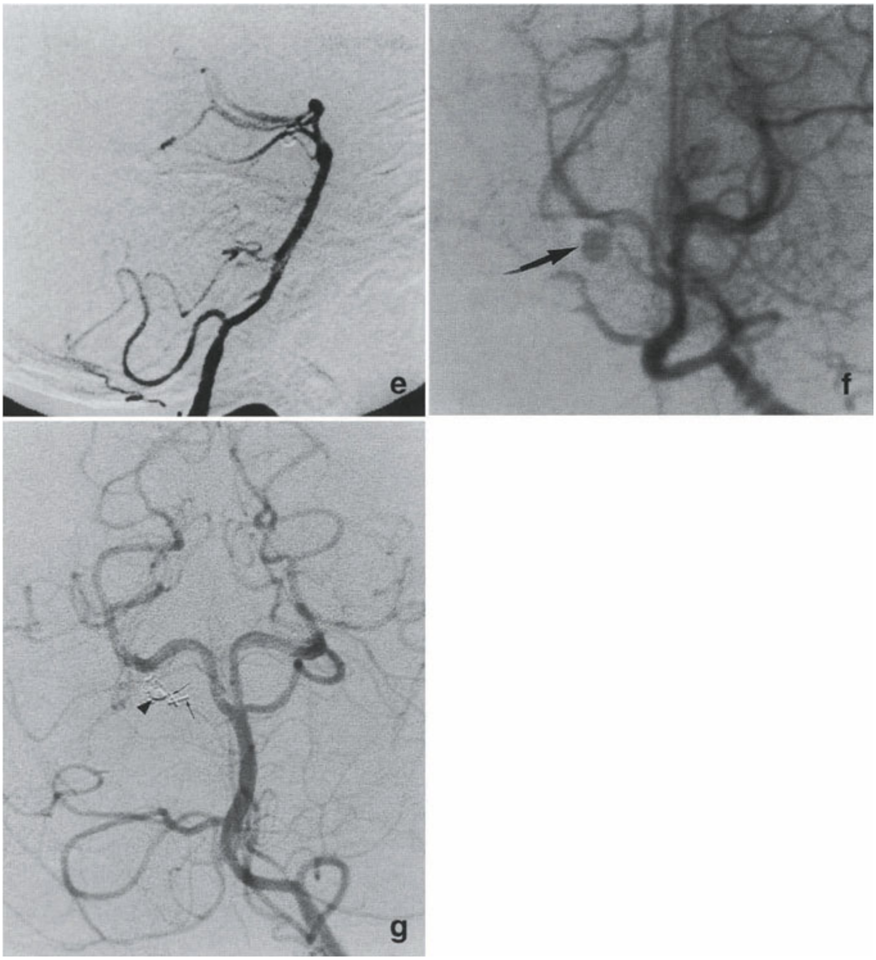

Fig. 6 (e–g)

lateral view. (e) Same as "c", lateral view. (f) As foreseable, the six month follow-up angiogram showed that the aneurysm had re-expanded (arrow). (g) Two GDC-10 "CRESCENT" (6 mm in length—see text) were therefore detached into the superior cerebellar artery, proximal to the aneurysm (two small arrows) occluding the artery. The angiogram shows complete exclusion of the aneurysm. The distal superior cerebellar artery territory fills via collaterals. The procedure was uneventful. Arrowhead points at GDCs utilized in the first session

Aggressive treatment of symptomatic vasospasm should be performed only after the aneurysm is treated, and includes the so-called triple H therapy (Hypertension, Hypervolemia, Hemodilution), transluminal angioplasty (Fig. 6), and intra-arterial papaverine injection. The presence of vasospasm does not contraindicate the endovascular treatment of aneurysms with the GDC system. In a recent study on 69 patients presenting with a grade I to III SAH, and treated with GDCs within the first 72 hours post-hemorrhage, Murayama [52] demonstrated a 23% incidence of symptomatic vasospasm (16 out of 69 patients). Twelve of these 16 patients were in excellent or good clinical condition at the six month follow-up. The overall outcome in these 69 patients was excellent in 79%, good in 8%, fair in 6%, poor in 4%, and death in 3% (2 cases).

Beyond the scope of this chapter are other possible complications post-SAH such as hydrocephalus, cerebral edema, hyponatremia, pulmonary complications, hepatic dysfunction, deep venous thrombosis, seizures, and cardiac complications.

The neurological condition of patients after an SAH is the most important factor in predicting the final clinical outcome and can be evaluated according to Hunt and Hess grading scale [40].

Grade I—Asymptomatic or minimal headache and slight nuchal rigidity.

Grade II—Moderate to severe headache, nuchal rigidity, no neurological deficit other than cranial nerve palsy.

Grade III—Drowsiness, confusion, or mild focal deficit.

Grade IV—Stupor, moderate to severe hemiparesis, responding to pain but not to voice, possible early decerebrate rigidity.

Grade V—Deep coma, decerebrate rigidity, pupils not reactive to light.

Patients with true incidental or with unruptured aneurysms are classified as Grades 0. The clinical presentation of the patient (grading) does not affect the feasibility of the endovascular treatment of aneurysms, with the GDC system.

It is estimated that approximately two percent of the population will have an intracranial aneurysm; one half of these patients will not become symptomatic. Most of the remaining patients will present with an intracranial bleeding at a rate of 10 cases per 100,000 population per year. Of these, 50% will die and 30% will ultimately have a good outcome with the aneurysm excluded from the blood circulation [76]. Although aneurysms are considered not to be inherited lesions, sporadic instances of a familial incidence of saccular aneurysms have been reported [71]. In 15% to 25% of patients diagnosed with an intracranial aneurysm there may be an additional intracranial aneurysm (multiple aneurysms). Multiple aneurysms may be treated in the same session with the GDC technique (Fig. 7), even if they are in different territories (i.e. anterior and posterior circulation) [47].

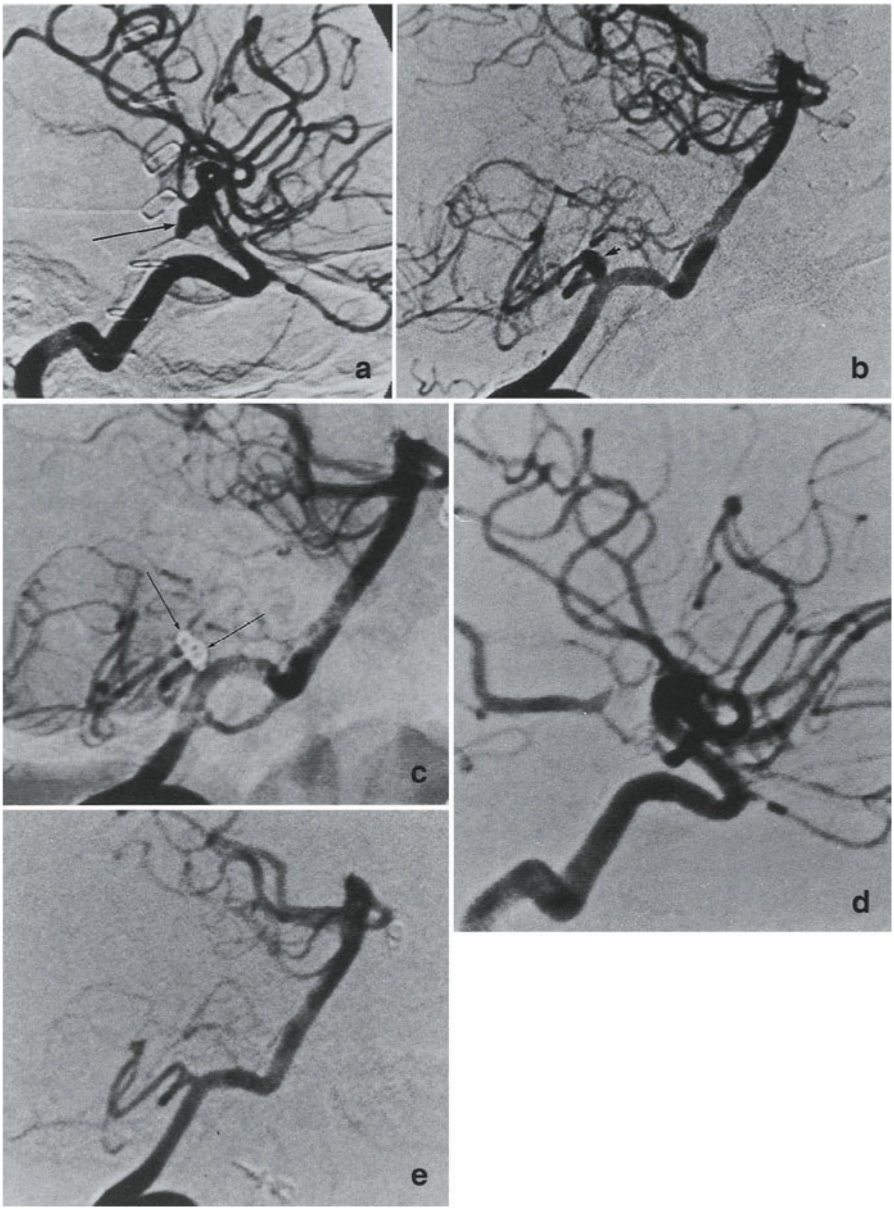

Fig. 7. (a) This 49 year old woman presented with an SAH and the cerebral angiogram showed a posterior communicating artery aneurysm. Surgical clipping failed and she was referred for endovascular treatment. The angiogram shows a small PCom aneurysm, with a broad base (arrow). (b) This angiogram shows an additional aneurysm, located at the origin of the posterior inferior cerebellar artery (arrow). Both aneurysms were treated in the same session with the GDC-10 system. (c) One GDC-10 (4×10) was detached in the PCom aneurysm (not shown). Two GCD-10 (total length 16 cm) were delivered and detached into the PICA aneurysm (arrows). (d) The 18 month follow-up angiogram shows complete occlusion of PCom aneurysm. (e) The 18 month follow-up angiogram shows complete occlusion of the PICA aneurysm. At the four year clinical follow-up the patient was in excellent condition

Age and Sex

The average age at which aneurysms rupture is 52. Fifteen percent of patients presenting with an aneurysmal SAH are 30 years old or younger, and about 10% are 60 or older [61]. Sixty-five percent of patients presenting with an SAH are women [42]. There is, however, a clear prevalence of males having anterior communicating artery aneurysms whereas women have a prevalence of carotid-ophthalmic aneurysms [77].

Indications for Treatment

The primary purpose of treatment of ruptured aneurysms is to prevent the often fatal rebleeding. In untreated ruptured aneurysms, the rebleeding rate is 4% in the first 24 hours, 19% in the first two weeks, and 50% within six months of the first hemorrhage. The second hemorrhage has a 50% mortality rate. Ideally, the aneurysm should be excluded from the blood circulation as soon as possible after the first hemorrhage to avoid a second hemorrhage and to allow aggressive management of the possible post-hemorrhagic vasospasm.

It is estimated that incidental aneurysms bleed at a rate of 1 to 2 percent per year. Surgical or endovascular treatment carries low morbi-mortality rates for incidental aneurysms, and therefore it should be recommended that these aneurysms be treated [76]. It has to be considered, however, that the surgical treatment of posterior circulation aneurysms is objectively difficult and carries higher morbi-mortality rates [41].

The rationale for treatment of aneurysms presenting with symptoms due to compression of surrounding nervous structures (the so called "mass effect") is to avoid persistent or increased mass effect and, perhaps more importantly, to prevent an intracranial hemorrhage.

Endovascular Treatment

A less invasive approach to brain aneurysms, utilizing vessels as natural channels to reach the aneurysm via the endovascular route, would be valuable. Treatment via the endovascular route has the special advantage of avoiding craniotomy, brain retraction, surgical vessel manipulation, possible perforator injury and possible post operative infections. It would also reduce post treatment hospital stay and recovery time. The guiding concept being that aneurysms constitute a vessel disease and that their treatment should ideally involve only blood vessels. The present technology produces soft microcatheters (less than 1 mm in diameter) that allow catheterization of intracranial vessels and arterial aneurysms.

The endovascular treatment of aneurysms may be divided in two broad categories: a) Occlusion (sacrifice) of the arterial axis ("parent vessel") harboring the aneurysm; and b) Occlusion of the aneurysm, with preservation of the parent artery.

Endovascular Aneurysm Treatment with Sacrifice of the Arterial Axis

Permanent occlusion of the parent artery is utilized for the treatment of giant intracavernous carotid aneurysms [5, 13], some high-risk giant supraclinoid carotid aneurysms [14], some high-risk giant or large posterior circulation aneurysms [4], fusiform aneurysms [16], some dissecting aneurysms [37] and pseudo aneurysms. With the patient awake and under systemic heparinization, the parent vessel can be sacrificed after clinical tolerance is tested with a 30 minute temporary balloon occlusion. The arterial axis can then be occluded with coils or detachable balloons. References indicate the largest published series on this subject.

Endovascular Aneurysm Treatment with Preservation of the Parent Artery

In the seventies and eighties the endovascular approach, using inflatable and detachable balloons, had been proposed as a therapeutic alternative in selected cases of intracranial saccular aneurysms, with preservation of the parent artery [12, 38, 59, 68]. Due to the risk of intraprocedural or delayed aneurysm rupture [39], the high procedure-related morbi-mortality rates in acutely ruptured aneurysms, and the high rate of failures, this method of treatment did not become popular and was mainly reserved for highly inoperable lesions.

Recently [1, 3, 8, 9, 17–37, 43, 44, 46–49, 51, 53–56, 58, 66, 67, 69, 70, 72, 74, 75, 78, 79], a new endovascular method with controllable and detachable platinum coils (GDC - Target Therapeutics - Freemont, California) has been developed to provide a less invasive and safer approach to intracranial aneurysms: these coils, used to densely fill the aneurysm, are very soft and less traumatic on the aneurysmal wall. They adopt the aneurysm shape without causing distortion of the fragile wall of the aneurysm. It is also believed that their softness allows them to adapt to the systolic blood pulsation rather than opposing to it. This possible redistribution of the systolic energy on the entire mass of the complex aneurysm-coils could be the factor explaining the difference with other occlusive endovascular devices (namely balloons) that have the characteristic of transmitting, rather than absorbing, the water-hammer effect of the systole. Since their first clinical use in early 1990 [20, 23], GDC coils have been utilized in many neuro-endovascular centers. At the present time, more than 20,000 patients have been treated with this technique worldwide in more than 450 centers.

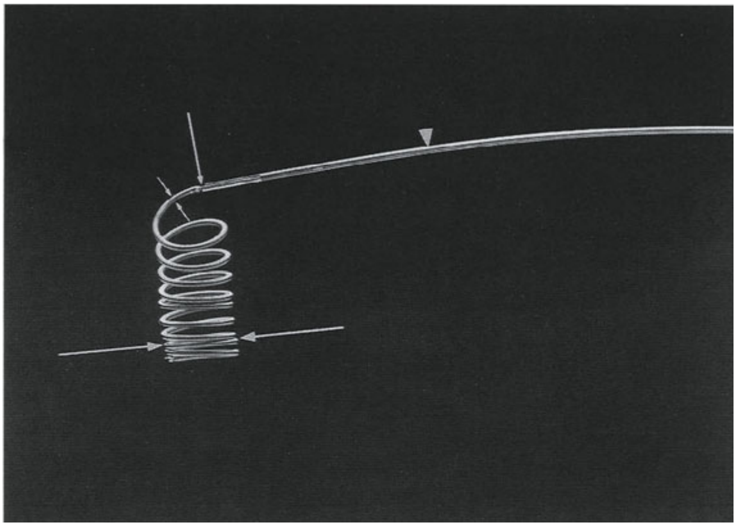

Fig. 8. Photograph of a GDC-10 "3 × 8" (3 mm in circular memory and 8 cm in length, when straightened). Arrowhead points at the stainless steel delivery wire. Single arrow points at the "junction" that undergoes electrolytic breakdown (junction of second GDC generation). The diameter of the platinum coil (0.010 inches - 0.25 mm, between two short arrows), and the GDC circular memory (3 mm, between two long arrows) are illustrated

Description of the GDC

A GDC coil is constituted by a platinum coil soldered to a stainless steel delivery wire (Fig. 8). The platinum coil is utilized to fill the aneurysm, while the delivery wire is used to push the coil into the aneurysm. The platinum portion is deposited and detached in the aneurysm. It is radiopaque and can be clearly distinguished, on fluoroscopy, from the much less radiopaque delivery wire. The platinum portion of a GDC is detached (typically in 1 to 3 minutes) from the delivery wire by electrolysis of the distal part of the delivery wire (Fig. 9). This is achieved by the passage of a 1 mA direct electric current. During passage of the current the intra-aneurysmal platinum is positively charged and this induces the formation of an "electrothrombus" in the aneurysm (vide infra) (Fig. 10).

The platinum portion (coil) of the GDC has to have different physical properties. Depending upon the type of aneurysm to be treated, one will select the appropriate GDC. GDCs have to be soft enough not to rupture the fragile aneurysmal wall and stiff enough not to be taken by the flow and migrate out of the aneurysm. GDCs are effective and safe if their physical properties remain within these two borders. Softness and stiffness

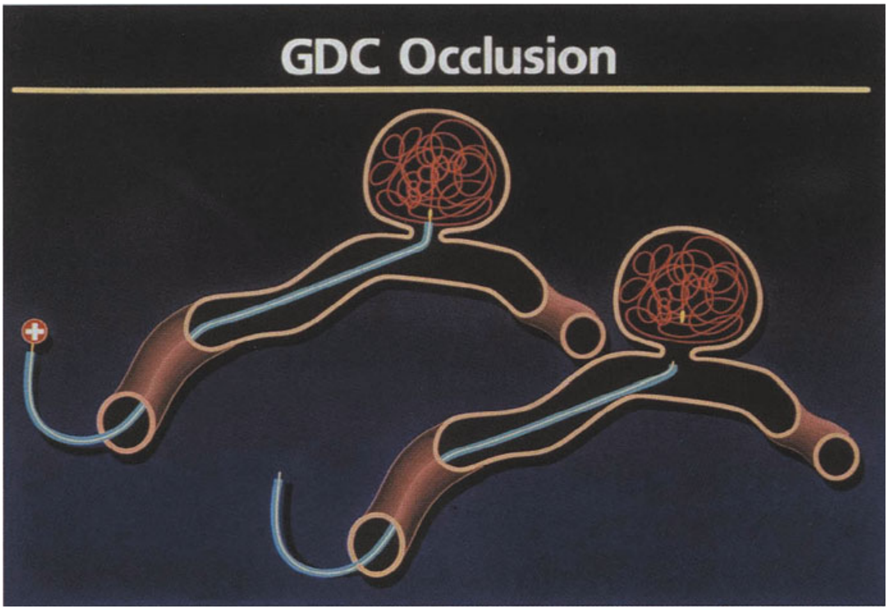

Fig. 9. Diagram showing the electrolytic detachment of the platinum intra-aneurysmal portion of a GDC from the stainless steel delivery wire. Electrolytic detachment is elicited by applying a 1 milliAmpere - 3 Volts direct positive electric current to the proximal end of the delivery wire. Detachment typically occurs in 1 to 3 minutes

have to be balanced in a delicate equilibrium. Every inclination toward excessive softness may lead to coil migration and every inclination toward stiffness leads to possible aneurysm perforation.

There are four physical factors that characterize the platinum portion of a GDC: 1. Circular memory; 2. Diameter of the coil; 3. Diameter of the platinum wire; 4. Length.

1. Circular Memory (Figs. 8 and 11)

All GDCs have a circular memory. This allows the GDC to remain in the aneurysm whereas a straight coil would have the tendency of migrating into the parent vessel. Currently, GDCs have a circular memory variable from 2 to 20 mm (2, 3, 4, 5, 6, 7, 8, 9, 10, 11, 12, 14, 16, 18, and 20 millimeters).

The so called 2D-GDC are now available. Their distal loop has a circular memory smaller than the rest of the coil (Fig. 12). This may allow easier deployment of the first (distal) loop of the first coil into the aneurysm avoiding migration of the tip of the coil into the distal parent artery.

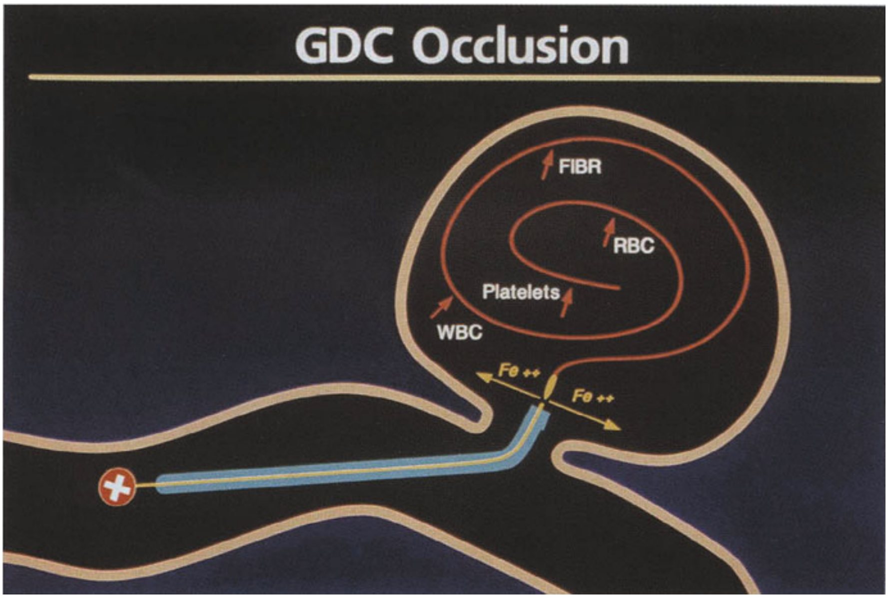

Fig. 10. Diagram representing the effects of electric current in an aneurysm. The positively changed intra-aneurysmal platinums attracts the negatively changed red blood cells (RBC), white blood cells (WBC), platelets, and fibrinogen, thus initiating thrombus formation. At the same time the electric current induces migration of ferrous ions (Fe ++) from the stainless steel, thus dissolving it and detaching the platinum component within the aneurysm

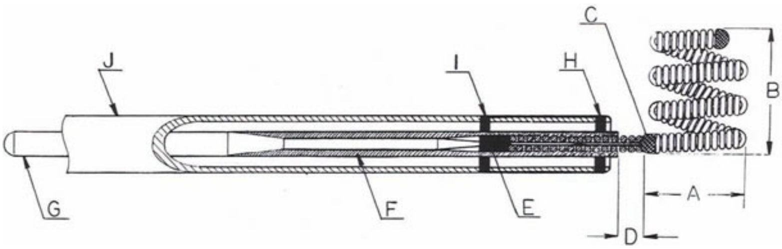

Fig. 11. Diagram of the GDC (first generation) and of the Tracker-GDC. *A* diameter of the circular memory; *B* the distal portion (2–30 cm in length) made of coiled platinum wire; *C* microsolder connecting the platinum coil to the stainless steel delivery wire; *D* uninsulated portion of the stainless steel delivery wire that undergoes electrolytic breakdown; *E* 0.5 cm long platinum radiopaque market on the delivery wire; *F* teflon insulation of the delivery wire; *G* proximal portion of the delivery wire, to be connected with the positive electrode of the GDC power source; *H–I* distal and proximal radiopaque markers on the Tracker-GDC (the distance between these two markers is 3 cm); *J* Tracker-GDC microcatheter

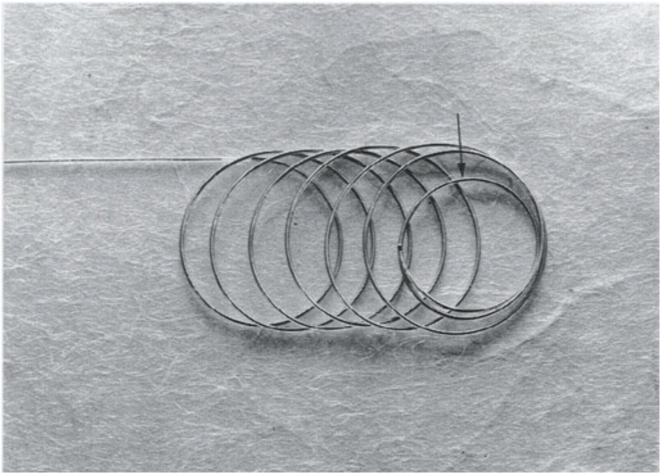

Fig. 12. The Two-Diameters GDC (2D-GDC) is shown. The distal $1\frac{1}{2}$ loops of the platinum coil (arrow) have a circular memory that is 75% of the primary helix. This facilitates the delivery of the tip of the coil inside the aneurysm

2. Diameter of the Coil (Fig. 8)

GDCs-10, GDCs-10 "soft", GDCs-18, and GDCs-118 "soft" are currently available. GDC-10 (and GDCs-10 "soft") have a diameter of 0.010 in. (0.25 mm) (0.0095 in. for the "soft"), are more delicate, are used for small aneurysms, and can be delivered through both Tracker 10 and, with some precautions, Tracker 18 catheters. GDC-18 have a diameter of 0.015 in. (0.375 mm), are less malleable, are used for large and giant aneurysms, and can be delivered through the Tracker 18 only. GDCs-18 "soft" have a diameter of 0.0135 in.

3. Diameter of the Platinum Wire

The platinum wire that constitutes the GDCs may have five different diameters: GDC-10 are constructed with 0.002 in. (0.05 mm) platinum wire; GDCs-10 "soft" with 0.00175 in. platinum (Fig. 13); GDC-18 are constructed with 0.003 in. (0.075 mm) (up to 14 mm in circular memory) or 0.004 in. (0.1 mm) (16, 18, and 20 mm in circular memory) platinum wire. GDCs-18 "soft" have a 0.00225 in. platinum wire. The thinner the platinum wire, the softer the coil (Fig. 13).

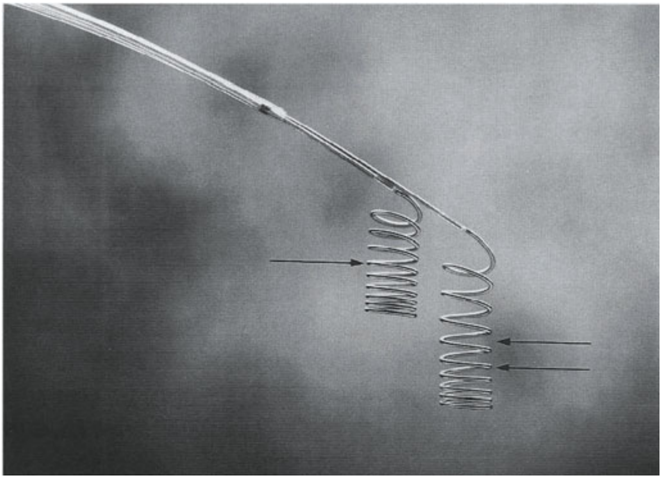

Fig. 13. Comparison between GDC-10 (arrow) and GDC-10 "soft" (two arrows), exposed to the gravitational force. GDC-10 soft are utilized in the treatment of small acute aneurysms to decrease the possibility of intraprocedural aneurysm rupture. GDC-10 soft are 38% softer than the standard GDC-10

4. Length

The length of a GDC, when straightened, is variable from 2 to 30 cm.

Every centimeter of a GDC-10 weighs 5.6 mg. Every centimeter of a GDC-18 weighs 12.6 milligrams. In practice, 180 centimeters of GDC-10 (or 80 centimeters of GDC-18) weighs 1 gram.

In peculiar cases, straight or "CRESCENT shaped", 4 to 10 mm long GDCs may be utilized to occlude distal and small arteries nourishing "peripheral" aneurysms (Fig. 6).

Polarity of the Vessel Wall

In 1953, Sawyer [63, 64, 65] and co-workers reported on a series of experiments in dogs and showed that the intima of a vessel has a constant negative charge (between −3 and −15 milliVolts) when compared to the adventitia. Due to this negative charge, the negatively charged blood components (white and red blood cells, platelets, fibrinogen) are typically repelled from the intima, decreasing the possibility of organization of an intravascular thrombus. If the intima is injured, immediate reversal of the electrical polarity takes place so that it becomes positively charged, attracting the negatively charged blood elements: this phenomenon may play an important role in post-traumatic vascular clotting.

Electrothrombosis

White blood cells, red blood cells, platelets, and fibrinogen are negatively charged. In 1952, Bigelow and De Foyes [6] demonstrated that platelets migrated to the positive pole of an electrophoretic cell. In 1953, Sawyer and Pate [63, 64, 65] used a direct electric current through heparinized blood to precipitate blood components around the anode (positively charged electrode); they were able to assess that these components were red blood cells, white blood cells, platelets, and fibrinogen. To perform this in vitro experiment, they used direct electric current from 2 mA to 10 mA for 30 minutes. With a current of up to 3 mA, the weight of the thrombus was directly proportional to the coulombs (mA x min.) of electricity. These findings demonstrated that a positively charged electrode positioned in the blood will attract these negatively charged components, promoting thrombus formation.

Several authors have performed in vivo experiments in order to confirm the actual occurrence of thrombus formation applying a positive direct electric current to an electrode positioned inside the lumen of a vessel. In 1961, Salazar [62] was able to completely occlude the coronary arteries in dogs by applying an intravascular electric current (0.5 mA) for two hours. In 1965, Araki [2] studied electrical thrombosis using both internal (positive) and external (negative) electrodes with 3 mA direct electric current for 1 hour. They showed that using this technique, a thrombus could be formed in the carotid artery of dogs in 90% of cases. Thrombus formation was reduced if the artery was infused with heparin. Thompson, in 1977 [73] elicited electrothrombosis of the aorta, femoral artery, and common carotid artery in rabbits by applying an electric current (10 mA, 9V) to a platinum or stainless steel endovascular electrode (anode).

Based upon the *in vitro* and *in vivo* experiments described above, it is possible to say that: 1) if a positive direct electric current is applied within a vessel, a thrombus will precipitate on the positive electrode (anode); 2) the size and weight of thrombus is directly proportional to the coulombs (mA x minutes) of electricity delivered; and 3) platinum appears to produce the largest clots and is not affected by electrolysis.

Chen, in 1994 [10], performed a series of *in vitro* experiments on heparinized blood (one unit of heparin per ml of blood) of swine. He confirmed (unpublished data) that the weight of the "electrothrombus" is directly proportional to current and time. He also measured the weight of the thrombus for different values of current and time. This is the result of the study. Three minutes—1mA: 10 mg thrombus; 3 minutes—2mA: 12 mg thrombus; 3 minutes—3mA: 26 mg thrombus; 3 minutes—10 mA: 85 mg thrombus.

Tenjin, in 1995 [72], published the results of treatment with GDCs of experimental aneurysms in monkeys. The standard 1 mA current was utilized. He examined the surface of the platinum coil with scanning electron microscopy one hour after the treatment. The surface of the coil was covered with a thin layer of leukocyte, fibrinlike material, and other proteins.

These two recent experimental studies, and the studies of previous investigators, suggest that with the electric current presently utilized (1 mA) only minimal electrothrombus is formed. Electric current increase (up to 5 mA) might allow increased intraaneurysmal thrombus formation with no side effects.

Electrolysis

Nearly 200 years ago it was found that water breaks down into hydrogen and oxygen when an electric current is passed through it. This was discovered after the scientist Alessandro Volta made the first electric battery capable of producing continuous current. When wires were connected to both terminals of a battery and their ends were dipped into a tank of water to act as electrodes, it was found that gas bubbles formed in the water at each electrode. It was also found that hydrogen gas was given off at the negative electrode and oxygen gas was given off at the positive electrode. It was then discovered that some of water had been decomposed into its elements. This process was called electrolysis.

Electrolysis also occurs when two iron electrodes connected to a source of direct electric current are dipped into a solution. Under these conditions, the immersed end of the positive wire dissolves, and the other wire recruits the migrating ferrous ions from the anode to the cathode. Electrolysis is the process by which GDCs are detached from the stainless steel (iron) delivery wire. Noble metals such as platinum are not affected by this phenomenon.

Miller [50] utilized 5 to 10 mA direct electric current to produce a thrombus in the citrated blood of dogs; stainless steel or platinum were constituents of the electrodes. They proved that platinum is three to four times more thrombogenic than stainless steel, that stainless steel dissolves during the passage of current by electrolysis, and that there is no difference in the size of the clot if the diameter of the platinum electrode is changed from 0.25 to 0.9 mm.

Piton [57] tested various metals in normal saline. This included silver, copper, platinum and stainless steel electrodes, all 0.5 mm. in diameter. They applied 10 mA direct electric current to these electrodes and showed that the silver electrode underwent electrolysis in 22 minutes and stainless steel electrode in 12 minutes; the copper electrode was rapidly affected by oxidation and the platinum was not electrolyzed.

Aneurysm Treatment with the GDC Technique: Patient Preparation

General anesthesia with intubation should be utilized for patients that are uncooperative or for small aneurysms (requiring high quality motionless road mapping). To accomplish precise aneurysm catheterization without touching the aneurysmal wall and to manage possible intraprocedural complications, general anesthesia must be utilized in the treatment of small aneurysms in the acute phase of SAH. Neuroleptic analgesia may be utilized in cooperative patients with large or giant unruptured lesions. To prevent thromboembolic complications, in the subacute-chronic phase post-SAH or in unruptured aneurysms a bolus of 3,000 units of heparin I.V. is administered at the beginning of the procedure, as soon as the femoral introducer is in the femoral artery. This is followed by 1,000 units of heparin I.V. every following hour. Heparin (5,000 units/lt) is always used in the pressurized solutions of saline that are utilized to continuously flush the catheters. In recently ruptured aneurysms, heparin is only used in the flushing solutions. In acute aneurysms, systemic heparinization may be instituted, during the treatment and after the detachment of the first coils, as soon as the "bleeding site" of the aneurysm is no longer seen on the angiogram. The additional coils can be added to fill the center of the aneurysm.

Principles of Treatment

The GDC technique includes various steps. The tip of a Tracker microcatheter is positioned into the aneurysm with the aid of a micro guidewire (Fig. 14). Through the microcatheter, the platinum portion of a GDC coil is introduced into the aneurysm while still soldered to the stainless steel delivery wire. In the microcatheter the coil assumes a straight configuration. As soon as it exits the tip of the microcatheter the coil folds on itself with a predetermined circular memory. If there is any coil deposit into the parent vessel, the coil may be withdrawn and repositioned into the aneurysm. The platinum portion of the GDC coil is radiopaque and this allows fluoroscopic visualization while it is being positioned within the aneurysm. The platinum coil is very soft and will adapt to the size and shape of the aneurysm with a minimal increase in intraluminal pressure. When the detachable platinum coil is seen to be in proper position inside the aneurysm, a 1 mA direct electric current is applied to the proximal end of the delivery wire. The negative ground electrode is connected to the skin of the groin or of the shoulder using an hypodermic needle or a conductive pad. The positively charged intra-aneurysmal platinum attracts the negatively charged blood elements (white and red blood cells, platelets, and fibrinogen). At the same time the current dissolves the stainless steel delivery wire proximal to the solder between platinum and stainless steel, by electrolysis. These phenomena typically occur in one to three minutes, detaching the platinum coil inside the aneurysm. The platinum coil becomes a dense mesh that holds the thrombus decreasing the possibility of its displacement into the parent artery and into the distal vascular tree. Additional GDC coils will be detached into the aneurysm to completely, and densely, fill its sac and neck (Fig. 14).

Aneurysm Treatment

A 6 French femoral artery sheath allows placement of a 6 French, thin walled, soft tip, non-tapered guiding catheter into the internal carotid or vertebral artery (Cordis Envoy, or Target FasGuide). For small posterior circulation aneurysms, a 5 French guiding catheter may be used. The guiding catheter must be continuously flushed with heparinized and pressurized saline utilizing a side-arm adapter. The guidewire is introduced through the valve of this side-arm adapter so to maintain continuous flushing when entering the carotid or vertebral artery with the guiding catheter. This helps preventing thromboembolic complications.

Gentle, hand-injection of contrast should be utilized, rather than pump injection, when performing angiograms in patients having intracranial aneurysms. This helps prevent aneurysm rupture during the angiogram.

A diagnostic angiogram is performed through the guiding catheter in order to obtain the best view of the aneurysm sac and neck, well separated from the parent vessel. At times, multiple attempts will be required to find this "working projection" (Fig. 2). If this working projection cannot be identified, the procedure should be aborted. There are no standard projections that can be suggested for every particular kind of aneurysm since every aneurysm is different and, perhaps, the correct projection has to be "invented" every time. The experience of the operator plays an important role here. There are, however, some general principles. Anterior communicating artery aneurysms and basilar bifurcation aneurysms should be treated in antero-posterior (AP) view, in order to have full control of the

Fig. 14. (a) The vertebral artery angiogram shows a small (4 mm) basilar bifurcation aneurysm (long arrow) with a small neck. The radiopaque tip of the microcatheter (Tracker-10 GDC) is in the aneurysm (short arrow), too close to the aneurysmal wall. Ideally, the tip should be in the center of the aneurysm. (b) Plain X-Ray film showing the first coil in place. This first coil is a GDC-10 (4 mm in circular memory and 6 cm in length). Several loops of the coil cross the area of the neck of the aneurysm (good predicting factor of complete aneurysm occlusion with additional smaller GDCs). (c) Two more smaller GDCs (3×6 soft and 2×6 soft) were utilized to fill the center of the aneurysm, within the first coil. Complete occlusion of the aneurysm

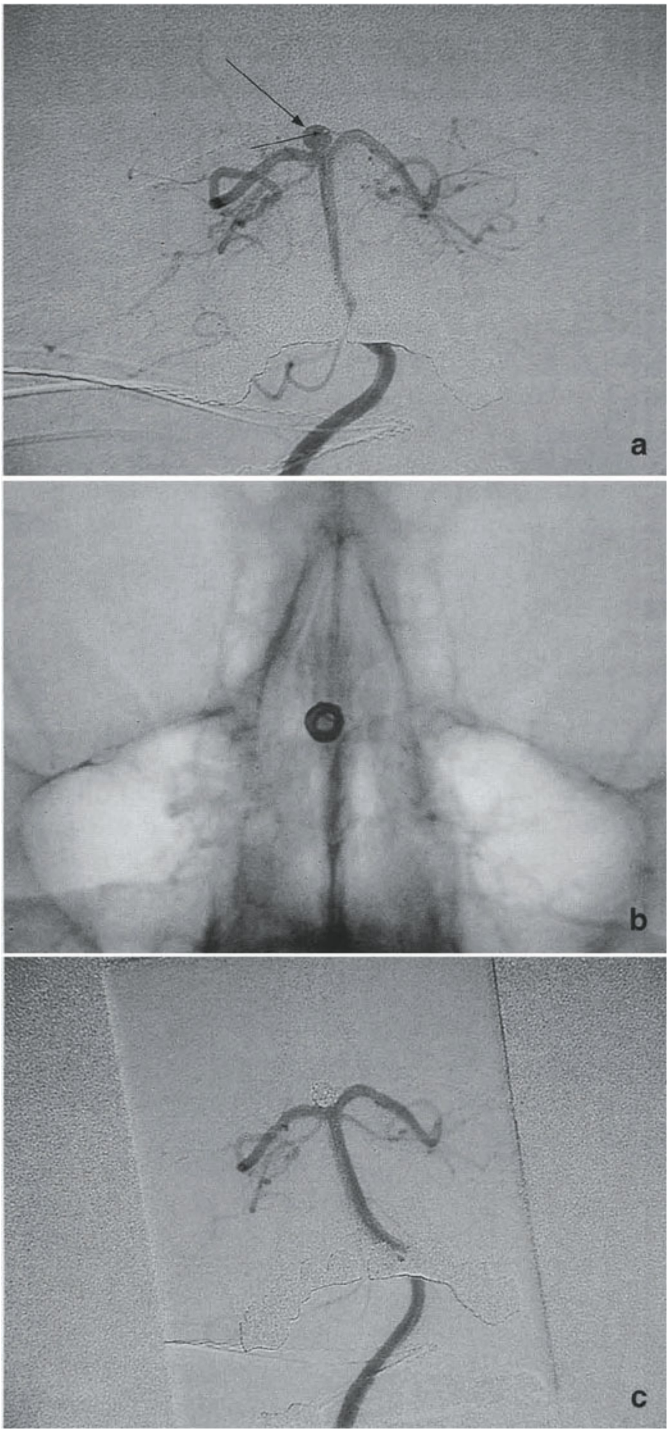
a
b
c

area of the aneurysm neck and not to deposit any coil in the parent vessel. The correct cranio-caudal incidence of the AP X-ray tube, however, has to be determined evaluating the lateral view, so that the AP incidence is perpendicular to the axis of the neck of the aneurysm. Carotid-ophthalmic, para-ophthalmic, and middle cerebral artery aneurysms often require complex oblique views using either the lateral or the AP X-ray tube.

A road map is then obtained in order to perform a safe catheterization of the aneurysm and to deliver the first coil avoiding any deposit into the parent vessel. Subsequent coils will be delivered using regular fluoroscopy: the first coil, in fact, constitutes a landmark delineating the border aneurysm-parent artery.

Through the guiding catheter, a Tracker 10 microcatheter with two markers or a Tracker 18 microcatheter with two markers is navigated into the brain vascular channels. The (softer) Tracker 10 is always used in small and in acute aneurysms. The Tracker 18 is used for unruptured large or giant aneurysms. The tip of the microcatheter has to be steam-shaped to conform it to the anatomical configuration of the aneurysm-parent vessel complex. This step is a very important one in that, if correctly performed, it prevents possible kinking of the microcatheter and makes the aneurysm catheterization easy, fast, and atraumatic. Paraophthalmic aneurysms are those that require the highest complexity of this distal curve. Here again operator experience plays a role. Curvature of the microcatheter tip is often not necessary for basilar bifurcation, ICA bifurcation aneurysms, and for all aneurysms originating in the same direction (axis) of the parent artery. A guidewire such as Seeker 10 or Seeker 14 is used in combination with the Tracker 10 or 18, respectively. During the catheterization maneuvers, the tip of both the Tracker and the guidewire should not touch the wall of the aneurysm. When the guidewire is withdrawn, forward movement of the microcatheter can be expected and prevented. In cases of tortuous vasculature, and in elderly patients, the Fastracker 10 or 18 with two markers are now available. The outer hydrophilic layer reduces the friction between the catheter and the inner arterial wall, allowing more distal catheterization. Sudden forward movements of the Fastracker can be expected and therefore great care should be paid when maneuvering this catheter in proximity of the aneurysm. Backward movement of this catheter can also be expected when delivering the GDC into the aneurysm.

Once the tip of the Tracker is inside the aneurysm, a controlled (1 drop every 5 seconds), pressurized heparinized continuous flush is connected to the Tracker hub via a side-arm adapter, in order to prevent the blood from flowing back into the microcatheter. This reduces the friction when advancing the GDC (blood is more viscous than saline). Intra-aneurysmal angiograms should be avoided, with the exception of peculiar cases, mostly aneurysms in which the saccular or fusiform nature has to be determined

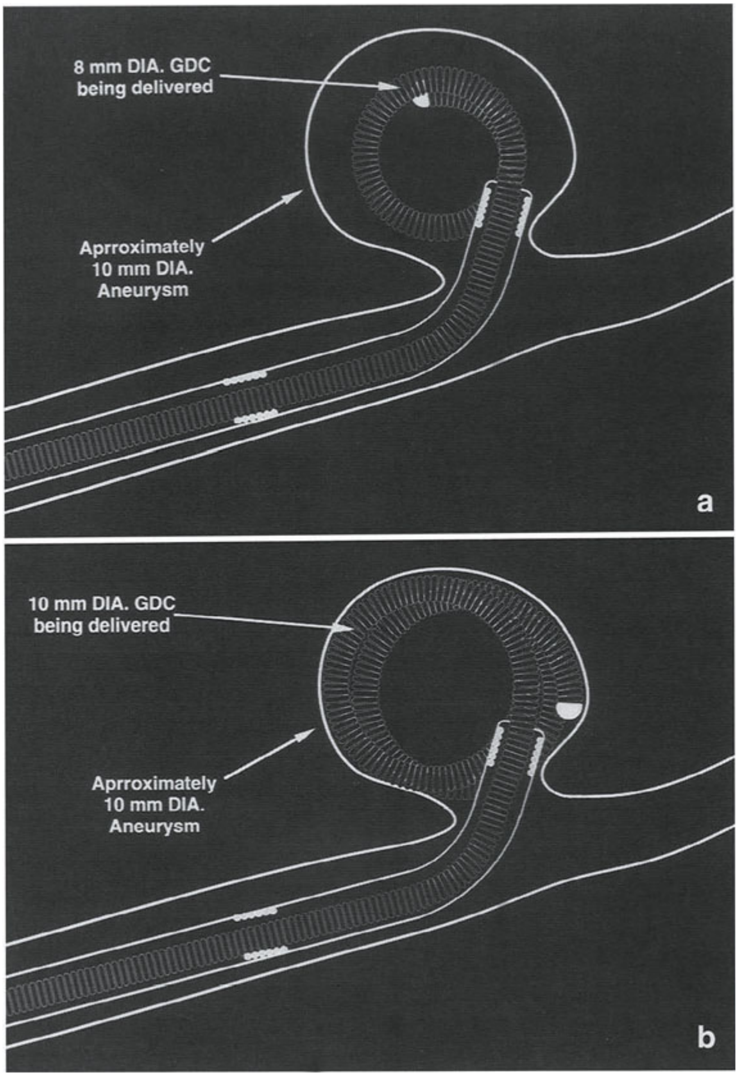

Fig. 15. (a) Drawing representing wrong selection of the first GDC. If this 8 mm coil is detached in a 10 mm aneurysm, an aneurysm neck remnant may remain at the end of the procedure. (b) Correct selection of the size of the first coil. With several loops of the first coil crossing the area of the neck of the aneurysm it is possible to predict a complete aneurysm occlusion

(Fig. 2). A first GDC coil is delivered through the microcatheter. This first GDC coil should have the largest possible circular memory for that given aneurysm (Figs. 14–15), in order to cross the neck area with several loops and to form an intra-aneurysmal "basket" (Figs. 14–15). Subsequent, progressively smaller GDC coils are delivered to fill the center of the aneurysmal sac within the basket formed by the first coil (Fig. 18).

As already mentioned, there are two main versions of GDCs, GDCs-10 and GDCs-18 (Figs. 16–17). Both kinds can be delivered through the Tracker 18 microcatheter. However, only short GDC-10 should be utilized with the Tracker 18. The GDCs-18 can be delivered only through the Tracker 18 microcatheter. The GDCs-18 are heavier and less malleable than the GDC-10. Currently, there are 50 types of GDC (Figs. 16–17). The first number is the diameter of the circular memory in millimeters; the second number is the length of the coil (in centimeters) when straightened. *GDC-10*: 2 × 2 soft, 2 × 3 soft, 2 × 4, 2 × 4 soft, 2 × 6 soft, 2 × 8, 2 × 8 soft, 3 × 3 soft, 3 × 4, 3 × 4 soft, 3 × 6, 3 × 6 soft, 3 × 8, 3 × 8 soft, 3 × 10 soft, 3 × 12, 4 × 6, 4 × 10, 5 × 10, 5 × 15, 6 × 10, 6 × 20, 7 × 10, 7 × 30, 8 × 10, 8 × 20, 8 × 30, 9 × 15, 9 × 30, 10 × 30. *GDC-18*: 2 × 4 soft, 2 × 8 soft, 3 × 4 soft, 3 × 8 soft, 4 × 6 soft, 4 × 10 soft, 5 × 15, 5 × 20, 6 × 20, 7 × 30, 8 × 20, 8 × 30, 9 × 15, 9 × 30, 10 × 30. 12 × 30, 14 × 30, 16 × 30, 18 × 30, 20 × 30.

If there is any deposit in the parent vessel or if the first coil has a too small, or too large, circular memory, the GDC may be partially withdrawn and repositioned or exchanged for a different sized one. The manoeuvre of coil withdrawal is a delicate one and should be avoided if possible. In fact the coil may become stretched into the microcatheter and this could lead to further technical difficulties. This is more likely to occur with the softer and more malleable GDC-10. It is recommended to release the tension of the microcatheter (that is pulling it in the aneurysm neck area) before the manoeuvre of coil withdrawal is initiated. This manoeuvre is then performed slowly and intermittently to allow the axial pulling force to be transmitted progressively to the entire coil without eliciting the stretching mechanism.

Once the coil is considered properly positioned, electrothrombosis and electrolytic coil detachment are elicited by applying a 1 mA direct electric current.

Proper pre-detachment positioning is insured by two markers (Fig. 18). The function of the two markers is explained as follows: The GDC coil has a 0.5 cm long radiopaque marker (made of platinum). It is positioned in the stainless steel delivery wire 3 cm proximal to the platinum-stainless steel junction. Another radiopaque platinum marker, 3 cm proximal to the tip, is on the special Tracker microcatheter. These markers, on both the coil and the microcatheter have been added with the purpose of increasing the safety of the procedure. After detachment of the first coil, it is difficult to visualize the platinum-stainless steel junction of the second and subsequent coils within the intra-aneurysmal coil mesh. The proximal radiopaque markers (in the parent vessel and outside the aneurysm) allow pre-

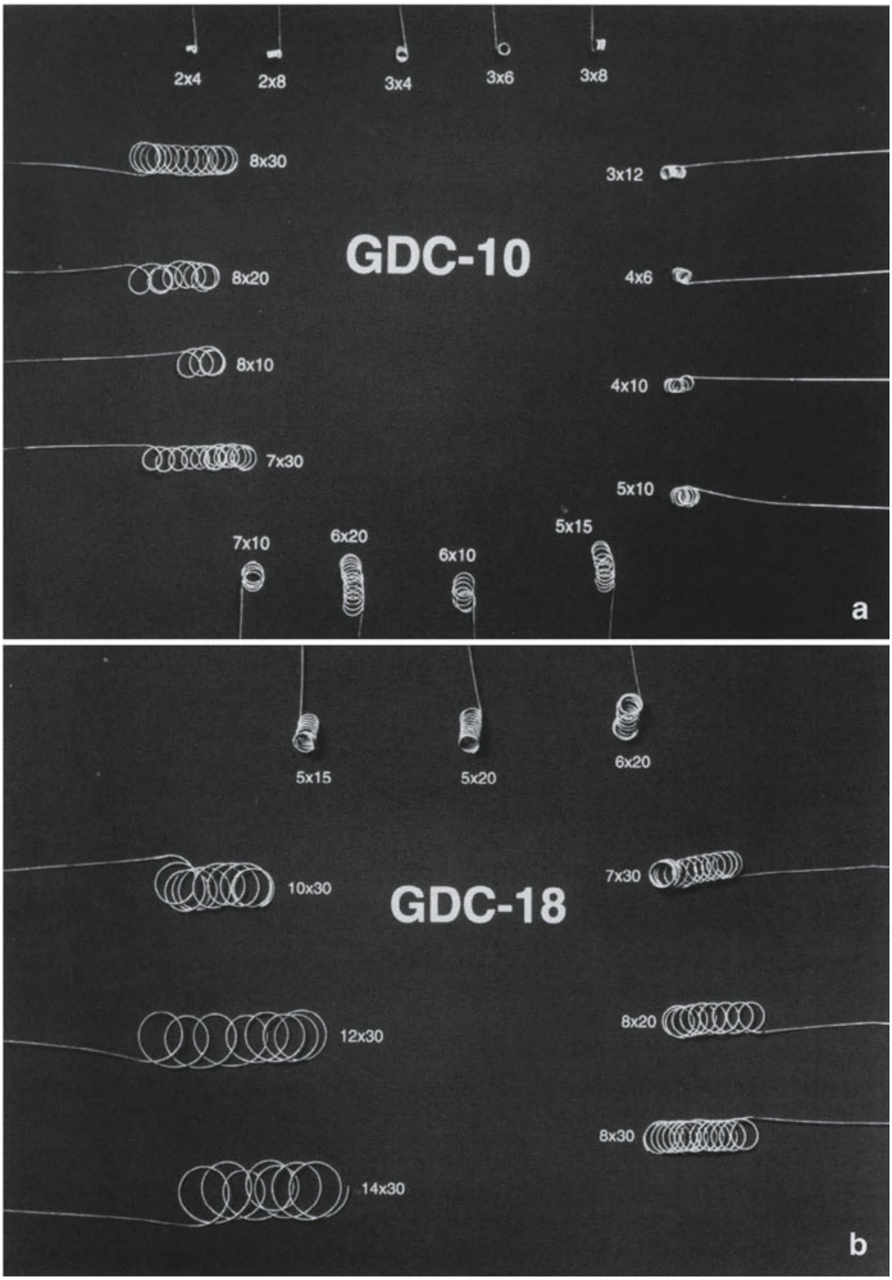

Fig. 16. (a) Photograph showing some of the different types of GDCs-10. The first number is the diameter of the circular memory in millimeters. The second number is the length of the platinum coil, if straightened, in centimeters. (b) Same, for the GDCs-18

GDC®-10
Guglielmi Detachable Coil

Sizing Chart

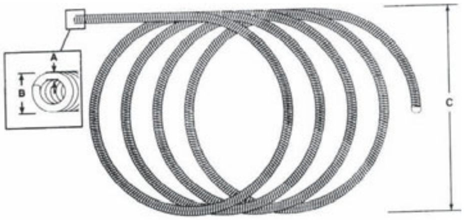

GDC-10 Part Number	Platinum Core Wire Diameter (A)	GDC Primary Coil Diameter (B)	GDC Helical Diameter (C)	Overall Length
341202 *soft*	0.00175"	0.0095"	2mm	2cm
341203 *soft*	0.00175"	0.0095"	2mm	3cm
341204 *soft*	0.00175"	0.0095"	2mm	4cm
341206 *soft*	0.00175"	0.0095"	2mm	6cm
341208 *soft*	0.00175"	0.0095"	2mm	8cm
341303 *soft*	0.00175"	0.0095"	3mm	3cm
341304 *soft*	0.00175"	0.0095"	3mm	4cm
341306 *soft*	0.00175"	0.0095"	3mm	6cm
341308 *soft*	0.00175"	0.0095"	3mm	8cm
341310 *soft*	0.00175"	0.0095"	3mm	10cm
340204	0.002"	0.010"	2mm	4cm
340208	0.002"	0.010"	2mm	8cm
340304	0.002"	0.010"	3mm	4cm
340306	0.002"	0.010"	3mm	6cm
340308	0.002"	0.010"	3mm	8cm
340312	0.002"	0.010"	3mm	12cm
340406	0.002"	0.010"	4mm	6cm
340410	0.002"	0.010"	4mm	10cm
340510	0.002"	0.010"	5mm	10cm
340515	0.002"	0.010"	5mm	15cm
340610	0.002"	0.010"	6mm	10cm
340620	0.002"	0.010"	6mm	20cm
340710	0.002"	0.010"	7mm	10cm
340730	0.002"	0.010"	7mm	30cm
340810	0.002"	0.010"	8mm	10cm
340820	0.002"	0.010"	8mm	20cm
340830	0.002"	0.010"	8mm	30cm
340915	0.002"	0.010"	9mm	15cm
340930	0.002"	0.010"	9mm	30cm
340103	0.002"	0.010"	10mm	30cm

Target Therapeutics • 47201 Lakeview Blvd., Fremont, California, 94538 • 800-345-2498

Fig. 17. (a) List of the GDC-10 currently available. GDC-2D and GDC-10 "Comma" (see text and Figs. 6g and 12) are not listed. (b) Same, for GDCs-18

GDC®-18
Guglielmi Detachable Coil

Sizing Chart

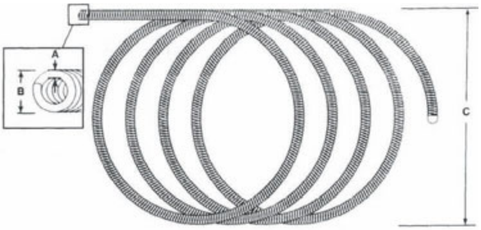

GDC-18 Part Number	Platinum Core Wire Diameter (A)	GDC Primary Coil Diameter (B)	GDC Helical Diameter (C)	Overall Length
351204 *soft*	0.00225"	0.0135"	2mm	4cm
351208 *soft*	0.00225"	0.0135"	2mm	8cm
351304 *soft*	0.00225"	0.0135"	3mm	4cm
351308 *soft*	0.00225"	0.0135"	3mm	8cm
351406 *soft*	0.00225"	0.0135"	4mm	6cm
351410 *soft*	0.00225"	0.0135"	4mm	10cm
350515	0.003"	0.015"	5mm	15cm
350520	0.003"	0.015"	5mm	20cm
350620	0.003"	0.015"	6mm	20cm
350730	0.003"	0.015"	7mm	30cm
350820	0.003"	0.015"	8mm	20cm
350830	0.003"	0.015"	8mm	30cm
350915	0.003"	0.015"	9mm	15cm
350930	0.003"	0.015"	9mm	30cm
350103	0.003"	0.015"	10mm	30cm
350123	0.003"	0.015"	12mm	30cm
350143	0.003"	0.015"	14mm	30cm
350163	0.004"	0.015"	16mm	30cm
350183	0.004"	0.015"	18mm	30cm
350203	0.004"	0.015"	20mm	30cm

TARGET
THERAPEUTICS®

Target Therapeutics • 47201 Lakeview Blvd., Fremont, California, 94538 • 800-345-2498

Fig. 17 (*continued*)

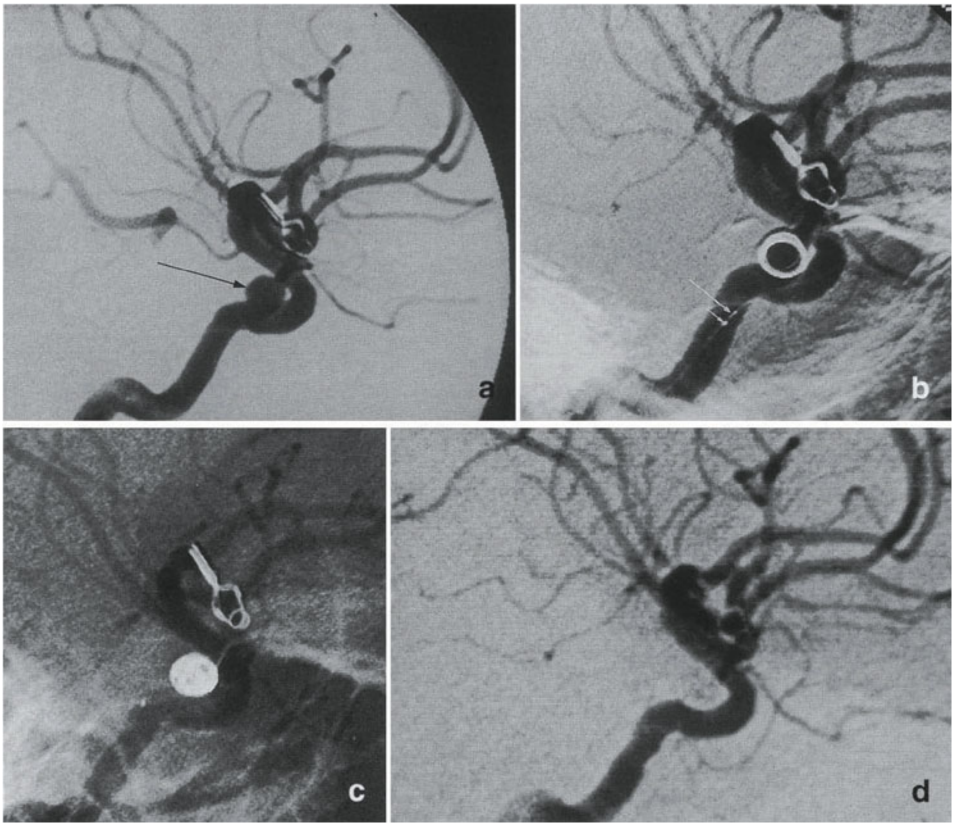

Fig. 18. (a) Internal carotid artery angiogram showing a small superior hypophyseal aneurysm (arrow) with a small neck. A surgical clip on a previously treated anterior communicating aneurysm is also visible. (b) Pre-detachment angiogram: the first coil is ready to be electrolytically detached. Proper positioning is ensured by the two markers, one on the microcatheter (short arrow) and one on the GDC delivery wire (long arrow). See also text. (c) Subsequent coils were utilized to densely fill the center of the aneurysm. (d) Final angiogram showing complete aneurysm occlusion

cise placement of the junction within the aneurysm even if the actual junction cannot be visualized. It is imperative that the junction emerges from the microcatheter for no more that 2 mm. Because of its relative stiffness, the stainless steel portion could potentially perforate the aneurysm if advanced too far. Alignment of the proximal radiopaque markers on the microcatheter and the GDC (in the parent artery) assures that the junction is no more than 2 mm beyond the microcatheter tip. Subsequent, progressively smaller, GDCs are delivered and detached to fill the center of the aneurysm, within the basket formed by the first coil.

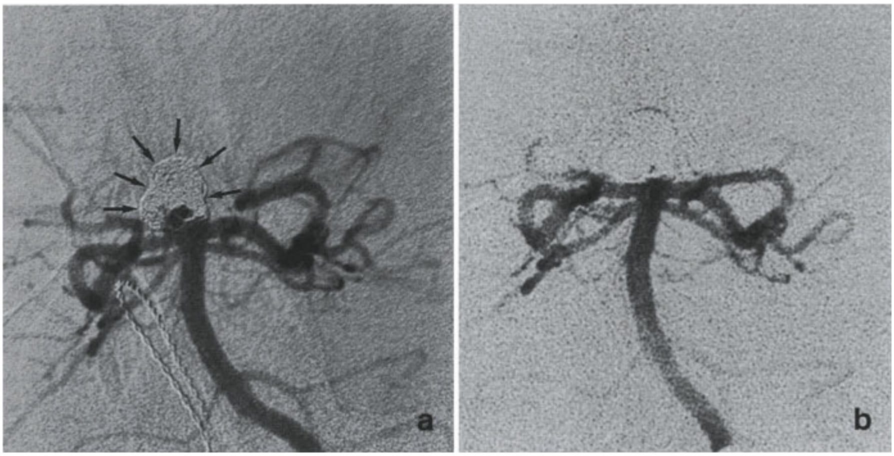

Fig. 19. (a) This 30 year old woman presented with acute SAH from a wide-necked basilar bifurcation aneurysm. Two GDC sessions were performed achieving subtotal aneurysm occlusion (not shown). This $3\frac{1}{2}$ year follow up angiogram show some degree of coil compaction with re-exposure of the base of the aneurysm to the blood flow (arrows point at the perphery of the aneurysm). (b) At the third session, four additional GDCs were detached at the base of the aneurysm. The final angiogram at the end of the third GDC session is shown. The patient is neurologically intact

Once a dense aneurysm packing is achieved (Fig. 18), the procedure is terminated. The Tracker is very slowly removed from the aneurysm. A final post treatment angiogram is performed to assess the degree of aneurysm occlusion and the configuration and patency of the distal vascular tree. Heparin may be reversed with protamine sulfate. In wide-necked aneurysms, and if there is some coil impingement upon the parent vessel, heparin is not reversed and aspirin (325 mg/day for one week) may be administered to reduce the risk of distal embolization.

A strict protocol of follow-up angiograms has to be implemented. Follow-up angiograms are performed usually at three months, twelve months, two years, and four years (Figs. 3, 7, and 19).

Results of Treatment

The degree of aneurysm occlusion varies depending upon many factors. The size of the aneurysm neck appears to be, however, the most important factor in predicting whether an aneurysm can be completely or incompletely occluded. Aneurysms with a small neck (<4 mm) can be completely occluded: a small neck holds the coils in place allowing dense aneurysm packing with little risk of coil migration or impingement upon the parent artery. A dense coil packing is clearly important in the neck area. Bridging with a dense meshwork of coils the neck area is a determinant factor in preventing their compaction toward the body of the aneurysm by the pulsatile blood flow.

It is possible to completely occlude 90% of small-necked aneurysms (Figs. 2, 3, 7, 14, and 18). In the remaining 10% of cases a residual neck is left unoccluded at the end of the procedure.

Wide-necked aneurysms (neck size >4 mm) are more difficult to totally occlude because of the risk of coil herniation in the parent artery. This technical difficulty results in the detachment of fewer coils than necessary. Bridging the entire neck area with a dense meshwork of coils is often impossible. Therefore the large area of the orifice of the aneurysm (neck) exposes the loose coil meshwork to the pulsatile blood flow. This leads to progressive compaction of coils in many cases, particularly in giant lesions. It is possible to completely occlude 15% of these wide-necked aneurysms. In the remaining cases a residual neck is seen at the final angiogram (Fig. 19).

If compaction of coils is seen at follow-up angiogram the aneurysm can be re-treated with GDC (Fig. 19). Surgical clipping, if feasible, or a combined endovascular and surgical approach to exclude the aneurysm from the circulation, can also be performed. In giant lesions, this may be accomplished by endovascular balloon or coil occlusion of the internal carotid artery, with or without an extra-intracranial by pass. If the posterior communicating arteries are normally developed, vertebral artery occlusion with balloons or coils, or surgical clipping of the basilar artery can be performed [35].

Fusiform, dissecting, and pseudoaneurysms can be completely occluded, with sacrifice of the arterial axis [16, 36] (Figs. 4 and 5).

In some cases the aneurysm is "endovascularly explored" with GDC and the decision may be taken not to detach GDC due to their instability, particularly in wide-necked lesions [35].

In some instances the aneurysm cannot be catheterized with the microcatheter. As already mentioned, recent materials such as the new generation of guiding catheters, the hydrophilic Fastracker with two markers, and low-friction micro-guidewires, have clearly reduced the number of aneurysms that cannot be catheterized, especially in elderly patients with tortuous vasculature. Since the introduction of these new materials, the rate of failure of aneurysm catheterization has dropped from 10% to almost 0%.

Appropriate patient selection criteria are part of the learning curve, and may also have an influence on the rate of complications (vide infra) and on the incidence of the need for further treatment after GDC. At UCLA, the number of patients requiring two GDC sessions has droped from 18% in the first 100 patients to 9% in the second 100 patients. The number of patients requiring 3 GDC session has dropped from 8% to 1%.

The number of cases requiring non-GDC additional endovascular or surgical treatment has dropped from 20% in the first 100 patients to 6% in the second 100 patients. The number of giant lesions treated in the first 100 patients was 25, and this number has dropped to 16 in the second 100 patients [45].

Complications

1. Aneurysm Rupture

As well documented in the neurosurgical literature, intracranial aneurysms may acutely rupture during their manipulation [15] at a rate of 15%–20%. This appears to be also the case in the endovascular approach, although at a lower rate. In the first 150 aneurysms treated at this institution, there were six cases of aneurysm rupture during the procedure. All ruptures occurred in small aneurysms. Of these, five were in the acute phase of the SAH, and one was incidental. Four of these six patients were in good Hunt and Hess grading, while two were in grades IV and V. In all six cases it was possible to stop quickly the hemorrhage. One of these patients required subsequent aneurysm clipping, while in the remaining five cases the aneurysm was completely occluded with GDC. The four patients that were originally in grades 0 to III made an excellent recovery, while the two patients in grades IV and V eventually died.

To summarize, the final outcome can be good and it seems related to the pre-existing grade.

To prevent the frightening occurrence of intraprocedural aneurysm rupture, some criteria need to be adopted, particularly in small aneurysms: a) General anesthesia should be utilized; b) Very cautious aneurysm catheterization should be performed; c) The microcatheter should have the correct distal curve in order not to touch the aneurysmal wall; d) It is preferable to position the microcatheter tip in the neck of the aneurysm rather than near the fundus; e) Only GDCs-10 "soft" should be utilized in lesions smaller than 4 mm in diameter. GDC-10 "soft" should also be utilized to fill the center of small aneurysms (4 mm in diameter or more) after the delivery of large, normal GDC-10; f) All the above mentioned steps should be followed, one by one, particularly in small and acutely ruptured aneurysms.

If an aneurysm ruptures during the procedure: a) Heparinization should be reversed immediately with protamine sulphate; b) The aneurysm treatment must be quickly completed by adding more coils; c) A CT should be performed, and, if appropriate, a ventricular drainage may be placed; d) If the aneurysm is not completely occluded with GDC, surgery should be considered.

2. *Aneurysm Rebleeding*

In the first 200 patients treated at this institution, there was one case of aneurysm rebleeding. This was a giant right posterior communicating artery aneurysm that had bled twice before treatment with GDC. Fifty days after treatment the patient re-hemorrhaged. An emergency angiogram showed that the phenomenon of coil compaction, as described above, had occurred, re-exposing the neck and a small part of the body of the aneurysm to the blood flow. In this case, as rarely occurs, the original rupture side was near the neck of the aneurysm. The residual portion was immediately treated with GDC achieving complete occlusion of the aneurysm in two different sessions. Six months, 16 months, and 3 years angiograms confirmed persistent aneurysm occlusion and at the 3 years clinical follow-up the patient has a residual mild left upper extremity weakness.

3. *Aneurysm Bleeding*

In the first 200 patients treated at this institution, a first bleeding (fatal in four cases) occurred in four giant and one large aneurysm, one to two years after partial GDC treatment. These lesions were inoperable (3 cases) or had previously undergone unsuccessful surgical exploration (one giant and one large lesion). Of the four giant lesions, 3 were partially thrombosed, and 2 were fusiform dilatations of the basilar apex, incorporating the posterior cerebral and superior cerebellar arteries.

4. *Thromboembolic Events*

In the first 200 patients treated at this institution, transient, mild clinical worsening (mild mono-hemiparesis, hemianopsia, dysphasia, sensory deficit) was observed in 4% of cases. These symptoms resolved within 24–48 hours and were probably due to micro-thromboembolic events.

Permanent neurological deficit due to thromboembolism occurred in 2% of patients (two cases of hemianopsia, one case of mild hemiparesis, and one case of severe hemiparesis). In 2 of these four cases the source of the embolus was the guiding catheter.

Our current protocol includes the use of systemic heparinization during the procedure. In acute cases, however, heparin is used in the flushing solutions only. Aspirin is also administered for one week if there is contrast stagnation in the network of coils within the neck area. Aspirin, for one year or more, is also prescribed if there is any coil deposit in the parent artery.

Morbid-mortality Rates

The procedure-related permanent morbidity rate is 3%. The procedure-related mortality rate is 1.5% (2 patients that were treated while in Grade IV or V). Considering only patients that were treated in Grades 0–I–II–III, the procedure-related mortality is 0%.

The rate of complications may be influenced by the learning curve of the operators. At UCLA, procedure-related permanent morbidity due to thromboembolic events has dropped from 4% in the first 100 patients to 0% in the second 100 patients. Procedure-related deaths from 2% to 0%. Coil migration from 2% to 0% [45].

Clinical Follow-ups

In April 1990 the first GDC procedure (ever) was performed, in a patient harboring an intracranial aneurysm. At the same institution (UCLA), the 100th patient was treated in February 1994. In early 1996 a campaign of clinical follow-up studies was carried out to assess the mid-term (defined as follow-up greater than two years) clinical status of these first 100 consecutive patients [45]. Follow-up information was obtained either by clinical examination, or from reports of the referring physician or from telephonic conversation with the patient (or patient's relatives).

In seven patients the follow-up is still pending. The average mid-term clinical outcome period in the 93 remaining patients is $3\frac{1}{2}$ years (range: 2 years to $5\frac{1}{2}$ years). According to a modified Glasgow Outcome Scale, patients were included in one of the following categories: excellent (neurologically intact, without any detectable neurologic deficit), good (mild hemiparesis, cranial nerve palsy or other deficit that does not interfere with daily functions or work), fair (significant hemiparesis, aphasia, confusion or other deficit which interferes with daily activities or prevents a return to work), poor (coma or severe neurologic deficit rendering the patient totally dependent upon family or nursing staff), dead. Considering the outcome of neurological deficits preexisting to the procedure, these deficits were classified as improved, unchanged or worsened at the date of clinical follow-up.

Six patients died of unrelated causes (three cases of myocardial infarction, one case of A.I.D.S., one case of marantic endocarditis, and one case of Moya-Moya) prior to reaching two-year survival.

Of nine patients treated in Hunt and Hess grades IV or V, one had a fair outcome, two had a poor outcome, and six died from the consequences of the initial hemorrhage, with no rebleeding.

A total of 18 patients underwent additional treatment after GDC (clipping in 8 cases and parent vessel sacrifice in 10 cases). None of these 18 patients experienced post-GDC hemorrhage in the time period between the

GDC procedure and the non-GDC additional treatment. The mid-term clinical outcome of these 18 patients did not show any significant difference from the outcome of the patients that had GDC as their definitive treatment.

Clinical mid-term outcomes of the remaining 60 patients who had GDCs as their definitive treatment was classified as excellent in 72% (43 cases), good in 13% (8 cases), fair in 5% (3 cases), poor in 2% (1 case), and dead in 8% (5 cases). All five deaths were in patients with giant lesions. The mid-term post-GDC hemorrhage rate is 0% for small aneurysms, 4% (one case) for large aneurysms, and 33% (4 cases) for giant aneurysms.

In 52 patients the neurologic status at admission was unchanged or improved while in 3 cases it was worsened, at the mid-term clinical follow-ups.

The results of this study indicate that, in small and large aneurysms, the GDC system is safe and effective in preventing rebleeding in the mid-term period (2 to 5 1/2 years, average 3 1/2 years). Giant lesions still constitute a formidable challenge and, in this subset of patients, results are less satisfying, although with significant exceptions.

Recent refinements of the GDC technique (new GDC sizes and shapes, new microcatheters, "soft" GDCs, shorter detachment time) are already allowing improvement of results.

The learning curve and the experience of the operator are important factors in determining completeness of treatment, appropriate indication for treatment, and morbi-mortality rates.

Longer-term clinical follow-up studies, on the same group patients, will be necessary to determine the longer-term efficacy of the GDC system.

Further Development of the GDC System

The technique of endovascular occlusion of intracranial aneurysms with the GDC coils was developed during an experimental research begun in January of 1989. A new technique for the surgical construction of experimental lateral saccular aneurysms on the common carotid artery of the swine was developed [29]. This technique involved the end-to-side suturing of an isolated segment of vein to an artery. During a short period of parent artery clamping, an elliptic arteriotomy was fashioned through the open-ended vein graft. The open end of the vein graft was then tied and the clamps were removed to form an aneurysmal vein pouch. The main advantage of this technique lies in the short period necessary for vascular clamping, which prevents severe endothelial injury and prolonged postoperative arterial spasm. Both small-necked aneurysms and wide-necked aneurysms can be created with this technique. This animal model was then used to develop the technique of endovascular occlusion of saccular aneurysms with electrolytically detachable GDC coils.

Although the technique of endovascular occlusion of intracranial aneurysms with GDC coils was first applied in the clinical setting more than 8 years ago (March 6, 1990) [23], experimental research is still ongoing. An in vitro study of electrothrombosis [10] using GDC was recently performed. This research showed that it is actually possible to form a thrombus around a platinum anode and that the weight of the thrombus is directly proportional to the current and the time used. Experiments were also performed to study the relationship of heparin concentration and the amount of thrombus formed by electrothrombosis.

In further investigations, wide-necked lateral aneurysms were surgically created and metallic stents were implanted in the parent artery and across the aneurysm neck. A microcatheter was then introduced into the aneurysm through the stent network. GDC were delivered into the aneurysm sac to produce thrombosis. This technique allowed tight packing of coils, for occlusion of wide-necked aneurysms without danger of coil herniation or migration into the parent artery.

New GDC coils of different sizes, shapes, softness, and new physical structures of the platinum-stainless steel junction are continuously tested and evaluated in the experimental setting. Currently available GDC have a junction of 2nd generation. This junction allows a faster detachment time (2–3 min). Third and 4th generations are being tested in the research setting.

Recent possible improvements of the GDC system are currently being tested in the animal laboratory. It seems that with the electric current presently utilized (1 mA), only a thin layer of proteins is deposited on the surface of the GDC [72]. It is believed that higher currents (up to 5 mA) may enhance electrothrombosis without producing unwanted side effects (vide supra).

A new ground electrode is being investigated as a substitute for the needle electrode currently used at the groin. This electrode is formed by a small conductive adhesive pad to be placed on the skin of the shoulder.

A new version of the power supply (Fig. 20) might determine the correct placement of the platinum-stainless steel junction with an acoustic signal. This would substitute the platinum markers on the Tracker and on the GDC (vide supra), with consequent easier aneurysm treatment. An acoustic signal (already incorporated in the latest version of the GDC power supply) also determines when electrolytic detachment has occurred.

The hydrophilic Fastracker-GDC is now available for easier catheterization of aneurysms. This catheter should be utilized in cases of difficult vascular anatomy (see above).

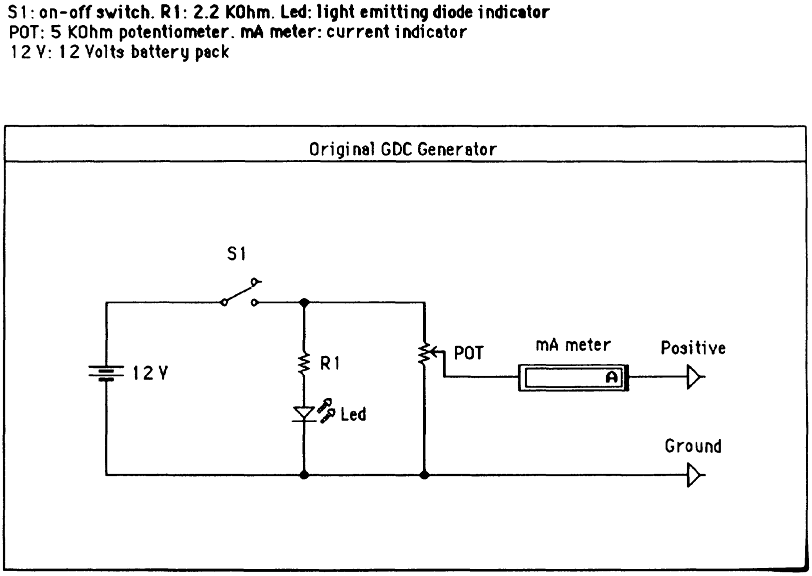

Fig. 20. Schematic of the original power supply, utilized for the experimental development of the GDC technique

A softer version of GDC-10 for small, acute aneurysms is under development and has already been utilized in the clinical setting, with excellent results.

Non-stretchable GDCs, and GDCs with two diameters (2D-GDC) (Fig. 12) are under development: these technical modifications are currently utilized in the clinical setting.

Conclusions

This technique of endovascular occlusion of intracranial aneurysms with GDC coils has been applied, so far, in patients with high surgical risk or inoperable aneurysms. This peculiar population of patients can be divided into two categories: patients that were difficult to treat surgically because of the anatomical configuration of the aneurysm (giant or large, wide-necked aneurysms), and patients with operable lesions (small, narrow-necked aneurysms) but where medical problems or poor grading contraindicated surgery. The best angiographic-anatomical results were obtained in the second category: the size of the neck of the aneurysm is the most important factor for treatment success, using the GDC technique.

The results of immediate and mid term clinical and angiographic follow-up studies indicate that: a) Small-necked aneurysms (neck <4 mm) can be completely occluded. In these cases, follow-up angiograms (up to 5 years) show that the GDC system is capable of permanently occluding small-necked intracranial aneurysms. Clinical follow-ups (up to 6 years) are excellent. b) Wide-necked aneurysms (neck >4 mm) often end up with post-treatment remnants. Follow-up angiograms may show coil compaction inside the aneurysm with re-exposure of portion of the aneurysm to the blood flow. In these cases further GDC treatment and/or a combined approach (endovascular-surgical) should be considered. Unoccluded portions of aneurysms may rupture, particularly in giant, terminal-type aneurysms. Clinical follow-ups (up to 6 years) are promising, considering the particular characteristics of the patient population (posterior circulation, high risk lesions, surgical failures).

Summarizing, small-necked aneurysms appear particularly suited to endovascular GDC treatment. Wide-necked aneurysms should be treated with the GDC technique if surgery carries a high risk.

Continued angiographic and clinical monitoring of the initial group of patients and those of other investigators will help determine the longer-term durability of this technique.

References

1. Ahuja A, Hegenrother R, Strother C, *et al* (1993) Platinum coil coatings to increase thrombogenicity: A preliminary study in rabbits. Am J Neuroradiol 14: 794–798
2. Araki C, Handa H, Yoshida K, *et al* (1996) Electrically induced thrombosis for the treatment of intracranial aneurysms and angiomas. In: deVet AC (ed) Proceedings of the Third International Congress of Neurological Surgery, Copenhagen, 1995. Excerpta Medica, Amsterdam, Vol 110, pp 651–654
3. Apsimon T, Khangure M, Ives J, *et al* (1995) The Guglielmi coil for trans-arterial occlusion of intracranial aneurysm: preliminary Western Australian experience. J Clin Neurosci 2: 26–35
4. Aymard A, Gobin P, Hodes J, *et al* (1991) Endovascular occlusion of vertebral arteries in the treatment of unclippable vertebrobasilar aneurysms. J Neurosurg 74: 393–398
5. Berenstein A, Ransohoff J, Kupersmith M, *et al* (1984) Transvascluar treatment of giant aneurysms of the cavernous carotid and vertebral arteries. Functional investigation and embolization. Surg Neurol 21: 3–12
6. Bigelow FS, De Foyes JF (1953) Cited by Sawyer P, Pate J. Am J Physiol 175: 103–107
7. Black SPW, Leo HL, Carson WL (1988) Recording and measuring the interior features of intracranial aneurysms removed at autopsy: method and initial findings. Neurosurgery 22: 40–43
8. Bradac GB, Riva M, Bergui M (1995) Endovascular coil embolisation of cerebral aneurysms. Riv Neuroradiol 8: 637–644

9. Chaloupka J, Guglielmi G, Vinuela F (1993) Direct thrombosis of aneurysms. Letter to the editor. J Neurosurg 78: 1006–1007
10. Chen H, Guglielmi G, Ji C: Unpublished data
11. Civit T, Auque J, Marchal JC, *et al* (1996) Aneurysm clipping after endovascular treatment with coils: a report of eight patients. Neurosurgery 38: 955–961
12. Debrun G, Lacour P, Caron JP, *et al* (1975) Inflatable and released balloon technique. Experimentation in dog-application in man. Neuroradiology 9: 267–271
13. Debrun G, Fox A, Drake C, *et al* (1981) Giant unclippable aneurysms: treatment with detachable balloons. Am J Neuroradiol 2: 167–173
14. Fox AJ, Vinuela F, Pelz D, *et al* (1987) Use of detachable balloons for proximal artery occlusion in the treatment of unclippable cerebral aneurysms. J Neurosurg 66: 40–46
15. Giannotta S, Oppenheimer J, Levy M, *et al* (1991) Management of intraoperative rupture of aneurysm without hypotension. Neurosurgery 28: 531–535
16. Gobin P, Vinuela F, Gurian J, *et al* (1996) Treatment of large and giant fusiform intracranial aneurysms with Guglielmi detachable coils. J Neurosurg 84: 55–62
17. Graves V, Strother CM, Rappe AH (1993) Treatment of experimental canine carotid aneurysms with platinum coils. Am J Neuroradiol 14: 787–793
18. Graves V, Strother C, Duff T, *et al* (1995) Early treatment of reptured aneurysms with Guglielmi Detachable Coils: Effect on subsequent bleeding. Neurosurgery 37: 640–648
19. Guglielmi G, Viñuela F, Sepetka I, *et al* (1991) Electrothrombosis of saccular aneurysms via endovascular approach. Part 1: Electrochemical basis, technique, and experimental results. J Neurosurg 75: 1–7
20. Guglielmi G, Viñuela F, Dion J, *et al* (1991) Electrothrombosis of saccular aneurysms via endovascular approach. Part 2: Preliminary clinical experience. J Neurosurg 75: 8–14
21. Guglielmi G, Vinuela F (1992) Endosaccular treatment of intracranial saccular aneurysms with GDC platinum detachable coils: Small-necked aneurysms. In: Pasqualin A, Da Pian R (eds) New trends in management of cerebrovascular malformations. Proceedings of the International Conference, Verona, Italy, June 8–12, 1992. Springer, Wien New York, 1994, pp 269–271
22. Guglielmi G, Viñuela F, Duckwiler G, *et al* (1992) Endovascular treatment of posterior circulation aneurysms by electrothrombosis using electrically detachable coils. J Neurosurg 77: 515–524
23. Guglielmi G, Vinuela F, Briganti F, *et al* (1992) Carotid-cavernous fistula due to a ruptured intracavernous aneurysm: endovascular treatment by electrothrombosis with detachable coils. Neurosurgery 31: 591–597
24. Guglielmi G (1992) Embolization of intracranial aneurysms with detachable coils and electrothrombosis. In: Viñuela F, Halbach V, Dion J (eds) Interventional neuroradiology. Raven, New York, pp 63–75
25. Guglielmi G (1992) Endovascular treatment of intracranial aneurysms. In: Viñuela F, Dion J, Duckwiler G (eds) Neuroimaging clinics of North America. Saunders, Philadelphia, pp 269–278

26. Guglielmi G (1992) Endosaccular endovascular treatment of intracranial aneurysms with the Guglielmi detachable coil (GDC) system. In: Takakura K, Sasaki T, (eds) Cerebrovascular surgery. Proceedings of the 3rd International Workshop on Cerebrovascular Surgery, October 17–19, 1992, Tokyo, Japan. pp 90–93
27. Guglielmi G, Vinuela F, Dion J, *et al* (1992) Answer to Hilal SK, Solomon RA: Endovascular treatment of aneurysms with coils. Letter to the editor. J Neurosurg 76: 337–338
28. Guglielmi G (1993) Endovascular treatment of intracranial aneurysm with detachable coils and electrothrombosis. In: Valavanis A (ed) Interventional neuroradiology. Springer, Berlin Heidelberg New York Tokyo, pp 111–122
29. Guglielmi G, Ji C, Massoud T, *et al* (1994) Experimental saccular aneurysms. Part 1: A new model in swine. Neuroradiology 36: 547–550
30. Guglielmi G (1994) Answer to Scotti G, Righi C: The Hypoteloric Happy Face Sign. A misleading indicator of complete aneurysm closure with GDC coils. Am J Neuroradiol 15: 796–797
31. Guglielmi G, Vinuela F (1994) Intracranial aneurysms: Guglielmi electrothrombotic coils. In: Hopkins LN (ed) Neurosurgery clinics of North America. Saunders, Philadelphia, Vol 5, N 3, pp 427–436
32. Guglielmi G, Vinuela F, Duckwiler G, *et al* (1995) High-flow, small hole arteriovenous fistulae: treatment with electrodetachable (GDC) coils. Am J Neuroradiol 16: 325–328
33. Guglielmi G (1995) Answer to Molyneux A, Byrne J, Renowden S: Guglielmi coils in ruptured aneurysms. Am J Neuroradiol 16: 612–613
34. Guglielmi G (1998) Treatment of intracranial berry aneurysms. In: Mawad M (ed) Interventional and therapeutic neuroradiology. Springer, Berlin Heidelberg New York Tokyo (in press)
35. Gurian J, Martin N, King W, *et al* (1995) Neurosurgical management of cerebral aneurysms following unsuccessful or incomplete endovascular embolization. J Neurosurg 83: 843–853
36. Gurian J, Vinuela F, Gobin P, *et al* (1995) Aneurysm rupture after parent vessel sacrifice: Treatment with Guglielmi detachable coil embolization via retrograde catheterization: Case report. Neurosurgery 37: 1216–1221
37. Halbach V, Higashida R, Dowd C, *et al* (1993) Endovascular treatment of vertebral artery dissections and pseudoaneurysms. J Neurosurg 79: 183–191
38. Hieshima GB, Grinnell VS, Mehringer CM (1981) A detachable balloon for transcatheter occlusions. Radiology 138: 227–228
39. Higashida R, Halbach V, Barnwell S, *et al* (1990) Treatment of intracranial aneurysms with preservation of the parent vessel: results of percutaneous balloon embolization in 84 patients. Am J Neuroradiol 11: 633–640
40. Hunt WE, Hess RM (1968) Surgical risk as related to time of intervention in the repair of intracranial aneurysms. J Neurosurg 28: 14–20
41. Khanna RK, Malik GM, Qureshi N (1996) Predicting outcome following surgical treatment of unruptured intracranial aneurysms: a proposed grading system. J Neurosurg 84: 49–54

42. Kongable GL, Lanzino G, Germanson T, *et al* (1996) Gender-related differences in aneurysmal subarachnoid hemorrhage. J Neurosurg 84: 43–48
43. Lylyk P, Vinuela F, Dion J, *et al* (1993) Therapeutic alternatives for vein of Galen vascular malformations. J Neurosurg 78: 438–445
44. McDougall C, Halbach V, Dowd C, *et al* (1996) Endovascular treatment of basilar tip aneurysms using electrolytically detachable coils. J Neurosurg 84: 393–399
45. Malisch T, Guglielmi G, Vinuela F, *et al* (1997) Intracranial aneurysms treated with the Guglielmi detachable coils: Midterm clinical results in 100 consecutive patients. J Neurosurg 87: 176–183
46. Massoud T, Guglielmi G, Vinuela F, *et al* (1994) Saccular aneurysms in Moya Moya disease. Endovascular treatment using electrically detachable coils. Surg Neurol 41: 462–467
47. Massoud T, Guglielmi G, Vinuela F, *et al* (1996) Multiple intracranial aneurysms involving the posterior circulation: Endovascular treatment with electrolytically detachable coils. Am J Neuroradiol 17: 549–554
48. Massoud T, Turjman F, Ji C, *et al* (1995) Endovascular treatment of fusiform aneurysms with stents and coils: Technical feasibility in a swine model. Am J Neuroradiol 16: 1953–1963
49. Mawad M, Mawad J, Cartwright J, *et al* (1995) Long-term histopathologic changes in canine aneurysms embolized with Guglielmi detachable coils. Am J Neuroradiol 16: 7–13
50. Miller MD, Johnsrude IS, Limberakis AJ, *et al* (1978) Clinical use of transcatheter electrocoagulation. Radiology 129: 211–214
51. Molineaux A, Ellison D, Morris J, *et al* (1995) Histological findings in giant aneurysms treated with Guglielmi detachable coils. J Neurosurg 83: 129–132
52. Murayama Y, Malisch T, Guglielmi G, Mawad M, *et al* (1998) Incidence of vasospasm after Guglielmi detachable coil treatment of acutely ruptured aneurysms. Neurosurg 87: 830–835
53. Nichols D (1993) Endovascular treatment of the acutely ruptured intracranial aneurysm. Commentary. J Neurosurg 79: 1–2
54. Nichols D, Meyer F, Piepgras D, *et al* (1994) Endovascular treatment of intracranial aneurysms. Mayo Clinic Proc 69: 272–285
55. Ogilvy C, Choi IS (1996) Guglielmi coils. Letter to the editor. J Neurosurg 84: 302–303
56. Pierot L, Boulin A, Castaings L, *et al* (1966) Selective occlusion of basilar artery aneurysms using controlled detachable coils. Report of 35 cases. Neurosurgery 38: 948–954
57. Piton J, Billerey J, Constant P, *et al* (1996) Selective vascular thrombosis induced by a direct electrical current: Animal experiments. J Neuroradiol 5: 139–152
58. Quintana F, Diez C, Gutierrez A, *et al* (1996) Traumatic aneurysms of the basilar artery. Am Neuroradiol 17: 283–285
59. Romodanov A, Scheglov V (1982) Intravascular occlusion of saccular aneurysms of the cerebral arteries by means of a detachable balloon catheter. In:

Krayenbuhl H (ed) Advances and technical standards in neurosurgery, vol 9. Springer, Wien New York, pp 25–48
60. Rossitti S (1995) Arterial caliber and shear stress. Studies on cerebral and retinal vessels in man. Thesis: Department of Neurosurgery, Institute of Clinical Neuroscience, Goteborg University, Sweden, pp. 7–10
61. Sahs A, Perret G, Locksley H, Nishioka (eds) (1969) Intracranial aneurysms and subarachnoid hemorrhage: a cooperative study. Lippincot, Philadelphia
62. Salazar A (1961) Experimental myocardial infarction. Induction of coronary thrombosis in the intact closed chest dog. Circ Res 9: 1351–1356
63. Sawyer P, Pate J (1953) Bio-electric phenomena as an etiologic factor in intravascular thrombosis. Am J Physiol 175: 103–107
64. Sawyer P, Pate J, Weldon C (1953) Relations of abnormal and injury electric potential differences to intravascular thrombosis. Am J Physiol 175: 108–112
65. Sawyer P, Pate J (1953) Electric potential differences across the normal aorta and aortic grafts of dogs. Am J Physiol 175: 113–117
66. Scotti G, Righi C, Mele A, *et al* (1994) Therapeutic neuroradiology: cost/benefit ratio. Riv Neuroradiol 7: 735–744
67. Scotti G, Righi C, Simionato F, *et al* (1994) Endovascular therapy of intracranial aneurysms with Guglielmi detachable coils (GDC). Riv Neuroradiol 7: 723–733
68. Serbinenko F (1974) Balloon occlusion and catheterization of major cerebral vessels. J Neurosurg 41: 125–145
69. Solomon R, Fink M, Pile-Spellman J (1994) Surgical management of unruptured intracranial aneurysms. J Neurosurg 80: 440–446
70. Standard S, Chavis T, Wakhloo A, *et al* (1994) Retrieval of a Guglielmi Detachable Coil after unraveling and fracture: case report and experimental results. Neurosurgery 35: 994–999
71. Stebbens W (1989) Etiology of intracranial berry aneurysms. J Neurosurg 70: 823–831
72. Tenjin H, Fushiki S, Nakahara Y, *et al* (1995) Effect of Guglielmi detachable coils on experimental carotid artery aneurysms in primates. Stroke 26: 2075–2080
73. Thompson W, Pizzo S, Jackson D, *et al* (1977) Transcatheter electrocoagulation: a therapeutic angiographic technique for vessel occlusion. Invest Radiol 12: 146–153
74. Tress B, Mitchell P (1995) Endovascular treatment of intracranial aneurysms. J Clin Neurosci 2: 24–25
75. Turjman F, Massoud T, Ji C, *et al* (1994) Combined stent implantation and endosaccular coil placement for treatment of experimental wide-necked aneurysms: a feasibility study in swine. Am J Neuroradiol 15: 1087–1090
76. Weir B, Macdonald R (1994) Intracranial aneurysms and subarachnoid hemorrhage: an overview. In: Wilkins RH, Rengachary SS (eds) Neurosurgery, Vol 2. McGraw-Hill, New York, pp 2191–2213
77. Yasargil MG (1984) Pathological considerations. In: Yasargil MG (ed) Microneurosurgery. Thieme, Stuttgart, pp 280–281

78. Vinuela F, Duckwiler G, Guglielmi G (1993) Commentary: Electrolytically detachable microcoils. Am J Neuroradiol 14: 337–339
79. Zubillaga A, Guglielmi G, Vinuela F, *et al* (1994) Endovascular occlusion of intracranial aneurysms with electrically detachable coils: correlation of aneurysm neck size and treatment results. Am J Neuroradiol 15: 815–820

Benign Intracranial Hypertension

Pseudotumour cerebri: Idiopathic Intracranial Hypertension

J. D. SUSSMAN[1], N. SARKIES[2], and J. D. PICKARD[3]

[1] Academic Neurology Department, University of Sheffield,
[2] Neuro-ophthalmology Department, and [3] Academic Neurosurgery Unit,
University of Cambridge, Addenbrooke's Hospital, Cambridge (U.K.)

With 8 Figures and 2 Tables

Contents

Life with Benign Intracranial Hypertension

What's in a name?

I'm angry, cross, annoyed
At a very misguided man
The one who names diseases
With inappropriate, ill suited titles.
Benign Intracranial Hypertension is the label
That doctors place on me.
If I met that man face to face
I would demand that he justify that name.
And tell me what's benign:
I find the word an insult to my suffering.
It implies it's OK, harmless, curable,
Slight, superficial, easily treatable.
I know it's not life-threatening
In a mortal sense,
But it's killing my living.
I haven't worked for months
In the job I love,
Had countless lumbar punctures
And needles in other parts.
Operations with tubing and valves
Inserted in unsymmetrical patterns around my body.

Symptoms too numerous to list.
My marriage is under constant strain
And my children suffer,
That really hurts.
Will I be home next week or not?
I want to get on with living,
Have a routine or normality.
Yes, I'm angry all right
What right did he have to label all this benign.
I have a right to be exasperated, infuriated
With his lack of imagination and understanding.
Surely he could have come up with something,
Something just a little more grand,
Something to portray my distress,
To evoke a little understanding in people standing near,
To induce a little sympathy for me.
Come on someone please,
Start now with this disease
Let's have a renaming ceremony,
But please, remember, invite me.

Liz Galfskiy
Winchester, UK

1. Definition and Historial Aspects

Benign intracranial hypertension is a diagnosis of exclusion characterised by the signs, symptoms and proof of raised intracranial pressure in the absence of localising neurological signs, obstruction or deformation of the ventricular system, in an alert and orientated patient (Modified Dandy Criteria, Table 1, 1–4). Traditionally Quincke (1897) [5] and Nonne (1904) [6] have been credited with the original descriptions of BIH. However, Johnston's (1992) [7] scholarly historical review makes clear that other authors had previously described relevant cases including Lawford (1881), Carter (1887) and Taylor (1890).

Furthermore, most of the cases described by Quincke as serous meningitis would not now fall within the definition of BIH nor would some of those of Nonne (1904) who originally coined the term pseudotumour cerebri. The historical advent of new technology including lumbar puncture, pneumoencephalography, CT, MRI, CSF infusion studies and PET has facilitated diagnosis but the pathophysiology remains an enigma. Cases with headache but without papilloedema [8], and papilloedema without headache [9] have been described which do not preclude the diagnosis. The terms pseudotumour cerebri (Nonne 1904) and benign intracranial hypertension (Foley 1955) [10] have historically been treated as synonymous, however given the high incidence of damage to vision, the term benign is

Table 1. *Modified Dandy's Criteria for the Diagnosis of BIH*

1. Signs and symptoms of raised intracranial pressure
2. No localizing neurological signs, in an awake and alert patient, apart from a VIth nerve palsy or rarely another false localizing sign.
3. Normal neuroradiology except for small ventricles or empty sella.
4. Documented raised CSF pressure (25 cmH_2O or more) but with a normal CSF composition.
5. No cause for the raised intracranial pressure with exclusion of structural or systemic causes of elevated intracranial venous sinus pressure.
6. Benign clinical course apart from visual deterioration.

(Modified from Rhakrishman *et al.* 1994) [11]

losing currency, and the syndrome tends to be referred to as pseudotumour cerebri (PTS), which best describes the disease phenotype. The term idiopathic intracranial hypertension is used once investigations have excluded a cause.

2. Incidence

BIH is uncommon. A similar annual incidence is found in Iowa and Louisiana, and in Libya, at roughly 1 to 1.7 per 100,000 per year rising to 19.3 in obese women aged 20–44 [12]. It is eight times more common in adult women than in men [13], though in childhood the incidence is approximately equal in both sexes [14].

3. Clinical Symptoms and Signs

The classical symptoms of BIH include novel headache (80–99%) disturbances of visual acuity including obscurations (40–68%), diplopia (22–40%), pulsatile intracranial noises and tinnitus (4–60%), photopsia (54%), nausea and vomiting (22–32%; 50% in children), dizziness (8–18%), retrobulbar pain on eye movements (22%), alteration of consciousness (4–10%). A range of other symptoms are occasionally reported, and up to 5% of patients may be asymptomatic. The history is usually less than 3 months at the time of presentation. The incidence of various symptoms will reflect the speciality of the reporting physician or surgeon.

3.1 Visual Symptoms of Papilloedema

Many patients with papilloedema may be visually asymptomatic. The first symptom noticed by many patients is often a transient obscuration of

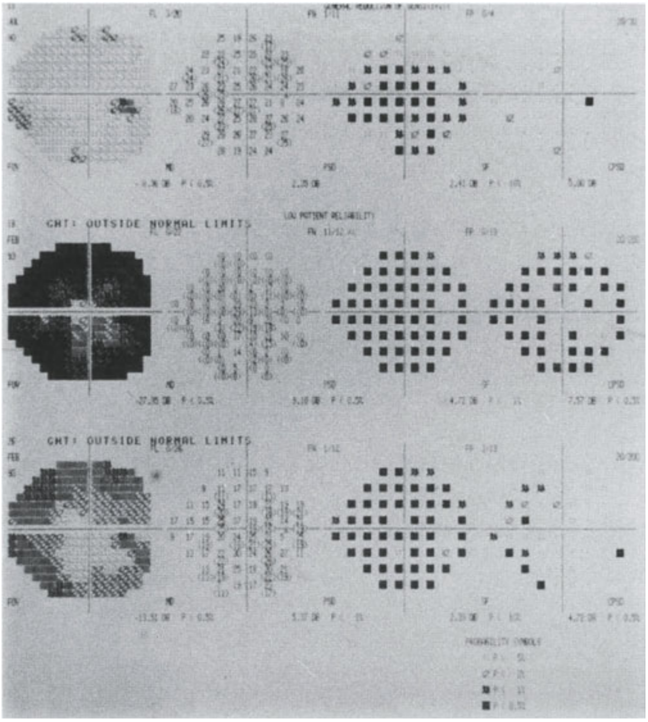

Fig. 1. Automated perimetry (Humphrey). Top: normal field; middle: peripheral constriction; bottom: superior arcuate field loss with nasal step and enlargement of the blind spot

vision which may occur many times each day, and is frequently precipitated by change of posture [15]. Obscurations do not predict permanent visual failure but their presence increases the risk, and should expedite early and aggressive management [16]. The aetiology of transient obscurations is not known: alternative theories suggest that they are due to pressure on the optic chiasm or intracranial portion of the optic nerve or ischaemia of the optic nerve head. Enlargement of the blind spot may be the only visual sign of papilloedema, and is frequently unnoticed by the patient. The visual field progressively becomes involved with arcuate defects, concentric constriction, ring scotomas, centra-caecal scotomas and finally loss of central vision (Fig. 1).

3.2 Visual Field Studies—Automated Perimetry versus Goldmann Kinetic Techniques

Visual field examinations are best performed with either a Goldmann manual perimeter or a computed automated perimeter. The Goldmann

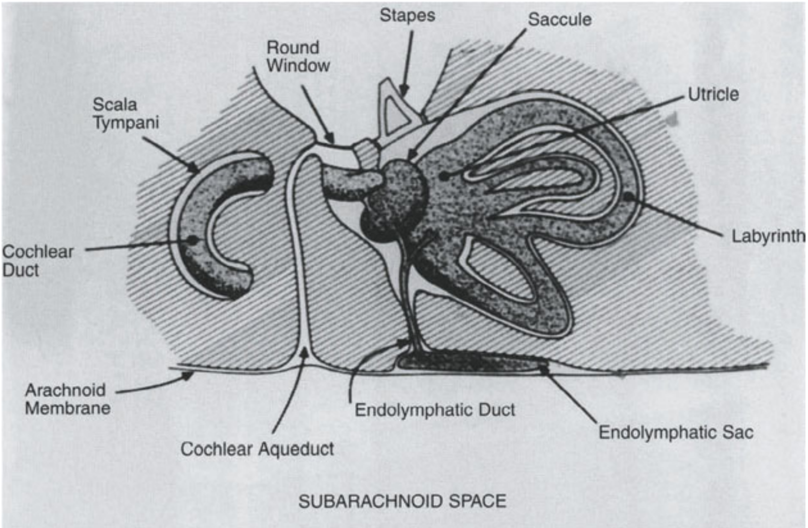

Fig. 2. Subarachnoid space. Diagram of anatomy of the cochlear aqueduct (with grateful thanks to Dr. R. Marchbanks)

method is a kinetic technique: a skilled technician is essential for an accurate examination. Computerized automated fields are more sensitive but require an attentive, motivated and alert patient.

3.3 Miscellaneous Symptoms

Single case reports exist of oculomotor, trochlear and facial palsies that resolved with resolution of the BIH. Nystagmus and ataxia have also been described. BIH may cause persisting CSF fistulae to develop. Johnston has reported a few patients presenting with disturbances of consciousness, ranging from drowsiness to syncopal episodes presumably related to the very high ICP [7]. The precise mechanism remains obscure in the absence of brain shift or significant reductions in Cerebral Blood Flow. Tinnitus, deafness and intracranial bruits may relate to transmission of raised CSF pressure through a patent cochlear aqueduct to increase perilymphatic pressure in the inner ear (see Fig. 2) [17,18].

Occasional patients may present with severe pain in the neck, arms and back possibly as the result of dilated spinal root sleeves. A number of patients with a lumbo-peritoneal shunt for BIH may complain of back and neck pain and even root pain when the shunt is not functioning [7].

Obesity is common in females together with a history of menstrual irregularity. However there is no consistent pattern of endocrine abnor-

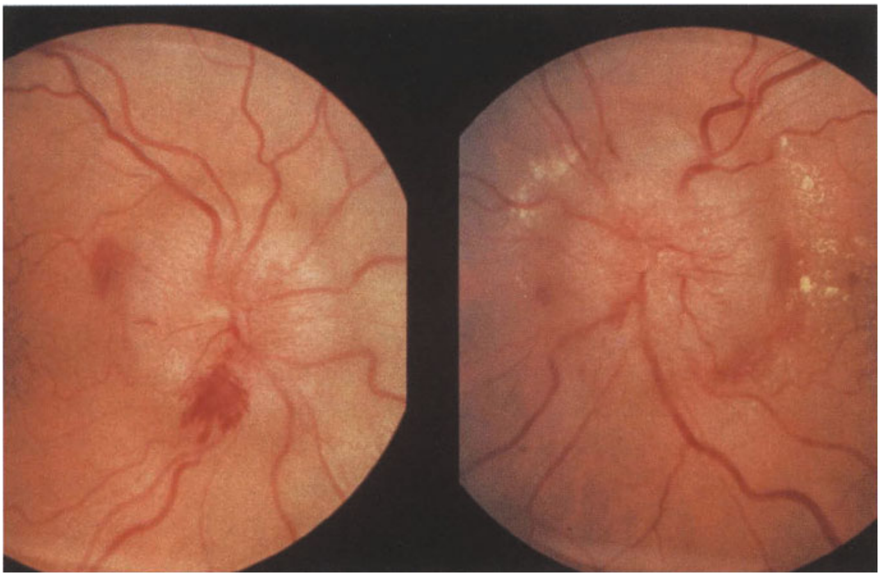

Fig. 3. Colour fundus photograph showing bilateral papilloedema

mality despite the empty sella and periodic interruption to portal blood supply. Careful history—taking may reveal a craving for salt [139].

3.4 Signs

The conventional signs are papilloedema (Fig. 3) with a variety of patterns of visual loss (acuity and fields) and VIth nerve palsies. Other cranial nerve palsies have been described including III, IVth, VII and hemifacial spasm, however great care must be taken to exclude occult lesions which may give rise to these signs, such as a glomus jugular tumour or arteriovenous malformations.

Papilloedema has been classified into four types viz: early, fully developed, chronic and atrophic [20,21].

Early Papilloedema

Early papilloedema may be suspected when the disc becomes hyperaemic, the edge becomes blurred and the disc itself becomes elevated from the surrounding retina. The hyperaemia results from dilatation of capillaries on the surface of the disc. Frequently the earliest sign of papilloedema is visible in the nerve fibre layer which appears "choked" by the hold-up of axoplasm in the axons. The best technique to visualise elevation of the optic disc is slit lamp biomicroscopy with a fundus lens which allows a three dimensional view. Other signs that have been described in early papilloedema include the dilatation of superficial veins on the surface of the disc, associated with small haemorrhages either on the surface of the disc or in the peripapillary region. The absence of spontaneous venous pulsation in the central retinal vein is often regarded as a cardinal sign of disc oedema, but spontaneous venous pulsations occur in only about 80% of normal subjects, and the CSF pressure may be transiently reduced below 200 mm of water even in patients with raised intracranial pressure so this sign is not entirely reliable. In cases where there is doubt, serial observations are advisable.

Once papilloedema has become established, haemorrhages around the disc margin become more obvious, and cotton wool spots or focal retinal infarcts, signs of ischaemic damage to the axons may develop. The disc swelling may be manifest predominantly with haemorrhages or with cotton wool spots (Fig. 4).

Associated Fundal Abnormalities

Circumferential lines may rarely be seen around the disc indicating compression of the posterior pole of the eye from a distended optic nerve sheath (Paton's lines). Haemorrhages and exudates tend to follow a radial distribution around the disc, because the nerve fibres in the macula have a fan-shaped appearance. When the rise in intracranial pressure has been rapid, subhyaloid haemorrhages may occur, which may rarely break into the vitreous. Peripheral retinal haemorrhages are rare in papilloedema. Choroidal folds may occur in patients with papilloedema as a result of pressure on the posterior globe from a distended optic nerve sheath. Subretinal neovascularization near the disc may occur when the papilloedema has become chronic.

Chronic Papilloedema

When papilloedema persists, haemorrhages and exudates slowly resolve and the disc develops a rounded appearance. The central cup becomes obliterated (Fig. 5).

Ultimately the disc swelling subsides and the disc becomes atrophic with narrowed, sheathed retinal vessels. The time for these changes to evolve is dependent upon many factors. Patients have been observed in whom the development of optic atrophy from acute papilloedema has occurred in as little as 6 weeks.

In some cases, optico-ciliary vessels may develop as papilloedema evolves from the chronic to the atrophic stage. These vessels bypass from the retinal to the ciliary circulation and are thought to result from chronic

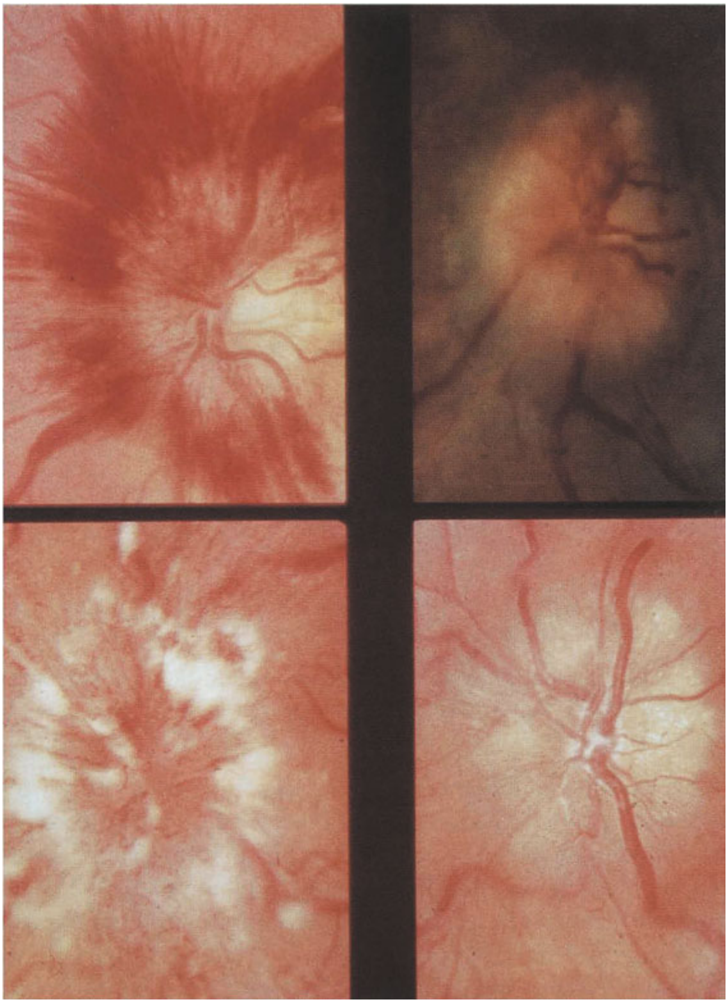

Fig. 4. Composite colour photograph of papilloedema. Top left: acute haemorrhagic papilloedema; bottom left: acute decompensated papilloedema with cotton wool spots; top right: chronic papilloedema with optico-ciliary shunt vessels; bottom right: chronic "vintage" papilloedema

obstruction of the normal venous drainage. The development of white spots on the optic disc resembling disc drusen also indicates chronicity.

Fluorescein Angiography in the Diagnosis of Early Papilloedema

There are occasional cases in which an appearance similar to papilloedema may be simulated by congenitally anomalous discs. In these cases, a fluorescein angiogram may be useful to confirm whether the papilloedema is

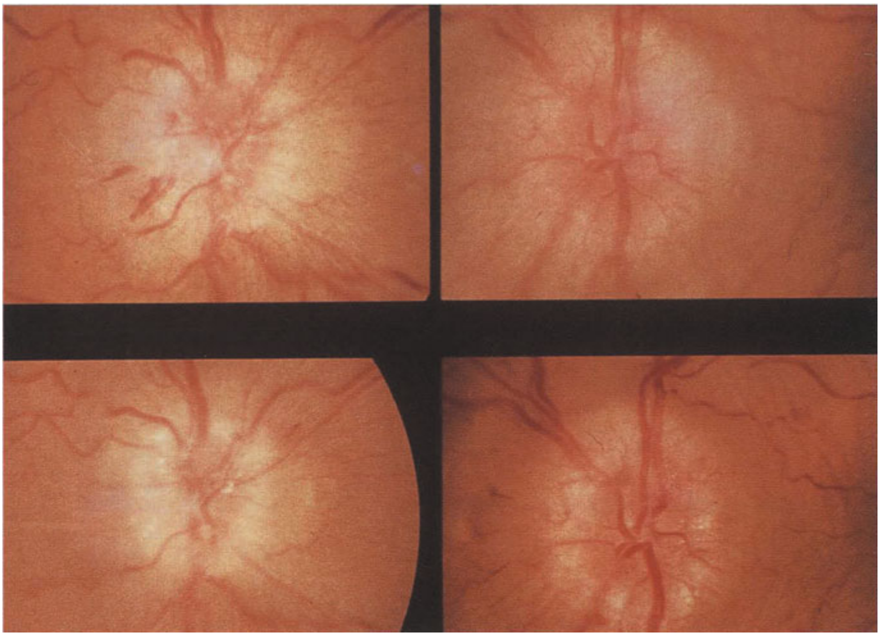

Fig. 5. Colour photograph showing papilloedema before (above) and after (below) right optic nerve sheath fenestration

real. In true papilloedema, there is leakage of dye from the disc margin soon after intravenous injection of 5 millilitres of 10% fluorescein sodium into a superficial arm vein. The test is not absolutely specific since certain disc anomalies such as eg. disc drusen, may also cause leakage of dye from the disc margin. In most cases, careful observation with a slit lamp is often sufficient to establish the correct diagnosis.

The Prognosis of Papilloedema

The prognosis of papilloedema is dependent upon the cause. In many cases it is not possible to judge the visual prognosis from examination of the disc alone. The presence of severe venous engorgement, retinal haemorrhages and exudates is of no prognostic significance. Once the disc has become pale and atrophic, permanent loss of nerve fibres has already occurred, and the prognosis is especially poor if the retinal arteries are narrowed. Most of these patients have evidence of visual dysfunction on testing visual acuity, colour vision and visual fields. Tertiary referral centre studies have emphasized that vision may be permanently damaged by papilloedema due to BIH. For example in Corbett's study [22], in which a group of 57 patients with a diagnosis of pseudotumour cerebri were followed for 5–41 years, severe visual impairment occurred in 14 patients (26%), and in over 80% patients, the CSF pressure remained elevated regardless of the therapy the patients had been given. Studies based on symptomatic patients ascertained from the general population describe a more benign, self-limiting course.

Pathophysiology of Papilloedema

In the most satisfactory animal models of papilloedema, inflatable balloons are introduced into the subarachnoid space to produce raised intracranial pressure [23, 24]. General points of agreement are: (1) Papilloedema only occurs if the meningeal spaces surrounding the optic nerve and intracranial are patent. (2) Papilloedema does not occur in an eye in which antecedent optic atrophy has destroyed most or all of the nerve fibres. (3) Axonal transport is abnormal in patients with papilloedema as well as in patients with other causes of disc swelling.

Using labelled amino acids. Tso and Hayreh [25] showed that both the fast and slow components of axonal transport were held up in the region of lamina cribosa of the optic disc in monkeys with experimental raised intracranial pressure. The accumulation of axoplasm resulted in the swelling of axons which was seen on electron microscopy. The slow component of axonal transport was also abnormal in other forms of experimental disc swelling [26].

Radius and Anderson [27] showed that changes in fast transport occurred only after the development of disc swelling, implying that changes in slow transport may be the primary abnormality. Parhad *et al.* (1980) have demonstrated disc swelling in guinea pigs and dogs with the drug B-B′-iminodipropionitrile (IDPN), which selectively and directly blocks axonal transport [28].

A number of questions remain unresolved. It is not known whether a relationship exists between the severity of axonal transport obstruction and the clinical degree of optic disc swelling.

The extent to which axonal transport obstruction is compatible with normal conduction of nerve impulses, is also unknown.

Whether the aetiology of axonal transport obstruction in papilloedema is mechanical, ischaemic, or due to an abnormality of autoregulation of the optic nerve head blood supply is also uncertain.

4. Investigations

4.1 Imaging

In order to establish whether a case satisfies the modified Dandy criteria (Table 1) a CT or MR scan is required, together with contrast enhancement to rule out arteriovenous malformations. MR cerebral angiography

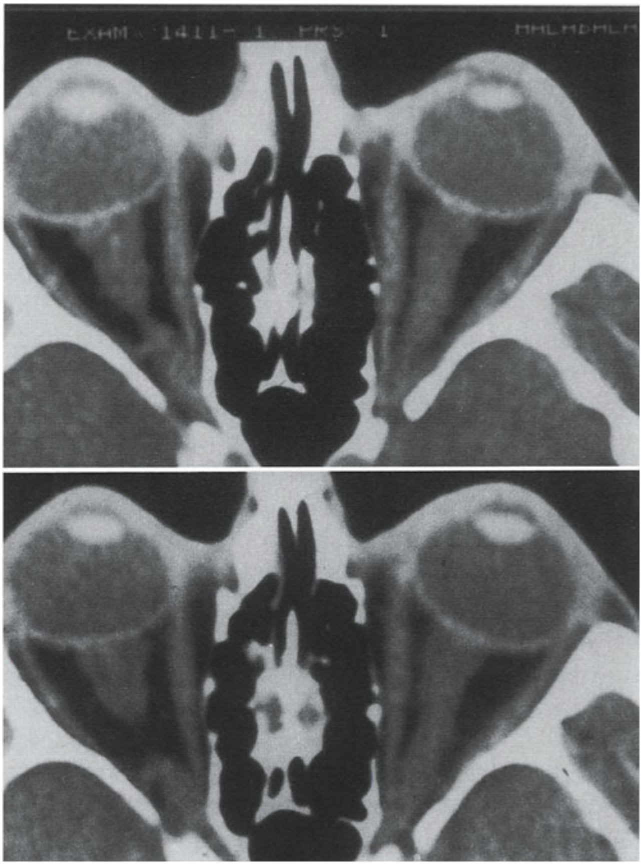

Fig. 6. CT scan of orbits showing optic nerve sheath enlargement in chronic papilloedema

should be performed to exclude any abnormalities of venous drainage [29]. CT of the orbits may show significantly larger optic nerve sheaths in PTC than in controls (Fig. 6). The normal outward convexity of the optic nerve head may be replaced by either flattening or concavity and a good correlation between the degree of abnormality and the severity of visual loss is seen [30]. This technique has not yet been applied prospectively to determine whether the abnormality will be present in patients before the appearance of significant visual morbidity and if so whether it will be predictive of a poor outcome. There remains debate over whether the ventricles are reduced in size ("slit-like; vide infra). The old ventriculography/ encephalography literature was reasonably consistent in documenting normal sized ventricles—indeed, some patients had modest ventricular enlargement [7,10]. Current CT data is not in agreement despite there being

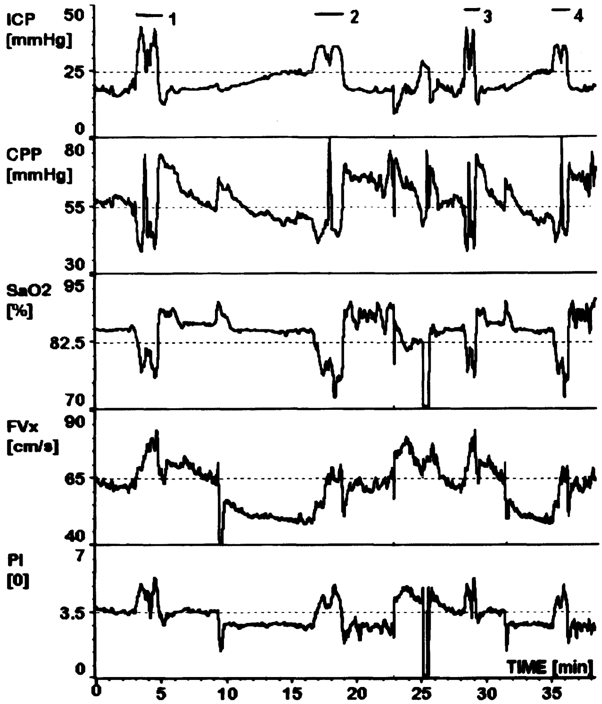

Fig. 7. Recording of a four hour period of continuous signal monitoring while the patient (with morbid obesity and visual failure) was asleep

no confounding variable of anaesthesia with nitrous oxide to complicate interpretation [31,32]. Reid's study was important in using the patient as their own control: ventricular volume increased significantly with successful treatment. There is an increased incidence of empty sella (55–95%).

4.2 CSF Studies

CSF pressure must be documented prior to any treatment once a normal CT scan has been obtained. Lumbar puncture in the obese patient requires a skilled operator if false-negative results and needle phobia are not to result. The patient needs to be relaxed and the opening pressure measured with the head and legs extended. Normally a simple measurement of raised CSF pressure (>25 cmH_2O or 18 mmHg) is sufficient if the clinical features are typical. Where the CSF pressure is unexpectedly normal, prolonged CSF pressure recording through a lumbar catheter (or even intracranial transducer) for a few hours or overnight is necessary. Such recordings will reveal not only raised baseline CSF pressure but also plateau and B waves (Fig. 7).

CSF pressure measurements may be combined with a CSF infusion using either a one or two needle technique and preferably with a more sophisticated computerized technique [33] than the original Katzmann-Hussey method. When care is taken an increased resistance to CSF absorption is confirmed [34, 41]. Unfortunately there is no substantial literature on CSF production rates. CSF should be normal in composition. CSF protein may be low and has been taken to reflect a dilutional effect (vide infra) [42, 43]. There is debate over whether CSF protein is inversely related to the opening CSF pressure.

Both radioisotope cisternography and MRI might be capable of revealing whether the cortical subarachnoid space and basal cisterns are dilated as an explanation for a low CSF protein. Isotope cisternography is notoriously difficult to interpret on a quantative basis; features such as a delayed flow and prolonged parasagittal stasis are reported in some 20% of normal subjects [44]. Free communication between all CSF spaces with neither convexity block nor ventricular reflux is the most consistent finding in BIH. Early studies suggesting that there might be reduced isotope clearance have not been confirmed in the majority of patients [7, 24, 41]. The technique is too crude to detect anything but the type of complete obstruction of CSF flow seen over the convexities in communicating hydrocephalus. MR scanning has not yet been used in sufficiently large numbers of patients and the early results are conflicting both with regard to possible cerebral/periventricular oedema and CSF volumes.

4.3 Haematology

Haematological investigations should include a full blood count to exclude myeloproliferative or lymphoproliferative disorders. If any abnormality is suspected then haematological advice should be sought and marrow aspiration or trephine may be required. A full thrombophilia screen should be performed including prothrombin time, KCCT, thrombin time, fibrinogen, protein C, total and free protein S, IgG and IgM anticardiolipin antibodies, the dilute Russell's viper venom time (DRVVT), and factor V Leyden. Any prolonged DRVVT should be correctable with the addition of serum. Antiphospholipid antibody testing is technically challenging and should be performed in an experienced laboratory [45].

A screen for inflammatory disease should be performed including ESR, C reactive protein, autoantibodies including DNA antibodies and extractable nuclear antigens. Plasma electrophoresis and immunoglobulin levels should be measured to exclude myeloma.

5. Aetiology—Causes and Associations

An extensive collection of clinical associations has been described (Table 2). Varying definitions of the condition have been utilised by differing studies,

Table 2

Proven associations	
Obesity	Female sex in adulthood
Recent weight gain	Systemic hypertension
Probable associations	
Cranial venous hypertension	Hematological
Cardiogenic or pulmonary right heart failure	Leukaemia
	Iron deficiency anaemia
Arteriovenous malformations	Polycythaemia
Cerebral venous occlusion	Myeloma
Congenital absence	POEMS syndrome
Prothrombotic disorders	Endocrine
Inflammatory processes	Addison's disease
Otitic hydrocephalus	Hypoparathyroidism
Mastoiditis	Nutritional disorders
SLE	Hyper/hypovitaminosis A
Behcet's syndrome	Medication
Sarcoidosis	Vitamin A, retinoids
Head injury	Tetracyclines
Pregnancy and puerperium	Nalidixic acid
Increased resistance to flow across arachnoid villi	Lithium
	Danazol
Post meningitis	Ethinyloestradiol
Post subarachnoid haemorrhage	Amiodarone
Raised CSF protein	Anabolic steroids
Spinal tumours	Corticosteroid withdrawal
Guillain Barre syndrome	
Possible associations not yet subjected to (adequate) case controlled studies	
Childhood hypothyroidism, or	Ketoprofen
Thyroid replacement therapy in childhood	Nitrofurantoin
	Familial
Indomethacin	
Associations no longer accepted	
Menarche	Diabetes
Menstrual irregularities	Multivitamins
Thyroid abnormality	Oral contraceptives
Minor trauma	

with part of the confusion arising from the choice of terminologies. The modified Dandy criteria have become the accepted definition of idiopathic intracranial hypertension, in which raised intracranial pressure exists, but without a cause being found (Table 1). There is, however, no consensus as to which investigations are required to exclude all causes of the condition, and a number of cases are described with CSF abnormalities which would preclude their inclusion from other series. If a cause is found, but in all other respects the case fulfils the modified Dandy criteria, then it is reasonable to use the term pseudotumour cerebri. A further problem arises from attempts to ascribe causation rather than association with any abnormal finding. For example, in more than half of the cases of BIH said by the literature to be associated with steroid therapy, the steroids were being given for SLE [46] which is also associated with the condition.

A number of case-controlled studies have attempted to critically assess some of the putative associations [46–48] though insufficient numbers of cases with the rarer causes were available for the statistical methods used [49], and it is possible that a number of false negative associations have therefore been recorded.

Obesity and recent weight gain are strongly associated with BIH in both women and men [13, 47, 50]. Systemic hypertension has also been demonstrated to be more common in patients than controls [13, 22, 50]. Some of the commonly accepted associations, however, such as menstrual irregularity and minor head injury, have been demonstrated to be spurious [13, 46, 48, 50, 51].

A variety of endocrine abnormalities have been described in association with pseudotumour cerebri [52–54]. An association with Addison's disease is probable, and the number of reports in cases of hypoparathyrodism is unlikely to be a coincidence [55, 56]. Thyroid abnormalities are reported in association with PTC [57]. Case control studies refute this connection, but with far too few cases for statistical validity [13, 50]. There are a number of cases associated with vitamin A deficiency in infancy [58].

A large literature on drug precipitants of PTC has built up over the past three decades. An association with vitamin A toxicity or retinoid use is now well established [46]. Tetracyclines are strongly implicated [46], with the majority of cases in healthy teenage girls taking the drug for acne. The combination of vitamin A or retinoids plus tetracycline appears to further increase the risk. Other drugs which appear implicated include danazol [59, 60], lithium [61, 62], ethinyloestradiol [46] and nalidixic acid [63].

Nine cases of PTC associated with thyroid replacement therapy, all in children aged 13 or less, are certainly suggestive of some form of association, though since the vast majority of cases of hypothyroidism in this age group are caused by chronic autoimmune thyroiditis, an immune mechanism may be implicated [46, 64]. A link with steroid use or its withdrawal has frequently been cited [13, 46, 54, 65, 66] though with CSF pleocytosis in some of the cases. As has been mentioned, many of those given steroids were receiving treatment for SLE, so the drug association must be regarded as tentative. The oral contraceptive pill though commonly claimed to be implicated, is excluded by case-controlled studies [47, 48], though given the well recognised association with thromboembolic disease, this is rather surprising. Five cases of BIH are associated with amiodarone therapy, for arrhythmias in the absence of heart failure, all in patients aged over 50 [46].

There have been occasional reports implicating nitrofurantoin [67, 68], and indomethacin [69] or ketoprofen [70] in Bartter's syndrome, but in insufficient numbers for their significance to be clear [46]. A number of familial cases of BIH have been reported; two pairs of obese sisters [71, 72], a mother and son, both obese [73], and three obese sisters [74]. In another family a mother and two of four daughters has pseudotumour cerebri, and a son, communicating hydrocephalus [75]. It has been suggested that there may be a hereditable defect in CSF absorption, though they may be explained by coincidence or familial obesity.

Intracranial venous sinus thrombosis giving rise to the inappropriately termed 'otitic hydrocephalus' is well recognised in association with middle ear and mastoid infection [10]. Venous sinus thrombosis may result from a variety of inflammatory vasculitic conditions such as Behcet's disease [76] and SLE [76–79] though these are frequently excluded from the diagnosis on the basis of their association with focal neurological signs. Closed head injury [80], and pregnancy and the puerperium [81] are also associated with PTC through sinus thrombosis. However, actual venous obstruction has also been purported to be a cause of hydrocephalus. Whether venous obstruction results in BIH or hydrocephalus may depend upon associated anomalies and the distensibility of the cortical subarachnoid space (vide infra).

Any coagulopathy may give rise to intracranial venous sinus occlusion, including disseminated intravascular coagulation, polycythaemia [82], essential thrombocythaemia [83], and sickle cell anaemia. Three quarters of cases of POEMS syndrome [84] and myeloma unassociated with Shimpo's disease, intracranial plasmacytoma or POEMS, are recognised in association with PTC, though the mechanism is not yet determined [85]. Congenital deficiency of clotting factor inhibitors is now recognised as the basis for the familial prothrombotic disorders [86]. Congenital deficiency of protein C is almost always associated with PTC [87], and cerebral venous thrombosis is well recognised in association with deficiency of plasminogen [88], protein S [89], or antithrombin III [76, 90], and with factor V Leyden. Antiphospholipid antibodies are a family of clotting inhibitors including lupus anticoagulants and anticardiolipin antibodies which are associated with the tendency for thromboembolic episodes. These antibodies have been associated with PTC caused by sinus thromboses [91, 92]. A variety of other associations have been made, including iron deficiency anaemia [93] and raised CSF protein arising from thoracolumbar cord tumour [94] or Guillain Barre syndrome [95]. Since angiography has not been a standard part of the work-up for PTC, no correlation exists between the putative 'causes' found, and angiographic abnormalities. In a study of sixteen patients with BIH, half of the patients were found to have occlusion of at least once the major dural venous sinuses [34]. The literature describes a number of cases of BIH with prothrombotic pathologies but with investigations failing to identify sinus thrombosis [83].

To investigate the proposition that undetected thrombosis might be a significant cause of PTC, clotting abnormalities were sought in a mixed prospectively and retrospectively investigated cohort of 38 patients with PTC. Antiphospholipid antibodies were found in 31% of patients, and a further 16% had raised fibrinogen without antiphospholipid antibodies. Seven patients who were prospectively studied underwent angiography within one month of the onset of symptoms. No angiographic abnormalities were detected although three had antiphospholipid antibodies, one had a raised fibrinogen, and another, antithrombin III deficiency. One patient, a diabetic on insulin developed her PTC while recovering from an episode of ketoacidosis with profound dehydrational polycythaemia [96]. These findings must raise the possibility of undetected thrombus in pseudotumour cerebri. It has been suggested that antiphospholipid antibodies might arise as a consequence of endothelial damage brought about by antiendothelial antibodies [44], which might increase the resistance to CSF absorption in the absence of detectable thrombosis. In spite of a large literature on PTC, a number of critical questions remain unanswered. The variation in terminology has given rise to confusion since cases have been defined as idiopathic without cerebral angiography having been performed. In order to devise rational therapy it will be necessary to seek the thrombotic risk factors already discussed, and routinely perform angiography in order to establish which apparent causes give rise to the condition and by which mechanism.

6. Pathophysiology of Raised CSF Pressure in BIH

Which intracranial compartment (brain, blood or CSF) becomes too big for the compensatory mechanisms controlling intracranial pressure?

6.1 Brain (Diffuse Cerebral Oedema)

There has been much debate over the presence of radiological signs of brain swelling in BIH [1,10]. There are considerable potential errors (20–

30%) in the measurement of ventricular volume with any technique [97]. Allowing for such errors, Reid found that ventricular size was either normal or reduced in the symptomatic phase of BIH compared with age-matched controls, and increased slightly in size in some patients with resolution of the symptoms [31]. Weisberg [98] found normal CT appearances in half of his patients and evidence of 'brain swelling' in the other half (small ventricles, poorly defined cisterns, enlarged optic nerves). Obliteration of the basal cisterns was an unusual feature of BIH. There appeared to be no abnormal tissue density or contrast enhancement in the white or grey matter and Reid found no change in the Hounsfield numbers. These authors suggested that the lack of change in Hounsfield numbers did not exclude the presence of brain swelling due to either raised cerebral blood volume or increased brain water. They proposed that an increase in the protein content of oedema fluid might mask any decrease in Hounsfield numbers brought about by increased brain water. They did not however address the observation that there is a low CSF protein in many patients with BIH, which rather contradicts their suggestion that there is no increase in total CSF volume but an increased cerebral extracellular protein concentration.

Two more recent studies using age/sex matched controls came to contradictory conclusions. Jacobsen found no evidence of small ventricles [99] whereas Rothwell suggested the opposite [32]. Diffusion weighted MR has suggested that in 7 of 12 BIH patients the apparent diffusion coefficient of water was increased in the subcortical white matter [100]. There was no correlation between apparent diffusion coefficient for water and CSF outflow resistance or duration of symptoms but a suggestion of a correlation between ADC and CSF pressure.

Direct evidence of brain swelling came from the histological study of Sahs & Joynt [101] on brain biopsies. Intracellular and extracellular oedema was described but such histological assessment is fraught with artifact. More recently Wall [102] found no evidence of oedema at post-mortem in two patients though not at a stage when the BIH was active. Potassium transport across the blood-brain barrier has been reported to be normal in BIH [103].

The fact that patients with BIH are so well and the EEG is usually normal [10, 104, 105] might be unexpected were severe brain oedema to be the cause. Although gross neurological function and electrical activity may be preserved in the presence of vasogenic oedema and less so in interstitial or hydrocephalic oedema, they most certainly are not preserved in cytotoxic oedema.

There is no evidence on CT scanning of either vasogenic or interstitial oedema in BIH. Obliteration of the cisterns in any other condition is associated with coma and impending doom. Furthermore, lumbar puncture in these latter circumstances may precipitate tentorial herniation but this just does not occur in BIH, hence the safety of serial lumbar punctures and lumbo-peritoneal shunts.

Finally, patients reassessed when asymptomatic may still have raised pressure, even though any ventricular compression has returned to normal [22, 41, 106].

6.2 Cerebral Blood Volume

In 1937 Dandy [1] suggested that changes in cerebral blood volume and cerebral vasomotor instability might play a part in BIH. Following subtemporal decompression, he observed 'marked variations in the degree of intracranial pressure from time to time and the changes from one extreme to the other and in either direction may occur, at times at least, very rapidly, i.e. over a period of a few minutes .... fright, fatigue, mental or physical, and sudden nervousness may cause the decompression to become more tense very rapidly'.

Foley [10] found that cerebral blood flow in three cases was at the upper limit of normal which is in keeping with the normal conscious level and EEG (Kety-Schmidt nitrous oxide method). In contrast. Raichle [107] found a small reduction in cerebral blood flow in nine patients using intracarotid injection of ^{15}O-tagged water after angiography and an increase in cerebral blood-volume (using ^{15}O-labelled carboxyhaemoglobin) with no change in cerebral oxygen consumption. CSF drainage did not affect these values. This degree of change in cerebral blood volume was not sufficient to account for the intracranial hypertension, and may have reflected the normal vasodilation of the cerebral vessels to raised intracranial pressure. In one patient, cerebrovascular reactivity to hypocapnia and hypercapnia was unaffected as determined by the arteriovenous oxygen technique. In contrast, Mathew [108] found that cerebral blood volume was increased in two patients with BIH, a change which did not resolve with decompression. Brooks [109] found no change in cerebral blood flow, cerebral blood volume, cerebral oxygen consumption or oxygen extraction in five conscious patients with BIH using the inhalation of tracer amounts of $C^{15}O_2$, $^{15}O_2$ and ^{11}CO with PET scanning. These authors suggested that Raichle's results might have reflected the confounding effects of anaesthesia and angiography contrast media. It is surprising that no increase in cerebral blood volume was found in the study of Brooks *et al.* (1985) since the autoregulatory response to falling cerebral perfusion pressure is dilatation, as has been demonstrated by a number of experimental studies. It should be emphasized however, that cerebral blood volume is difficult to measure accurately.

6.3 Increased CSF Volume

CSF Hypersecretion or Reduced Absorption Due Either to Obstruction of the Cranial Venous Outflow or Increased Resistance Across the Arachnoid Villi

BIH might theoretically arise from an increase in the total CSF volume. If this were so, ventricular dilation might be expected, but is not found.

Unfortunately, no good estimates of CSF volume are available in BIH, given the invasive nature of the ventriculo-lumbar perfusion technique that would be required. It is the common experience however of many neurosurgeons from Dandy (1937) onwards, that the cortical subarachnoid space may be deeper than usual in BIH, leading to the term 'hypertensive meningeal hydrops' of Davidoff and Dyke (1937) [110]. Foley (1955) [10] felt that external hydrocephalus could not develop following arachnoid villus or sinus obstruction, without some dilation of the ventricles, since they and the subarachnoid space are in communication and under equal pressure. He dismissed the deep subarachnoid space seen at craniotomy or through a burr hole as an 'artefact due merely to opening the skull and dura when fluid from the ventricles, even if they are small, is displaced into that part of the subarachnoid space which has been opened to atmospheric pressure'. If fluid is added to a completely patent, freely communicating CSF containing space, it will be accommodated primarily in the most capacious and most distensible part, the subarachnoid space (spinal, convexity and basal) [111]. The hallmark of communicating hydrocephalus on cisternography is a convexity block with ventricular reflux: in BIH, the cortical subarachnoid space is completely patent, and no ventricular reflux occurs. Furthermore, for hydrocephalus to develop, a transmantle pressure gradient has to develop between ventricle and cortical subarachmnoid space (Fig. 8).

The low CSF protein found in many patients [42, 43, 105] may be attributed to a dilutional effect of the normal protein secretion in an excess CSF volume. Fishman (1980) extrapolating from experimental data obtained from water loading, argued that the rate of protein clearance from the CSF may be increased in response to intracranial hypertension. This view is contrary to the results of cisternography and steady-state CSF infusion studies which certainly do not indicate enhanced CSF clearance. Condon have described an NMR sequence which highlights all the intracranial CSF. In one patient with BIH reported in this preliminary communication, both ventricular and extraventricular CSF volumes were reduced compared with some control patients. It will be interesting to see further results with this technique and whether it can be used to resolve the volume of the spinal subarachnoid space.

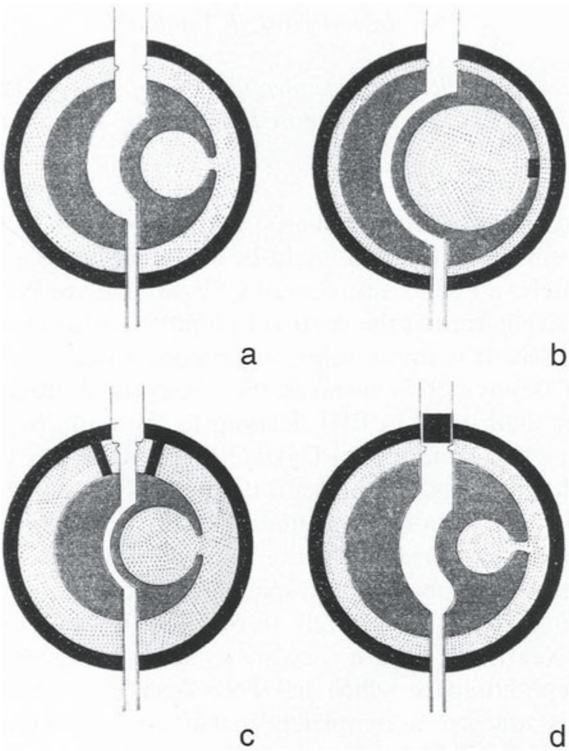

Fig. 8. Schematic representation of the three components of the intracranial system, the incompressible brain tissue (shaded), the vascular system open to atmosphere, and the C.S.F. (dotted); (B) during ventricular obstruction; (C) when there is obstruction at or near the points of outlet of the C.S.F.; (D) when there is obstruction of the venous outlet (reproduced with permission of the Guarantors of Brain)

6.3.1 Hypersecretion

CSF secretion rate would have to increase very considerably for intracranial pressure to rise to the levels seen in BIH if it were the only abnormality in the Katzman-Hussey test, infusion of 0.76 ml/min of mock CSF (in addition to the normal CSF secretion rate of 0.3–0.4 ml/min) only increases intracranial pressure up to some 15 mmHg. In the absence of rigorous data obtained by ventriculo-cisternal perfusion, the estimation of CSF production from withdrawal of CSF in imprecise and the results differ between authors, but do not suggest gross hypersecretion [41, 37, 39, 113]. Preliminary MR studies have again raised the possibility of increased CSF secretion at least in a minority of patients [114].

6.3.2 Reduced CSF Absorption

There is considerable evidence in favour of the concept that reduced CSF absorption is the final common pathway linking the many causes of BIH. CSF absorption is a passive process that obeys 'Ohm's Law' (Davson *et al.* 1970) [115]:

$$\text{CSF absorption } \alpha \frac{(P_{csf} - P_{sss})}{R_o}$$

(P_{sss} = superior sagittal sinus pressure: R_o = resistance to flow across the arachnoid villi).

The normal pressure gradient between cortical venous pressure, CSF pressure and sagittal sinus pressure is: $P_{vco} > P_{csf} > P_{sss}$.

Following clinical or experimental venous sinus obstruction, ICP rises: $P_{vco} = P_{sss} > P_{csf}$ [116, 34].

Following sinus obstruction, in both patients and animals, CSF absorption falls without any change in the resistance to flow across the absorptive channels (R_o). None of the animals showed any increase in brain weight to suggest cerebral oedema, nor did any develop ventricular dilatation [116]. Whether venous obstruction results in BIH or hydrocephalus may depend upon associated anomalies and the distensibility of the cortical subarachnoid space [117]. Although it is generally assumed that there is no evidence of sinus thrombosis in non-otitic cases of BIH, Janny *et al.* (1980) [34] found that sinus obstruction was present in three such cases. Magnetic resonance angiography suggests that sinus occlusion may be more common than was previously thought.

In patients with BIH in whom there is no sinus obstruction, the normal pressure gradient ($P_{vco} > P_{csf} > P_{sss}$) is normal or slightly increased. The CSF resistance to drainage, estimated using steady-state CSF infusion tests (both constant volume and constant pressure modifications of the (Katzman-Hussey test) is increased an average threefold in the majority of patients [34–40]. Malm has recently argued that the increased outflow resistance was insufficient to explain the rise in CSF pressure and noted elevated sagittal sinus pressure in over half of their patients. They suggested that BIH was variably the result of both vasogenic oedema and reduced CSF absorption. MR should eventually resolve this debate. Raised CSF protein concentration increases R_o but it is uncertain whether the increase in R_o is sufficient to account for the rise in ICP ($ICP = If \times R_o + P_{sss}$) where If is the rate of CSF formation [39]. Isotope cisternography has been discussed earlier: the most consistent finding in BIH is that there is free communication between all CSF spaces with neither convexity block nor ventricular reflux. Acute steroid withdrawal may precipate BIH in some patients and, in dogs, doubles the resistance to CSF absorption across the arachnoid villi with no evidence of cerebral oedema or hydrocephalus [116]. Both hyper- and hypovitaminois A cause BIH in man and animals. In rats and calves, for example, hypovitaminois A provokes intracranial hypertension, increases resistance to CSF absorption, and structural alterations in the arachnoid villi [119]. The dura matter was thicker and less pliable in both species and the arachnoid granulations were enlarged, with increased interstitial fibrous and accumulation of PAS-positive electron dense debris. One intriguing possibility concerns the recently resurrected concept of lymphatic drainage of the brain whereby interstitial fluid circulates within the perivascular spaces of the brain to drain in part via the nasal lymphatics into the deep cervical lymphatics. Ablation of nasal lymphatics by cervical lymphadenectomy produces modest hydrocephalus in 80% of rats. It remains to be shown whether such a system exists in man and what is its quantitative significance under different circumstances.

7. Management

The rational management of patients with BIH should involve the multi disciplinary collaboration between neurosurgeon/neurologist and ophthalmologist. BIH is sufficiently uncommon and ill-understood to warrant a subspecialist approach. The paucity of data derived from randomized controlled trials of therapy is a testament to our failure to organize a multicentre approach to studies of BIH. Too many patients have not been adequately investigated. For example, few patients have had angiography and it is therefore unclear whether thrombosis, arachnoid granulation dysfunction, or some other pathology has been the cause.

Furthermore, the symptomatic state of patients was often not defined, so that when a treatment was regarded as successful, it is unclear whether the author was referring to the resolution of headaches or the lack of further visual decline.

There are theoretical hazards behind the treatments used. CSF shunting to diminish the pressure gradient across the arachnoid villi might reduce the flow of water across the membrane possibly allowing more obstructive scar tissues to form. Successful early symptomatic treatment might thus result in the condition becoming chronic. One might also be concerned that a patient with sinus thrombosis would deteriorate if subjected to overvigorous dehydration therapy. It must also be noted that the resolution of symptoms may occur without normalisation of CSF pressure which may persist for many years, and that patients apparently in remission may still be at risk of visual loss. The low risk and capricious occurrence of blindness in relatively young obese females presenting to the physician with headache, papilloedema without visual symptoms and a negative CT Scan can so easily lull him into a sense of false security. Do not many cases of

BIH resolve spontaneously (11.5%, Johnston *et al.* [120] 1981; 35% Greer 1968) [121]. He might even dismiss the brisk, more aggressive approach of his neurosurgical and ophthalmic colleagues as a reflection of their surgical personalities. Why do surgeons fret about patients with BIH who are thin and male? BIH is sufficiently uncommon that it may be some time before the physician (after years of happily managing his patients by gentle admonitions to diet, a little diuretic and the odd lumbar puncture) is confronted abruptly by visual failure.

What overall plan of management minimises the risk to sight in a few yet does not put the majority at undue risk of treatment complications? The following strategy reflects our consensus and largely coincides with that described by Weisberg (1975) [105], Johnston *et al.* (1981) [120], Ahlskog and O'Neill (1982) [122], Corbett and Thompson [19], and Radhakrishnan *et al.* (1994) [11]. It is essential to have a locally agreed protocol and not to allow management to drift.

7.1 *Initial Assessment*

(1) Establish the diagnosis
(a) History and examination—look for a cause, although it is unusual to find one (Table 2) and treat.
(b) CT and MR Scan must be normal; magnetic resonance angiography should be performed.
(2) Establish accurate baselines for vision and c.s.f. pressure
(a) Vision (acuity and fields)
Ophthalmological examination should include testing of visual fields and visual acuity and fundus photography to document the optic disc appearance.

The aim of the ophthalmological evaluation of patients with BIH is to prevent permanent loss of visual function. The decision to operate upon a patient with BIH should depend upon their visual function, measured by perimetry and best corrected visual acuity. These tests are subjective and therefore skilled interpretation of the results in conjunction with an assessment of the optic discs is essential. Patients have to learn how to perform field tests, especially automated quantitative perimetry, so that the first evaluation of the visual fields should be repeated to confirm that the abnormalities are real. In some patients the results of quantitative perimetry remain unreliable after repeated testing, and in these patients more emphasis should be placed upon the results of alternative techniques, eg. confrontation fields, the tangent screen or Goldmann perimeter. The size of the blind spot is critically dependent upon the elevation of the surrounding retina caused by swelling of the disc, and it is possible to reduce the size of the blind spot in patients with papilloedema with a correcting hypermetropic lens. The frequency of testing is somewhat arbritrary, but Corbett and Thompson (1989) recommend initial monthly checks.

(b) CSF pressure

The swelling of the optic disc must be caused by increased intracranial pressure. CSF pressure varies in BIH and lumbar puncture may need to be repeated if the pressure is unexpectedly low—it should be at least 18 mmHg (25 cmH_2O). As noted previously a permanent chart recording of CSF pressure for 30 minutes obtained via a lumbar puncture may be useful for subsequent comparison particularly if more than one clinician is involved. CSF should be removed (30–50 ml) both to reduce CSF pressure and also for laboratory examination for protein, sugar and cytology. The lumbar puncture should be repeated a few days to a week later.

(3) Treatment

If there has been no obvious benefit following lumbar puncture a two week therapeutic trial of corticosteroids (dexamethasone 4 mg q.d.s. with ranitidine or cimetidine) is commonly used, but remains controversial (vide infra). If there is no response (visual symptoms, acuity or fields; CSF pressure on repeat lumber puncture) or the suspicion of further deterioration during the two-week trial of steroids, further liaison should be sought with the ophthalmologist to discuss proceeding with surgical therapy. If there is any contraindication to a lumbo-peritoneal shunt (multiple previous laparotomies, Crohn's disease or peritonitis, for example), a ventriculo-atrial shunt is easier to establish via a non-dominant frontal burr hole than from the posterior parietal route. Multiple lumbar punctures are best avoided as they might make lumbo-peritoneal shunt insertion difficult. If faced with a patient with rapidly deteriorating vision on presentation, steroids should be started and, at the same time a lumbar spinal drain inserted for 72 hours. If vision continues to deteriorate an MR scan should be performed to exclude any lesion initially missed. If the CSF pressure is proven to be normal, the ophthalmologist should again be consulted over the exact intraocular mechanism and whether he feels that optic nerve sheath fenestration is relevant. As patients with BIH are often managed by a variety of specialists, good collaboration between them is essential.

Young obese females presenting with headache alone, no visual symptoms and no acuity or field changes can probably be managed more conservatively and would be suitable for a randomised trial of, say, weight reduction alone versus weight reduction plus two weeks of steroids or a diuretic. Weekly monitoring of symptoms and vision would still be required.

7.2 Pregnancy

Digre *et al.* (1984) [123] reviewed their own cases of BIH occurring in pregnancy, and the world literature, and came to the following conclusions.

(1) BIH occurs in pregnancy at about the same rate as in non-pregnant women.
(2) BIH can occur in any trimester, although it usually appears in the first half of pregnancy.
(3) Patients with BIH during pregnancy have the same spontaneous abortion rate as the general population.
(4) Visual outcome for pregnant women with BIH is the same as for women with BIH who are not pregnant
(5) Pregnant patients with BIH should be treated in the same way as any other patient with BIH except that excessive calorie restriction should be avoided and therapy minimised in the first trimester.
(6) Therapeutic abortion to limit progression of disease is not indicated.
(7) Subsequent pregnancy does not increase the risk of recurrence of BIH above the risk of recurrence in any other women with BIH, and is associated with normal outcome.

7.3 The Evidence for Therapeutic Efficacy

What criteria for therapeutic success should be used? The degree of papilloedema does not correlate with intracranial pressure, hence the latter has to be measured directly. Visual deterioration may not relate precisely to intracranial pressure and the patient's symptoms often resolve despite intracranial pressure failing to return completely to normal. Hence a pragmatic approach must be adopted, and the effects of treatment on both CSF pressure and visual outcome should be examined.

7.4 No Treatment

There is no adequate series of untreated patients who fulfilled all the criteria for BIH. In two series, 11.5% and 35% of patients appeared to undergo spontaneous resolution of symptoms,, but this may be an underestimate of the natural history of the condition in the community [120, 121].

7.5 Weight Reduction Including Bariatric Surgery

Greer (1968) [121] advocated weight reduction but many of his obese patients still underwent surgery. This approach is only relevant in obese patients and has only been used as the sole method of treatment in one small series of patients who were given a rice diet, however it was notable that there were no late visual failures. Unfortunately, details of visual acuity and fields were not provided (Newborg 1974) [124]. Clinical experience suggests that significant weight loss through dieting may ameliorate headache and the response to dehydrating agents matches a patient's weight loss as discussed below. Weight gain certainly precipitates BIH in many patients [125]. More direct evidence has come from Sugerman's [126] recent study of surgically induced weight loss on BIH in morbid obesity. CSF pressure returned to normal levels in all 8 operated patients with morbid obesity and Pickwickian syndrome with retention of carbon dioxide. Such surgery is not appropriate for patients with rapidly deteriorating vision. Corbett has highlighted this unusual benefit: in his experience other treatments leave up to 80% of patients with BIH with pathologically elevated CSF pressures even where papilloedema has resolved. Effects of changes in intra-abdominal pressure on CSF pressure are unlikely to explain the effect of surgery: CSF pressure is not raised in either pregnancy or obesity. This innovation in the treatment of BIH should not be used lightly—complications include incisional hernia, bleeding from marginal ulcers, stomal stenosis, small bowel obstruction, anastomotic leakage, peripheral neuropathy and even Wernicke's encephalopathy.

Finally, a careful dietary history may reveal salt-craving [139]. Anecdotally a low salt diet may help but it is difficult to achieve consistent patient compliance as with any dietary advice.

7.6 Serial Lumbar Punctures

Repeat lumbar punctures are useful in the early stages of management and should be repeated once before starting any other form of therapy except, as noted, where vision is failing rapidly. Multiple lumbar puncture (10–20) are best avoided, since they might make the surgeon's life difficult when trying to establish a lumbo-peritoneal shunt and carry a small risk of arachnoiditis, backache and implanted epidermoid tumour within the spinal canal. 24% of the patients in Weisberg's (1975) [105] series of 120 patients had a normal pressure by the second lumbar puncture performed a few days after the first and all these 24% had an initial opening pressure of less than 350 mm CSF (26 mmHg). Johnston *et al.* (1981) [120] found that serial lumbar punctures (mean of 9) proved adequate as the sole treatment in 39% of a series of 67 patients. The initial CSF pressure was however relatively low (mean 210mm CSF) and in the 61% who did not respond, the opening pressure was greater than 300 mm CSF. The responders therefore appeared to have had a milder version of the syndrome. Since ICP is reported to return to normal within two hours of lumbar puncture, the mechanism of action of the lumbar punctures is unclear, though an inexperienced operator might be supposed to prove more effective by inflicting multiple dural holes and hence predispose to persistant CSF leakage! (Bulens *et al.* 1979 [128]; Johnston *et al.* 1981) [120].

Rhakrishman [11] has postulated that relief of elevated ICP by lumbar puncture alleviates compression of arachnoid villi (thereby improving CSF egress), which may be a secondary factor in some patients. Nine lumbar punctures are certainly not a benign experience for the patients, and a maximum of 4 has been recommended.

7.7 Drug Therapy

Given the extensive literature on BIH, remarkably few drug therapy studies have even been performed, and in those which have, no untreated control groups were used. This is a particularly significant deficiency in view of the highly variable natural history of the disease and its variable propensity for spontaneous resolution.

Diuretics, Acetazolamide and Digoxin

Jefferson and Clark (1976) [129] provided the only substantial data for a diuretic used alone in BIH, in a study comparing the efficacy of oral urea, oral glycerol, hydroflumethiazide or chlorthalidone. This study of 25 patients used blind spot area but not CSF pressure, as a measure of response, and demonstrated the resolution of Papilloedema in 6–12 weeks, with chlorthalidone providing the quickest "time-to-cure".

There were no patients in this small series with severe late visual failure and no controls. In all patients who responded to treatment, impressive weight loss was described though without further comment. The patients who did not respond, did not show significant weight loss. Since patients with BIH are not oedematous, it must be assumed that the 10% weight loss shown by most patients was not a result of diuresis which would have made the patients feel quite unwell. The experience of others, using diuretics albeit anecdotal, has been much less convincing (Greer 1968 [121]; Weisberg 1975 [105]; Bulen *et al.* 1979 [128]; Johnston *et al.* 1981) [120].

There is no particular logic as to which diuretic might prove most efficacious, although acetazolamide is well known to reduce CSF production by up to 50% but for only a few hours after each dose [130]. Carbonic anhydrase inhibitors act to reduce the secretion of CSF by inhibiting production of carbonic acid, and hence bicarbonate from water and CO_2 within the choroid plexus. An oral dose of 4 g/day decreased CSF pressure in one study of patients with BIH. If given intravenously however it will increase intracranial pressure despite reducing CSF production, by inducing vasodilatation. This observation highlights the importance of cerebral haemodynamics over and above that of CSF secretion. Rhakrishman [11] recommended an initial does of 250 mg q.i.d., increasing to 500 mg q.i.d. Neither Weisberg (1975) [105] nor Bulens *et al.* (1979) [128] were impressed by the efficacy of acetazolamide but Ahlskog and O'Neill (1982) [122] quoted evidence suggesting that the slow-release form of acetazolamide might be more effective. Acetazolamide is associated with a range of side effects, including nausea, paraesthesiae, drowsiness, general malaise, metabolic acidosis, altered taste and renal calculi. Acetazolamide may also result in a range of hypokalaemic interactions. Furthermore, aspirin reduces the excretion of acetazolamide with a risk of toxicity, and lithium excretion may be enhanced. Cardiac glycosides reduce CSF formation but are not effective in BIH (Weisberg 1975) [105]. Glycerol was introduced by Bucknell and Walsh (1964) [132] and used in BIH by Absolon (1966) [133]. However, glycerol apparently produces anorexia, nausea and vomiting, and Weisberg (1975) [105] found that to keep CSF pressure down required the equivalent of 4000 calories/day, which is counter productive in obese patients. Frusemide has also been used as as diuretic in the treatment of PTC. Its activity is independent of diuresis and acts via carbonic anhydrase, where it is less potent than acetazolamide [135]. Experimental treatments which have been reported include hyperbaric oxygen therapy, intravenous barbituate, D1 antagonists, and vasopressin [135–138].

One problem with all medication is that it may lead to procrastination, poor quality of life and delayed referral for definitive treatment. Since no prospective randomised trial has ever demonstrated that any drug is superior to any other, or that any drug is capable of diminishing papilloedema, a rational "best guess" approach would have to depend on investigations as discussed. If significant visual loss or deteriorating vision is found, then surgical intervention should be seriously considered. In the absence of demonstrable risk to vision, symptomatic treatment should commence with diet and with acetazolamide, or if side effects are unacceptable, with frusemide. If this fails, oral steroids should be introduced. No consensus exists on the management of sagittal sinus thrombosis in this context, though many might feel that it should be treated in the standard manner with anticoagulation, provided no risk factors are present (vide infra).

Corticosteroids

There is a view that steroids should not be used because of their potential side effects and risk of precipitating BIH [13] though for others it has become the mainstay of treatment [140]. Paterson *et al.* (1961) [141] first suggested the use of prednisone in the treatment of BIH, a suggestion which met with a mixed reception. Weisberg (1975) [105] made the important observation that headache and papilloedema improved rapidly within 72 hours of starting steroids in 13 of 15 patients who had not responded to serial lumbar punctures. Symptoms did not recur when the steroids were stopped after 7–14 days. In 81% of 37 patients, steroids effected resolution of signs and symptoms of BIH (Johnston *et al.* 1981) [120]. In the remaining seven patients, additional treatment was required either because of side-effects or because the intracranial hypertension did not resolve. All patients who responded to steroids showed improvement in three to four days and steroids could be stopped in 7–14 days No patient with BIH who did not show a response in one week subsequently improved on a more prolonged course of steroids. Five of the 37 patients who responded initially, subsequently relapsed (13.5%) When steroids were given for two months, the complication rate rose to 13% (diabetes mellitus, peptic ulceration, fluid retention, obesity and psychosis). A short course of dexamethasone with either ranitidine or cimetidine (7–14 days) is much less likely to be accompanied by such complications. Corbett *et al.* (1982) [22] have drawn attention to the effects of steroids on intraocular pressure, and the consequent need for close collaboration with an opthalmologist during the management of this condition.

Steroids have been criticised (Jefferson and Clark 1976 [129], quoting Winn 1974 and Hulme 1975) for their lack of immediate effect on CSF pressure despite the resolution of symptoms. Indeed, CSF pressure is reported not to fall over one week after starting steroids (Johnston *et al.* 1981) [120], though it may do so later. Dogs given high dose steroids do not show any change in CSF absorption, although acute steroid withdrawal was reported to result in an increase in resistance to flow across the arachnoid complex [142]. Steroids have also been reported to reduce CSF production [143,144] though other mechanisms may account for the efficacy of steroids. However, within hours of starting steroids the intracranial elastance (volume pressure response to 1 ml changes in CSF volume) is reduced (Pickard 1973 unpublished observations). The mean intracranial pressure may therefore not be reduced but its sensitivity to small fluctuations in CSF volume or cerebral blood volume may be diminished.

In summary, there is a role for a two week course of dexamethasone (4 mg q.i.d), provided the patient's vision is not rapidly deteriorating and is kept under supervision, which should then be tailed off. If symptoms or signs recur, surgical action is required rather than further courses of steroids [125, 11]. Prolonged corticosteroids of course have many side-effects and some authors consider than they may provoke re-occurence or maintenance of papilloedema and BIH.

7.8 Surgery

Indications

It is important to emphasize that in many patients symptomic BIH is self-limiting even though CSF pressure and outflow resistance often remain high, even when symptoms have resolved. Surgery is reserved for those patients in whom vision is deteriorating when first referred, who cannot tolerate drugs, are non-compliant or who cannot be relied upon to attend followup clinics, or where disc swelling/visual loss and/a severe headache persist despite medication.

Subtemporal Decompression

This technique was first described by Dandy (1937) [1]. However, in spite of its use multiple lumbar punctures were still needed in these patients, and those of other series, to control intermittent bulging of the decompression and in the management of visual deterioration (Greek 1968 for review) [121]. In Johnston *et al.*'s series (1981) [120], the vision in 5 of 43 patients continued to deteriorate despite subtemporal decompression. There is a significant surgical complication rate of 12% which includes epilepsy, otorrhoea and brain damage [127]. No measurements of intracranial compliance and CSF outflow resistance have been taken following this procedure to determine whether decompression functions to increase compliance or to increase CSF absorption by exposure to the temporalis fascia and galea.

CSF Shunts

Jackson and Snodgrass (1955) [145] first inserted shunts (ventriculo-peritoneal and lumbo-peritoneal) into 10 patients with BIH as part of their series of 62 peritoneal shunts, and regarded this group of patients as the more successful, but the exact results were not recorded. At first glance, lumbo-peritoneal shunts appear easier to insert in patients with BIH as the ventricular catheter does not need to be established within small ventricles, and this approach to management has found wide acceptance for patients failing to respond to serial lumbar puncture and drugs (Vander Ark *et al.* 1971 [146]; Weisberg 1975 [105]; Vassilouthis and Uttley 1979 [140]; Johnston *et al.* 1981) [120]. Many patients are obese however, and positioning on the table is important if the peritoneal catheter is to be placed reliably within the peritoneal cavity. Many revisions of L-P Shunts are the predictable result of delegation of an apparently simple procedure to an untutored trainee.

Weisberg (1975) [105] found shunts to be successful in all five patients refractory to more conservative treatment. Similarly Johnston *et al.* (1981) [120] found lumbo-peritoneal shunts to be successful in all eight patients so treated. Two of six ventriculo-peritoneal shunts required revision or removal for infection. In Rosenberg's [147, 148] series 34 patients treated with CSF diversion operations were retrospectively analysed. They had collectively undergone a total of 64 lumboperitoneal shunts and 7 ventricular shunts.

Only 9/34 (26%) were cured after a single procedure, and only 25% of shunts functioned for longer than 6 months. 20% of the reoperations were required for low pressure headaches. The vision of 12 patients (35%) showed continuing visual loss, four of whom did so while their shunts were considered to be functioning normally. Shunt failure with recurrence of symptoms occurred as late as 7 years following shunting [147]. After pooling the results from six American centers it was concluded that CSF diversion techniques failed 53% of patients [148]. The complication rate of lumbo-peritoneal shunts has reduced with the advent of percutaneous placement, modern silicone catheters and tethering techniques to avoid migration of the tubing (infection, spinal arachnoiditis, obstruction, low pressure headaches, subdural haematomas) (Selman *et al.* 1980) [149]. Unfortunately it is now recognised that an L-P shunt that functions too well for too long may result in secondary descent of the cerebellar tonsils [150]. In one of our patients, sub occipital headache was accompanied by palatal myoclonus. A difficulty which arises with lumbo-peritoneal shunts is knowing whether they are patent and functioning without recourse to lumbar puncture both to measure CSF pressure and for an isotope shuntogram. In patients with a complicated history of multiple treatments, recurrence and hysterical features, inclusion of a subcutaneous reservoir in the shunt system permits painless access, albeit with the small risk of bacterial colonisation. The majority of patients appear to require a functioning shunt for only a few months until the episode of BIH spontaneously resolves (Johnston *et al.* 1981) [120] but there is no need to remove a shunt unless specifically indicated.

Neurosurgeons and ophthalmologists who have an interest in BIH inevitably collect a number of patients with refractory problems. Each specialty can cite anecdotal examples of the failure of each other's favourite technique. A combined approach is essential. Cisterno-pleural or cisterno-peritoneal shunt may sometimes be required when other forms of shunt and optic sheath fenestration (wide infra) have failed or caused side-effects [151].

Optic Nerve Sheath Fenestration

"... relatively straightforward ophthalmic procedure, similar in style to a squint operation; it therefore has advantages over the more major neurosurgical procedures usually used to relive raised CSF pressure" (Tompkins and Spalton 1984) [152].

"This procedure is not done at many institutions, because there is a risk of visual loss after the operation" (Ahlskog and O'Neill 1982) [122].

"It is not a technically simple procedure and potential complications exist..." (Knight *et al.* 1986) [158].

"This operation relieves the pressure on the optic nerve head but does nothing to relieve intracranial hypertension" (Kaye *et al.* 1981) [153].

Recently there has been renewed interest in the operation of optic nerve sheath fenestration, first described by de Wecker in 1872 [154]. In monkeys with experimental papilloedema, a window created in the optic nerve sheath of one eye relieved both the ipsilateral swelling and sometimes that on the other side.

Techniques

With the medial approach, after a conjunctival peritomy, the medial rectus is disinserted leaving a frill of tendon attachment to the globe through which a traction suture may be placed. Malleable retractors are then used to retract the orbital fat to gain access to the optic nerve sheath, surrounded by the ciliary vessels. Damage to these vessels risks optic disc and choroidal infarction. The nerve sheath is grasped with toothed forceps and incised with a long-handled knife or long-handled scissors. In cases of papilloedema, incision of the sheath is accompanied by a gush of cerebrospinal fluid.

Lateral approaches to the nerve sheath involve either a lateral orbitotomy, or access without bone removal via a lateral canthotomy, or even an eyelid crease incision. The major risk via the lateral approach is damage to the temporal ciliary vessels, despite the better exposure afforded. Debate continues over the best method of creating a fistula:slit, window, valve with or without mitomycin.

Complications

Many ocular complications of optic nerve sheath fenestration have been reported. Transient ocular motility problems are common. Permanent tonic pupils occur more frequently after the lateral decompression route [155]; corneal dellen and supporative keratitis may occur after the medial approach due to conjunctival swelling (Sergott *et al.* 1988) [156]. Other sight threatening complications have included optic nerve trauma, angle closure glaucoma and dacryocystitis (Flaherty and Sergott 1992) [157], optic nerve haematoma and orbital haemorrhage dacryocystitis (Flaherty and Sergott 1992) [157], optic nerve haematoma and orbital haemorrhage (Corbett *et al.* 1988) [155], optic disc and choroidal infarcts (Knight *et al.* 1986) [158], peripapillary haemorrhages and chorio-retinal scarring (Spoor *et al.* 1992) [159], central and branch retinal artery occlusion (Plotink *et al.* 1993) [160].

Results Including Long Term Follow up

Three studies published in 1988 have documented an improvement in visual function in patients with idiopathic intracranial hypertension after this procedure. The improved visual results have to be balanced against the risk of complications to the eye.

In Corbett's [155] study of 40 eyes in 28 patients, the operation was performed via a lateral orbitotomy. Visual acuity improved in 12, and remained the same in 22 eyes; visual fields improved in 21 eyes and remained the same in 10 eyes. Eight eyes in five patients continued to lose acuity postoperatively; in each of these eyes there was a concomitant loss of visual field. In a further 2 eyes visual field loss developed, though visual acuity was preserved.

Two studies employed the medial route to decompress the optic nerve sheath. In Brourman's [161] study of 10 eyes in 6 patients, visual acuity improved in 3 eyes, remaining the same in 7. Visual field improved in all eyes. In Sergott's [156] series of 29 eyes, visual acuity improved in 19/29 eyes and visual field improved in all eyes.

More recently, Acheson *et al.* [162] reported their 15 years experience with the medial approach that visual acuity and fields either improved or stabilized in 17/20 eyes and four patients required optic nerve sheath decompression despite previous shunting or subtemporal decompression. However, five patients required shunts or subtemporal decompression after optic nerve sheath decompression because of persistent headache in three cases and for uncontrolled visual failure in two cases. Kelman [163] found that optic nerve sheath fenestration resulted in visual improvement in 12 patients with progressive visual loss despite functioning lumboperitoneal shunts.

Curiously, headache has been reported to be reduced in some 50–75% of patients after this procedure but with no long term follow up. In a quarter of such cases, however, headaches requiring diuretic therapy returned within 3–8 months, though not associated with deteriorating vision. It is not clear whether this was associated with a rise in intracranial pressure since this was not measured. It is however known that chronically raised pressure may persist without a decline in visual function (45), and in those cases in which CSF pressure has been measured in the immediate post operative period following optic nerve fenestration the pressure has been found to remain high.

The follow-up intervals in most studies varies widely (1 week to 8 years in Corbett's study), so it is important to note from a later report that 32% experience deterioration of visual function more than six months after surgery (Spoor and McHenry 1994) [159]. Long term follow up is required with careful monitoring of discs, acuity and fields, whatever the method of surgical management.

Mechanism of Effect of Optic Nerve Sheath Fenestration

Two mechanisms have been suggested: CSF absorption by orbital tissues or fibrosis within or around the nerve blocking transmission of raised CSF pressure to the optic nerve head. In a CT study of four patients from one day to four months post operatively with intrathecally injected contrast, complete filling of the subarachniod space around the optic nerve was identified, suggesting that extensive fibrosis around the nerve does not take place [161]. No dye leakage was seen in the orbit but this is probably not surprising given that it would be present in small amounts, and would be rapidly absorbed.

7.9 Management of Cerebral Venous Thrombosis

No consensus exists on the management of venous sinus thrombosis in a literature which is based almost exclusively on individual or serialised case reports. Diuretics, steroids, platelet inhibitors, pentobarbital-induced coma, surgical intervention, and systemic or local thrombolytic therapy have all been used in individual cases. Strong opposition to the use of thrombolysis had arisen because of the risk of spontaneous intracerebral haemorrhage. However in a blinded placebo controlled study of patients receiving KCCT-monitored intravenous heparin treatment, the mortality was 30% amongst the controls, with no deaths amongst those treated. In the same paper, a retrospective group of patients with both sinus thrombosis and intracerebral haemorrhage were examined. Even in the presence of haemorrhage, mortality was reduced by heparin therapy from 69% to 15% [165]. This conclusion is supported in a retrospectively collected series of cases in which intravenous heparin prevented all deaths [166]. While it may be tempting to extrapolate from these series to PTC-related sinus thrombosis, it must be recognised that a diagnosis of sinus venous thrombosis is usually made on a sick person with focal neurological signs, and that spontaneous intracerebral haemorrhage is not associated with PTC. The natural history of the two forms of thrombosis is different, with no deaths arising from PTC. It is possible that the two categories represent opposite ends of a disease spectrum, with differing rates of thrombus occlusion, or with primarily inflammatory or vascultitic disease giving rise to the more severe end of the spectrum, and thrombotic disease, the less severe cases. Currently no study has examined the efficacy of thrombolytic therapy in cerebral thrombosis presenting as PTC.

Acknowledgements

The authors are very grateful to Dr. Robert Marchbanks for permission to use Fig. 2 and to Liz Galfskiy of Winchester, UK for permission to reproduce her

poem first published in LINK magazine (Association of Spina Bifada and Hydrocephalus) December 1996/January 1997, Issue 167, Hydrocephalus Network News Page IV. This review is in part an update of a previous review [167].

Address for reprints: Prof. J. D. Pickard, Box 167, Academic Neurosurgical Unit, Addenbrooke's Hospital, Cambridge, U.K., CB22QQ.

References

1. Dandy WE (1937) Intracranial pressure without brain tumor. Ann Surg 106: 492–513
2. Hoffman HJ (1982) How is pseudotumor cerebri diagnosed? Arch Neurol 43: 167–168
3. Corbett JJ, Mehta MP (1983) Cerebrospinal fluid pressure in normal obese subjects and patients with pseudotumor cerebri. Neurology 33: 1386–1388
4. Smith JL (1985) Whence pseudotumor cerebri? J Clin Neuro Ophthalmol 5: 55–56
5. Quincke H (1897) Ueber meningitis serosa und verwandte Zustände. Dtsch Z Nervenheilkde 9: 140–168
6. Nonne M (1904) Über Fälle vom Symptomkomplex "Tumour cerebri" mit Ausgang in Heilling (Pseudotumor cerebri); Über letal verlaufene Fälle von "Pseudotumour cerebri" mit Sektionsbefund. Dtsch Z Nervenheilkde 27: 169–216
7. Johnston IH (1992) The pseudotumor syndrome. MD Thesis, University of Dundee, Scotland
8. Lipton HL, Michelson PE (1972) Pseudotumor cerebri syndrome without papilledema. JAMA 220: 1591–1592
9. Rush JA (1980) Pseudotumor cerebri. Clinical profile and visual outcome in 63 patients. Mayo Clin Proc 55: 541–546
10. Foley J (1955) Benign forms of intracranial hypertension—"toxic" and "otitic" hydrocephalus. Brain 78: 1–41
11. Radhakrishnau K, Ahlskog E, Garrity JA, Kurland LT (1994) Idiopathic intracranial hypertension. Mayo Clin Proc 69: 169–180
12. Durcan FJ, Corbett JJ, Wall M (1988) The incidence of pseudotumor cerebri: population studies in Iowa and Louisiana. Arch Neurol 45: 875–877
13. Digre KB, Corbett JJ (1988) Pseudotumor cerebri in men. Arch Neurol 45: 866–872
14. Lessell S (1992) Paediatric pseudotumor cerebri (Idiopathic intracranial hypertension). Surv Ophthalmol 37: 155–166
15. Cogan DG (1961) Blackouts not obviously due to carotid occlusion. Arch Ophthalmol 66: 180–187
16. Orcutt JC, Page NGR, Sanders MD (1984) Factors attending visual loss in benign intracranial hypertension. Ophthalmology 91: 1303–1312
17. Sismanis A (1987) Otologic manifestations of benign intracranial hypertension syndrome: diagnosis and management. Laryngoscope 97: 1–17
18. Reid A, Marchbanks RJ, Bateman D, Martin AM, Brightwell AP, Pickard JD (1989) Mean intracranial pressure monitoring by a non-invasive audiological technique—a pilot study. J Neurol Neurosurg Psychiatry 52: 610–612

19. Corbett JJ, Thompson HS (1989) The rational management of idiopathic intracranial hypertension. Arch Neurol 46: 1049–1051
20. Hoyt W, Beeston D (1996) The Ocular Fundus in Neurologic Disease. CV Mosby, St. Louis
21. Sanders MD (1979) A classification of papilloedema based on fluorescein angiographic study of 69 cases. Trans Ophthalmol Soc UK 89: 177–192
22. Corbett JJ, Savino PJ, Thompson HJ, *et al* (1982) Visual loss in pseudotumor cerebri: follow-up of 57 patients from 5 to 41 years and a profile of 14 patients with permanent severe visual loss. Arch Neurol 39: 461–474
23. Hedges TR, Weinstein JD, Crystle CD (1964) Orbital vascular response to acutely increased intracranial pressure in the rhesus monkey. Arch Ophthalmol 71: 226–237
24. Hayreh SS (1964) Pathogenesis of oedema of the optic disc (papilloedema). Br J Ophthalmol 48: 522–543
25. Tso MOM, Hayreh SS (1977a,b) Optic disc oedema in raised intracranial pressure III A pathologic study and IV Axoplasmic transport in experimental papilloedema. Arch Ophthalmol 95: 1448–1462
26. Minckler DS, Bunt DH (1977) Axoplasmic transport in ocular hypotony and papilloedema in the monkey. Arch Ophthalmol 95: 1430–1436
27. Radins RL, Anderson DR(1980) Fast axonal transport in early experimental disc edema. Invest Ophthalmol Vis Sci 19: 158–168
28. Parhad IM, Griffin JW, Cork LC, *et al* (1980) IDPN intoxications: a toxic model of disc swelling. J Neuropath Exp Neurol 39: 380–385
29. Medlock MD, *et al* (1992) Children with cerebral venous thrombosis diagnosied with magnetic resonance imaging and magnetic resonance angiography. Neurosurgery 31: 870–875
30. Gibby WA, *et al* (1993) Pseudotumor cerebri: CT findings and correlation with vision loss. Am J Roentgenol 160: 143–146
31. Reid AC, Matheson MJ, Teasdale G (1980) Volume of the ventricles in benign intracranial hypertension. Lancet ii: 7–8
32. Rothwell PM, Gibson RJ, Sellar RJ (1994) Computed tomographic evidence of cerebral swelling in benign intracranial hypertension. J Neurol Neurosurg Psychiatry 57: 1407–1409
33. Czosnyksa M, Whitehouse H, Smieleroski P, Simac S, Rickard JD (1996) Testing of cerebrospinal compensatory reserve in shunted and non-shunted patients. J Neurol Neurosurg Psychiatry 60: 549–558
34. Janny P, Chazul J, Colnet G, Irthum B, Georget AM (1980) Benign intracranial hypertension and disorders of CSF absorption. Surgical Neurology 15: 168–174
35. Martins AN (1973) Resistance to drainage of cerebrospinal fluid: clinical measurements and significance. J Neurol Neurosurg Psychiatry 36: 313–318
36. Calabrese VP, Selhorst JB, Harbisons JW (1978) Cerebrospinal fluid infusion tests in pseudotumor cerebri. Trans. Am Neurol Assoc 103: 146–150
37. Mann JD, Johnson RN, Butler AB, Bass BH (1979) Impairment of cerebrospinal fluid circulatory dynamics in pseudotumor cerebri and response to steroid treatment. Neurology (Minn) 29: 550

38. Sklar FH, Beyer CWJV, Ramanatham M, Cooper PR, Clark WK (1979) CSF dynamics in patients with pseudotumor cerebri. Neurosurgery 5: 208–216
39. Ropper AH, Marmarou A (1984) Mechanisms of pseudotumor in Guillain-Barre syndrome. Arch Neurol 41: 259–261
40. Gjerris F, Sorensen PS, Paulson OB (1985) ICP conductance to CSF outflow and CBF in patients with benign intracranial hypertension (pseudotumor cerebri). Ann Neurol 17: 158–162
41. Johnston IH, Patterson A (1974a,b) Benign intracranial hypertension I Diagnosis and Prognosis II CSF pressure and circulation. Brain 97: 289–312
42. Chandra V, Bellur SN, Anderson RJ (1986) Low CSF protein concentration in idiopathic pseudotumor cerebri. Ann Neurol 19: 80–82
43. Johnston PK, Corbett JJ, Maxner CE (1991) CSF protein and opening pressure in idiopathic intracranial hypertension (pseudotumor cerebri). Neurology 41: 1040–1042
44. James AE, Harbert JC, Hoffer DB, Deland FH (1974) CSF imaging in benign intracranial hypertension. J Neurol Neurosurg Psychiatry 37: 1053–1058
45. Creagh MD, *et al* (1919) Screening for the lupus acnticoagulant and anti-cardiolipin antibody in women with fetal loss. J Clin Pathol 44: 45–47
46. Griffin JP (1992) A review of the literature on benign intracranial hypertension associated with medication. Adverse Drug React Toxicol Rev 11: 41–58
47. Giuseffi V, *et al* (1991) Symptoms and disease associations in idipoathic intracranial hypertension (pseudotumor cerebri): a case-control study. Neurology 41: 239–244
48. Ireland B, Corbett JJ, Wallace RB (1990) The search for causes of pseudotumor cerebri: A preliminary case-control study. Arch Neurol 47: 315–320
49. Cochran WG (1954) Biometrics 10: 417
50. Wall M, Giuseffi V, Rojas PB (1989) Symptoms and disease associations in pseudotumor cerebri: A case controlled study. Neurology 39 [Suppl]: 210
51. Wall M (1991) Idiopathic intracranial hypertension. Neurologic Clinics 9: 73–95
52. Walsh FB (1952) Papilledema associated with increased intracranial pressure in Addison's disease. Arch Ophthalmol 47: 86
53. Boudin G, Funck-Brentano JL, Gayno M (1956) Maladie d'Addison par aplasie surrenale et syndrome para-biermerien. Bull Soc Méd Höp Paris 66: 1736–1740
54. Greer M (1963) Benign intracranial hypertension: II Following corticosteroid therapy. Neurology 13: 439–441
55. Bronsky D, *et al* (1958) Idiopathic hypoparathyroidism and pseudohypoparathyroidism: case reports and review of the literature. Medicine (Balt) 37: 317–352
56. Sheldon RS, *et al* (1987) Hypoparathyroidism and pseudotumor cerebri: An infrequent clinical association. Can J Neurol Sci 14: 622–625
57. Dickman MS, Somasundaram M, Brzozowski L (1980) Pseudotumor cerebri and hyperthyroidism. NY State J Med 80: 1118–1120

58. Karsakis EJ, Bass NH (1982) Benign intracranial hypertension induced by deficiency of vitamin K during infancy. Neurology 32: 1292–1295
59. Shah A, *et al* (1987) Danazol and benign intracranial hypertension. Br Med J 294: 1323
60. Hamed LM, *et al* (1989) Am J Ophthalmol 107: 105–110
61. Saul RF, Hamburger HA, Selhorst JB (1985) Pseudotumor cerebri secondary to lithium carbonate. J Am Med Assoc 253: 2869–2870
62. Levine SH, Puchalski C (1990) Pseudotumor cerebri associated with lithium therapy in two patients. J Clin Psychiatry 51: 251–253
63. Mukherjee A, *et al* (1990) Benign intracranial hypertension after nalidixic acid overdose in infants. Lancet 335: 1602
64. Van Dop C, *et al* (1983) Pseudotumor cerebri associated with initiation of levothyroxine therapy for juvenile hypothyroidism. N Engl J Med 308: 1076–1080
65. Vyas CK, *et al* (1981) Steroid-induced benign intracranial hypertension. Postgrad Med J 57: 181–182
66. Neville BGR, Wilson J (1970) Benign intracranial hypertension following corticosteroid withdrawal in children. Br Med J 3: 554
67. Korzets A, *et al* (1988) Pseudotumor cerebri and nitrofurantoin. Drug Intell Clin Pharm 22: 345
68. Mushet GR (1977) Pseudotumor and nitrofurantoin therapy. Arch Neurol 34: 257
69. Konomi H, *et al* (1978) Indomethacin causing pseudotumor cerebri in Bartter's syndrome. N Engl J Med 298: 855
70. Larizza D, *et al* (1979) Ketoprofen causing pseudotumor cerebri in Bartter's syndrome. N Engl J Med 300: 796
71. Buchheit WA, *et al* (1969) Papilloedema and idiopathic intracranial hypertension: Report of a familial occurrence. N Engl J Med 280: 938–941
72. Howe J, Saunders M, Clarke P (1973) Familial benign intracranial hypertension. Acta Neurochir (Wien) 29: 173–175
73. Rothman AP, Brust JCM (1974) Pseudotumor cerebri: report of a familial occurrence. Arch Neurol 30: 110–111
74. Traviesa DC, *et al* (1976) Familial benign intracranial hypertension. J Neurol Neurosurg Psychiatry 39: 420–423
75. Johnston I, Morgan MK (1991) A familial coincidence of pseudotumor cerebri and communicating hydrocephalus. Neurourgery 28: 727–729
76. Bousser MG, *et al* (1985) Cerebral venous thrombosis: a review of 38 cases. Stroke 16: 199–213
77. Kaplan RE, *et al* (1985) Pseudotumor cerebri associated with cerebral venous sinus thrombosis, internal jugular vein thrombosis, and systemic lupus erythematosis. J Pediatr 107: 266–268
78. Bettman JW, *et al* (1968) Papilledema and asymptomatic intracranial hypertension in systemic lupus erythematosus. Arch Ophthalmol 80: 189–193
79. Carlow TJ, Glaser JA (1974) Pseudotumor cerebri syndrome in systemic lupus erythematosus. JAMA 228: 197–200

80. Kinal ME (1967) Traumatic thrombosis of dural venous sinuses in closed head injuries. J Neurosurg 27: 142–145
81. Carroll JD, Leak D, Lee HA (1966) Cerebral thrombophlebitis in pregnancy and the puerperium. Quart J Med 35: 347
82. Melamed E, *et al* (1976) Aseptic cavernous sinus thrombosis after internal carotid arterial occlusion in polycythaenia vera. J Neurol Neurosurg Psychiatry 39: 320–324
83. Esack A, Thompson G, Burmester H (1989) Benign intracranial hypertension and essential thrombocythaemia. J Neurol Neurosurg Psychiatry 52: 914
84. Casalé Turu A, *et al* (1992) Oedeme de la papille et syndrome de POEMS. Ophthalmologica 205: 144–148
85. Wasan H, *et al* (1992) Myeloma and benign intracranial hypertension. Br Med J 304: 685
86. Greaves M, Preston FE (1993) Clinical and laboratory aspects of thrombophilia in recent advances in blood coagulation. Churchill Livingstone, London, pp 119–140
87. Massons J, *et al* (1992) Cerebral venous thrombosis and hereditary protein C deficiency. Neurologia 7: 34–38
88. Schutta HS, *et al* (1991) Cerebral venous thrombosis associated with plasminogen deficiency. Stroke 22: 401–405
89. Cros D, *et al* (1990) Superior saggital sinus thrombosis in a patient with protein S deficiency. Stroke 21: 633–636
90. Ambruso DR, Jacobson LJ, Hathaway WE (1980) Inherited antithrombin III deficiency and cerebral thrombosis in a child. Paediatrics 65: 125–131
91. Mokri B, Jack CR, Petty GW (1993) Pseudotumor syndrome associated with cerebral venous sinus occlusion and antiphospholipid antibodies. Stroke 24: 469–472
92. Levine SR, *et al* (1987) Cerebral venous thrombosis with lupus anticoagulants: report of two cases. Stroke 18: 801–804
93. Ikkala E, Laitinen L (1963) Papilloedema due to iron deficiency anaemia. Acta Haematol 29: 368–370
94. Risdale L, Moseley I (1978) Thoracolumbar intraspinal tumours. Presenting features of raised intracranial pressure. J Neurol Neurosurg Psychiatry 41: 737–745
95. Morley JB, Reynolds H (1966) Papilloedema and the Landry-Guillain-Barre syndrome. Case reports and a review. Brain 89: 205–222
96. Sussman JD, Leach M, Greaves M, Maliar, Davies-Jomes GAD (1997) Potentially pro-thrombotic abnormalities of coagnitation in benign intracranial hypertension J Neurol Neurosurg Psychiatry 62: 229–233
97. Wyper DJ, Pickard JD, Matheson MS (1979) Accuracy of ventricular volume estimation. J Neurol Neurosurg Psychiatry 42: 345–350
98. Weisberg LA (1985) Computed tomography in benign intracranial hypertension. Neurology 35: 1075–1078
99. Jacobson DM, Karanjia PN, Olson KA, Warner JJ (1990) Computed tomography ventricular size has no predictive value in diagnosing pseudotumor cerebri. Neurology 40: 1454–1455

100. Gideon P, Sorenson PS, Thomsen C, Stahlberg F, Gjerris F, Henriksen O (1995) Increased brain water self-diffusion in patients with idiopathic intracranial hypertension. Am J Neuroradiol 16: 381–387
101. Sans AL, Joynt RJ (1956) Brain swelling of unknown cause. Neurology (Minn) 6: 791–803
102. Wall M, Pollar JD, Sadon AA, Kardon R (1995) Idiopathic intracranial hypertension—lack of histologic evidence for cerebral edema. Arch Neurol 52: 141–145
103. Brooks DJ, Beaney RP, Lammertsma AA (1984) Quantitative measurement of bloodbrain barrier permeability using Rubidium-82 and positron emission tomography. J Cereb Blood Flow Metab 4: 535–545
104. Boddie HG, Banna M, Bradley WG (1974) 'Benign' intracranial hypertension A survey of the clinical and radiological features and longterm prognosis. Brain 97: 313–326
105. Weisberg LA (1975) Benign intracranial hypertension. Medicine 54: 197–207
106. Kaye AH, Tress BM, Brownbill D, King J (1982) ICP in patients with the empty sella syndrome without benign intracranial hypertension. J Neurol Neurosurg Psychiatry 45: 209–216
107. Raichle ME, Grubb RL, Phelps Me, Gado MH, Caronna J (1978) Cerebral haemodynamics and metabolism in pseudotumor cerebri. Ann Neurol 4: 104–111
108. Mathew NT, Meyer JS, Ott EO (1975) Increased cerebral blood volume in benign intracranial hypertension. Neurology (Minn) 25: 646–649
109. Brooks DJ, Beaney RP, Leenders KL, Marshall J, Thomas DJ, Jones T (1985) Regional cerebral oxygen utilisation blood flow and blood volume in benign intracranial hypertension studied by positron emission tomography. Neurology 35: 1030–1034
110. Davidoff LM, Dyke CG (1937) Hypertensive meningeal hydrops. Am J Ophthalmol 20: 908–927
111. Lofgren J, Zwetnow NW (1973) Cranial and spinal components of the cerebrospinal fluid pressure volume curve. Acta Neurol Scand 49: 575–585
112. Fishman RA (1980) Cerebrospinal fluid in diseases of the nervous system. Sanders, London
113. Donaldson JO (1981) Pathogenesis and pseudotumor cerebri syndromes. Neurology 31: 877–880
114. Gideon P, Sorenson PS, Thomsen C, Stahlberg F, Gjerris F, Henriksen O (1994) Assessment of CSF dynamics and venous flow in the superior sagittal sinus by MRI in idiopathic intracranial hypertension: a preliminary study. Neuroradiology 36: 350–354
115. Davson HG, Hillingsworth MB, Segal (1970) The mechanism and drainage of the cerebrospinal fluid. Brain 93: 665–678
116. Johnston IH (1975) The definition of a reduced CFS absorption syndrome; a re-appraisal of benign intracranial hypertension and related conditions. Medical Hypotheses 1: 10–14

117. Sante Rose C, Lacombe J, Pierre-Kahn A, Renieu, D, Hirsch JF (1984) Intracranial venous sinus hypertension—cause or consequence of hydrocephalus in infants? J Neurosurg 60: 727–736
118. Malm J, Kristensen B, Morkgren P, Ekstedt J (1992) CSF hydrodynamics in idiopathic intracranial hypertension: a long term study. Neurology 42: 851–858
119. Hayes KC, McCombs HL, Faherty TP (1971) The fine structure of Vitamin A deficiency II arachnoid granulations and CSF pressure. Brain 94: 213–224
120. Johnston I, Paterson A, Besser M (1981). The treatment of benign intracranial hypertension: a review of 134 cases. Surg Neurol 16: 218–224
121. Greer M (1968) Management of benign intracranial hypertension. Clin Neurosurg 15: 161–172
122. Ahlskog E, O'Neill BP (1982) Pseudotumor cerebri. Annals of Internal Medicine 97: 249–256
123. Digre KL, Varner MW, Corbett JJ (1984) Pseudotumor cerebri and pregnancy. Neurology (Cleveland) 34: 721–729
124. Newborg B (1974) Pseudotumor cerebri treated by rice/reduction diet. Arch Int Med 133: 802–807
125. Wall M, George D (1991) Idiopathic intracranial hypertension: A prospective study of 50 patients. Brain 114: 155–180
126. Sugerman HJ, Felton WL III, Salvant JB (1995) Effects of surgically induced weight loss on idiopathic intracranial hypertension in morbid obesity. Neurology 45: 1655–1659
127. Corbett JJ (1996) Surgical management of papilloedema. In: Festschrift for WB Hoyt. (In Press)
128. Bulens C, De Vries VAEJ, Van Crevel H (179) Benign intracranial hypertension. A retrospective and follow-up study. J Neurol Sci 40: 147–157
129. Jefferson A, Clark J (1976) Treatment of benign intracranial hypertension by dehydrating agents with particular reference to the measurement of the blind spot area as a means of recording improvement. J Neurol Neurosurg Psychiatry 39: 627–639
130. Rubin RC, Henderson ES, Ommaya AK (1966) The production of cerebrospinal fluid in man and its modifications by acetazolamide. J Neurosurg 25: 430–436
131. Gucer G, Viernstein L (1978) Longterm intracranial pressure recording in the management of pseudotumor cerebri. J Neurosurg 49: 256–263
132. Buckell M, Walsh L (1964) Effect of glycerol by mouth on raised intracranial pressure in man. Lancet 2: 1151–1152
133. Absolon MJ (1966) Unusual presentation of benign intracranial hypertension. Early treatment with oral glycerol. Br J Ophthalmol 50: 683–686
134. Javaheri S (1991) Role of NaCl cotransport in cerebrospinal fluid production: effects of loop diuretics. J Appl Physiol 71: 795–800
135. Luongo C, *et al* (1992) Hyperbaric oxygen therapy in the treatment of benign intracranial hypertension. Follow-up of a preliminary study. Minerva Anestesiol 58 [Suppl 1]: 97–98

136. Maruishi M, *et al* (1992) Successful treatment of increased intracranial pressure by barbiturate therapy in a patient with severe sinus thrombosis after failure of osmotic therapy. A case report. Acta Neurochir (Wien) 120: 88–91
137. Faraci FM, Mayhan WG, Heistad DD (1990) Effect of vasopressin on production of cerebrospinal fluid: possible role of vasopressin (Vl)-receptors. Am J Physiol 258: R94–98
138. Boysen SJ, Alexander A (1990) Net production of cerebrospinal fluid is decreased by SCH-23390. Ann Neurol 27: 631–635
139. Rosner MJ (1995) Personal Communication
140. Vassilouthis J, Uttley D (1979) Benign intracranial hypertension: clinical features and diagnosis using computed tomography and treatment. Surg Neurol 12: 389–392
141. Paterson R, DePasquale N, Mann S (1961) Pseudotumor cerebri. Medicine 40: 85–99
142. Johnston I, Gilday DL, Hendrick EB (1974) The effects of steroids and steroid withdrawal on CSF absorption. An experimental study in dogs. J Neurosurg 42: 690–695
143. Sato O, Hara M, Asai T (1973) The effect of dexamethasone phosphate on the production rate of cerebrosponal fluid in the subarachnoid space of dogs. J Neurosurg 39: 480–484
144. Weiss MH, Nulsen FE (1970) The effect of glucocorticoids on CSF flow in dogs. J Neurosurg 32: 452–458
145. Jackson JJ, Snodgrass SR (1955) Peritoneal shunts in the treatment of hydrocephalus and increased intracranial pressure. A 4 year survey of 62 patients. J Neurosurg 12: 216–222
146. Vander Ark GD, Kemple LG, Smith DR (1971) Pseudotumor cerebri treated with lumbo-peritoneal shunt. J Am Med Assoc 217: 1832–1834
147. Rosenberg M, *et al* (1989) The efficacy of shunting procedures in pseudotumor cerebri. Neurology 38 [Suppl]: 209
148. Rosenberg ML, Corbett JS, *et al* (1993) Cerebrospinal fluid diversion procedures in pseudotumor cerebri. Neurology 43: 1071–1072
149. Selman WR, Spetzler RF, Wilson CB, Grollmus JW (1980) Percutaneous lumboperitoneal shunt: review of 130 cases. Neurosurgery 6: 255–257
150. Chumas PD, Armstrong DC, Drake JM, Kulkarni AV, Hoffman HJ, Humphreys RP (1993) Tonsillar herniation: the rule rather than the exception after lumboperitoneal shunting in the peadiatric population. J Neurosurg 78: 568–573
151. Johnston IH, Sheridan MM (1993) CSF shunting from the cisterna magna: a report of 16 cases. Br J Neurosurg 7: 39–43
152. Tomkins CM, Spalton DJ (1984) Benign intracranial hypertension treated by optic nerve sheath decompression. J Royal Soc Med 77: 141–144
153. Kaye AH, Galbraith JEK, King J (1981) Intracranial pressure following optic nerve decompression for benign intracranial hypertension. J Neurosurg 55: 453–456
154. De Wecker L (1872) On incision of the optic nerve in cases of neuroretinitis. 1st Ophthalmic Congr Rep 4: 11–14

155. Corbett JJ, Nerad JA, Tse DT, Anderson RL (1988) Results of optic nerve sheath fenestration for pseudotumor cerebri: the lateral orbitotomy approach. Arch Ophthalmol 106: 1391–1397
156. Sergott RC, Savino PJ, Bosley TM (1988) Modified optic nerve sheath decompression provides longterm visual improvement for pseudotumor cerebri. Arch Ophthalmol 106: 1384–1390
157. Flaherty PM, Sergott RC (1992) Optic nerve sheath decompression. Ophthalmol Clin North Am 1: 395–404
158. Knight RSG, Fielder AR, Firth JL (1986) Benign intracranial hypertension: visual loss and optic nerve sheath fenestration. J Neurol Neurosurg Psychiatry 49: 243–250
159. Spoor TC, McHenry JG (1993) Longterm effectiveness of optic nerve sheath decompression for pseudotumor cerebri. Arch Ophthalmol III: 632–635
160. Plotnik JC, Kosmorsky GS (1993) Operative Complications of optic nerve sheath decompression. Ophthalmology 100: 683–690
161. Brourman ND, Spoor TC, Ramacki JM (1988) Optic nerve sheath decompression for pseudotumor cerebri. Arch Ophthalmol 106: 1378–1383
162. Acheson JF, Green WT, Sanders MD (1994) Optic nerve sheath decompression for the treatment of visual failure in chronic raised intracranial pressure. J Neurol Neurosurg Psychiatry 57: 1426–1429
163. Kelman SE, Heaps R, Wolf A, Elman HJ (1992) Optic nerve decompression surgery improves visual function in patients with pseudotumor cerebri. Neurosurgery 30: 391–395
164. Foley KM (1977) Is benign intracranial hypertension a chronic disease? Neurology 27: 388 (Abstract)
165. Einhaupl KM, *et al* (1991) Heparin treatment in sinus venous thrombosis. Lancet 338: 597–600
166. Bousser MG, *et al* (1985) Cerebral venous thrombosis: a review of 38 cases. Stroke 16: 199–213
167. Pickard JD (1987) Which patients with benign intracranial hypertension can we help? In: Warlow C, Garfield J (eds) More dilemmas in the management of the neurological patient. Churchill Livingstone, Edinburgh, pp 156–170
168. Kirkpatrick PJ, Meyer T, Sarkies N, Pickard JD (1994) Papilloedema and visual failure in a patient with nocturnal hypoventilation. J Neurol Neurosurg Psychiatry 57: 1546–1547

Subject Index

Springer-Verlag and the Environment

WE AT SPRINGER-VERLAG FIRMLY BELIEVE THAT AN international science publisher has a special obligation to the environment, and our corporate policies consistently reflect this conviction.

WE ALSO EXPECT OUR BUSINESS PARTNERS – PRINTERS, paper mills, packaging manufacturers, etc. – to commit themselves to using environmentally friendly materials and production processes.

THE PAPER IN THIS BOOK IS MADE FROM NO-CHLORINE pulp and is acid free, in conformance with international standards for paper permanency.